UILU-ENG-92-2009

CIVIL ENGINEERING STUDIES

HYDRAULIC ENGINEERING SERIES NO. 41

ISSN: 0442-1744

SENSITIVITY OF FLOOD ROUTING MODELS TO VARIATIONS OF MOMENTUM EQUATION COEFFICIENTS AND TERMS

By

RENJIE XIA

and

BEN CHIE YEN

DEPARTMENT OF CIVIL ENGINEERING
UNIVERSITY OF ILLINOIS AT
URBANA-CHAMPAIGN
URBANA, ILLINOIS
FEBRUARY 1992

CIVIL ENGINEERING STUDIES
HYDRAULIC ENGINEERING SERIES NO. 41

SENSITIVITY OF FLOOD ROUTING MODELS TO VARIATIONS OF MOMENTUM EQUATION COEFFICIENTS AND TERMS

By

RENJIE XIA

and

BEN CHIE YEN

DEPARTMENT OF CIVIL ENGINEERING
UNIVERSITY OF ILLINOIS AT
URBANA-CHAMPAIGN
URBANA, ILLINOIS
FEBRUARY 1992

ABSTRACT

The Saint-Venant equations consist of a continuity equation and a well-known dynamic wave equation. The dynamic wave equation is actually a simplification of a more complicated exact momentum equation obtained by assuming some coefficients as constants and neglecting some terms involved in the exact momentum equation. In this study, a systematic and comprehensive investigation is conducted to detect the sensitivity of flood-routing models to the variations of the coefficients and terms in the exact momentum equation.

This study is divided into two aspects. The first one considers the impacts of the coefficients (ß, k, and k') on the solutions of the equations. These impacts can be obtained by comparing the solutions of the Saint-Venant equations (ß = k = k' = 1) with those of the exact momentum and continuity equations (ß, k, and k' have various values).

The second aspect is concerned with the relative contributions of the terms in the exact momentum equation (such as local and convective accelerations, pressure, channel slope, friction slope, and internal stresses) under various flow and downstream boundary conditions. In addition, the contribution of each term due to the variations of the coefficients (ß, k, and k') is also detected.

In both aspects, different downstream boundary conditions are tested in order to investigate the downstream backwater effect which has been generally ignored by other researchers in their study of unsteady flow simulations.

The results investigated in this study show: (a) The importance of the coefficients is in a descending order as k, k', and ß. (b) The impacts of the coefficients on the solutions of the equations are greatly influenced by the channel slope and downstream boundary condition. (c) The contributions of the terms are closely related to the downstream boundary condition, and slightly influenced by the variations of the coefficients. (d) The pressure term is significant for either convectively decelerating or accelerating water surface profiles. Based on the results, criteria for proper selection of the equations (the exact momentum and continuity equations or the Saint-Venant equations) as well as the lower level approximations (the noninertia or kinematic wave model) are proposed.

ACKNOWLEDGMENTS

This research was done while the first author was working part-time with the Illinois State Water Survey. Support of computer time was provided by the Research Board and the Graduate College of the University of Illinois at Urbana-Champaign. This report is essentially the same as the Ph.D. thesis of the first author under the supervision of the second author, omitting the appendices which are summary tables of computed results.

TABLE OF CONTENTS

LIST OF FIGURES

LIST OF TABLES

LIST OF SYMBOLS

A	Flow cross-sectional area perpendicular to x
A_0	Reference flow cross-sectional area
A_*	A/A_0
B	Width of the cross section at the free surface
B_0	Reference width
B_*	B/B_0
b	Bottom width of a trapezoidal channel
b_0	Reference bottom width
b_*	b/b_0
C	Chezy Factor
C_f	Factor
c	Kinematic wave speed
c^+	Forward characteristics
c^-	Backward characteristics
c'	Pressure-head correction
c_*	Dimensionless celerity
c_{*r}	Relative dimensionless celerity
D	Diameter of a circular channel
F	$\sqrt{gB/A}$
F_0	$V_0/\sqrt{gh_0}$
F_r	Froude number
f	Weisbach coefficient
f_c	Coefficient
G_1	Cross-sectional geometry function
G_2	Cross-sectional geometry function
G_3	Cross-sectional geometry function

G_4	Cross-sectional geometry function
G_5	Cross-sectional geometry function
g	Gravitational acceleration
h	Flow depth normal to x
h_0	Reference flow depth
h_*	h/h_0
h'	Perturbation depth
h_d	Flow depth of downstream boundary
h_{d*}	h_d/h_0
h_n	Normal flow depth
h_u	Uniform flow depth
h_{ua}	Average height of water level above h_u
h_w	Wave amplitude
h_{w*}	h_w/h_0
h_{**}	Dimensionless depth amplitude function
K	Piezometric pressure correction coefficient
K'	Ambient piezometric pressure correction coefficient
K'_{ni}	Ambient piezometric pressure correction coefficient in tensor form
K_1	Wave celerity
K_2	Wave dispersion coefficient
K_d	Diffusivity due to channel irregularities
L	Length
L_0	Reference length
L_w	Wavelength of disturbance
m	Exponent
n	Manning resistance factor
n_0	Reference Manning resistance factor

n_*	n/n_0
P	Local piezometric pressure
$\overline{P}$	Mean value of P
P'	Turbulent fluctuation of P
Q	Discharge
Q_0	Reference discharge
Q_*	Q/Q_0
Q'	Perturbation discharge
Q_n	Normal discharge
q	Discharge per unit width
q_0	Reference discharge
q_*	q/q_0
q'	Perturbation discharge
q_L	Lateral flow rate per unit length of x
R	Hydraulic radius
R_0	Reference hydraulic radius
R_*	R/R_0
r	Normal displacement of σ with respect to space or time
r_k	Radius of curvature of channel bottom
S_0	Channel slope
S_f	Friction slope
T	Force due to internal stresses acting normally to A
T_0	Reference force
T_*	T/T_0
T_{ij}	Force due to internal stresses in tensor form
T_r	Time-of-rise of inflow hydrograph
t	Time
t_0	Reference time

t_*	$V_0 t/L_0$
t_w	Duration
t_{w*}	t_w/t_0
U_x	X component of the lateral flow velocity
u	Local point velocity
u_i	Instantaneous local velocity component along the ith direction
u_j	Instantaneous local velocity component along the jth direction
$\bar{u}_i$	Temporal average of u_i
$\bar{u}_j$	Temporal average of u_j
V	Mean velocity of flow over A
V_0	Reference velocity
V_*	V/V_0
V'	Perturbation Velocity
V_i	Mean velocity component along the ith direction
V_j	Mean velocity component along the jth direction
V_w	Monoclinal wave velocity
V_{**}	Dimensionless velocity amplitude function
x	Distance along the longitudinal direction
x_*	x/L_0
Z	Stage
z	Side slope
z_d	Elevation of the channel bottom above the datum plane
β	Momentum flux correction coefficient or Boussinesq coefficient
β_{nij}	Momentum flux correction coefficient or Boussinesq coefficient in tensor form
Ω_*	Dimensionless complex propagation factor

γ	Specific weight of the liquid
γ_a	Cross-sectional average specific weight of the fluid
θ	Angle between the x direction and a horizontal plane
ρ	Fluid density
$\overline{\rho}$	Temporal average of ρ
ρ_a	Cross-sectional mean fluid density
ρ_h	Mean fluid density along flow depth
κ	Kinematic flow number
σ	Perimetric bounding cross-sectional area A
σ_*	Dimensionless wave number
τ_x	Boundary shear stress in x-direction
τ_{ij}	Deformation stress
ϕ	Central angle of a circular channel
ϕ_0	Reference central angle
ω	Frequency
ω	Constant wave speed
Δt	Small time increment
Δt_*	$V_0 \Delta t / L_0$
Δx	Small distance increment
Δx_*	$\Delta x / L_0$
θ	Time weighting factor
Π	Constant attenuation parameter
$\zeta(x,Z)$	Width of irregular cross section at point (x,Z)
ζ_1	Coefficient of nondimensional finite difference equation
ζ_2	Coefficient of nondimensional finite difference equation
η_1	Coefficient of nondimensional finite difference equation
η_2	Coefficient of nondimensional finite difference equation

δ_1 Coefficient of nondimensional finite difference equation

δ Logarithmic decrement

ε Ratio of characteristic surface gradient to bed gradient

ς Square of Froude number

1. INTRODUCTION

Unsteady flow is characterized by the time dependence of the flow. It is one of the most frequently encountered types of flow in nature. Unsteady flow problems cover a wide range of phenomena including flood movement and surge in rivers, channels and sewers, overland surface runoff, and tidal motion.

Flood movement, i.e., the propagation of flood waves along rivers or channels, is a widely investigated classical subject. The process of tracing the movement of a flood wave is known as flood routing. The literature shows that engineers have been concerned with the behavior of flood waves and tried to route them down rivers or channels for at least the past hundred years.

Flood routing generally is an unsteady flow problem. The solution and simulation of flood routing can commonly follow two approaches, i.e., hydrologic approach and hydraulic approach. While both hydrologic and hydraulic approaches utilize conservation of mass, the hydraulic approach explicitly considers dynamic effects of flow, whereas the hydrologic approach does not and simply regards the volume of water in a channel reach as a single-valued function of discharge. Over the years different models in both groups have been developed along separate lines. In general, models which result from the hydrologic approach are numerous and simple in flood routing, but they are less precise in their physical description of the phenomenon. With the development of high speed computers and advancement in numerical techniques, models which result from the hydraulic approach have become

increasingly popular and reached a high level of sophistication.

One-dimensional unsteady flow can be mathematically represented by a pair of nonlinear hyperbolic-type first-order partial differential equations which are derived from a consideration of the conservation of mass and momentum. These equations are generally referred to as the Saint-Venant equations which include a well-known dynamic wave equation and a continuity equation. Currently, there exist a number of models for the solution of these equations. Most proposed models are based on finite difference numerical techniques. In addition to one-dimensional modeling, there are many two-dimensional and three-dimensional models for various unsteady flow problems. These two-dimensional and three-dimensional modelings are useful, but often not necessary, since for many problems only the one-dimensional solution is needed.

Over the years many investigators have studied flood routing problems. They set up various models, developed or improved numerical schemes, investigated their solutions and applied these models to specific field problems. However, there is a basic problem which is seldom considered, namely, all the models are based on the Saint-Venant equations or their simplifications; but the so-called complete dynamic wave equation in the Saint-Venant equations comes from a more complicated exact momentum equation (Yen, 1973) by assuming constant values for some of the coefficients (i.e., momentum flux correction coefficient, ß, and pressure correction coefficients, k and k') and by neglecting certain terms (such as local acceleration, convective acceleration,

pressure, internal stresses and lateral flow) in the exact momentum equation. Therefore, a question has to be asked, namely, how significant are these assumptions on the solution of the equations. In order to settle this question, two aspects should be investigated separately. The first one is the study of the importance of the coefficients, and the second is the contributions of the terms in the exact momentum equation. The objective of this research is to increase the understanding of the above question and find out the difference between the solutions of the exact momentum and the complete dynamic wave equations. This objective will be accomplished through evaluating the theory of unsteady flow, briefly reviewing relevant literature, processing a numerical procedure, and analyzing the results of the aforementioned aspects concerned with the coefficients and terms in the exact momentum equation. To investigate the importance of the coefficients, it should be mentioned that for real flow, all the coefficients (ß, k and k') vary simultaneously, that means, when one coefficient varies, others must be influenced; but in this study a kind of hypothetical analysis has been performed to simplify the complication of real problems by changing one coefficient at a time.

2. THEORY

Unsteady flow can be described mathematically by a continuity equation and a momentum equation. Historically, a fundamental derivation of the one-dimensional gradually varied equations of unsteady flow has been laid mostly by the 19th century hydraulicians, Coriolis, Saint-Venant, and Boussinesq. Developments considering the terms reflecting turbulence effects were made by Keulegan (1938) and Keulegan and Patterson (1943). Further progress has been made by Strelkoff (1969), Chen and Chow (1971) and others. Yen (1971, 1973) performed a much more thorough development and derived a set of equations describing the unsteady, spatially-varied, turbulent, free-surface flow of a viscous nonhomogeneous fluid in a channel of arbitrary cross sectional and alignment geometry with erodible boundary by integrating the point-form equations of continuity, momentum, and energy over a cross-sectional area of the channel.

2.1. Mathematical Representation

The pair of hyperbolic-type partial differential equations representing mathematically the flow of an incompressible homogeneous fluid in an open channel can be written in the following form of a continuity equation and a exact momentum equation (Yen, 1973)

$$\frac{\partial A}{\partial t} + \frac{\partial Q}{\partial x} = q_L \qquad (2.1)$$

$$\frac{1}{gA}\frac{\partial Q}{\partial t} + \frac{1}{gA}\frac{\partial}{\partial x}\left(\frac{\beta}{A}Q^2\right) + \frac{\partial}{\partial x}(kh\cos\theta)$$

$$+ (k-k')\frac{h\cos\theta}{A}\frac{\partial A}{\partial x} = S_0 - S_f + \frac{1}{\gamma A}\frac{\partial T}{\partial x} + \frac{q_L U_x}{gA} \qquad (2.2)$$

in which Q is discharge, t is time, x is the distance along the longitudinal direction, A is flow cross-sectional area perpendicular to x, h is flow depth normal to x as shown in Fig. 2.1, θ is the angle between the x direction and a horizontal plane, S_0 is the channel slope ($S_0 = \sin\theta$), S_f is the friction slope, β is a momentum flux correction coefficient, k is a piezometric pressure correction coefficient in order to account for the nonhydrostatic pressure distribution, k' is a ambient piezometric pressure correction coefficient, T is the force due to internal stresses acting normally to A, γ is specific weight of the liquid, g is gravitational acceleration, q_L is the lateral flow rate per unit length of x, and U_x is the x component of the lateral flow velocity.

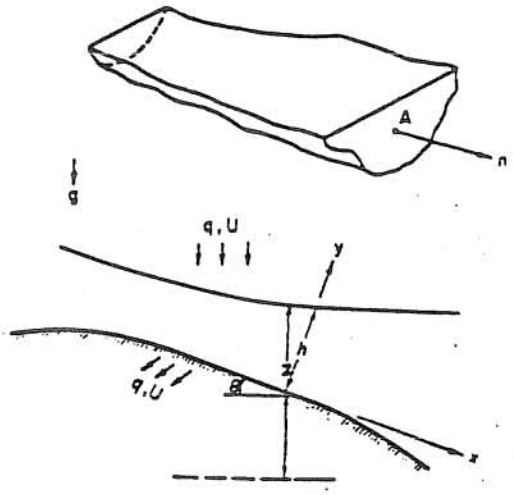

Fig. 2.1 Open Channel Flow

The first equation states the principle of conservation of mass. The three terms in this equation physically represent, in their order of appearance, the time rate of change of storage, the spatial rate of change of discharge and the lateral flow.

The second equation states the law of conservation of linear momentum in the x direction. The physical meaning of each of the terms in this exact momentum equation will be discussed later in section 2.3.

Equations (2.1) and (2.2) can also be written alternatively in the form of Q and h or V and h (V is mean velocity of flow over cross-sectional area, A) by defining the discharge, Q, at a channel section as Q = VA and carefully dealing with the derivatives of area, A.

The proper expression of flow cross-sectional area, A, is

$$A = \int_0^h \zeta(x,Z)\, dZ \tag{2.3}$$

in which $\zeta(x,Z)$ is a width of an irregular cross section at point (x,Z) (Fig. 2.2 from Liggett, 1975).

By using the Leibnitz rule and assuming that the channel bed is nonerodiable, the time derivative of A is

$$\frac{\partial A}{\partial t} = \frac{\partial}{\partial t}\int_0^h \zeta(x,Z)\, dZ = \int_0^h \frac{\partial}{\partial t}\zeta(x,Z)\, dZ + \zeta(x,Z)\left.\frac{\partial Z}{\partial t}\right|_0^h$$

$$= \zeta(x,h)\frac{\partial h}{\partial t} = B\frac{\partial h}{\partial t}$$

in which B is the channel width at the water surface.

The x-derivative of A is slightly more complex

$$\frac{\partial A}{\partial x} = \frac{\partial}{\partial x}\int_0^h \zeta(x,Z)\ dZ = \int_0^h \frac{\partial}{\partial x}\zeta(x,Z)\ dZ + \zeta(x,Z)\ \frac{\partial Z}{\partial x}\Big|_0^h$$

The integral is often written as

$$\int_0^h \frac{\partial}{\partial x}\zeta(x,Z)\ dZ = \left(\frac{\partial A}{\partial x}\right)_h$$

Thus,

$$\frac{\partial A}{\partial x} = \int_0^h \frac{\partial}{\partial x}\zeta(x,Z)\ dZ + B\frac{\partial h}{\partial x} = \left(\frac{\partial A}{\partial x}\right)_h + B\frac{\partial h}{\partial x}$$

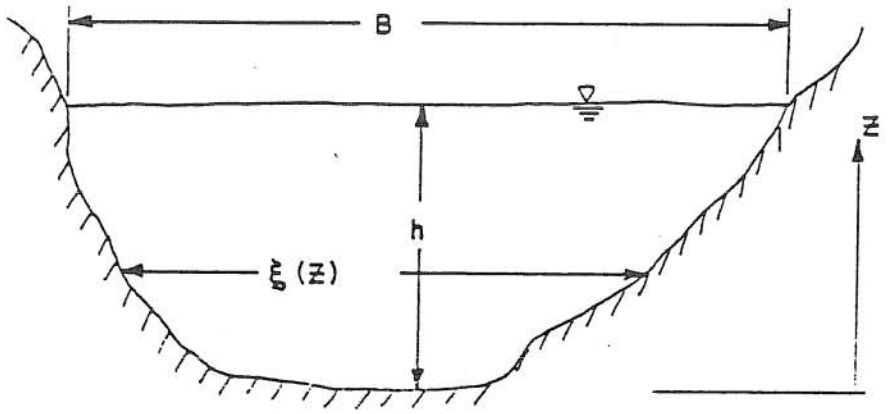

Fig. 2.2 Cross Section of a Channel of Arbitrary Shape

Yen (1973) mentioned that $(\partial A/\partial x)_h = 0$ only if the following assumptions are used: the channel bed is nonerodible or the time rate of change of bed profile is slow, and the channel is straight and prismatic. Thus, Eqs. (2.1) and (2.2) become:

$$\frac{\partial h}{\partial t} + \frac{1}{B}\frac{\partial Q}{\partial x} = \frac{q_L}{B} \tag{2.4}$$

$$\frac{1}{gA}\frac{\partial Q}{\partial t} + \frac{1}{gA^2}\left(\beta\frac{\partial Q^2}{\partial x} + Q^2\frac{\partial \beta}{\partial x} - \frac{\beta Q^2 B}{A}\frac{\partial h}{\partial x}\right) + h\cos\theta\frac{\partial k}{\partial x}$$

$$+ k\frac{\partial}{\partial x}(h\cos\theta) + (k-k')\frac{B h\cos\theta}{A}\frac{\partial h}{\partial x} = S_0 - S_f + \frac{1}{\gamma A}\frac{\partial T}{\partial x} + \frac{q_L U_x}{gA} \tag{2.5}$$

or

$$\frac{\partial h}{\partial t} + \frac{A}{B}\frac{\partial V}{\partial x} + V\frac{\partial h}{\partial x} = \frac{q_L}{B} \tag{2.6}$$

$$\frac{1}{g}\frac{\partial V}{\partial t} + \frac{V^2}{g}\frac{\partial \beta}{\partial x} + (2\beta - 1)\frac{V}{g}\frac{\partial V}{\partial x} + h\cos\theta\frac{\partial k}{\partial x}$$

$$+ k\frac{\partial}{\partial x}(h\cos\theta) + \left[(\beta - 1)\frac{V^2}{g} + (k - k')h\cos\theta\right]\frac{B}{A}\frac{\partial h}{\partial x}$$

$$= S_0 - S_f + \frac{1}{\gamma A}\frac{\partial T}{\partial x} + \frac{q_L(U_x - V)}{gA} \tag{2.7}$$

Eqs. (2.4) and (2.5) are in the so-called conservation form since the discharge, Q, is regarded as conservational, and Eqs. (2.6) and (2.7) are in the so-called nonconservation form.

2.2. Physical Meaning and Values of Coefficients Involved in Exact Momentum Equation

In the exact momentum equation, Eq. (2.2), the most important coefficients, which may produce an influence on the solutions of Eqs. (2.1) and (2.2), are ß, k and k'.

2.2.1. Momentum Flux Correction Coefficient or Boussinesq Coefficient

The momentum flux correction coefficient or Boussinesq coefficient, ß, reflects the extent of the nonuniform distribution of velocity over a cross-section. In 1877, Boussinesq first proposed it. It is defined as

$$ß = \frac{\int_A u^2 \, dA}{V^2 \, A} \approx \frac{\Sigma \, u^2 \Delta A}{V^2 \, A} \tag{2.8}$$

in which u is the local point velocity, A is the cross-sectional area and V is the mean velocity over A.

Yen (1973) defined ß as a tensor and expressed it as

$$ß_{nij} = \frac{\int_A \bar{\rho} \, \bar{u}_i \, \bar{u}_j \, dA}{\rho_a \, V_i \, V_j \, A} \tag{2.9}$$

in which ρ_a is the cross-sectional mean fluid density, u_i and u_j are the instantaneous local velocity component along the ith or jth direction, V_i and V_j are the mean velocity component along the ith or jth direction, and the quantities with bar, $\bar{\rho}$, $\bar{u}_i$, $\bar{u}_j$, represent temporal averaging over turbulent fluctuation.

The value of ß can be obtained from measured velocity distribution. It is obvious that when the velocity distribution is strictly uniform across the channel section, the value of ß is equal to unity.

Kolupaila (1956) suggested the values of ß for practical purposes as listed in Table 2.1.

Table 2.1 Values of ß for Various Channels

Channels	Value of ß		
	Min	Average	Max
Regular channel, flumes, spillways	1.03	1.05	1.07
Natural streams and torrents	1.05	1.10	1.17
Rivers under ice cover	1.07	1.17	1.33
River valleys, overflooded	1.17	1.25	1.33

Chow (1959) wrote that for channels with regular cross section and fairly straight alignment, the effect of nonuniform velocity distribution on the computed velocity head and momentum is small. Therefore, ß is often assumed to be unity. In general, the value of ß for fairly straight prismatic channels varies approximately from 1.01 to 1.12. For channels with complex cross section ß may exceed 1.2 and can vary quite rapidly from section to section in case of irregular alignment. In addition, ß is usually greater in steep channels than in mild channels.

Henderson (1966) mentioned that the value of ß is never less than unity, and the further the flow departs from uniform, the greater the value of ß becomes.

Yen (1973) gave the value of ß as follows: (a) ß = 1 for constant density and uniform velocity distribution over A or for two-dimensional flow with uniform velocity distribution and linearly varying density over depth. (b) ß = 1.20 for a parabolic velocity distribution. (c) ß = 1.33 for linearly varying velocity over depth.

In addition, for extremely nonuniform velocity distribution ß can reach a very large value. An example is a channel with narrow and deep cross-sectional shape and large roughness. Because of the influence of resistance of the sides and bed of the channel on the flow velocity and low location of the maximum velocity, the velocity distribution becomes very nonuniform, thus, the value of ß may be much greater than 1.33.

2.2.2. Piezometric Pressure Correction Coefficient

The piezometric pressure correction coefficient, k, accounts for pressure variation on the flow cross section. It is a function of pressure distribution and the cross-sectional shape and is not a function of velocity distribution.

Yen (1973) defined it as

$$k = \frac{\int_A \overline{P}\, dA}{\gamma_a\, A\, h\, \cos\theta} \qquad (2.10)$$

in which h is the mean depth of flow and averaged over turbulent fluctuation, γ_a is the cross-sectional average specific weight of the fluid, P is the local piezometric pressure, and θ is the angle between the channel bed and a horizontal plane.

Chow (1959) wrote that the application of the hydrostatic law to the pressure distribution in the cross section of a flowing channel is valid only if the flow filaments have no acceleration components in the plane of cross section. This type of flow is theoretically known as parallel flow. Uniform flow is a parallel flow. Gradually varied flow is not this kind of flow, but it is

so mild that the streamlines can be assumed to have neither appreciable curvature nor divergence. Therefore, for practical purposes, the hydrostatic law of pressure distribution is applicable to gradually varied flow as well as uniform flow. For curvilinear flow, the pressure distribution over the section deviates from the hydrostatic. Thus, the hydrostatic law of pressure distribution is not valid. For example, in concave flow the centrifugal forces are pointing downward to reinforce the gravity action; so the resulting pressure is greater than the hydrostatic pressure of a parallel flow. In convex flow the centrifugal forces are acting upward against the gravity action; the resulting pressure is less than the hydrostatic pressure of a parallel flow. In order to account for this deviation from hydrostatic, the piezometric pressure correction coefficient, k, is introduced as a correction for curvilinear flows. It can easily be seen that the value of k is greater than 1.0 for concave flow, less than 1.0 for convex flow, and equal to 1.0 for parallel flow.

Yen (1973) gave the value of k as follows: (a) $k = 1$ for constant density fluid and hydrostatic pressure distribution over A or constant piezometric pressure over A. (b) $k = \rho_h/\rho_a$ for constant piezometric pressure over A, in which ρ_a is the cross-sectional mean fluid density and ρ_h is the mean fluid density along the depth of flow, h.

Chow (1959) introduced a simplified formula to calculate the piezometric pressure correction coefficient as

$$k = 1 + \frac{1}{Qh} \int_A c' u \, dA \approx 1 + \frac{v^2}{gr_k} \qquad (2.11)$$

in which Q is discharge, A is flow cross-sectional area, u is the local point velocity of flow, V is the mean velocity, h is depth of flow, g is gravitational acceleration, r_k is the radius of curvature of channel bottom, and c' is the pressure-head correction with a dimension of length (c' is defined approximately as hu^2/gr_k and is positive for concave flow, negative for convex flow, and zero for parallel flow). From Eq. (2.11) the value of k can be roughly estimated. The relationship between k and the radius of curvature for different mean flow velocities is demonstrated in Fig. 2.3. In general, the closer to unity the value of k, the

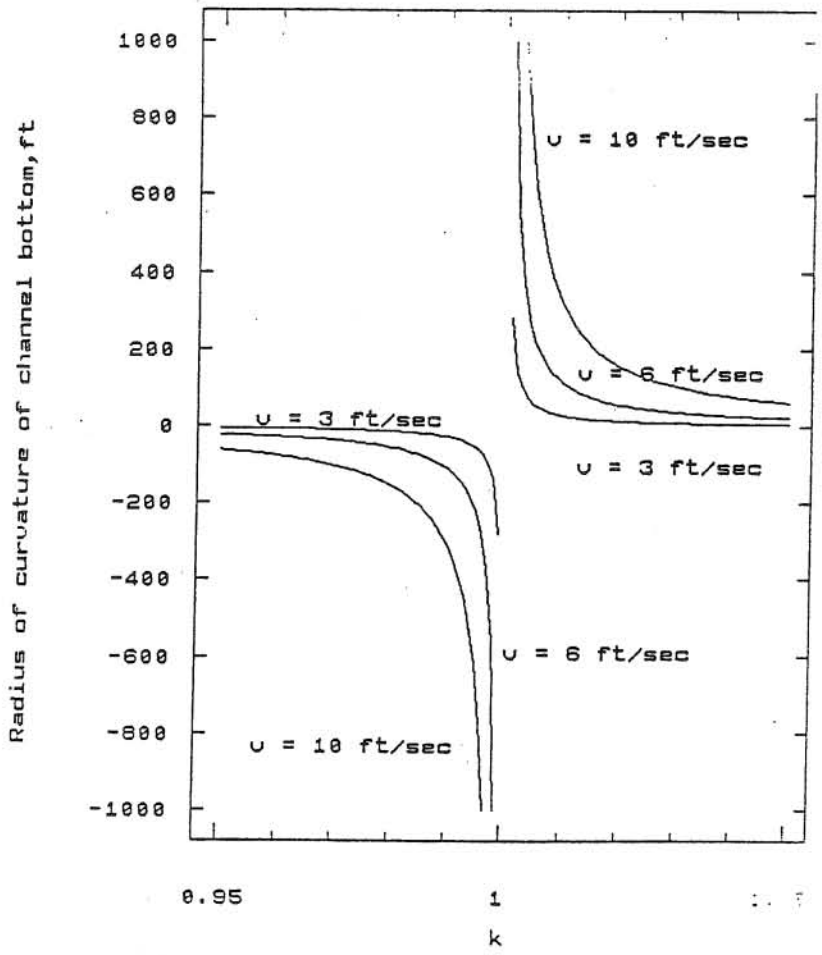

Fig. 2.3 Relationship between k and Radius of Curvature

larger the magnitude of the radius of curvature of channel bottom, i.e., the flatter the channel bed. Furthermore, the value of k deviates appreciably from unity when the flow velocity is high. Figure 2.3 shows that for the same radius of curvature, the larger the flow velocity, the further the value of k departs from unity. From Fig. 2.3, if the mean velocity, V, is assumed as 6 ft/sec, the radius of curvature, r_k, corresponding to the case of k = 1.05 (or 0.95) and the case of k = 1.01 (or 0.99) is equal to 22.5 ft and 111.9 ft, respectively. The values of r_k reflect that the cases of k = 1.05 and 0.95 can be encountered only in unusual situations, for example, spillways or channels with sharply curved bottom, whereas the cases of k between 1.01 and 0.99 are more common.

2.2.3. Ambient Piezometric Pressure Correction Coefficient

The ambient piezometric pressure correction coefficient, k'_{ni}, reflects the effect of the ambient pressure when there is a spatial change in flow cross section, i.e., nonuniform flow.

Yen (1973) defined it as

$$k'_{ni} = \frac{-\int_{\sigma} \left(\bar{P}\frac{\partial \bar{r}}{\partial x_i} + \overline{P'\frac{\partial r'}{\partial x_i}}\right) d\sigma}{\gamma_a h \cos\theta \frac{\partial A}{\partial x_i}} \qquad (2.12)$$

in which σ is the perimeter bounding cross-sectional area A, r is the normal displacement of σ with respect to space or time, and P' and r' represent the turbulent fluctuation of P and r with respect to its mean value, $\bar{P}$ and $\bar{r}$, respectively.

For constant density and hydrostatic pressure distribution over nonfluctuating A and σ, the value of k' is equal to unity.

2.2.4. Further Remarks

From the preceding sections 2.2.1 to 2.2.3, it is realized that only for some special situations ß, k and k' are equal to unity or can be approximated as unity, and at this time the exact momentum equation becomes the well-known dynamic wave equation if the internal stresses and lateral flow are not considered. For complicated cases, ß, k and k' are not equal to unity. Therefore, two questions arise: if there exists a difference in the solutions between the exact momentum equation and the complete dynamic wave equation with simplifying assumption of ß, k and k' being unity, and, if yes, how much is the difference.

In addition, it should be considered that the variations of ß, k and k' are simultaneous, i.e., while one coefficient varies other coefficients must vary. For example, Figure 2.4 shows that a free overfall occurs where the bottom of a flat channel is discontinued. The velocity distribution is uniform and pressure distribution is hydrostatic at the position very far from the downstream brink. However, as the flow approaches the brink, the pressure distribution becomes nonhydrostatic, and the value of k should be less than unity. Finally, at the brink, the pressure distribution is a bow because the free overfall enters the air in the form of a nappe and the pressure on the upper or lower surface of the nappe should be equal to zero. Thus, k varies from unity to a magnitude less than unity along the channel. At this time,

because of the free overfall the velocity of flow increases along the channel from upstream to the brink, and the value of ß should become gradually greater than unity. Therefore, this example shows that in this study, only varying one coefficient while keeping other coefficients constant is only a hypothetical and fundamental investigation.

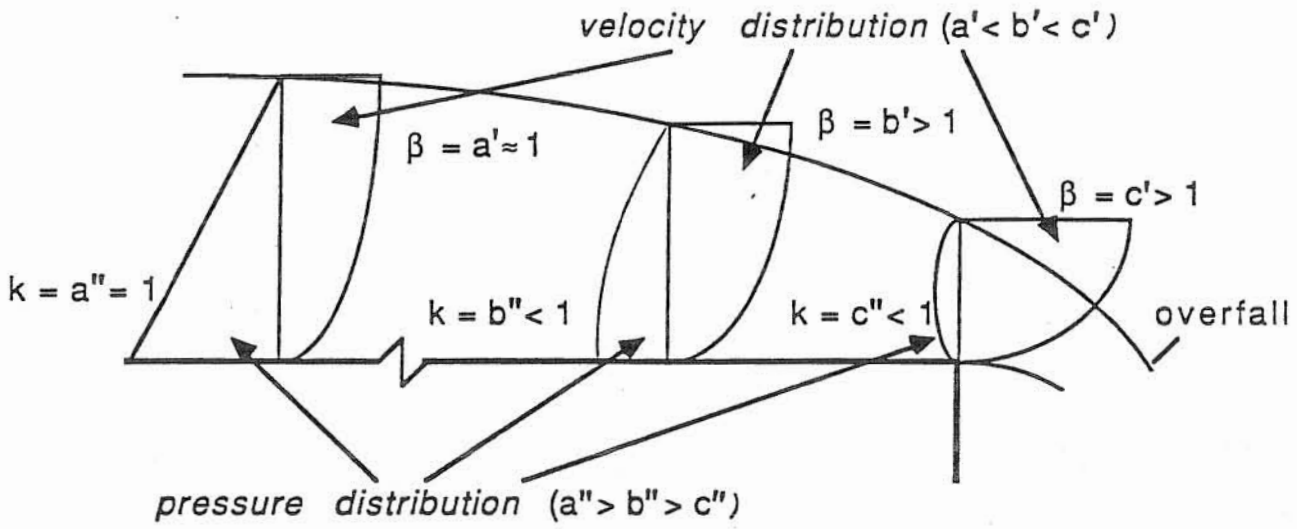

Fig. 2.4 Example for Variations of ß and k

2.3. Physical Meaning of Terms Involved in Exact Momentum Equation

There are seven terms in the exact momentum equation, Eq. (2.2). They are the local acceleration, convective acceleration, pressure term, channel slope, friction slope, internal stress term, and lateral flow. In addition, the variables $\partial\beta/\partial x$ and $\partial k/\partial x$ will also be discussed in this section.

2.3.1. Local Acceleration

The local acceleration, $\partial Q/\partial t$, represents the rate of time change of momentum flux. For steady flow, this term is equal to

zero. For unsteady flow, if an acute change occurs in Q during a short period of time this term may reach a large value. For example, when flow controlling structures are quickly operated, when a dam is broken down, and when a heavy rain falls on a small watershed this term is significant.

2.3.2. Convective Acceleration

The convective acceleration, $\partial(\beta Q^2/A)/\partial x$, represents the rate of spatial change of momentum flux. The value of this term is equal to zero for uniform flow. For gradually varying flow, since the change in depth is gradual and the streamlines are nearly parallel, i.e., the curvature of streamlines is mild, the value of this term could be small. But, for spatially rapidly varying flow the curvature of streamlines can be very large and the flow profile may become virtually discontinuous. Therefore, the flow depth, the flow velocity and the velocity distribution may significantly vary in a short distance and the value of this term may become very large. Examples include flow over a weir or dam, flow in curved or bent rivers and channels, propagation of surge or bore due to dam break or other reasons, and flow in nonprismatic channels, particularly, with sudden contractions or expansions vertically, horizontally, or both. For such cases, the sudden change of flow depth and flow velocity will lead to significant convective acceleration.

2.3.3. Pressure Term

The pressure term, $\partial(khcos\theta)/\partial x + [(k-k')hcos\theta/A]\partial A/\partial x$, is composed of two portions: $\partial(khcos\theta)/\partial x + (khcos\theta/A)\partial A/\partial x$ represents the rate of spatial change of the piezometric pressure acting on the cross section; $(k'hcos\theta/A)\partial A/\partial x$ represents the component of the force due to the mean and fluctuating ambient piezometric pressure acting on the boundary surface.

The value of this term is zero for steady uniform flow. For gradually varied flow, since the pressure distribution is assumed to be hydrostatic, the flow depth, the pressure distribution, and two correction coefficients, k and k', do not change very significantly in a short reach, so the value of this term could be small. For rapidly varied flow, the situation is just opposite, therefore, the value of this term becomes large. The value of the pressure term is also related to the channel slope and downstream boundary condition. Under certain conditions, for example, when the channel slope is relatively mild and there is a downstream backwater effect, this pressure term may become more important.

As to a comparison of values of the aforementioned three terms, generally speaking, the magnitude of the local acceleration is of the same order as that of the convective acceleration and their signs usually are opposite; while the two acceleration terms are smaller than the pressure term. In this study, because the values of the coefficients, ß, k and k', are considered not necessarily equal to unity, the magnitudes of the convective acceleration term and the pressure term could vary with the values of ß, k and k'. It is possible that for a certain combination of

ß, k and k' the convective acceleration term becomes relatively important when compared to the pressure term.

2.3.4. Channel Slope

The channel slope, S_0, represents the component of the gravitational force. With the x direction defined along the channel bed, the angle between the channel bed and a horizontal plane is θ, and $S_0 = \sin\theta$. In general, S_0 is variable for rivers and natural conveyance channels. But it is conventionally assumed that S_0 is independent of t. Its value can be obtained by direct measurement. In this study, the choice of the value of S_0 obeys the following rule: the flow remains subcritical. The reason is that for supercritical flow, because the velocity of flow is very high the free water surface in the channel becomes very unstable, and supercritical flow will break into a series of roll waves or slugs, known as pulsating flow. However, the exact momentum and continuity equations do not contain terms specifically considering the phenomenon of pulsating flow.

2.3.5. Friction Slope

The friction slope, S_f, accounts for the resistance due to external boundary shear stresses in the x direction. It is defined as (Yen and Wenzel, 1970 and Yen et al., 1972)

$$S_f = \int_\sigma \frac{\tau_x}{\gamma R} \, d\sigma \qquad (2.13)$$

in which τ_x is the effective boundary shear stress in the x-direction, γ is specific weight of the fluid, R is the hydraulic radius and σ is the perimeter bounding the cross-sectional area A.

From the expression it is clear that if the boundary shear stress, τ_x, is directly measured or computed from the velocity profile in the inner-law region and if R is known, the value of S_f can be calculated. However, τ_x is usually not available and S_f has to be estimated by other means. In common practice, the frictional resistance is assumed to be the same as that of the steady uniform flow at the same depth and velocity, i.e., assuming S_f is equal to S in each of the following Manning, Chezy, and Weisbach resistance formulas

$$S = \frac{n^2 V^2}{2.21 R^{4/3}} \tag{2.14}$$

$$S = \frac{V^2}{C^2 R} \tag{2.15}$$

$$S = \frac{f V^2}{8gR} \tag{2.16}$$

in which n is Manning's factor, C is Chezy's factor, and f is Weisbach's coefficient.

These formulas are based on the assumption of steady uniform flow; they do not truly represent the actual friction slope. However, satisfactory methods of evaluating the value of S_f have not yet developed. Thus, using the slope in the above three formulas as S_f is only an approximation. Approximations are

sometimes available. For example, Rouse (1965) mentioned that the effects and errors due to using the slope in the Manning, Chezy, and Weisbach equations as S_f are probably negligible when the flow is gradually varied. Yen and Wenzel (1970) studied steady spatially varied flow and demonstrated that for a certain given rainfall if the direct effect of the lateral flow in the momentum equation is negligible and if the assumption that ß is constant can be justified, S_f can be approximated by the Manning, Chezy, or Weisbach formula.

The values of Manning's n and Weisbach's f and the relationship between them have been well established for steady uniform flow of a homogeneous incompressible fluid. Yen (1973) wrote that from a theoretical viewpoint the Weisbach coefficient, f, is probably the most suitable in hydraulic analysis since f is dimensionless and can be found from the Moody diagram as a function of the Reynolds number and the relative boundary roughness. However, the validity of using the Moody diagram values for cases other than steady uniform flow has always been subject to question. Baltzer and Lai (1968) showed a variation of Manning's n obtained from a natural channel (Fig. 2.5). From Fig. 2.5, it is obvious that the value of n gradually tends to a small range as Reynolds number becomes large. Yen (1975 and 1986) suggested that for flows with sufficiently large Reynolds number over a rigid boundary with a given surface roughness in a prismatic channel, Manning's factor, n, is nearly constant over a wide range of depth. Thus, the Manning equation is introduced to represent friction slope, S_f, and n is treated approximately as a constant in this study.

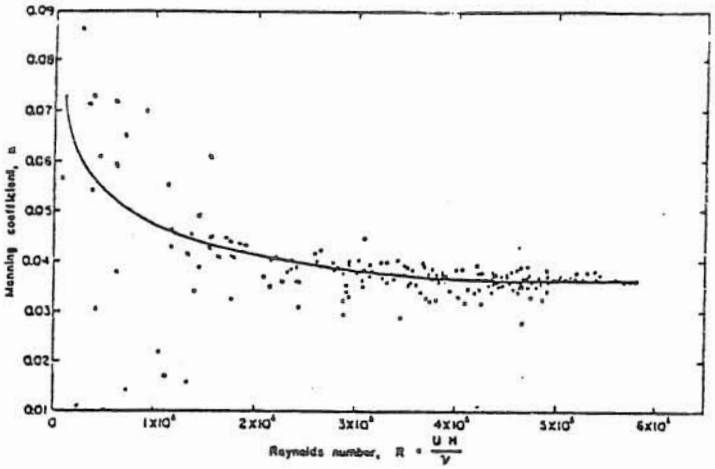

Fig. 2.5 Manning n vs. Reynolds Number for Three-mile Slough near Rio Vista, California (From Baltzer and Lai)

2.3.6. Internal Stresses

The internal stress term, $(1/\gamma A)\partial T/\partial x$, represents the rate of spatial change of the internal deformation stresses of the mean motion acting on the cross section. Yen (1973) defined the force, T_{ij}, due to internal stresses as

$$T_{ij} = \int_A \bar{\tau}_{ij} \, dA \qquad (2.17)$$

in which τ_{ij} is the deformation stresses and the bar indicates averaging over turbulence.

The value of this term is related to the ratio between viscous stresses and Reynolds stresses. For fully developed turbulence, the internal stresses may be large. But, for most open channels the variation of the internal stresses with respect to the flow direction x, $\partial T/\partial x$, is relatively small. Therefore, the term is often neglected conventionally.

2.3.7. Lateral Flow

The lateral flow term, $q_L U_x/gA$, represents the momentum influx of the lateral flow. The value of q_L is positive for lateral inflow and negative for lateral outflow.

Lateral flow is an important phenomenon. It changes the discharge in the flow direction and alters the velocity distribution in the main flow section. But, due to time limitation this term is not considered in this study.

2.3.8. Rate of Spatial Change of ß and k

The term, $\partial ß/\partial x$, represents the rate of spatial change of the velocity distribution along the flow direction and it is a portion of the convective acceleration term.

According to section 2.2, the value of ß is probably related to the shape of the cross section, roughness of the channel (bed and banks), alignment of the channel (straight or curved), channel slope, sediment concentration, and depth of flow. Therefore, if any of these quantities has an abrupt change in a short distance, for example, the cross-sectional width of a channel is suddenly expanded or contracted, the value of ß varies and the variation leads to a significant magnitude of $\partial ß/\partial x$. In this study, for a one-dimensional, rigid, straight and prismatic open channel, the value of ß may be closely related to the flow depth if S_0 and n are approximately regarded as constants, and if the effect of sediment concentration is not considered. In addition, this study focuses on the gradually varying flow, i.e., the depth of flow varies only

gradually, thus, the change of the value of ß is also gradual. Therefore, $\partial ß/\partial x$ is small or negligible.

The term, $\partial k/\partial x$, represents the rate of spatial change of the pressure distribution of flow along the flow direction, and it is a portion of the pressure term. From the description of section 2.2, the value of k reflects the pressure distribution on a cross section. If the pressure distribution has an abrupt change in a short distance, for example, if the radius of curvature of the channel bottom is suddenly varied, the magnitude of $\partial k/\partial x$ could be large and not negligible. But, similar to ß, when one-dimensional, rigid, straight and prismatical channel and gradually varied flow are considered, the importance of $\partial k/\partial x$ is relatively small.

2.3.9. Further Remarks

According to the description of the preceding sections 2.3.1 through 2.3.7, it is without question that for various special situations some of the terms in the exact momentum equation can be safely neglected as compared to others. Many investigators studied the terms and provided valuable information. But, all the previous studies assumed ß, k and k' as unity. Therefore, it is necessary to compare the contributions of all the terms for other cases where ß, k and k' cannot be considered as equal to unity.

2.4. Approximations to Exact Momentum Equation

2.4.1. Saint-Venant Equations

Since the exact momentum equation is too complicated to solve and requires a considerable amount of detailed data, most

investigators have conveniently assumed the coefficients considered in the exact momentum equation to be constants, implicitly or explicitly involving the following assumptions:

(a) The pressure distribution over A is hydrostatic, hence $k = k' = 1$.

(b) The cross-sectional velocity distribution remains unchanged along the x direction, implying the momentum flux correction coefficient, β, remains a constant. Often it is assumed that the velocity distribution is uniform, hence $\beta = 1$.

(c) The spatial gradient of the force due to internal stresses is small, hence the $\partial T/\partial x$ term is negligible.

(d) The angle between the x direction and a horizontal plane, θ, is constant and independent of x, hence $\cos\theta$ is constant.

(e) There is no lateral flow, hence $q_L = 0$.

The result is the well-known dynamic wave equation which can be expressed in terms of either discharge, Q, or flow cross-sectional average velocity, V,

$$\frac{1}{gA}\frac{\partial Q}{\partial t} + \frac{1}{gA}\frac{\partial}{\partial x}\left(\frac{Q^2}{A}\right) + \frac{\partial h}{\partial x} - (S_0 - S_f) = 0 \qquad (2.18)$$

or

$$\frac{1}{g}\frac{\partial V}{\partial t} + \frac{V}{g}\frac{\partial V}{\partial x} + \frac{\partial h}{\partial x} - (S_0 - S_f) = 0 \qquad (2.19)$$

One of Eqs. (2.18) and (2.19) together with the continuity equation in either of the following two types

$$\frac{\partial A}{\partial t} + \frac{\partial Q}{\partial x} = 0 \qquad (2.20)$$

or

$$\frac{\partial h}{\partial t} + \frac{A}{B}\frac{\partial V}{\partial x} + V\frac{\partial h}{\partial x} = 0 \qquad (2.21)$$

form a pair of equations which are customarily referred to as the Saint-Venant equations and also called shallow water wave equations because flood-routing problems generally involve shallow waves, namely, the whole cross section of the body of water is disturbed by the shallow-water wave movement.

It is clear that these assumptions simplify the equations for solutions. But they do not precisely reflect the flow process.

2.4.2. Various simplified Approximations

Although the complete dynamic wave equation, Eq. (2.18) or Eq. (2.19), is simpler than the exact momentum equation, it together with the continuity equation and appropriately specified initial and boundary conditions, is still rather tedious and computationally costly to solve. Therefore, many investigators have tried to find alternative solution methods and acceptable simplifications of the complete dynamic wave equation.

There are different levels of approximation to the complete dynamic wave equation. By referring to Eqs. (2.18) or (2.19), if the local acceleration, $\partial Q/\partial t$ or $\partial V/\partial t$, is relatively small as compared to other terms, and hence dropped, the approximation is called a quasi-steady dynamic wave. If both the local and convective acceleration terms are dropped, the approximation is a noninertia model. If, in addition to dropping both inertia terms,

the pressure term, $\partial h/\partial x$, is also dropped by comparing it with the channel slope and friction slope the approximation is known as kinematic wave. All the approximations are illustrated in Fig. 2.6.

$$\frac{1}{gA}\frac{\partial Q}{\partial t} + \frac{1}{gA}\frac{\partial}{\partial x}\left(\frac{Q^2}{A}\right) + \frac{\partial h}{\partial x} - (S_0 - S_f) = 0$$

$$\frac{1}{g}\frac{\partial V}{\partial t} + \frac{V}{g}\frac{\partial V}{\partial x} + \frac{\partial h}{\partial x} - (S_0 - S_f) = 0$$

Kinematic wave

Noninertia

Quasi-steady dynamic wave

Complete dynamic wave

Fig. 2.6 Simplifications of Saint-Venant Equations

2.4.2.1. Kinematic Wave Approximation

The kinematic wave approximation is based on neglecting the acceleration and pressure terms in the complete dynamic wave equation. According to the finite difference form of the continuity equation, i.e., linearized or nonlinearized form, the kinematic wave approximation can be classified into a linear kinematic wave approximation and a nonlinear kinematic wave approximation. The kinematic wave is the simplest among the different approximations of the Saint-Venant equations. It requires only one boundary condition in addition to the initial condition. The lone boundary condition is specified at the upstream boundary, hence it enables the solution to disregard the

downstream boundary condition. The biggest disadvantage of the kinematic wave approximation is its ignorance of the downstream backwater effect.

In order to explain the disadvantage of the kinematic wave approximation, a prismatic channel is considered and a water surface stage, Z, which is equal to $h\cos\theta + z_d$ (z_d is the elevation of the channel bottom above a datum plane) is introduced herein, then the continuity equation can be written as

$$\frac{\partial Z}{\partial t} + \frac{A}{B}\frac{\partial V}{\partial x} + V\frac{\partial Z}{\partial x} + VS_0 = 0 \qquad (2.22)$$

If the Chezy equation or the Manning equation is used to describe the friction slope, the kinematic wave approximation, i.e., $(S_f - S_0) = 0$, can be written as

$$\frac{V^2}{C^2 R} - S_0 = 0 \qquad (2.23)$$

or

$$\frac{V^2 n^2}{2.21 R^{4/3}} - S_0 = 0 \qquad (2.24)$$

in which R is the hydraulic radius, C is Chezy factor, and n is Manning resistance factor. The two equations can be used to determine the rate of change of velocity with respect to water surface elevation, i.e., dV/dZ. Furthermore, the continuity equation can be written as

$$\left(\frac{A}{B}\frac{dV}{dZ} + V\right)\frac{\partial Z}{\partial x} + \frac{\partial Z}{\partial t} = -VS_0 \qquad (2.25)$$

and the total differential of water surface elevation can be considered as

$$\frac{dZ}{dt} = \frac{dx}{dt}\frac{\partial Z}{\partial x} + \frac{\partial Z}{\partial t} \tag{2.26}$$

Thus, an expression of the kinematic wave speed can be obtained

$$c = \frac{dx}{dt} = \frac{A}{B}\frac{dV}{dZ} + V \tag{2.27}$$

and the characteristic form of the kinematic wave equation can be derived as

$$\frac{dZ}{dt} = - VS_0 \tag{2.28}$$

Whereas the Saint-Venant equations possess two characteristic directions (Chow, 1959, pp. 587-588; Henderson, 1966, pp. 288-289), the kinematic wave equation possesses only one characteristic direction. Therefore, it is clear that kinematic waves can travel only downstream and, consequently, the kinematic wave approximation cannot consider the influence of any downstream control.

Furthermore, the kinematic wave approximation has no mechanism to attenuate the flood peak. Results of numerical solution often indicate attenuation and distortion of a flood wave, however, this apparent attenuation and distortion is actually due to inaccuracy of the finite difference approximation. In other words, it is a numerical damping rather than a physical damping of the flood waves.

2.4.2.2. Noninertia Approximation

The noninertia approximation, a more appropriate name than the often used misnomer diffusion wave, neglects only the two acceleration terms, so it is a significant improvement over the kinematic wave approximation. It allows the specification of a boundary condition at the downstream to account for the backwater effect. Therefore, the noninertia approximation has wide application potential. Keefer (1974) compared the noninertia model with the complete dynamic wave model and confirmed that the two models produce similar results, but the noninertia model is simpler than the complete dynamic wave model. Akan and Yen (1977 and 1981) also demonstrated that this model is nearly as accurate as the dynamic wave model and as efficient in computer time as the kinematic wave model for routing flow in open channels. In addition, Akan and Yen (1977 and 1981) and Katopodes (1982) demonstrated that the noninertia model possesses the ability of accounting for the downstream backwater effect.

The advantage of the noninertia approximation accounting for the downstream backwater effect can be explained by considering a prismatic channel and introducing a water surface stage, $Z = h\cos\theta + z_d$. The continuity equation and momentum equation can be written respectively as

$$\frac{\partial Z}{\partial t} + \frac{A}{B}\frac{\partial V}{\partial x} + V\frac{\partial Z}{\partial x} + VS_0 = 0 \qquad (2.29)$$

$$\frac{\partial Z}{\partial x} = -S_f \qquad (2.30)$$

By writing first the sum, and then the difference, of Eqs. (2.29) and (2.30), two new equations are obtained:

$$\frac{\partial Z}{\partial t} + \frac{A}{B}\frac{\partial V}{\partial x} + (V+1)\frac{\partial Z}{\partial x} = -VS_0 - S_f \qquad (2.31)$$

$$\frac{\partial Z}{\partial t} + \frac{A}{B}\frac{\partial V}{\partial x} + (V-1)\frac{\partial Z}{\partial x} = -VS_0 + S_f \qquad (2.32)$$

or

$$\frac{\partial Z}{\partial t} + \left(\frac{A}{B}\frac{dV}{dZ} + (V+1)\right)\frac{\partial Z}{\partial x} = -VS_0 - S_f \qquad (2.33)$$

$$\frac{\partial Z}{\partial t} + \left(\frac{A}{B}\frac{dV}{dZ} + (V-1)\right)\frac{\partial Z}{\partial x} = -VS_0 + S_f \qquad (2.34)$$

By comparing Eqs. (2.33) and (2.34) with the basic equations of partial differentiation, namely

$$dZ = \frac{\partial Z}{\partial t}\,dt + \frac{\partial Z}{\partial x}\,dx \qquad (2.35)$$

$$\frac{dZ}{dt} = \frac{\partial Z}{\partial t} + \frac{dx}{dt}\frac{\partial Z}{\partial x} \qquad (2.36)$$

the expressions of two possible wave speeds can be obtained as

$$c^+ = \frac{dx}{dt} = \frac{A}{B}\frac{dV}{dZ} + (V + 1) \qquad (2.37)$$

$$c^- = \frac{dx}{dt} = \frac{A}{B}\frac{dV}{dZ} + (V - 1) \qquad (2.38)$$

Physically, this means that a disturbance will propagate in both the upstream and downstream directions. Therefore, this approximation is closer to reality than the kinematic wave for which the disturbance propagates only along the c^+ direction downstream.

2.4.2.3. Quasi-steady Dynamic Wave Approximation

The quasi-steady dynamic wave approximation ignores the local acceleration term in the Saint-Venant equations. It differs from the noninertia approximation by including the convective acceleration term in the momentum equation. Under certain conditions the convective acceleration term is important, such as long duration, small amplitude flood waves propagating in highly nonuniform open channels where the local acceleration is small as compared to the convective acceleration and hence it can be neglected, whereas the convective acceleration cannot be ignored.

2.4.2.4. Further Remarks

In order to further understand the aforementioned various approximations, some major features of a theoretical comparison of the quasi-steady dynamic wave, noninertia and kinematic wave models are depicted in Table 2.2 (Yen, 1986). Based on this table and the description of the sections 2.4.2.1 through 2.4.2.3, the noninertia model appears to be simpler than the complete dynamic wave, more realistic than the kinematic wave and more accurate than the quasi-steady dynamic wave.

Table 2.2 Theoretical Comparison of Approximations to Complete Dynamic Wave Equation

	Kinematic wave	Noninertia model	Quasi-steady dynamic wave
Boundary condition required	1	2	2
Account for downstream backwater effect and flow reversal	NO	YES	YES
Damping of flood peak	NO	YES	YES
Account for flow acceleration	NO	NO	Only convective acceleration
Solution accuracy	Depend on Δx and Δt used		Usually less accurate than noninertia

3. BRIEF LITERATURE REVIEW

The exact momentum equation together with the continuity equation describes the propagation of flood waves more exactly than the Saint-Venant equations. However, because the exact momentum equation is very complicated and was proposed relatively recently, no work has been done towards its solution. Since the beginning of the century, many investigators working in this area have contributed to solving the Saint-Venant equations. How to efficiently, accurately, and economically solve Saint-Venant equations is always an important research subject. Therefore, it will be helpful to review previous work in the field. Because related literature abound (e.g., Miller and Yevjevich, 1975) only selected studies are mentioned here.

Due to the nonlinear nature of the Saint-Venant equations it is impossible to obtain an explicit analytical solution to the flood propagation problem. Therefore, various methods to acquire approximate solution have been attempted. These methods can be divided into two categories:

(a) analytically applying a linearized form of the equations and simplified boundary conditions;

(b) numerically applying the finite difference approximations of the nonlinear form of the equations by using digital computers.

3.1. Analytical Solutions

All the methods of analytical solutions proposed by previous investigators used the Saint-Venant equations as the basic

equations, and often assumed $\beta = 1$ and $k = k' = 1$. They also involved at least the following assumptions (Sevuk, 1973) to reduce the Saint-Venant equations to a mathematically amenable form:

(a) linearization of the Saint-Venant equations by using a reference flow condition, for example, V_0 or q_0 and h_0 of a steady uniform condition, and by introducing small perturbations in the velocity $V = V_0 + V'$ or the discharge $q = q_0 + q'$, and the flow depth $h = h_0 + h'$;

(b) relaxation of the downstream boundary condition;

(c) assumption of a constant resistance factor for Manning's n, Weisbach's f or Chezy's C;

(d) a constant cross section of the channel, usually wide rectangular.

With these assumptions, after the Saint-Venant equations are linearized, the equations can be reduced to a second-order linear partial differential equation which can be integrated analytically. The attractiveness of an analytical solution is that quantities can be obtained directly from the analytical solution. The disadvantages of an analytical solution are the severe limitations on the conditions for which the solution is valid and results from the analytical solution of the simplified equations can only be regarded as approximate. Thus, analytical methods are not used to solve the exact momentum equation in this study. But they are useful in verifying the numerical solutions for some special conditions.

3.1.1. Complete Dynamic Wave Model

The Saint-Venant equations without lateral flow can be written as

$$\frac{\partial A}{\partial t} + \frac{\partial Q}{\partial x} = 0 \tag{3.1}$$

$$\frac{1}{gA}\frac{\partial Q}{\partial t} + \frac{1}{gA}\frac{\partial}{\partial x}\left(\frac{Q^2}{A}\right) + \frac{\partial h}{\partial x} - (S_0 - S_f) = 0 \tag{3.2}$$

The friction slope, S_f, is related to the discharge by

$$Q = AC_f R^m \sqrt{S_f} \tag{3.3}$$

in which C_f is a factor and m is an exponent. When the Chezy formula is used, C_f = C (Chezy factor) and m = 0.5. When the Manning formula is used, C_f = 1.486/n (n is Manning's resistance factor) and m = 2/3. When the Weisbach formula is used, $C_f = (8g/f)^{0.5}$ (f is Weisbach's coefficient) and m = 0.5.

For a wide rectangular channel with small channel slope, the discharge per unit width q = Q/B and area A = Bh, where B is the width of the cross section at the free surface. Furthermore, the hydraulic radius, R, can be approximated by the depth h when the channel is wide rectangular. Hence, Eqs. (3.1) and (3.2) can be written for a unit width as

$$\frac{\partial h}{\partial t} + \frac{\partial q}{\partial x} = 0 \tag{3.4}$$

$$h^2\frac{\partial q}{\partial t} + 2hq\frac{\partial q}{\partial x} + (gh^3 - q^2)\frac{\partial h}{\partial x} - gh^3\left(S_0 - \frac{q^2}{C_f{}^2 h^{2(1+m)}}\right) = 0 \tag{3.5}$$

By assuming C_f independent of t and x, differentiation of Eq. (3.5) with respect to time t, aided with Eq. (3.4), yields a nonlinear second-order partial differential equation as follows:

$$(gh - V^2)\frac{\partial^2 q}{\partial x^2} - 2V\frac{\partial^2 q}{\partial x \partial t} - \frac{\partial^2 q}{\partial t^2} - 3gS_0\frac{\partial q}{\partial x} - \frac{(6m-3)gV^2}{3C_f{}^2h^{2m}}\frac{\partial q}{\partial x}$$

$$- \frac{2gV}{C_f{}^2h^{2m}}\frac{\partial q}{\partial t} + 3g\frac{\partial h}{\partial x}\frac{\partial q}{\partial x} + \frac{2V}{h}\left(\frac{\partial q}{\partial x}\right)^2 + \frac{2V}{h}\frac{\partial h}{\partial x}\frac{\partial q}{\partial t} = 0 \qquad (3.6)$$

By linearizing Eq. (3.6) about a reference discharge q_0, a reference velocity V_0 and a reference depth h_0, confining attention to a small range of fluctuations, q', (i.e., $q = q_0 + q'$) and assuming q_0 = constant, Eq. (3.6) can be reduced to the following linearized form

$$(gh_0 - V_0{}^2)\frac{\partial^2 q'}{\partial x^2} - 2V_0\frac{\partial^2 q'}{\partial x \partial t} - \frac{\partial^2 q'}{\partial t^2}$$

$$= 2(1+m)gS_0\frac{\partial q'}{\partial x} + \frac{2gS_0}{V_0}\frac{\partial q'}{\partial t} \qquad (3.7)$$

or

$$(1 - F_0{}^2)\frac{\partial^2 q'}{\partial x^2} - \frac{2F_0{}^2}{V_0}\frac{\partial^2 q'}{\partial x \partial t} - \frac{1}{gh_0}\frac{\partial^2 q'}{\partial t^2}$$

$$= 2(1+m)\frac{S_0}{h_0}\frac{\partial q'}{\partial x} + \frac{2S_0}{V_0 h_0}\frac{\partial q'}{\partial t} \qquad (3.8)$$

in which h_0 and V_0 indicate the values at the linearization discharge, q_0, and F_0 is equal to $V_0/\sqrt{gh_0}$.

The analytical solution of the second-order linear partial differential equation is often referred to as the complete linearized solution and was first obtained by Lighthill and Whitham (1955) and later generalized by Harley (1967).

Their solutions indicate that the center of mass of the flood wave travels at a wave velocity equal to $(1+m)V_0$. The front of the dynamic wave travels at a velocity $V_0 + \sqrt{gh_0}$ and the dynamic wave is rapidly damped out exponentially at a rate $[1 - (V_0/2\sqrt{gh_0})]$ (gS_0/V_0). The solution is valid for the situation of a wide rectangular channel, but errors will be created if it is used for a natural river or other channel shapes.

3.1.2. Noninertia Model

If the inertia terms in Eq. (3.2) are neglected, the momentum equation is simplified as

$$\frac{\partial h}{\partial x} = S_0 - S_f \tag{3.9}$$

When Eqs. (3.4) and (3.9) are treated in the same method of treating Eqs. (3.4) and (3.5), a nonlinear second order partial differential equation is obtained

$$\frac{\partial^2 q}{\partial x^2} = \frac{2q}{C_f{}^2 h^{2(1+m)}} \frac{\partial q}{\partial t} + \frac{2(1+m)q^2}{C_f{}^2 h^{(3+2m)}} \frac{\partial q}{\partial x} \tag{3.10}$$

By assuming the linearizing reference discharge q_0 or the reference depth h_0 to be constant, Eq. (3.10) is reduced to the following linearized form

$$\frac{\partial q'}{\partial t} + (1+m)V_0 \frac{\partial q'}{\partial x} = \frac{q_0}{2S_0} \frac{\partial^2 q'}{\partial x^2} \tag{3.11}$$

or

$$\frac{\partial h'}{\partial t} + (1+m)V_0 \frac{\partial h'}{\partial x} = \frac{q_0}{2S_0} \frac{\partial^2 h'}{\partial x^2} \tag{3.12}$$

in which $(1+m)V_0$ and $q_0/2S_0$ are designated as k_1 and k_2 and defined as a wave celerity and a wave dispersion coefficient, respectively. In general, $k_1 = (3/2)V_0$ if Chezy formula is used and $k_1 = (5/3)V_0$ if the Manning formula is used.

Equation (3.12) can also be derived in the following way: according to Eq. (3.9), the discharge for a wide channel can be expressed as

$$Q = BhC_f h^m \sqrt{\bar{s}_f} = BC_f h^{(1+m)} \left(S_0 - \frac{\partial h}{\partial x}\right)^{0.5} \tag{3.13}$$

Thus, differentiating Eq. (3.13) yields

$$\frac{\partial Q}{\partial x} = (1+m)\, BV \frac{\partial h}{\partial x} - \frac{BhV}{2(S_0 - \partial h/\partial x)} \frac{\partial^2 h}{\partial x^2} \tag{3.14}$$

By substituting Eq. (3.14) into Eq. (3.1), Eq. (3.15) is obtained as

$$\frac{\partial h}{\partial t} + (1+m)\, V \frac{\partial h}{\partial x} = \frac{hV}{2(S_0 - \partial h/\partial x)} \frac{\partial^2 h}{\partial x^2} \tag{3.15}$$

If $(S_0 - \partial h/\partial x)$ is approximately considered as s_0 and $h = h_0 + h'$ is introduced (h_0 is assumed as constant), Eq. (3.15) becomes Eq. (3.12).

The model, which was first formulated by Hayami (1951), was also called the diffusion wave and Eq. (3.10) was known as the diffusion-convection equation. However, Lighthill and Whitham (1955) derived the same type of diffusion-convection equation from the kinematic wave approximation. Therefore, for the sake of clarity, Yen (1986) suggested that the approximation of dropping both inertia terms of dynamic equation should be called the noninertia approximation.

Tingsanchali and Manandhar (1985) considered effects of channel irregularities and lateral flow and expressed the non-inertia equation as:

$$\frac{\partial h}{\partial t} + \frac{3}{2} V \frac{\partial h}{\partial x} = [K_d + \frac{hV}{2(S_0 - \partial h/\partial x)}] \frac{\partial^2 h}{\partial x^2} + q_L(x,t) \qquad (3.16)$$

in which K_d is diffusivity due to channel irregularities ($K_d = 0$ for a rectangular channel), V is flow mean velocity and is assumed to be equal to $C[h(S_0 - \partial h/\partial x)]^{0.5}$, C is Chezy roughness factor, $q_L(x,t)$ is lateral discharge per unit length of the tributary and per unit length of the main channel.

Tingsanchali and Manandhar (1985) developed the analytical noninertia model for flood routing with backwater effects and lateral flow. The noninertia equation is linearized about an average depth of (h_u+h_{ua}), in which h_u is uniform flow depth at the initial condition and h_{ua} is the average height of the water level above h_u, and solved by using boundary conditions which take into account the effects of backwater and lateral flow. The

applicability of the model is limited to slowly rising floods in which the effects of flow acceleration can be neglected, and to the flow case in which the Froude number is less than one-half. They found their result checked well with that obtained by the finite difference method using an implicit numerical scheme based on the Saint-Venant equations for unsteady open channel flow.

Wang and Yen (1987) expressed the noninertia equation for a wide rectangular channel as:

$$\frac{2S_0}{q_0}\frac{\partial q'}{\partial t} + \frac{3S_0}{h_0}\frac{\partial q'}{\partial x} = \frac{\partial^2 q'}{\partial x^2} \tag{3.17}$$

They further considered various cross sections, such as rectangular, trapezoidal and circular cross sections, and derived the different forms of the noninertia equation as follows:

For flow in a rectangular channel with width B

$$2B\frac{S_0}{Q_0}\frac{\partial Q'}{\partial t} + \left[\frac{3S_0}{h_0} - \frac{2S_0}{B}\left(\frac{1}{1 + 2h_0/B}\right)\right]\frac{\partial Q'}{\partial x} = \frac{\partial^2 Q'}{\partial x^2} \tag{3.18}$$

in which Q' is a small perturbation discharge. For flow in a trapezoidal channel with bottom width B and side slope z

$$\frac{2S_0}{Q_0}(2h_0 z + B)\frac{\partial Q'}{\partial t} + \left[\frac{3S_0}{h_0} - \frac{2S_0}{B}\left(\frac{1}{1 + 2h_0/B}\right) + \frac{3S_0 z}{B + zh_0}\right]\frac{\partial Q'}{\partial x} = \frac{\partial^2 Q'}{\partial x^2} \tag{3.19}$$

For flow in a circular channel with diameter D

$$\left[\frac{D}{2}\,\frac{\frac{\phi_0^2}{2!}-\frac{\phi_0^4}{4!}+\frac{\phi_0^6}{6!}-..}{\frac{\phi_0}{2}-\frac{\phi_0^3}{2^3 3!}+\frac{\phi_0^5}{2^5 5!}-..}\right]\frac{2S_0}{Q_0}\frac{\partial Q'}{\partial t}+$$

$$\frac{S_0\left[\frac{5\phi_0^4}{(3!)^2}+\frac{9\phi_0^8}{(5!)^2}+..-2\frac{7\phi_0^6}{3!5!}-2\frac{11\phi_0^{10}}{5!7!}-..\right]}{-\left[\frac{D}{4}\left(\frac{\phi_0}{2}-\frac{\phi_0^3}{2^3 3!}+\frac{\phi_0^5}{2^5 5!}-..\right)\left[\frac{\phi_0^5}{(3!)^2}+\frac{\phi_0^9}{(5!)^2}+..-2\frac{\phi_0^7}{3!5!}-..\right]\right]}\frac{\partial Q'}{\partial x}$$

$$=\frac{\partial^2 Q'}{\partial x^2} \qquad (3.20)$$

in which ϕ is central angle (in radians) of the free surface, Q_0 and ϕ_0 are reference discharge and corresponding central angle.

Wang and Yen (1987) considered an initial condition of a steady uniform flow and different boundary conditions, took the Laplace transformation of Eqs. (3.17) through (3.20), used means of convolution theorem, and obtained the analytical solutions of the model for various cross sections. The solutions are applicable to situations where the downstream backwater effect is significant, but are not applicable to supercritical flow.

3.1.3. Kinematic Wave Model

If both the inertia and pressure terms in Eq. (3.2) are neglected, the momentum equation is reduced to a kinematic wave equation

$$S_0 = S_f \qquad (3.21)$$

Equation (3.21) clearly demonstrates the distinguishing characteristic of the kinematic wave model, namely, instantaneously the discharge is always equal to the normal discharge, Q_n, and is thus a single-valued function of depth.

By combining Eqs. (3.3), (3.4) and (3.21) a nonlinear partial differential equation for a wide rectangular channel is obtained

$$\frac{\partial q}{\partial t} + \frac{(1+m)q}{h} \frac{\partial q}{\partial x} = 0 \tag{3.22}$$

Furthermore, by linearizing and assuming q_0 or h_0 = constant, a linearized form of the equation is

$$\frac{\partial q'}{\partial t} + (1+m)V_0 \frac{\partial q'}{\partial x} = 0 \tag{3.23}$$

or

$$\frac{\partial h'}{\partial t} + (1+m)V_0 \frac{\partial h'}{\partial x} = 0 \tag{3.24}$$

Equation (3.24) can also be derived in the following way: from Eq. (3.21), the discharge for a wide rectangular channel is expressed as

$$Q = AC_f R^m \sqrt{S_f} = BhC_f h^m \sqrt{S_0} = Q_n \tag{3.25}$$

Thus, differentiating Eq. (3.25) yields

$$\frac{\partial Q}{\partial x} = (1+m)\ BV_0 \frac{\partial h}{\partial x} \tag{3.26}$$

By substituting Eq. (3.26) in Eq. (3.1) and using $h = h_0 + h'$, Eq. (3.24) is obtained.

For the special case with initial condition

$$h'(x,0) = \sin \omega x \qquad (-\infty < x < \infty)$$

the solution of Eq. (3.24) is

$$h'(x,t) = \sin \omega(x - k_1 t)$$

The solution clearly indicates that the propagation of a sine wave with the kinematic-wave velocity or wave celerity k_1, will not produce any attenuation. In other words, a kinematic wave propagates downstream without dissipation and without considering the downstream boundary condition. Therefore, the model is applicable only to situations where the downstream backwater effect is insignificant.

The model was first introduced for flood-routing problems by Lighthill and Whitham (1955). Despite its deficiency of being unable to account for the downstream backwater effect, the kinematic wave model is the most extensively studied among the different approximations of the Saint-Venant equations.

3.2. Numerical Solutions

3.2.1. General Concept

Almost all the numerical models proposed by previous investigators are based on the Saint-Venant equations as a start. Numerical solutions of the Saint-Venant equations or their other simplified forms can be attempted by using various finite difference schemes which can be broadly classified into direct methods and characteristic methods. In the direct methods, finite

difference representation is based directly on primary equations. The direct methods can be classified into explicit and implicit methods. In the characteristic methods, the Saint-Venant equations are first transformed into a characteristic form, which is then used to develop the finite difference representation. The characteristic methods also can be classified further into explicit and implicit methods.

3.2.2. Direct Explicit Finite Difference Method

Isaacson et al. (1956) applied the direct explicit method to the movement of floods in the Ohio River. Subsequently, there have been many papers which used various computational schemes to solve various unsteady flow problems.

The explicit finite difference method is characterized by transforming the Saint-Venant equations into algebraic difference equations from which the unknowns are expressed explicitly as functions of known quantities, and are solved directly. According to the number and position of the grid points used in expressing the finite difference to approximate the derivatives, there are many different explicit schemes, for example, the unstable scheme, the diffusive scheme, L-shaped scheme, Leap-Frog scheme, Lax-Wendroff scheme, and Dronker's scheme. Details of some common schemes have been summarized by Lai (1986).

In general, explicit schemes are relatively easy to understand, easy to formulate, and easy to program. They provide the most direct solution. Unfortunately, they are also computationally highly inefficient because of numerical instability

problems. Even if a scheme is numerically stable, the solution may vary with the value of $\Delta t/\Delta x$ used, and often the accuracy is in doubt. To minimize the numerical instability most investigators have chosen their computational space and time intervals based on the Courant stability criterion

$$\Delta t \leq \frac{\Delta x}{V + \sqrt{gA/B}} \tag{3.27}$$

which does not necessarily guarantee the method to be stable. Because of the limitation on Δt for a selected Δx, the method becomes costly and thus impractical in routing long duration flood waves through a channel which has rapid variations in geometry requiring small distance increments Δx.

3.2.3. Direct Implicit Finite Difference Method

In the direct implicit finite difference method the Saint-Venant equations are transformed into a set of simultaneous algebraic difference equations and the unknowns are solved simultaneously by using an appropriate solution technique. The first detailed description of the implicit method was published by Richtmyer (1957). He applied an implicit scheme to heat propagation problems. Later, different implicit schemes, including four-point central scheme, non-central scheme, wide flange scheme, Tee scheme, Preissmann scheme, Vasilier scheme, and Abbott scheme, were developed. Various schemes for flood routing were discussed by Liggett and Cunge (1975) and Lai (1986).

Implicit schemes are more popular and generally preferred over explicit schemes because they allow large time steps and

reduce the computational effort. They are relatively more difficult and complicated to formulate and program, and require many more computations, but if done properly and carefully they can be computationally very efficient and stable. The finite difference computational grid sizes Δx and Δt, namely, space and time increments, can be chosen independently. But, there always is a numerical error as any finite difference approximation is applied and the error is a function of the space and time increments. In order to obtain the most accurate result from the implicit schemes, Price (1974) and Wormleaton and Karmegam (1984) suggested a criterion for selecting values of Δx and Δt when routing in a natural river, i.e., $\Delta x/\Delta t$ = the monoclinal wave velocity, V_w, which is approximately given by $V_w = 3Q/2A$ if the Chezy formula is used, or $V_w = 5Q/3A$ if the Manning formula is used. Price also gave a simple argument to demonstrate this criterion. Price (1985) further introduced a quantity, namely, constant attenuation parameter, Π, designated constant wave speed as ω, and summarized that for rivers Δt is usually defined such that $\Delta x > \Pi/\omega$ and for flood waves in artificial channels and storm sewers the choice of Δt may force Δx to be considerably less than Π/ω, so it is necessary to avoid inappropriate values of Δx and Δt. Implicit schemes are often quoted as numerically unconditionally stable. This statement is based on the linearized differential equation. For a nonlinear differential equation the numerical stability is, strictly speaking, not unconditional (Yen, 1986). For the case of extremely long reach in an open channel, even though the implicit scheme is stable it may converge to a wrong

answer because of an inaccurate representation of nonlinear terms (Wylie, 1970).

Among the numerous implicit schemes, Amein's four-point implicit scheme (Amein, 1968; Amein and Chu, 1975; Amein and Fang, 1970; Fread, 1971) has been shown to have the advantage of economy in computer time, accuracy, and stability under a wide range of time increments (Price, 1974; Ponce et al., 1978) and it has been applied to branched channels (Quinn and Wylie, 1972), surges in open channels (Chaudhry and Contractor, 1973), and rivers with tributaries (Fread, 1973). In this scheme the weighting factor, θ, which is used for time weighting, has been found to be important in the stability of numerical solutions. Its value ranges from zero to unity. Quinn and Wylie (1972) investigated the selection of θ and found that the numerical solution is strongly stable for values of θ given by $0.6 \leq \theta \leq 1.0$. Amein (1975) realized that the box scheme, i.e., $\theta = 0.5$, is accurate and stable for slowly varying flows. However, the box scheme produces numerical oscillations under certain transient conditions. Ponce (1978) pointed out that the weighting factor $\theta = 0.5$ is the 'theoretically better' value; however, it is impractical from the stability viewpoint. Joliffe (1984) wrote that experience has shown that for some flow simulations it is necessary to increase θ, from its lower limit, to ensure numerical stability. Amein (1975) presented a numerical model based on using $\theta = 1$ which makes the finite difference equations much simpler than those for $\theta = 0.5$. In a word, when the four-point implicit scheme is employed θ should be selected carefully.

3.2.4. Characteristic Method

In the characteristic method the Saint-Venant equations are transformed into four ordinary differential equations known as the characteristic equations

$$\frac{dx}{dt} = V + (g/F) = (V + c) = c^{+} \tag{3.28a}$$

$$\frac{dx}{dt} = V - (g/F) = (V - c) = c^{-} \tag{3.28b}$$

$$dV + Fdh = d(V+2c) = g(S_0 - S_f)dt \tag{3.29a}$$

$$dV - Fdh = d(V-2c) = g(S_0 - S_f)dt \tag{3.29b}$$

in which F is equal to $\sqrt{gB/A}$; c is equal to $\sqrt{gA/B}$; and c^{+} and c^{-} are the forward and backward characteristics, respectively.

The equations can be transformed into a finite difference form and solved numerically by using either implicit or explicit schemes with either the characteristic grid or a fixed rectangular grid. Presently, there are many different numerical schemes, but only some basic schemes are mentioned in next several sections. Furthermore, for the subject of the characteristic grid and a fixed rectangular grid, Wylie (1980) made an itemized comparison between them and summarized their advantages and disadvantages.

A number of papers have appeared in the past, in which characteristic methods were used for flood routing. The best known early characteristic method is the fixed mesh explicit method that was applied by Stoker (1953) to river flow problems. Later, the explicit characteristic method was applied to estuary flows by Lai (1965) and Baltzer and Lai (1968), and to the propagation of long

waves by Amein (1966). The implicit characteristic method was applied to streamflow routing by Amein (1968) and Fletcher and Hamilton (1967), and to overland flow by Liggett and Woolhiser (1967). Lai (1986, 1988) made a complete summary of the characteristic method.

The characteristic method is often considered to suit to a wide range of unsteady flow problems. It is more accurate than other numerical methods (Liggett and Woolhiser, 1967; Medowell, 1976). It deserves special attention because the close relationship between physical and mathematical properties makes this method a basic concept and tool in analyzing and understanding the complex problem of unsteady flow (Lai, 1986). It seems to handle relatively rapidly changing flows more effectively than other numerical methods (Lai, 1986). However, the characteristic method requires a large amount of interpolation and places a heavy demand on computer resources (Weinmann and Laurenson, 1979).

3.2.4.1. Courant Scheme

The scheme was first mentioned by Courant and Friedricks (1948). In this scheme a rectangular grid is imposed on the x-t plane as shown in Fig. 3.1. The value of the grid points A, M and

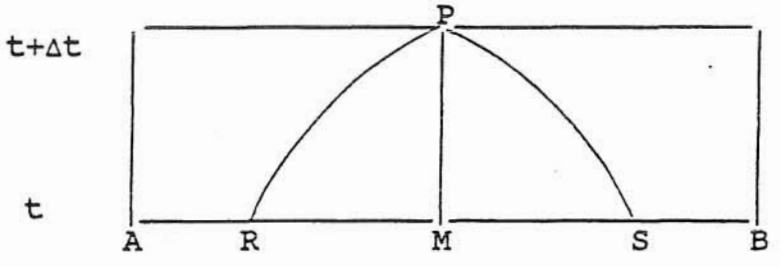

Fig. 3.1 Rectangular Computation Grid

B at a time t is known either as given initial values or as the results from previous computations. P is a grid point at time t + Δt where the solution will be sought.

The difference equations of Eqs. (3.28) and (3.29) are

$$x_P - x_R = (V + c)_M \, \Delta t \tag{3.30a}$$

$$x_P - x_S = (V - c)_M \, \Delta t \tag{3.30b}$$

$$V_P - V_R + F_M(h_P - h_R) = g(S_0 - S_f)_M \, \Delta t \tag{3.31a}$$

$$V_P - V_S - F_M(h_P - h_S) = g(S_0 - S_f)_M \, \Delta t \tag{3.31b}$$

It has been assumed that Δt is sufficiently small so that the characteristics PR and PS can be approximated by straight lines.

Generally speaking, the computative procedure is

(a) Determine the values of x_R and x_S by using Eq. (3.30).

(b) Compute the values of V_R, h_R, V_S and h_S by using linear interpolation between the adjacent grid points.

For point R and S, if U is used to represent the variables V or h the computative formulas are

$$U_R = U_M - \frac{U_M - U_A}{\Delta x} \quad (x_M - x_R) \tag{3.32}$$

and

$$U_S = U_M + \frac{U_M - U_B}{\Delta x} \quad (x_M - x_S) \tag{3.33}$$

If the flow condition is supercritical, Eq. (3.33) will become

$$U_S = U_M - \frac{U_M - U_A}{\Delta x} (x_M - x_S) \qquad (3.34)$$

(c) Obtain the unknown values of the V_P and h_P by using Eq. (3.31).

3.2.4.2. First-order Characteristic Scheme

The scheme was first described by Lin (1952) and Hartree (1952). Later, Lister (1960) made a more detailed description. It is an improvement over the Courant scheme. In this scheme the slopes are evaluated at the points R and S (Fig. 3.1).

The difference equations of Eqs. (3.28) and (3.29) are

$$x_P - x_R = (V + c)_R \Delta t \qquad (3.35a)$$

$$x_P - x_S = (V - c)_S \Delta t \qquad (3.35b)$$

$$V_P - V_R + F_R(h_P - h_R) = g(S_0 - S_f)_R \Delta t \qquad (3.36a)$$

$$V_P - V_S - F_S(h_P - h_S) = g(S_0 - S_f)_S \Delta t \qquad (3.36b)$$

In computation of this case, x_R and x_S can no longer be obtained directly from Eq. (3.35), they will be computed by using iterative computation.

Generally speaking, the computative procedure is as follows

(a) Obtain the first estimates of x_R and x_s by using Eq. (3.30).

(b) Substitute the estimates into Eqs. (3.32), (3.33) or (3.34) to compute V_R, h_R, V_S, h_S, $(V + c)_R$ and $(V - c)_S$.

(c) Obtain the second estimates of x_R and x_S by using Eq. (3.35), then substitute them back into Eqs. (3.32), (3.33) or (3.34) until the difference between the values of successive estimates reaches a specified tolerance.

(d) Using the calculated values of V_R, h_R, V_S and h_S, the unknown V_P and h_P can be obtained from Eq. (3.36).

3.2.4.3. Second-order Characteristic Scheme

The scheme also was first described by Hartree (1952) and later was detailed by Lister (1960). Sevuk (1973) made further modification. In this scheme the trapezoidal rule is applied. The difference equations of Eqs. (3.28) and (3.29) are

$$x_P - x_R = 0.5(V_P + c_P + V_R + c_R)\ \Delta t \tag{3.37a}$$

$$x_P - x_S = 0.5(V_P - c_P + V_S - c_S)\ \Delta t \tag{3.37b}$$

$$V_P - V_R + 0.5(F_P + F_R)(h_P - h_R) = 0.5g(S_P + S_R - 2S_0)\ \Delta t \tag{3.38a}$$

$$V_P - V_S - 0.5(F_P + F_S)(h_P - h_S) = 0.5g(S_P + S_S - 2S_0)\ \Delta t \tag{3.38b}$$

In this scheme quadratic interpolations are used in evaluating V_R, h_R, V_S and h_S. If U is used to represent the variables of V and h, the interpolation equations for points R and S are

$$U_R = U_M - \frac{(U_M - U_A)(x_M - x_R)}{2\Delta x} +$$

$$\frac{U_B - 2U_M + U_A}{2} \left(\frac{x_M - x_R}{\Delta x}\right)^2 \qquad (3.39)$$

$$U_S = U_M - \frac{(U_M - U_A)(x_M - x_S)}{2\Delta x} +$$

$$\frac{U_B - 2U_M + U_A}{2} \left(\frac{x_M - x_S}{\Delta x}\right)^2 \qquad (3.40)$$

The predictor-corrector method can be used to obtain the unknown values of V_P and h_P.

3.2.4.4. Other Schemes

There are many other schemes for solving the characteristic equations. They are mostly variations to the aforementioned schemes. For example, the specified interval scheme (Jolly and Yevjevich, 1974); various specified time interval schemes which include implicit scheme (Schmitz and Edenhofer, 1980, 1983), implicit time-line interpolation scheme (Goldberg and Wylie,1983), spatial reachout scheme (Chang and Richards, 1971), and temporal reachback scheme (Wylie, 1980); specified distance scheme (Sivaloganathan, 1978); and multimode scheme (Lai, 1988) which combines the four specified time interval schemes (implicit scheme, temporal reachback scheme, spatial reachback scheme, and classical scheme) into one which possesses all the advantages of each scheme. Further details of all the schemes can be obtained in the cited literature.

3.2.5. Comparison of Various Numerical Schemes

Because so many schemes have been proposed for solving the Saint-Venant equations numerically, many investigators have been concerned with identifying the best scheme or developing a good new scheme for the solutions of the equations. A number of papers have been published on comparison of numerical schemes. There have been comparative studies of different numerical schemes by Liggett and Woolhiser (1967), Strelkoff (1970), Yevjevich and Barnes (1970), Sevuk and Yen (1973), and Price (1974). The comparison tests of the accuracy and efficiency of the schemes are based on either results from a physical prototype or results from an exact analytical solution of the basic equations used to describe the flow of simple conditions.

Strelkoff (1970) examined the numerical stability of the characteristic and direct forms of the Saint-Venant equations. He indicated that the explicit numerical schemes, which are simple, but require small steps in time because of stability problems, are contrasted with implicit schemes that permit numerical solution over large time steps but require the solution of large sets of simultaneous algebraic equations at each step.

Yevjevich and Barnes (1970) studied two explicit schemes, namely, a diffusive scheme and a Lax-Wendroff scheme for routing subcritical open-channel flow through a single pipe and found them less suitable than the method of characteristics in Courant form using a fixed rectangular grid.

Building upon the work of Yevjevich and Barnes, Sevuk and Yen (1973) compared five schemes for flood routing through circular channels. Four of these schemes are method-of-characteristics schemes with fixed rectangular grids, and one is a four-point, box, noncentral direct implicit scheme. The first characteristic scheme is a scheme with the characteristic equations in canonical form, the second is a first-order semiexplicit scheme of linear characteristics, the third is a second-order semiimplicit scheme solved by a predictor-corrector method, and the fourth is a scheme in Courant form. For the last three characteristic schemes the Courant stability criterion was used to select Δt and Δx. They found that all the five schemes work reasonably well and are stable. Since the true solution of the differential equations is unknown they used the flood volume conservation as an error measure and found that the second-order characteristic scheme is most accurate but also most costly, roughly requiring twice as much computer time as the other schemes, while the Courant characteristic scheme has the largest error among the five schemes investigated.

Price (1974) compared four of the more important numerical second-order finite difference schemes, i.e., leap-frog explicit scheme, two-step Lax-Wendroff explicit scheme, four-point implicit scheme, fixed mesh implicit characteristic scheme, for flood routing with exact analytical solutions for the monoclinal wave. He concluded that (a) the implicit method of Amein (1970) is most accurate when $\Delta x/\Delta t$ is approximately equal to the speed of the monoclinal wave, (b) the fixed mesh implicit characteristic method is most accurate when $\Delta x/\Delta t$ is slightly smaller than the Courant

speed, (c) the implicit method is computationally faster than the other methods for a similar accuracy, (d) the greater the difference between the monoclinal wave speed and the Courant speed, the greater the advantage in using the implicit method, and (e) the time step for the implicit method must be chosen with caution if there are large differences in speeds for different parts of the flood wave, i.e., flooding over an extensive flood plain associated with the river. Price considered that the four-point implicit method is the most efficient method for flood routing problems.

The behavior and comparison of the numerical schemes can also be found in many other articles and books (Mahmood and Yevjevich, 1975; Miller and Yevjevich, 1975; Abbott, 1979; and Cunge et al., 1981). According to these previous investigations described in section 3.2., it is observed that the direct implicit method is a better means and the four-point finite difference scheme is a better scheme. Therefore, this scheme has been chosen for this study.

3.3. Study on Importance of Coefficients and Terms in Momentum Equation

The kind of study concerned with the applicability and sensitivity of the assumptions involved in simplifying the momentum equation from the exact form to the complete dynamic wave form has not been found. Few investigators have studied the importance of the coefficient, β, and none of k or k'. Although many investigators have compared the significance of each term in the complete dynamic wave equation, none of them have taken account of the backwater effect when calculating the contribution of each of

the terms. Some useful studies on the importance of the coefficient, ß, and terms in the momentum equation are discussed.

Yevjevich and Barnes (1970) made a sensitivity analysis on the effect of the momentum flux correction factor, ß, on computed results. Their investigation showed that the effect of ß appears to be small when the Saint-Venant equations are employed for routing typical flood waves through storm sewers.

Yu and McNown (1964) investigated the importance of the terms in the Saint-Venant equations and showed that when runoff measurements on airfield surfaces near Los Angeles were held, the two acceleration terms and the pressure term were each less than 1/100 of the S_0 or S_f term.

Ragan (1965) found that if local inflows are a significant part of the total flow, the convective acceleration term could not be neglected. Otherwise the error produced by ignoring this term becomes great and reduces the general computational accuracy.

Henderson (1966) gave the following values for 'an actual river in steep alluvial country' and a 'very fast-rising flood' as

Term	S_0,	$\frac{\partial h}{\partial x}$,	$\frac{V}{g}\frac{\partial V}{\partial x}$,	$\frac{1}{g}\frac{\partial V}{\partial t}$
Value, ft/mile	26,	1/2	1/8-1/4	1/20

It is shown that even in this case which should involve relatively large acceleration terms, the last three terms are very small compared to S_0.

Harder and Armacost (1966) mentioned that when a Missouri River flow was increased almost instantaneously from 24,000 cfs to

104,000 cfs, the acceleration terms were only about five percent of the friction term.

Iwasaki (1967) concluded by investigating actual flood records on the Kitakami River in Japan that the local and convective acceleration terms were at most one and a half percent of the pressure term.

From these studies, Miller and Cunge (1975) suggested that for many unsteady channel flows the acceleration terms are small relative to other terms and thus may be ignored without appreciable error. However, the resistance term must still be dealt with.

Henderson (1966) gave several rough expressions to reflect the relative ratios between the terms in wide rectangular channels for a given inflow hydrograph $q = q(t)$. Based on an assumption, $S_0 \approx S_f$, he obtained that

$$\frac{\partial h/\partial x}{S_0} \propto S_0^{-5/3} * \left(\begin{array}{c} \text{terms characteristic of the} \\ \text{inflow hydrograph alone} \end{array} \right)$$

$$O\left(-\frac{V}{g}\frac{\partial V/\partial x}{\partial h/\partial x}\right) = O\left(\frac{\partial (V^2/2g)/\partial x}{\partial h/\partial x}\right) = O(F_r^2)$$

$$O\left(\frac{1}{g}\frac{\partial V}{\partial t}\right) = O\left(\frac{V}{g}\frac{\partial V}{\partial x}\right)$$

He concluded that (a) the pressure term must become small as S_0 increases, (b) the local and convective acceleration terms are of the same order of magnitude, and (c) the two acceleration terms are of no higher order than the pressure term, unless F_r^2 (F_r is Froude number) >> 1. Thus, Henderson provided a criterion using

S_0 as a parameter to estimate the magnitudes of the local acceleration term, convective acceleration term, and pressure term. For intermediate slopes the magnitudes of the three terms are relatively large and they cannot be neglected, i.e., flood waves are best described by the complete dynamic equation. For gentle slopes the two acceleration terms are negligible but the pressure term is important, i.e., flood waves are best described by the noninertia equation. For steep slopes the three terms are not important and can be neglected, i.e., flood waves are best described by kinematic wave equation.

Some other researchers used Froude number, F_r, or kinematic flow number, κ, as dimensionless parameters to assess the magnitudes of the local acceleration, convective acceleration and pressure terms. For example, Miller and Cunge (1975) gave $F_r = 2$ (Chezy's formula was used) or $F_r = 1.5$ (Manning's formula was used) as a criterion to determine that the three terms should be kept or omitted. As $F_r = 2$ (or 1.5), the dynamic and kinematic waves have the same celerity, i.e., both waves are of equal importance. So, the kinematic wave model is absolutely valid. Woolhiser and Liggett (1967) used the kinematic flow number as a criterion to judge the validity of the kinematic model. They presented that as $\kappa > 20$ the kinematic model is very good. Overton (1972) reported that when $\kappa > 10$, the error in the kinematic approximation is decreasing rapidly and the aforementioned three terms can be safely neglected, i.e., the dynamic wave solution approaches the kinematic wave solution.

Jolly and Yevjevich (1974) investigated the contribution of each of the terms in the momentum equation. Unfortunately, among the three momentum equations cited and utilized in that article, only one is proper. Therefore, their conclusions and results are rather doubtful. More detailed commentary about that article can be found in Martin and Wiggert (1975) and Yen and Sevuk (1975).

Ponce and Simons (1977) applied the theory of linear stability to the Saint-Venant equations in wide channels of rectangular cross section. They calculated the propagation characteristics of various shallow water waves in open channels, namely, kinematic, diffusion (strictly speaking, it should be denoted as noninertia), steady dynamic, dynamic, and gravity waves. The propagation characteristics, i.e., the celerity and attenuation function, are expressed as a function of the steady uniform Froude number and the dimensionless wave number. They summarized that the entire wave number spectrum is divided into three bands: (a) a gravity band corresponding to the range of large values of the wave number; (b) a kinematic band corresponding to small wave number; and (c) a dynamic band corresponding to midspectrum values of the wave number. According to the analysis, the various approximate wave models can be compared to each other, and the accuracy of the kinematic model and the so-called diffusion wave model can be assessed.

Ponce et al. (1978) further investigated the applicability of kinematic and diffusion wave models for a sinusoidal shaped wave in a wide channel. They concluded that the channel slope and wave period are two important physical characteristics in determining

the applicability of the approximate models. The so-called diffusion model is shown to be applicable for a wider range of channel slopes and wave periods than the kinematic model. They indicated when the channel slope and wave period exceeds a certain limited range, only the complete dynamic wave model can be used to simulate the physical phenomena of the unsteady open channel flow. They gave the following inequalities as criteria to distinguish if the kinematic or diffusion model is valid

$$\frac{T_r S_0 V_0}{h_0} > N \tag{3.41}$$

$$T_r S_0 \, (g/h_0)^{1/2} > M \tag{3.42}$$

in which T_r is the time-of-rise of the inflow hydrograph, S_0 is the channel slope, g is gravitational acceleration, V_0 and h_0 are the steady uniform flow velocity and depth, and the recommended values of N and M are 85 and 15, respectively. Ponce (1989) wrote that if the first inequality is satisfied a wave is a kinematic wave, and the greater the left side of the second inequality, the more likely it is that the wave is a diffusion wave.

Ponce (1990) derived a generalized so-called diffusion wave equation with inertial effects on the basis of the linear analogs of the Saint-Venant equations and summarized four types of diffusion wave models, i.e., full inertial, local inertial, convective inertial and noninertial models. The definition of each of these models is dependent on whether the inertia terms (local and convective) are excluded from or included in the formulation. By comparing the hydraulic diffusivity of each of the four types

of models, Ponce concluded that for low Froude number, the noninertial model is shown to be a better approximation to the full inertial model than either local or convective models.

Fread (1979) also presented two inequalities as criteria to quantify the acceptable range of application for the kinematic and so-called diffusion models. The criteria are developed by estimating the magnitudes of the terms in the momentum equation. All the terms are normalized with the channel slope, and these ratios are further expressed with hydraulic variables, for example, channel slope, peak discharge, Manning n, time-of-rise of inflow hydrograph, cross-section parameters. The criteria are more complicated than those provided by Ponce et al., but, they are applicable for a wide range of practical channel shapes and typical inflow hydrograph shapes. Fread also concluded that the diffusion criterion permits a much larger range of channel characteristics and inflow hydrographs to be treated with the so-called diffusion model than with kinematic model for the same level of error index.

Ball (1988) investigated the importance and contributions of the terms in the momentum equation. He considered only the terms in the Saint-Venant momentum equation when it is applied to open channel flow in pipes. Ball concluded that as the almost full-pipe Froude number, F_p, increases, the magnitude and the importance of the pressure term, the convective acceleration term, the local acceleration term, and the lateral inflow acceleration term, decrease. This decrease in magnitude was of particular importance in consideration of the pressure term. It was found that the bed slope is the most important and the pressure term is the next most

important factor. For cases where lateral inflow was considered, it was found that the lateral inflow acceleration term, although significant in respect to other terms, did not have a substantial influence on the hydrograph propagation.

Price (1985) made a magnitude scale analysis of the Saint-Venant equations to see if some of the terms in the equations may be more important than others. He selected some typical scales in UK rivers: $\bar{Q} \propto 500\ m^3/s$; $\bar{A} \propto 300\ m^2$; $\bar{h} \propto 5\ m$; $\bar{S}_0 \propto 10^{-3}$; $\bar{g} = 9.81\ m/s^2$ and $\bar{t} \propto 10^5\ s$. Here, the imposition of a 'bar' denotes the scale for the variables, where $\bar{Q}$, $\bar{A}$, and $\bar{h}$ are the bankfull discharge, cross-sectional area, and depth, respectively, and $\bar{t}$ is the duration of the flood. According to the continuity equation, the length scale $\bar{x}$ of the flood wave is

$$\bar{x} \propto Qt/A \propto 1.7 * 10^5\ m = 170\ km$$

From the complete dynamic wave equation the ratios between the terms can be obtained as

$$\frac{|\partial Q/\partial t|}{|\partial (Q^2/A)/\partial t|} \propto 1$$

$$\frac{|\partial Q/\partial t|}{|gAS_0|} \propto \frac{\bar{Q}/\bar{t}}{gAS_0} \propto 1.7 * 10^{-3}$$

$$\frac{|gA(\partial h/\partial x)|}{|gAS_0|} \propto \frac{\bar{h}}{xS_0} \propto 2 * 10^{-2}$$

Furthermore, Price introduced two parameters: $\varepsilon = \bar{h}/\bar{x}\bar{S}_0$ which is the ratio of the characteristic surface gradient to the bed gradient, and $\varsigma = \bar{Q}^2/(\bar{g}\bar{A}^2\bar{h})$ which is the square of the Froude number of the flow. He further rewrote the complete dynamic wave equation

as

$$\frac{\varepsilon\varsigma}{A''}\left[\frac{\partial Q''}{\partial t''}+\frac{\partial}{\partial x''}\left(\frac{Q''^2}{A''}\right)\right]+\varepsilon\frac{\partial h''}{\partial x''}-S''_0+S''_f=0 \qquad (3.43)$$

in which the 'double prime' denotes the dimensionless form of the variables. For example, $Q'' = Q/\bar{Q}$, $A'' = A/\bar{A}$, $h'' = h/\bar{h}$, $S''_0 = S_0/\bar{S}_0$, $S''_f = S_f/\bar{S}_0$, $x'' = x/\bar{x}$ and $t'' = t/\bar{t}$. From these ratios and the equation, Price concluded that the first two inertia terms in the momentum equation are significantly smaller than the pressure term, and the pressure term is significantly smaller than S_0 or S_f, generally for rivers with subcritical flow $\varsigma \leq \varepsilon \leq 1$.

All the previous investigations provided very helpful knowledge about the importance of the coefficient, ß, and the contribution of each term in the momentum equation. Based on the information, the two subjects, namely, the importance of the coefficients and the contributions of the terms involved in the exact momentum equation, are further examined in this study.

4. DESCRIPTION OF NUMERICAL PROCEDURE

In order to investigate the importance of the coefficients and the contributions of the terms in the exact momentum equation, Eq. (2.2), this exact momentum equation together with a continuity equation is applied to flood routing for an open channel with specified conditions. The solutions are compared with those of the Saint-Venant equations by using the same numerical procedure, and the magnitudes of the terms in the exact momentum equation are analyzed. From the comparison and analysis performed in this study the sensitivity of the coefficients and terms in the exact momentum equation to the solutions can be realized.

4.1. Nondimensional Form of Exact Momentum and Continuity Equations

In order to obtain a general picture of the sensitivity of the coefficients and terms in the exact momentum equation, it would be helpful to convert the continuity equation, Eqs. (2.1) or (2.4) or (2.6), and the exact momentum equation, Eqs. (2.2) or (2.5) or (2.7), into a nondimensional form. The nondimensional equations are solved numerically by applying an implicit finite difference method.

We define

$$V_* = \frac{V}{V_0}\ ,\quad h_* = \frac{h}{h_0}\ ,\quad x_* = \frac{x}{L_0}\ ,\quad t_* = \frac{V_0}{L_0}\,t\ ,\quad B_* = \frac{B}{B_0}\ ,$$

$$A_* = \frac{A}{A_0}\ ,\quad Q_* = \frac{Q}{A_0V_0}\ ,\quad n_* = \frac{n}{n_0}\ ,\quad R_* = \frac{R}{R_0}\ ,\quad T_* = \frac{T}{T_0}\ ,$$

in which quantities with an asterisk subscript are dimensionless and those with the subscript ' 0 ' are quantities at a certain reference condition, i.e., L_0 is defined as a reference length, V_0 is the steady uniform flow velocity, h_0 is the depth when the flow is steady uniform, A_0, B_0 and R_0 are the cross-sectional area, width of cross section at the free surface and hydraulic radius corresponding to the depth h_0, respectively, n_0 and T_0 are Manning resistance factor and internal stresses for the steady uniform flow condition, and $t_0 = L_0/V_0$ is the time required to travel the distance L_0 with speed V_0.

Accordingly, the following expressions can be written,

$$\frac{\partial A}{\partial t} = \frac{A_0 V_0}{L_0} \frac{\partial A_*}{\partial t_*}, \qquad \frac{\partial A}{\partial x} = \frac{A_0}{L_0} \frac{\partial A_*}{\partial x_*},$$

$$\frac{\partial Q}{\partial t} = \frac{A_0 V_0^2}{L_0} \frac{\partial Q_*}{\partial t_*}, \qquad \frac{\partial Q}{\partial x} = \frac{A_0 V_0}{L_0} \frac{\partial Q_*}{\partial x_*},$$

$$\frac{\partial h}{\partial t} = \frac{h_0 V_0}{L_0} \frac{\partial h_*}{\partial t_*}, \qquad \frac{\partial h}{\partial x} = \frac{h_0}{L_0} \frac{\partial h_*}{\partial x_*},$$

$$\frac{\partial V}{\partial t} = \frac{V_0^2}{L_0} \frac{\partial V_*}{\partial t_*}, \qquad \frac{\partial V}{\partial x} = \frac{V_0}{L_0} \frac{\partial V_*}{\partial x_*},$$

Thus, if lateral flow is neglected, the equations of continuity and momentum, Eqs. (2.1) and (2.2) and Eqs. (2.4) through (2.7), can be written nondimensionally as

$$\frac{\partial A_*}{\partial t_*} + \frac{\partial Q_*}{\partial x_*} = 0 \qquad (4.1)$$

$$\frac{\partial Q_*}{\partial t_*} + \frac{Q_*^2}{A_*}\frac{\partial \beta}{\partial x_*} + \frac{2\beta Q_*}{A_*}\frac{\partial Q_*}{\partial x_*} - \frac{\beta Q_*^2}{A_*^2}\frac{\partial A_*}{\partial x_*}$$

$$+ (k - k')\frac{\cos\theta}{F_0^2} h_* \frac{\partial A_*}{\partial x_*} + \frac{\cos\theta}{F_0^2} h_* A_* \frac{\partial k}{\partial x_*} + \frac{\cos\theta}{F_0^2} k A_* \frac{\partial h_*}{\partial x_*}$$

$$= \kappa A_* \left(1 - \frac{Q_*^2 n_*^2}{A_*^2 R_*^{1.33}}\right) + \frac{T_0}{\gamma A_0 h_0 F_0^2}\frac{\partial T_*}{\partial x_*} \qquad (4.2)$$

$$\frac{\partial h_*}{\partial t_*} + \frac{A_0}{B_0 h_0}\frac{1}{B_*}\frac{\partial Q_*}{\partial x_*} = 0 \qquad (4.3)$$

$$\frac{\partial Q_*}{\partial t_*} + \frac{Q_*^2}{A_*}\frac{\partial \beta}{\partial x_*} + \frac{2\beta Q_*}{A_*}\frac{\partial Q_*}{\partial x_*} - \frac{\beta B_0 h_0}{A_0}\frac{B_* Q_*^2}{A_*^2}\frac{\partial h_*}{\partial x_*}$$

$$+ (k - k')\frac{\cos\theta h_0 B_0}{F_0^2 A_0} h_* B_* \frac{\partial h_*}{\partial x_*} + \frac{\cos\theta}{F_0^2} h_* A_* \frac{\partial k}{\partial x_*} + \frac{\cos\theta}{F_0^2} k A_* \frac{\partial h_*}{\partial x_*}$$

$$= \kappa A_* \left(1 - \frac{Q_*^2 n_*^2}{A_*^2 R_*^{1.33}}\right) + \frac{T_0}{\gamma A_0 h_0 F_0^2}\frac{\partial T_*}{\partial x_*} \qquad (4.4)$$

$$\frac{\partial h_*}{\partial t_*} + \frac{A_0}{B_0 h_0}\frac{A_*}{B_*}\frac{\partial V_*}{\partial x_*} + V_*\frac{\partial h_*}{\partial x_*} = 0 \qquad (4.5)$$

$$\frac{\partial V_*}{\partial t_*} + V_*^2\frac{\partial \beta}{\partial x_*} + (2\beta - 1) V_*\frac{\partial V_*}{\partial x_*} + (\beta - 1)\frac{B_0 h_0}{A_0}\frac{V_*^2 B_*}{A_*}\frac{\partial h_*}{\partial x_*}$$

$$+ (k - k')\frac{\cos\theta}{F_0^2}\frac{B_0 h_0}{A_0}\frac{B_* h_*}{A_*}\frac{\partial h_*}{\partial x_*} + \frac{\cos\theta}{F_0^2} h_*\frac{\partial k}{\partial x_*} + \frac{\cos\theta}{F_0^2} k\frac{\partial h_*}{\partial x_*}$$

$$= \kappa \left(1 - \frac{V_*^2 n_*^2}{R_*^{1.33}}\right) + \frac{T_0}{\gamma A_0 h_0 F_0^2}\frac{1}{A_*}\frac{\partial T_*}{\partial x_*} \qquad (4.6)$$

in which $F_0 = V_0/\sqrt{gh_0}$ is the Froude number based on reference quantities, V_0 and h_0, and $\kappa = gS_0L_0/V_0^2 = S_0L_0/F_0^2h_0$ is the Kinematic wave number.

In Eqs. (4.1) through (4.6) the Manning formula is introduced to represent friction slope, S_f. As described in section 2.3.5, using the Manning formula has an advantage. The value of Manning's roughness factor, n, is nearly constant over a wide range of depths for flows with sufficiently high Reynolds number over a rigid boundary with a given surface roughness in a prismatic channel. Therefore, $n_* \approx 1$ and this will simplify the equations.

Equations (4.1) through (4.6) contain three different sets of dependent variables. They are Q and A, Q and h, and V and h, respectively. The three sets of equations have similar mathematical properties. But there is no guarantee, and it is most unlikely, that the influences of the coefficients and the contributions of the terms on the solutions of the three sets of equations are identical because of the different dependent variables. Therefore, it is desirable to compare the numerical results of Eqs. (4.1) and (4.2) versus Eqs. (4.3) and (4.4) and Eqs. (4.5) and (4.6). However, since the investigative time has been limited, this study focuses only on the comparison of Eqs. (4.3) and (4.4) versus Eqs. (4.5) and (4.6).

4.2. Nondimensional Equations Considering Different Channel Shapes

In this study only the condition of a prismatic channel is simulated. The effect of the channel cross-sectional shape is investigated by using a hypothetical 54-mile long channel with wide

rectangular, rectangular or trapezoidal cross sections. The selection of a 54-mile length for the channel is referred to an example used by Chow (1959, pp. 596-600). For channels having these cross-sectional shapes, the nondimensional form of the exact momentum and continuity equations is shape dependent. Hence, the importance of the coefficients and terms in the exact momentum equation to the solutions of the equations could be different for different shapes. For different cross-sectional shapes of the channel, Eqs. (4.3) and (4.4) can be written as the following nondimensional equations in terms of the general nondimensional cross-sectional geometry functions, G_1, G_2 and G_3,

$$\frac{\partial h_*}{\partial t_*} + \frac{1}{G_1}\frac{\partial Q_*}{\partial x_*} = 0 \tag{4.7}$$

$$\frac{\partial Q_*}{\partial t_*} + \frac{{Q_*}^2}{G_2}\frac{\partial \beta}{\partial x_*} + \frac{2\beta Q_*}{G_2}\frac{\partial Q_*}{\partial x_*} - \frac{G_1 \beta {Q_*}^2}{{G_2}^2}\frac{\partial h_*}{\partial x_*}$$

$$+ (k - k')\frac{\cos\theta}{{F_0}^2} G_1 h_* \frac{\partial h_*}{\partial x_*} + \frac{\cos\theta}{{F_0}^2} G_2 h_* \frac{\partial k}{\partial x_*} + \frac{\cos\theta}{{F_0}^2} k G_2 \frac{\partial h_*}{\partial x_*}$$

$$= \kappa G_2 \left(1 - \frac{{Q_*}^2}{{G_2}^2 {R_*}^{1.33}}\right) + \frac{1}{G_3 {F_0}^2}\frac{\partial T_*}{\partial x_*} \tag{4.8}$$

For wide rectangular and rectangular channels, $G_1 = B_* = 1$, $G_2 = B_* h_* = h_*$ and $G_3 = \gamma B_0 {h_0}^2 / T_0$. For trapezoidal channels with bottom width b and side slope z,

$$G_1 = 2h_* + \frac{b_* - 2h_*}{1 + z\dfrac{h_0}{b_0}} \tag{4.9}$$

$$G_2 = h_*^2 + \frac{b_* h_* - h_*^2}{1 + z \frac{h_0}{b_0}} \tag{4.10}$$

$$G_3 = \frac{\gamma b_0 h_0^2}{T_0} \left(1 + z \frac{h_0}{b_0}\right) \tag{4.11}$$

in which b_* is defined as b/b_0 representing the longitudinal variation of the channel width where b_0 is a reference bottom width. The value of b_* is equal to unity when the channel is prismatic for which the value of b_0 is taken equal to that of b, and b_* is equal to B_* when the side slope z approaches zero, i.e., the trapezoidal channel becomes the rectangular channel.

Likewise, Eqs. (4.5) and (4.6) can be written as follows

$$\frac{\partial h_*}{\partial t_*} + \frac{h_*}{G_4} \frac{\partial V_*}{\partial x_*} + V_* \frac{\partial h_*}{\partial x_*} = 0 \tag{4.12}$$

$$\frac{\partial V_*}{\partial t_*} + V_*^2 \frac{\partial \beta}{\partial x_*} + (2\beta - 1) V_* \frac{\partial V_*}{\partial x_*} + (\beta - 1) G_4 \frac{V_*^2}{h_*} \frac{\partial h_*}{\partial x_*}$$

$$+ (k - k') \frac{\cos\theta}{F_0^2} G_4 \frac{\partial h_*}{\partial x_*} + \frac{\cos\theta}{F_0^2} h_* \frac{\partial k}{\partial x_*} + \frac{\cos\theta}{F_0^2} k \frac{\partial h_*}{\partial x_*}$$

$$= \kappa \left(1 - \frac{V_*^2}{R_*^{1.33}}\right) + \frac{1}{G_5 F_0^2} \frac{1}{h_*} \frac{\partial T_*}{\partial x_*} \tag{4.13}$$

in which G_4 and G_5 are nondimensional geometry functions. For wide rectangular and rectangular channel $G_4 = 1$, $G_5 = \gamma B_0 B_* h_0^2/T_0 = \gamma B_0 h_0^2/T_0$. For trapezoidal channel

$$G_4 = 2 - \frac{1}{1 + z \dfrac{h_0 h_*}{b_0 b_*}} \tag{4.14}$$

$$G_5 = \frac{\gamma b_0 b_* h_0^2}{T_0} \left(1 + z \frac{h_0 h_*}{b_0 b_*}\right) \tag{4.15}$$

4.3. Nondimensional Finite Difference Equations of Exact Momentum and Continuity Equations

Based on the depiction in section 3.2.3, the Amein's four-point implicit method is selected and applied to this study because of its economics and accuracy. In order to make the numerical solution strongly stable, the time weighting factor, θ, is taken equal to 0.6. The finite difference quotients are

$$\frac{\partial f_*}{\partial t_*} = \frac{1}{2\Delta t_*} \left(f_{*\,i+1}^{j+1} + f_{*\,i}^{j+1} - f_{*\,i+1}^{j} - f_{*\,i}^{j}\right); \tag{4.16}$$

$$\frac{\partial f_*}{\partial x_*} = \frac{\theta}{\Delta x_*} \left(f_{*\,i+1}^{j+1} - f_{*\,i}^{j+1}\right) + \frac{1-\theta}{\Delta x_*} \left(f_{*\,i+1}^{j} - f_{*\,i}^{j}\right); \tag{4.17}$$

$$f = \frac{\theta}{2} \left(f_{*\,i+1}^{j+1} + f_{*\,i}^{j+1}\right) + \frac{1-\theta}{2} \left(f_{*\,i+1}^{j} + f_{*\,i}^{j}\right), \tag{4.18}$$

in which f represents a variable, A, h, Q or V; the superscript denotes time discretization and subscript spatial discretization.

Thus, the nondimensional continuity and momentum equations, Eqs. (4.1) and (4.2), can be written in finite difference form as

$$(A_{*\,i+1}^{j+1} + A_{*\,i}^{j+1} - A_{*\,i+1}^{j} - A_{*\,i}^{j})$$

$$+ 2\,\frac{\Delta t_*}{\Delta x_*}\,[\theta(Q_{*\,i+1}^{j+1} - Q_{*\,i}^{j+1}) + (1-\theta)(Q_{*\,i+1}^{j} - Q_{*\,i}^{j})] = 0 \qquad (4.19)$$

$$(Q_{*\,i+1}^{j+1} + Q_{*\,i}^{j+1} - Q_{*\,i+1}^{j} - Q_{*\,i}^{j})$$

$$+ \zeta_1 \frac{[\theta(Q_{*\,i+1}^{j+1} + Q_{*\,i}^{j+1}) + (1-\theta)(Q_{*\,i+1}^{j} + Q_{*\,i}^{j})]}{[\theta(A_{*\,i+1}^{j+1} + A_{*\,i}^{j+1}) + (1-\theta)(A_{*\,i+1}^{j} + A_{*\,i}^{j})]}\;[\theta(Q_{*\,i+1}^{j+1} - Q_{*\,i}^{j+1}) + (1-\theta)(Q_{*\,i+1}^{j} - Q_{*\,i}^{j})]$$

$$+ \frac{\zeta_1}{2} \frac{[\theta(Q_{*\,i+1}^{j+1} + Q_{*\,i}^{j+1}) + (1-\theta)(Q_{*\,i+1}^{j} + Q_{*\,i}^{j})]^2}{[\theta(A_{*\,i+1}^{j+1} + A_{*\,i}^{j+1}) + (1-\theta)(A_{*\,i+1}^{j} + A_{*\,i}^{j})]^2}\;[\theta(A_{*\,i+1}^{j+1} - A_{*\,i}^{j+1}) + (1-\theta)(A_{*\,i+1}^{j} - A_{*\,i}^{j})]$$

$$+ \eta_1\,[\theta(h_{*\,i+1}^{j+1} + h_{*\,i}^{j+1}) + (1-\theta)(h_{*\,i+1}^{j} + h_{*\,i}^{j})]\,[\theta(A_{*\,i+1}^{j+1} - A_{*\,i}^{j+1}) + (1-\theta)(A_{*\,i+1}^{j} - A_{*\,i}^{j})]$$

$$+ \delta_1\,[\theta(A_{*\,i+1}^{j+1} + A_{*\,i}^{j+1}) + (1-\theta)(A_{*\,i+1}^{j} + A_{*\,i}^{j})]\,[\theta(h_{*\,i+1}^{j+1} - h_{*\,i}^{j+1}) + (1-\theta)(h_{*\,i+1}^{j} - h_{*\,i}^{j})]$$

$$= \Delta t_*\,\kappa\,[\theta(A_{*\,i+1}^{j+1} + A_{*\,i}^{j+1}) + (1-\theta)(A_{*\,i+1}^{j} + A_{*\,i}^{j})]$$

$$\{1 - \frac{(2)^{1.33}\,[\theta(Q_{*\,i+1}^{j+1} + Q_{*\,i}^{j+1}) + (1-\theta)(Q_{*\,i+1}^{j} + Q_{*\,i}^{j})]^2}{[\theta(A_{*\,i+1}^{j+1} + A_{*\,i}^{j+1}) + (1-\theta)(A_{*\,i+1}^{j} + A_{*\,i}^{j})]^2\,[\theta(R_{*\,i+1}^{j+1} + R_{*\,i}^{j+1}) + (1-\theta)(R_{*\,i+1}^{j} + R_{*\,i}^{j})]^{1.33}}\} \qquad (4.20)$$

in which $\zeta_1 = 4\beta \dfrac{\Delta t_*}{\Delta x_*}$,

$$\eta_1 = (k - k') \frac{\cos\theta}{F_0^2} \frac{\Delta t_*}{\Delta x_*} ,$$

$$\delta_1 = k \frac{\cos\theta}{F_0^2} \frac{\Delta t_*}{\Delta x_*} .$$

Likewise, Eqs. (4.7) and (4.8) can be written as

$$(h_{*\,i+1}^{j+1} + h_{*\,i}^{j+1} - h_{*\,i+1}^{j} - h_{*\,i}^{j})$$

$$+ \frac{4\Delta t_*}{\Delta x_*} \frac{[\theta(Q_{*\,i+1}^{j+1} - Q_{*\,i}^{j+1}) + (1-\theta)(Q_{*\,i+1}^{j} - Q_{*\,i}^{j})]}{[\theta(G_{1\,i+1}^{j+1} + G_{1\,i}^{j+1}) + (1-\theta)(G_{1\,i+1}^{j} + G_{1\,i}^{j})]} = 0 \qquad (4.21)$$

$$(Q_{*\,i+1}^{j+1} + Q_{*\,i}^{j+1} - Q_{*\,i+1}^{j} - Q_{*\,i}^{j})$$

$$+ 2\zeta_1 \frac{[\theta(Q_{*\,i+1}^{j+1} + Q_{*\,i}^{j+1}) + (1-\theta)(Q_{*\,i+1}^{j} + Q_{*\,i}^{j})]}{[\theta(G_{2\,i+1}^{j+1} + G_{2\,i}^{j+1}) + (1-\theta)(G_{2\,i+1}^{j} + G_{2\,i}^{j})]} [\theta(Q_{*\,i+1}^{j+1} - Q_{*\,i}^{j+1}) + (1-\theta)(Q_{*\,i+1}^{j} - Q_{*\,i}^{j})]$$

$$- \zeta_1 \frac{[\theta(G_{1\,i+1}^{j+1} + G_{1\,i}^{j+1}) + (1-\theta)(G_{1\,i+1}^{j} + G_{1\,i}^{j})][\theta(Q_{*\,i+1}^{j+1} + Q_{*\,i}^{j+1}) + (1-\theta)(Q_{*\,i+1}^{j} + Q_{*\,i}^{j})]^2}{[\theta(G_{2\,i+1}^{j+1} + G_{2\,i}^{j+1}) + (1-\theta)(G_{2\,i+1}^{j} + G_{2\,i}^{j})]^2}$$

$$[\theta(h_{*\,i+1}^{j+1} - h_{*\,i}^{j+1}) + (1-\theta)(h_{*\,i+1}^{j} - h_{*\,i}^{j})]$$

$$+\frac{\eta_1}{2}\left[\theta\left(G_{1\,i+1}^{j+1}+G_{1\,i}^{j+1}\right)+(1-\theta)\left(G_{1\,i+1}^{j}+G_{1\,i}^{j}\right)\right]\left[\theta\left(h_{*\,i+1}^{j+1}+h_{*\,i}^{j+1}\right)+(1-\theta)\left(h_{*\,i+1}^{j}+h_{*\,i}^{j}\right)\right]$$

$$\left[\theta\left(h_{*\,i+1}^{j+1}-h_{*\,i}^{j+1}\right)+(1-\theta)\left(h_{*\,i+1}^{j}-h_{*\,i}^{j}\right)\right]$$

$$+\frac{\delta_1}{2}\left[\theta\left(G_{2\,i+1}^{j+1}+G_{2\,i}^{j+1}\right)+(1-\theta)\left(G_{2\,i+1}^{j}+G_{2\,i}^{j}\right)\right]\left[\theta\left(h_{*\,i+1}^{j+1}-h_{*\,i}^{j+1}\right)+(1-\theta)\left(h_{*\,i+1}^{j}-h_{*\,i}^{j}\right)\right]$$

$$=\Delta t_*\,\kappa\,\frac{\left[\theta\left(G_{2\,i+1}^{j+1}+G_{2\,i}^{j+1}\right)+(1-\theta)\left(G_{2\,i+1}^{j}+G_{2\,i}^{j}\right)\right]}{2}$$

$$\left\{1-\frac{(2)^{3.33}\left[\theta\left(Q_{*\,i+1}^{j+1}+Q_{*\,i}^{j+1}\right)+(1-\theta)\left(Q_{*\,i+1}^{j}+Q_{*\,i}^{j}\right)\right]^2}{\left[\theta\left(G_{2\,i+1}^{j+1}+G_{2\,i}^{j+1}\right)+(1-\theta)\left(G_{2\,i+1}^{j}+G_{2\,i}^{j}\right)\right]\left[\theta\left(R_{*\,i+1}^{j+1}+R_{*\,i}^{j+1}\right)+(1-\theta)\left(R_{*\,i+1}^{j}+R_{*\,i}^{j}\right)\right]^{1.33}}\right\}$$

(4.22)

Similarly, from Eqs. (4.12) and (4.13) one has

$$\left(h_{*\,i+1}^{j+1}+h_{*\,i}^{j+1}-h_{*\,i+1}^{j}-h_{*\,i}^{j}\right)$$

$$+\frac{2\Delta t_*}{\Delta x_*}\frac{\left[\theta\left(h_{*\,i+1}^{j+1}+h_{*\,i}^{j+1}\right)+(1-\theta)\left(h_{*\,i+1}^{j}+h_{*\,i}^{j}\right)\right]}{\left[\theta\left(G_{4\,i+1}^{j+1}+G_{4\,i}^{j+1}\right)+(1-\theta)\left(G_{4\,i+1}^{j}+G_{4\,i}^{j}\right)\right]}\left[\theta\left(V_{*\,i+1}^{j+1}-V_{*\,i}^{j+1}\right)+(1-\theta)\left(V_{*\,i+1}^{j}-V_{*\,i}^{j}\right)\right]$$

$$+\frac{\Delta t_*}{\Delta x_*}\left\{\left[\theta\left(V_{*\,i+1}^{j+1}+V_{*\,i}^{j+1}\right)+(1-\theta)\left(V_{*\,i+1}^{j}+V_{*\,i}^{j}\right)\right]\left[\theta\left(h_{*\,i+1}^{j+1}-h_{*\,i}^{j+1}\right)+(1-\theta)\left(h_{*\,i+1}^{j}-h_{*\,i}^{j}\right)\right]\right\}$$

$$=0 \qquad (4.23)$$

$$(V_{*\,i+1}^{j+1} + V_{*\,i}^{j+1} - V_{*\,i+1}^{j} - V_{*\,i}^{j})$$

$$+ \zeta_2 \left[\theta(V_{*\,i+1}^{j+1} + V_{*\,i}^{j+1}) + (1-\theta)(V_{*\,i+1}^{j} + V_{*\,i}^{j})\right]\left[\theta(V_{*\,i+1}^{j+1} - V_{*\,i}^{j+1}) + (1-\theta)(V_{*\,i+1}^{j} - V_{*\,i}^{j})\right]$$

$$+ \eta_2 \left[\theta(G_{4\,i+1}^{j+1} + G_{4\,i}^{j+1}) + (1-\theta)(G_{4\,i+1}^{j} + G_{4\,i}^{j})\right]\left[\theta(h_{*\,i+1}^{j+1} - h_{*\,i}^{j+1}) + (1-\theta)(h_{*\,i+1}^{j} - h_{*\,i}^{j})\right]$$

$$\frac{\left[\theta(V_{*\,i+1}^{j+1} + V_{*\,i}^{j+1}) + (1-\theta)(V_{*\,i+1}^{j} + V_{*\,i}^{j})\right]^2}{\left[\theta(h_{*\,i+1}^{j+1} + h_{*\,i}^{j+1}) + (1-\theta)(h_{*\,i+1}^{j} + h_{*\,i}^{j})\right]}$$

$$+ \eta_1 \left[\theta(G_{4\,i+1}^{j+1} + G_{4\,i}^{j+1}) + (1-\theta)(G_{4\,i+1}^{j} + G_{4\,i}^{j})\right]\left[\theta(h_{*\,i+1}^{j+1} - h_{*\,i}^{j+1}) + (1-\theta)(h_{*\,i+1}^{j} - h_{*\,i}^{j})\right]$$

$$+ 2\delta_1 \left[\theta(h_{*\,i+1}^{j+1} - h_{*\,i}^{j+1}) + (1-\theta)(h_{*\,i+1}^{j} - h_{*\,i}^{j})\right]$$

$$= 2\Delta t_* \kappa \left\{1 - \frac{\frac{1}{4}\left[\theta(V_{*\,i+1}^{j+1} + V_{*\,i}^{j+1}) + (1-\theta)(V_{*\,i+1}^{j} + V_{*\,i}^{j})\right]^2}{\frac{1}{2}\left[\theta(R_{*\,i+1}^{j+1} + R_{*\,i}^{j+1}) + (1-\theta)(R_{*\,i+1}^{j} + R_{*\,i}^{j})\right]^{1.33}}\right\} \qquad (4.24)$$

in which $\zeta_2 = (2\beta - 1)\,\dfrac{\Delta t_*}{\Delta x_*}$,

$$\eta_2 = \frac{(\beta - 1)}{2}\,\frac{\Delta t_*}{\Delta x_*}\,.$$

4.4. Initial and Boundary Conditions

The initial flow condition is determined by computing the steady-flow water surface profiles throughout the channel. The flow treated in this study is in the subcritical regime. Hence, the initial condition is either convectively decelerating type profiles (M1 and S1 types) or convectively accelerating type profiles (M2 type).

For the upstream boundary condition, one positive phase of a sinusoidal wave is introduced, and the form is, for example, $h = h_w[1 - \cos(2\pi t/t_w)]$ in which h_w is wave amplitude and t_w is duration. If a dimensionless form is taken, this expression becomes $h_* = h_{w*}[1 - \cos(2\pi t_*/t_{w*}]$ in which h_{w*}, t_{w*} and t_0 are equal to h_w/h_0, t_w/t_0 and L_0/V_0, respectively. The introduced sinusoidal wave is shown in Fig. 4.1.

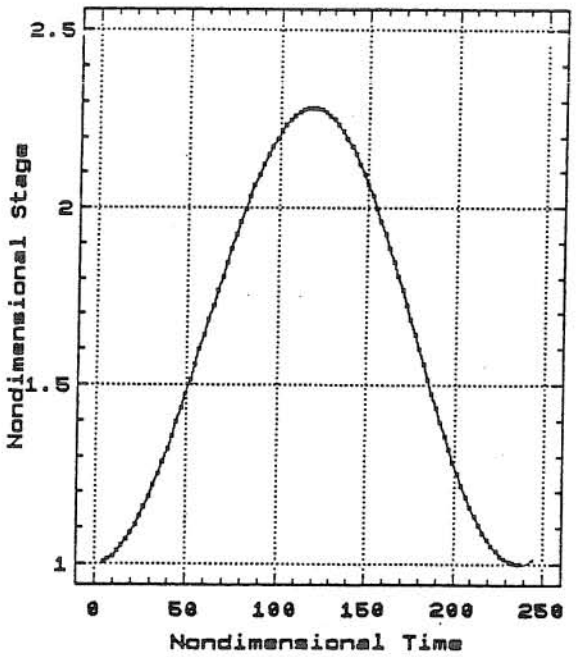

Fig. 4.1 Inflow Stage Hydrograph

For the downstream boundary condition, three different cases are selected:

(a) no downstream boundary restriction, i.e., no backwater effect;

(b) h_d = constant, i.e., the flow depth at downstream boundary does not change;

(c) $h_d = f(t)$, i.e., the flow depth at downstream boundary is a prescribed function of time.

Case (a) without downstream backwater effect for subcritical flows only is a hypothetical case often used by unsteady flow model simulators which cannot exist in reality. In such a hypothetical simulation the computation for a given time increment proceeds from upstream towards downstream and stops at the end of the channel. An equation is given for the channel end section to compute the flow variables using the information from upstream sections as well as that of the end section at the previous time. Depending on how the end section equation is formulated there are different versions. Nevertheless, this hypothetical case of no downstream backwater effect is equivalent to unsteady flow in an infinitely long channel. For practical reasons, the channel cannot be simulated as infinitely long. Instead, it is usually satisfactory to simulate over a sufficiently long channel such that additional length would produce insignificant differences at the end cross section of the channel. For the 54-mile long example channel adopted in this study, an additional 54 miles and an additional 162 miles are used making it a 108-mile and a 216-mile long channel, respectively, for case (a). It has been found that for the flows

tested, changes of depth at the 54-mile cross section between cases of the 108-mile and 216-mile long channels are negligible. Thus, the downstream boundary is positioned at 108th mile, and the simulated results for the first 54 miles of the 108-mile long channel are used as case (a) without downstream backwater effect.

For case (b), flow depth at the downstream boundary is kept constant throughout time. This case is similar to that of a river or a channel flowing into a very large reservoir or a lake.

For case (c), flow depth at the downstream boundary changes with time and four different typical situations are considered. First, the stage hydrograph at the downstream boundary is the same as that at the upstream boundary. This implies that the rises in stage of the main river and tributary stream are simultaneous. Second, the stage hydrograph at the downstream boundary is larger than that at the upstream boundary, for example, twice or one and a half times as great as the stage hydrograph at the upstream boundary (i.e., the same period while twice or one and a half times in amplitude). This situation is similar to that of a small tributary entering into a large main river. Third, the stage hydrograph at the downstream boundary is smaller than that at the upstream boundary, for example, one half or two thirds of the stage hydrograph at the upstream boundary (i.e., the same period while one half or two thirds in amplitude). This implies some special situations, for example, due to certain reasons the peak discharge of the tributary stream is larger than that of the main river. Fourth, the stage hydrograph at the downstream boundary is entirely opposite from that at the upstream boundary, i.e., although they

have the same period and amplitude, the times of reaching the minimum and peak stages are reversed.

4.5. Selection of Space and Time Increments

As described in section 3.2.3, the four-point implicit method is considered to have no stability limitations for the channel reach investigated, which is not very long, and this method has been shown to have the advantage of accuracy. However, in order to enhance the accuracy of the simulation results, the ratio of $\Delta t_*/\Delta x_*$ is carefully selected based on the suggestions of Price (1974 and 1985) and Wormleaton and Karmegam (1984). The size of Δx_* is first determined by comparing the solutions of the exact momentum and continuity equations in the nondimensional finite difference formulation for different values of Δx_*, e.g., 0.25, 0.5, 1 and 2, and a fixed size of Δt_*. Generally speaking, for the implicit method the smaller the size of Δx_*, the higher the accuracy, but the computation time becomes long and the computation cost increases. Therefore, Δx_* is so chosen that the difference between the solutions of the equations for two successive reductions in Δx_* becomes small enough to satisfy the required accuracy. After Δx_* is determined, the formula of the ratio of $\Delta t_*/\Delta x_*$ (or the ratio of $\Delta t/\Delta x$) described in section 3.2.3 and suggested by Price and Wormleaton and Karmegam, namely, $\Delta t_*/\Delta x_* = 3/5$ (or $\Delta t/\Delta x = 3A/5Q$), is adopted to calculate the size of Δt_*.

4.6. Consideration of Solution Method

In the simulation, the channel is divided into (N - 1) reaches. The continuity and momentum equations are applied to each reach separately. For a channel of length L (in this study L = 54 miles) having N (= 55) nodes (in this study the reference length L_0 is taken as 1 mile). For the (N - 1) reaches, 2(N - 1) equations can be written. There are 2N unknowns in the flow equations. If an upstream boundary condition and a downstream boundary condition are added, the modeling is closed and the flood routing problem in an open channel at every time increment can be completely solved using Newton's iteration method, the double-sweep method, or any other standard method, such as Gaussian elimination, or the matrix inversion. Newton's iteration method is employed in this study.

4.7. Determination of Tested Values of Coefficients and Estimation of Importance of Terms

Before solving the nondimensional finite difference equations it is necessary to determine the value of each of the coefficients and further estimate the importance of each of the terms involved in the exact momentum equation.

For the coefficients, the conventionally used values of β = 1, k = 1 and (k-k') = 0 are chosen as the basic reference. Based on the description in section 2.2, the impacts of β and k on the solutions of the equations are investigated for β = 1.0, 1.33 and 2.0, and k = 0.95, 0.99, 1.0, 1.01 and 1.05, respectively. The impact of k' in term of (k-k') is investigated for three different values, namely, -0.05, 0 and 0.05. Generally speaking, it is

common in open channel problems that the value of ß is less than 1.33 and the value of k is close to unity. The reason for choosing the value of ß as high as 2 is to consider the extreme condition of velocity distribution. This extreme nonuniform velocity distribution can be encountered in channels with narrow and deep cross-sectional shape and large roughness. If the effect of ß is not significant under this extreme condition the impact of ß on the solutions of the equations can be ignored. Similarly, the value of k is considered to be 0.95 and 1.05, which may occur in channels with sharply curved beds. Testing the impact of k under two extreme situations should be adequate to evaluate the importance of k.

As regards the terms, the channel slope, S_0, and the friction slope, S_f, are the most important terms. Their values generally are much greater than those of the pressure term and the two acceleration terms. In the numerical tests the magnitudes of the channel slope, S_0, are chosen such that the flow remains subcritical throughout the entire channel. Therefore, once typical flow discharge and Manning resistance factor, n, are determined, the range of S_0 can be obtained using the Manning formula and the formula calculating critical depth. The selected values of S_0 are equal to 0.00019, 0.00057, 0.00095 and 0.00114. In addition, because the flow is subcritical throughout the entire channel, the water surface profile is either the convectively decelerating type (M1 and S1) or the convectively accelerating type (M2) under various downstream boundary conditions.

According to the ratios between terms of the Saint-Venant equations given by Henderson (1966), the pressure term is of secondary importance and the two acceleration terms are even smaller in significance. Generally speaking, the two inertia terms are on an order smaller than the pressure term, unless $F_r^2 >> 1$, and the pressure term is smaller than either S_0 or S_f. However, the conditions considered in this study are broader and different from those considered by Henderson. First, because the flow considered in this research is subcritical and the selected channel slopes are mild, the pressure term could become relatively large. In fact, under some test conditions the magnitude of the pressure term is greatly increased. Second, since β, k and k' are not necessarily equal to unity, the value of either the convective acceleration term or the pressure term in the exact momentum equation is changed as compared to that in the complete dynamic wave equation, i.e., the convective term changes from $\partial(Q^2/A)/\partial x$ to $\partial(\beta Q^2/A)/\partial x$ and the pressure term from $\partial(h\cos\theta)/\partial x$ to $\partial(kh\cos\theta)/\partial x + [(k-k')(h\cos\theta/A)]\ \partial A/\partial x$. Thus, the contributions of the pressure term and the convective acceleration term may become more important. Third, as discussed previously, the assessment of the channel slope and the friction slope being the most important terms is made under the condition of no backwater effects. If there is a backwater effect the ratios between the terms could be different and the magnitudes of these terms, especially for the pressure term, depend to a great extent on the downstream flow depth. Furthermore, if the water surface profile is of interest, comparing the pressure term only with either S_0 or

S_f becomes unsatisfactory. A comparison between the pressure term and the difference, $(S_0 - S_f)$, is usually more useful.

Concerning the $\partial T/\partial x$ term, it is generally considered as an unimportant term and often neglected conventionally. In this study the impact of the term on the solutions is investigated by giving it some suitable values, then observing the solutions of the equations and evaluating its importance.

Because the contribution of each of the terms in the exact momentum equation is related to the downstream boundary condition, a nondimensional flow depth at the downstream boundary, $h_{d*} = h_d/h_0$ is introduced in this study and used as a variable to detect the relationship between the contributions of terms and the downstream boundary condition. Its values can be determined according to the following rules: (a) For the convectively decelerating type backwater profiles, the value of h_{d*} should be greater than unity and less than $1 + (S_0L/h_0)$. In order to ensure that there is no supercritical flow, the value of h_{d*} used should be sufficiently greater than unity. Hence, the values of h_{d*} are chosen from 1.44 to 2.53. (b) For the convectively accelerating type backwater profiles, the values of h_{d*} should be less than unity and greater than the nondimensional critical depth corresponding to a certain channel slope, S_0. In this study, five values of h_{d*}, from 0.31 to 1.0, are selected. At this time, it should be remarked that in a simulation run with changing time the value of h_{d*} is not constant. As the unsteady inflow at the upstream is entering into the channel, the hydrograph of h_{d*} at the downstream boundary will gradually vary from the initial given value of h_{d*} to a certain

value, then return back to the given value of h_{d*}, i.e., the hydrograph of h_{d*} consists of a rising limb and a receding one. Corresponding to a given upstream inflow, by using the critical depth formula, the value of h_{d*} at each time increment can be calculated.

4.8. Consideration and Organization of Test Runs

As just discussed, because S_0 and h_d/h_0 are also independent variables to be investigated, in addition to the coefficients, ß, k and k', there are five independent variables to be tested, namely, ß, k, (k-k'), S_0 and h_d/h_0. A summary of the test ranges of these variables is given in Table 4.1.

Table 4.1 Summary of Values of Variables Tested

Variable	Values
ß	1 1.33 2
k	0.95 0.99 1 1.01 1.05
k-k'	0.05 0 -0.05
S_0	0.00019 0.00057 0.00095 0.00114
h_d/h_0	1.44 1.66 1.80 2.02 2.53 (for convectively decelerating type profiles)
	0.31 0.50 0.70 0.80 1.00 (for convectively accelerating type profiles)

From the table it can be calculated that the total number of combinations of these variables is equal to (3 * 5 * 3 * 4 * 5) * 2 = 1800. Among these there are (1 * 1 * 1 * 4 * 5) * 2 = 40 cases where ß, k and k' are equal to unity while S_0 and h_d/h_0 are assumed to have different values, i.e., the cases of the Saint-Venant

equations. As mentioned in section 4.1, this study also compares Eqs. (4.3) and (4.4) in which the dependent variables are flow depth, h, and velocity, V, with Eqs. (4.5) and (4.6) in which the dependent variables are discharge, Q, and flow depth, h. Thus, the total number of combinations investigating the impacts of these coefficients, channel slope, and downstream boundary condition on the solutions of the equations expands to 2*1800 as the two forms (h, V vs. h, Q) of the equations are tested. Obviously, it is impractical and unnecessary to perform all the 3600 test runs. Therefore, two strategies are carried out in this study: (a) The combinations of these variables are chosen efficiently and reasonably. First, the situations that ß = 1 and the values of h_d/h_0 being equal to 1.44, 1.80 and 2.53 (corresponding to the convectively decelerating type profiles) are selected as representative while different values of other variables, k, k' and S_0, are investigated for wide rectangular channels (this means that only 1 * 5 * 3 * 4 * 3 = 180 test runs will be processed). By summarizing these results and observing a trend it is possible to use less than 180 test runs to achieve the required investigations for the cases of ß being equal to 1.33 and 2, for other cross-sectional shapes of the channel, and for the convectively accelerating type profiles. (b) The exact momentum and continuity equations in the form of h and V are regarded as primary equations, i.e., they are studied completely using the numerical procedure described above. Then, based on the results of the equations in the form of h and V, the exact momentum and continuity equations in the form of Q and h are further selectively investigated.

5. IMPORTANCE OF COEFFICIENTS INVOLVED IN EXACT MOMENTUM EQUATION

There is a large amount of results of flow depth, h, and flow velocity, V, or discharge, Q, generated for the sets of test runs described in Chapter 4. The difference between the solutions of the exact momentum and continuity equations and the Saint-Venant equations for the same flow and boundary conditions is given by subtracting the solution of the latter from that of the former at each distance-time increment. There are 55 distance increments and 100 time increments in each run. For simplicity and convenience, only the maximum absolute solution difference (the maximum value among all the differences at different space and time points in a run) and the maximum relative solution difference (the maximum absolute solution difference divided by the corresponding value of the solution of the Saint-Venant equations) are chosen as indices for comparison and discussion, and they are designated as MASD and MRSD, respectively. From the numerous calculations and comparisons the impacts of the coefficients, ß, k and k', on the solutions of the equations can be detected.

5.1. Wide Rectangular Channel

The results obtained from the equations in the form of flow depth, h, and velocity, V, for the simple case of a wide rectangular channel will be described in detail. The results are first presented for subcritical flow with an initial M1-type water surface profile. Later, the results for rectangular and trapezoidal channels and for initially M2-type profiles as well as

the results obtained from the equations in the form of h and Q will be depicted in two special sections and one chapter.

5.1.1. Impacts of k and k'

The impacts of the pressure correction coefficients, k and k', on the solutions of h and V of the exact momentum and continuity equations are summarized in Tables 5.1 through 5.4, in which two channel slopes, S_0 = 0.00019 and 0.00095, are chosen as examples. The zero values of MASD or MRSD for h/h_0 and V/V_0 in the tables imply that the solutions of the exact momentum and continuity equations are essentially the same as those of the Saint-Venant equations. The results for the case of S_0 = 0.00019 are also shown graphically in Figs. 5.1 through 5.4.

In Tables 5.1 and 5.2, k is varied from 0.95 to 1.05 while the values of ß and k' are fixed at unity, with or without downstream backwater effect. In reality, it is impossible that only k varies while ß and k' are kept constant. In natural rivers the three coefficients change simultaneously. However, investigating the simple situation is fundamental, i.e., first study the basic sensitivity of each of the coefficients, then the complex situations. From Tables 5.1 and 5.2, it is found that the maximum absolute or relative differences of h/h_0 are close to those of V/V_0 in magnitude as the water depth at the downstream boundary h/h_0 is small and the channel slope is large. If the downstream-boundary depth becomes large and the channel slope is small the distinction between the maximum absolute or relative differences of h/h_0 and those of V/V_0 increases. This indicates that the impact of k on

Table 5.1 Impact of Pressure Correction Coefficient k on Maximum Solution Difference of Flow Depth

(a) Absolute Difference

S_0=0.00019 ß=1, k'=1	No backwater effect	1.44	1.66	h_d/h_0= 1.80	2.02	2.53
	Maximum absolute solution difference of h/h_0					
k = 0.95	-0.0036	0.0274	-0.0250	-0.0361	-0.0547	-0.0874
k = 0.99	-0.0007	0.0052	-0.0051	-0.0072	-0.0107	-0.0164
k = 1	0.0000	0.0000	0.0000	0.0000	0.0000	0.0000
k = 1.01	0.0007	-0.0051	0.0051	0.0073	0.0106	0.0159
k = 1.05	0.0035	-0.0243	0.0259	0.0361	0.0513	0.0750
	Rate of change of solution difference with respect to k in %					
k varies 5% (0.95 to 1)	+7	-55	+50	+72	+109	+175
k varies 1% (0.99 to 1)	+7	-52	+51	+72	+107	+164
k varies 1% (1 to 1.01)	+7	-51	+51	+73	+106	+159
k varies 5% (1 to 1.05)	+7	-49	+52	+72	+103	+150

S_0=0.00095 ß=1, k'=1	No backwater effect	1.44	1.66	h_d/h_0= 1.80	2.02	2.53
	Maximum absolute solution difference of h/h_0					
k = 0.95	0.0019	0.0015	0.0017	0.0018	0.0022	-0.0066
k = 0.99	0.0006	0.0005	0.0006	0.0006	0.0009	-0.0022
k = 1	0.0000	0.0000	0.0000	0.0000	0.0000	0.0000
k = 1.01	-0.0003	-0.0002	-0.0003	-0.0003	0.0003	0.0029
k = 1.05	-0.0008	-0.0013	-0.0019	-0.0019	0.0020	0.0110
	Rate of change of solution difference with respect to k in %					
k varies 5% (0.95 to 1)	-4	-3	-3	-4	-4	+13
k varies 1% (0.99 to 1)	-6	-5	-6	-6	-9	+22
k varies 1% (1 to 1.01)	-3	-2	-3	-3	+3	+29
k varies 5% (1 to 1.05)	-2	-3	-4	-4	+4	+22

Table 5.1 (continued)

(b) Relative Difference

S_0=0.00019 ß=1, k'=1	No backwater effect	1.44	1.66	h_d/h_0= 1.80	2.02	2.53
	Maximum relative solution difference of h/h_0 in %					
k = 0.95	-0.29	1.44	-2.24	-3.13	-4.33	-6.03
k = 0.99	-0.06	0.27	-0.45	-0.62	-0.84	-1.01
k = 1	0.00	0.00	0.00	0.00	0.00	0.00
k = 1.01	0.06	-0.27	0.46	0.63	0.84	0.98
k = 1.05	0.29	-1.27	2.32	3.12	4.08	5.88
	Rate of change of solution difference with respect to k in %					
k varies 5% (0.95 to 1)	+6	-29	+45	+63	+87	+121
k varies 1% (0.99 to 1)	+6	-27	+45	+62	+84	+101
k varies 1% (1 to 1.01)	+6	-27	+46	+63	+84	+98
k varies 5% (1 to 1.05)	+6	-25	+46	+62	+82	+118

S_0=0.00095 ß=1, k'=1	No backwater effect	1.44	1.66	h_d/h_0= 1.80	2.02	2.53
	Maximum relative solution difference of h/h_0 in %					
k = 0.95	0.19	0.15	0.16	0.18	0.22	-0.51
k = 0.99	0.07	0.05	0.06	0.06	0.09	-0.20
k = 1	0.00	0.00	0.00	0.00	0.00	0.00
k = 1.01	-0.03	-0.01	-0.01	-0.01	0.02	0.29
k = 1.05	-0.08	-0.06	-0.08	-0.09	0.14	1.09
	Rate of change of solution difference with respect to k in %					
k varies 5% (0.95 to 1)	-4	-3	-3	-4	-4	+10
k varies 1% (0.99 to 1)	-7	-5	-6	-6	-9	+20
k varies 1% (1 to 1.01)	-3	-1	-1	-1	+2	+29
k varies 5% (1 to 1.05)	-2	-1	-2	-2	+3	+22

Table 5.2 Impact of k on Maximum Solution Difference of Flow Velocity

(a) Absolute Difference

S_0=0.00019 ß=1, k'=1	No backwater effect	h_d/h_0= 1.44	1.66	1.80	2.02	2.53
	Maximum absolute solution difference of V/V_0					
k = 0.95	-0.0081	-0.0294	0.0244	0.0353	0.0533	0.0998
k = 0.99	-0.0016	-0.0057	0.0053	0.0074	0.0109	0.0224
k = 1	0.0000	0.0000	0.0000	0.0000	0.0000	0.0000
k = 1.01	0.0016	0.0057	-0.0049	-0.0072	-0.0120	-0.0238
k = 1.05	0.0080	0.0275	-0.0262	-0.0374	-0.0602	-0.1169
	Rate of change of solution difference with respect to k in %					
k varies 5% (0.95 to 1)	+16	+59	-49	-71	-107	-200
k varies 1% (0.99 to 1)	+16	+57	-53	-74	-109	-224
k varies 1% (1 to 1.01)	+16	+57	-49	-72	-120	-238
k varies 5% (1 to 1.05)	+16	+55	-52	-75	-120	-234

S_0=0.00095 ß=1, k'=1	No backwater effect	h_d/h_0= 1.44	1.66	1.80	2.02	2.53
	Maximum absolute solution difference of V/V_0					
k = 0.95	-0.0006	-0.0013	-0.0013	-0.0012	-0.0012	0.0064
k = 0.99	-0.0001	-0.0003	-0.0002	-0.0002	-0.0002	0.0025
k = 1	0.0000	0.0000	0.0000	0.0000	0.0000	0.0000
k = 1.01	0.0001	0.0003	0.0002	0.0002	-0.0003	-0.0029
k = 1.05	0.0006	0.0013	0.0013	0.0013	-0.0019	-0.0101
	Rate of change of solution difference with respect to k in %					
k varies 5% (0.95 to 1)	+1	+3	+3	+2	+2	-13
k varies 1% (0.99 to 1)	+1	+3	+2	+2	+2	-25
k varies 1% (1 to 1.01)	+1	+3	+2	+2	-3	-29
k varies 5% (1 to 1.05)	+1	+3	+3	+3	-4	-20

Table 5.2 (continued)

(b) Relative Difference

S_0=0.00019 ß=1, k'=1	No backwater effect	1.44	1.66	h_d/h_0= 1.80	2.02	2.53
	Maximum relative solution difference of V/V_0 in %					
k = 0.95	-0.58	-1.46	3.53	4.03	6.67	16.25
k = 0.99	-0.11	-0.28	0.77	0.84	1.37	3.65
k = 1	0.00	0.00	0.00	0.00	0.00	-0.00
k = 1.01	0.12	0.28	-0.54	-0.83	-1.50	-3.88
k = 1.05	0.57	1.38	-2.86	-4.27	-7.53	-19.04
	Rate of change of solution difference with respect to k in %					
k varies 5% (0.95 to 1)	+12	+29	-71	-81	-133	-325
k varies 1% (0.99 to 1)	+11	+28	-77	-84	-137	-365
k varies 1% (1 to 1.01)	+12	+28	-54	-83	-150	-388
k varies 5% (1 to 1.05)	+11	+28	-57	-85	-151	-381

S_0=0.00095 ß=1, k'=1	No backwater effect	1.44	1.66	h_d/h_0= 1.80	2.02	2.53
	Maximum relative solution difference of V/V_0 in %					
k = 0.95	-0.05	-0.08	-0.10	-0.10	-0.12	0.64
k = 0.99	-0.01	-0.02	-0.02	-0.02	-0.02	0.25
k = 1	0.00	0.00	0.00	0.00	0.00	0.00
k = 1.01	0.01	0.02	0.02	0.02	-0.02	-0.29
k = 1.05	0.05	0.08	0.08	0.08	-0.16	-1.01
	Rate of change of solution difference with respect to k in %					
k varies 5% (0.95 to 1)	+1	+2	+2	+2	+2	-13
k varies 1% (0.99 to 1)	+1	+2	+2	+2	+2	-25
k varies 1% (1 to 1.01)	+1	+2	+2	+2	-2	-29
k varies 5% (1 to 1.05)	+1	+2	+2	+2	-3	-20

Table 5.3 Impact of Pressure Correction Coefficient k' on Maximum Solution Difference of Flow Depth

(a) Absolute Difference

S_0=0.00019 ß=1, k=1	No backwater effect	1.44	1.66	h_d/h_0= 1.80	2.02	2.53
	Maximum absolute solution difference of h/h_0					
k' = 0.95	0.0018	-0.0125	0.0130	0.0182	0.0262	0.0440
k' = 0.99	0.0004	-0.0026	0.0026	0.0036	0.0053	0.0081
k' = 1	0.0000	0.0000	0.0000	0.0000	0.0000	0.0000
k' = 1.01	-0.0004	0.0026	-0.0026	-0.0036	-0.0053	-0.0081
k' = 1.05	-0.0018	0.0133	-0.0126	-0.0181	-0.0269	-0.0467
	Rate of change of solution difference with respect to k'in %					
k'varies 5% (0.95 to 1)	-4	+25	-26	-36	-52	-88
k'varies 1% (0.99 to 1)	-4	+26	-26	-36	-53	-81
k'varies 1% (1 to 1.01)	-4	+26	-26	-36	-53	-81
k'varies 5% (1 to 1.05)	-4	+27	-25	-36	-54	-93

S_0=0.00095 ß=1, k=1	No backwater effect	1.44	1.66	h_d/h_0= 1.80	2.02	2.53
	Maximum absolute solution difference of h/h_0					
k' = 0.95	-0.0005	-0.0005	-0.0008	-0.0009	0.0008	0.0045
k' = 0.99	-0.0001	-0.0001	-0.0002	-0.0002	0.0001	0.0014
k' = 1	0.0000	0.0000	0.0000	0.0000	0.0000	0.0000
k' = 1.01	0.0003	0.0003	0.0003	0.0004	0.0005	-0.0012
k' = 1.05	0.0011	0.0008	0.0009	0.0010	0.0015	-0.0047
	Rate of change of solution difference with respect to k'in %					
k'varies 5% (0.95 to 1)	+1	+1	+2	+2	-2	-9
k'varies 1% (0.99 to 1)	+1	+1	+2	+2	-1	-14
k'varies 1% (1 to 1.01)	+3	+3	+3	+4	+5	-12
k'varies 5% (1 to 1.05)	+2	+2	+2	+2	+3	-9

Table 5.3 (continued)

(b) Relative Difference

S_0=0.00019 ß=1, k=1	No backwater effect	1.44	1.66	h_d/h_0= 1.80	2.02	2.53
	Maximum relative solution difference of h/h_0 in %					
k' = 0.95	0.15	-0.66	1.16	1.57	2.08	3.04
k' = 0.99	0.03	-0.13	0.23	0.31	0.42	0.50
k' = 1	0.00	0.00	0.00	0.00	0.00	0.00
k' = 1.01	-0.03	0.14	-0.23	-0.31	-0.42	-0.50
k' = 1.05	-0.14	0.70	-1.13	-1.55	-2.13	-3.23
	Rate of change of solution difference with respect to k'in %					
k'varies 5% (0.95 to 1)	-3	+13	-23	-31	-42	-61
k'varies 1% (0.99 to 1)	-3	+13	-23	-31	-42	-50
k'varies 1% (1 to 1.01)	-3	+14	-23	-31	-42	-50
k'varies 5% (1 to 1.05)	-3	+14	-23	-31	-43	-65

S_0=0.00095 ß=1, k=1	No backwater effect	1.44	1.66	h_d/h_0= 1.80	2.02	2.53
	Maximum relative solution difference of h/h_0 in %					
k' = 0.95	-0.05	-0.02	-0.04	-0.04	0.06	0.44
k' = 0.99	-0.01	-0.00	-0.02	-0.02	0.01	0.14
k' = 1	0.00	0.00	0.00	0.00	0.00	0.00
k' = 1.01	0.02	0.03	0.03	0.04	0.06	-0.11
k' = 1.05	0.11	0.08	0.09	0.10	0.15	-0.47
	Rate of change of solution difference with respect to k'in %					
k'varies 5% (0.95 to 1)	+1	+0	+1	+1	-1	-9
k'varies 1% (0.99 to 1)	+1	+0	+2	+2	-1	-14
k'varies 1% (1 to 1.01)	+2	+3	+3	+4	+6	-11
k'varies 5% (1 to 1.05)	+2	+2	+2	+2	+3	-9

Table 5.4 Impact of k' on Maximum Solution Difference of Flow Velocity

(a) Absolute Difference

S_0=0.00019 ß=1, k=1	No backwater effect	1.44	1.66	h_d/h_0= 1.80	2.02	2.53
	Maximum absolute solution difference of V/V_0					
k' = 0.95	0.0040	0.0140	-0.0127	-0.0184	-0.0265	-0.0744
k' = 0.99	0.0008	0.0028	-0.0025	-0.0036	-0.0055	-0.0124
k' = 1	0.0000	0.0000	0.0000	0.0000	0.0000	0.0000
k' = 1.01	-0.0008	-0.0028	0.0024	0.0036	0.0057	0.0116
k' = 1.05	-0.0040	-0.0144	0.0126	0.0182	0.0269	0.0686
	Rate of change of solution difference with respect to k'in %					
k'varies 5% (0.95 to 1)	-8	-28	+25	+37	+53	+149
k'varies 1% (0.99 to 1)	-8	-28	+25	+36	+55	+124
k'varies 1% (1 to 1.01)	-8	-28	+24	+36	+57	+116
k'varies 5% (1 to 1.05)	-8	-29	+25	+36	+54	+137

S_0=0.00095 ß=1, k=1	No backwater effect	1.44	1.66	h_d/h_0= 1.80	2.02	2.53
	Maximum absolute solution difference of V/V_0					
k' = 0.95	0.0003	0.0007	0.0006	0.0006	-0.0008	-0.0085
k' = 0.99	0.0001	0.0001	0.0001	0.0001	-0.0001	-0.0014
k' = 1	0.0000	0.0000	0.0000	0.0000	0.0000	0.0000
k' = 1.01	-0.0001	-0.0001	-0.0001	-0.0001	-0.0001	0.0014
k' = 1.05	-0.0003	-0.0007	-0.0006	-0.0006	-0.0006	0.0051
	Rate of change of solution difference with respect to k'in %					
k'varies 5% (0.95 to 1)	-1	-1	-1	-1	+2	+17
k'varies 1% (0.99 to 1)	-1	-1	-1	-1	+1	+14
k'varies 1% (1 to 1.01)	-1	-1	-1	-1	-1	+14
k'varies 5% (1 to 1.05)	-1	-1	-1	-1	-1	+10

Table 5.4 (continued)

(b) Relative Difference

S_0=0.00019 ß=1, k=1	No backwater effect	1.44	1.66	h_d/h_0= 1.80	2.02	2.53
	Maximum relative solution difference of V/V_0 in %					
k' = 0.95	0.29	0.70	-1.38	-2.10	-3.31	-12.06
k' = 0.99	0.06	0.14	-0.27	-0.41	-0.69	-2.02
k' = 1	0.00	0.00	0.00	0.00	0.00	0.00
k' = 1.01	-0.06	-0.14	0.26	0.41	0.71	1.89
k' = 1.05	-0.29	-0.72	1.37	2.07	3.36	11.13
	Rate of change of solution difference with respect to k'in %					
k'varies 5% (0.95 to 1)	-6	-14	+28	+42	+66	+241
k'varies 1% (0.99 to 1)	-6	-14	+27	+41	+69	+202
k'varies 1% (1 to 1.01)	-6	-14	+26	+41	+71	+189
k'varies 5% (1 to 1.05)	-6	-14	+27	+41	+67	+223

S_0=0.00095 ß=1, k=1	No backwater effect	1.44	1.66	h_d/h_0= 1.80	2.02	2.53
	Maximum relative solution difference of V/V_0 in %					
k' = 0.95	0.02	0.04	0.04	0.04	-0.06	-0.86
k' = 0.99	0.01	0.01	0.01	0.01	-0.01	-0.14
k' = 1	0.00	0.00	0.00	0.00	0.00	0.00
k' = 1.01	-0.01	-0.01	-0.01	-0.01	-0.01	0.14
k' = 1.05	-0.02	-0.04	-0.05	-0.05	-0.06	0.50
	Rate of change of solution difference with respect to k'in %					
k'varies 5% (0.95 to 1)	-0	-1	-1	-1	+1	+17
k'varies 1% (0.99 to 1)	-1	-1	-1	-1	+1	+14
k'varies 1% (1 to 1.01)	-1	-1	-1	-1	-1	+14
k'varies 5% (1 to 1.05)	-0	-1	-1	-1	-1	+10

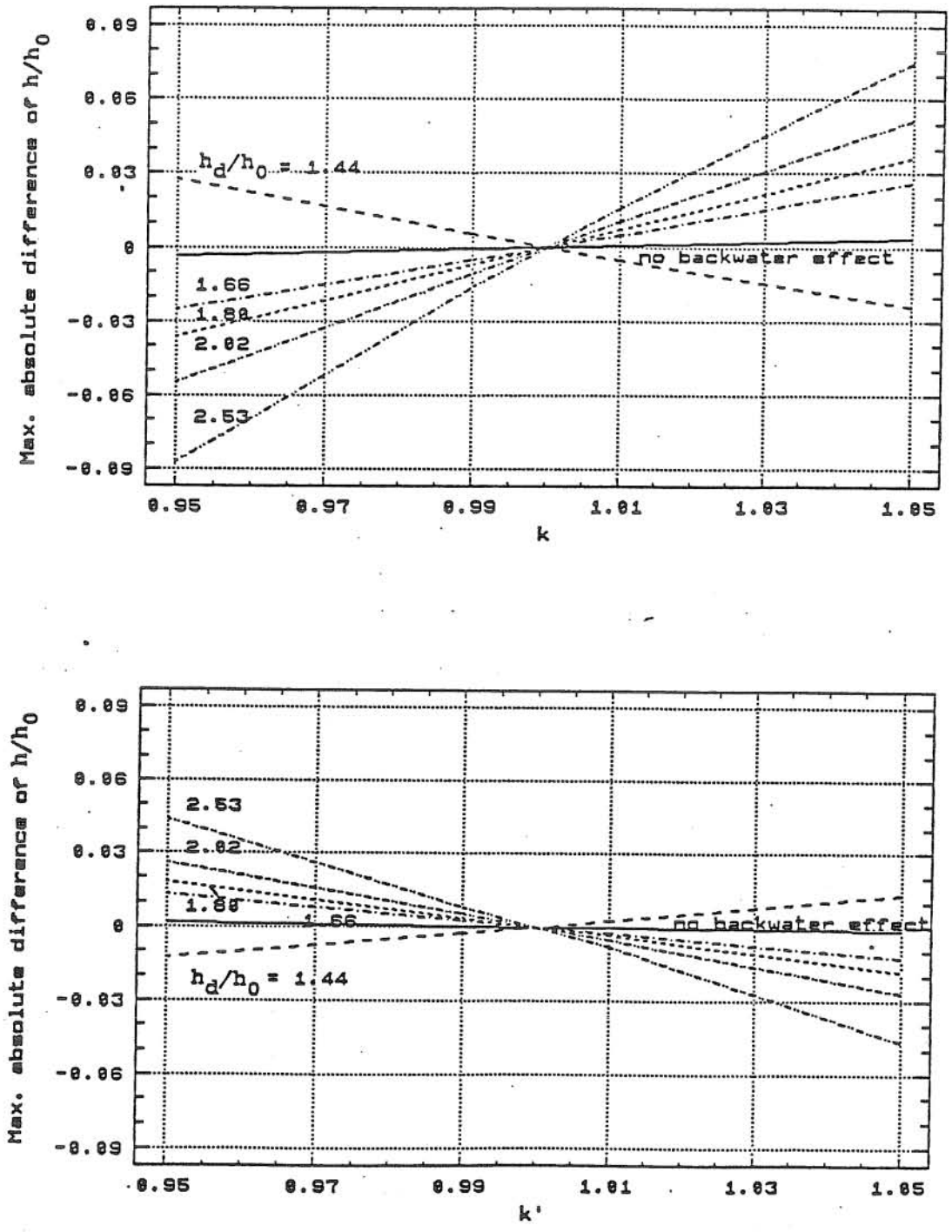

(a) Absolute Difference

Fig. 5.1 Variation of Maximum Solution Difference of h/h_0 with k and k' for S_0 = 0.00019

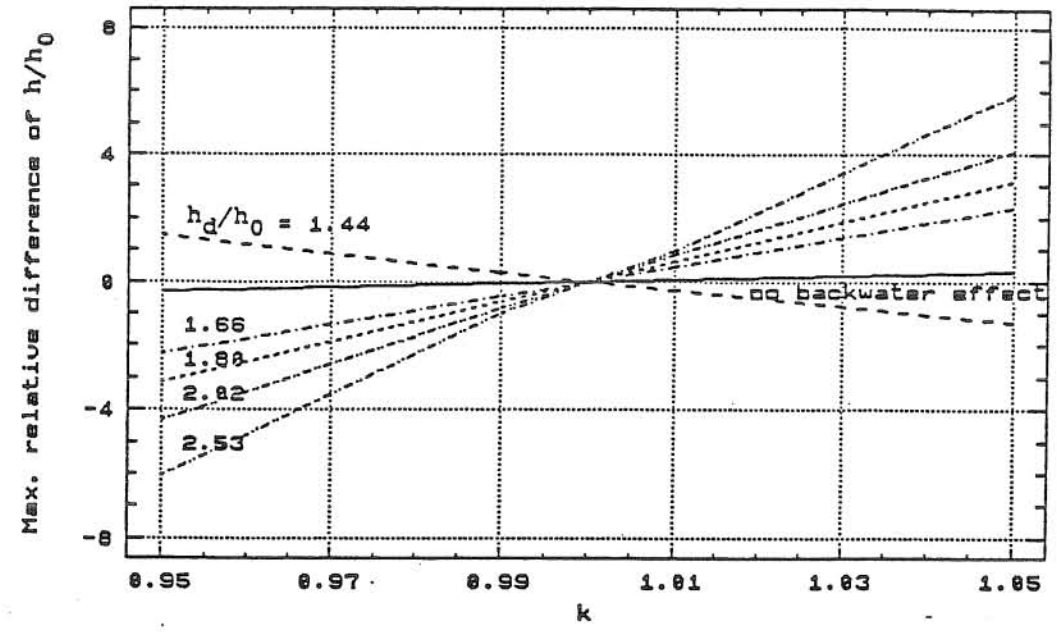

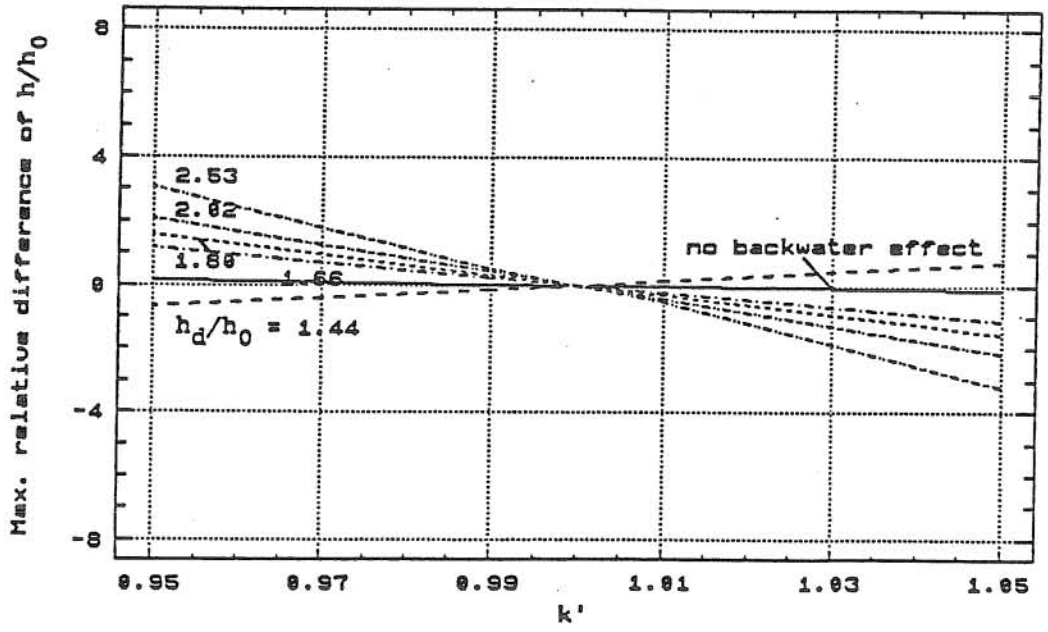

(b) Relative Difference

Fig. 5.1 (continued)

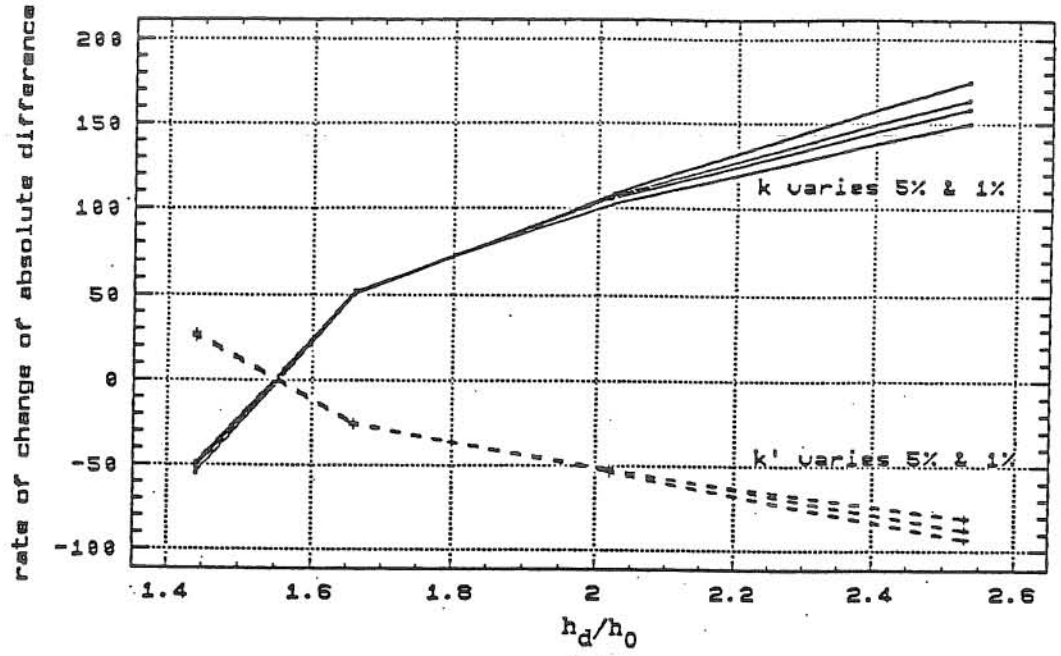

(a) Absolute Difference

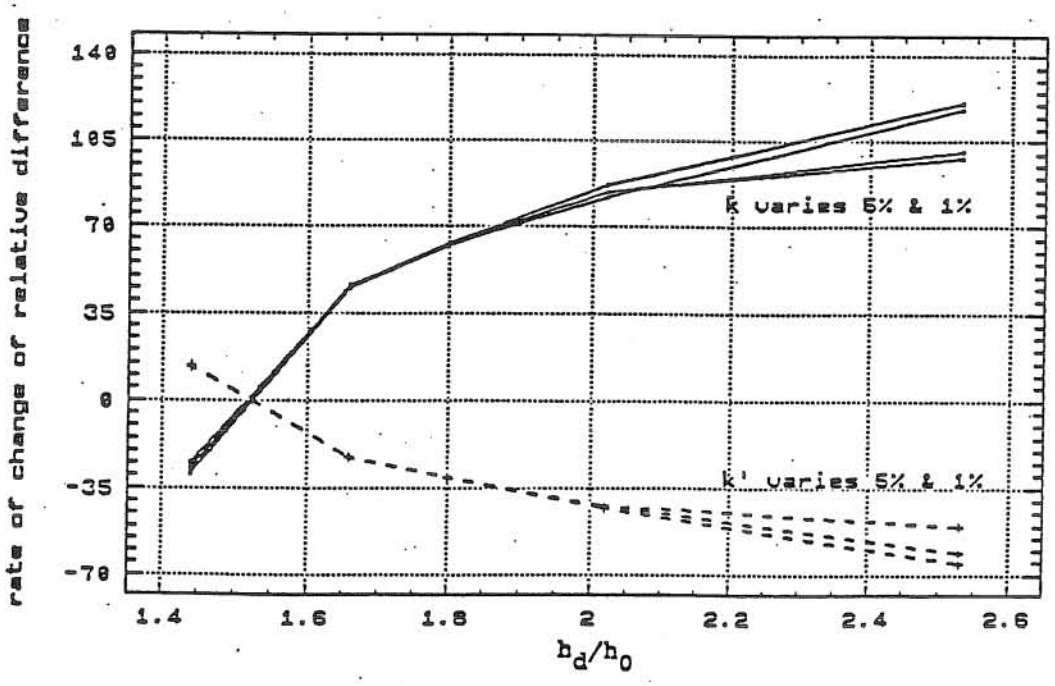

(b) Relative Difference

Fig. 5.2 Variation of Rate of Change of Maximum Solution Difference of h/h_0 with k and k'

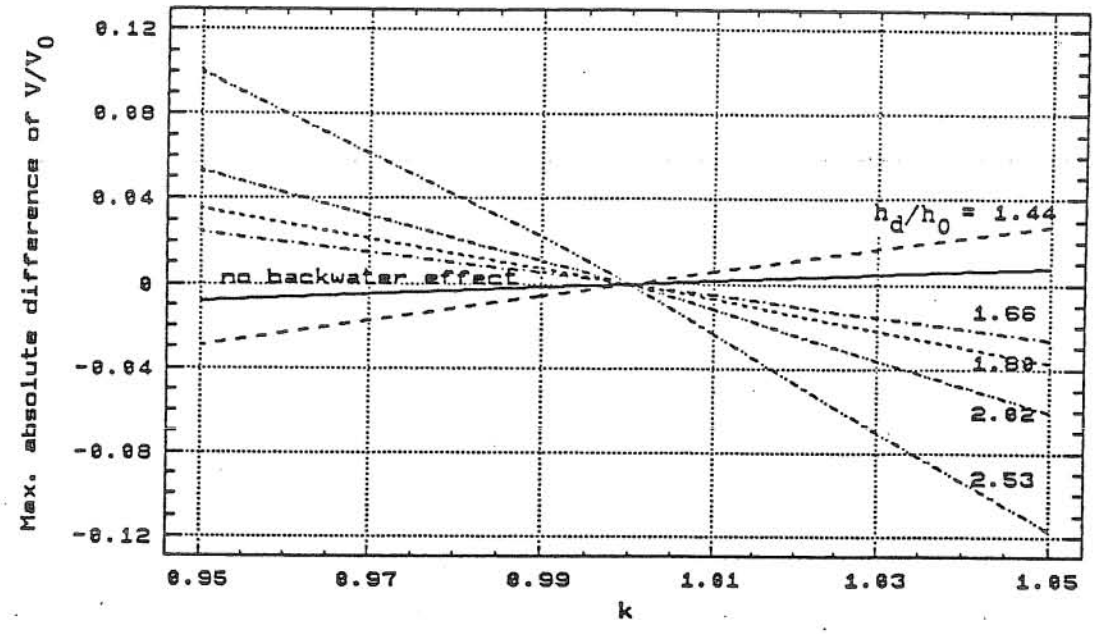

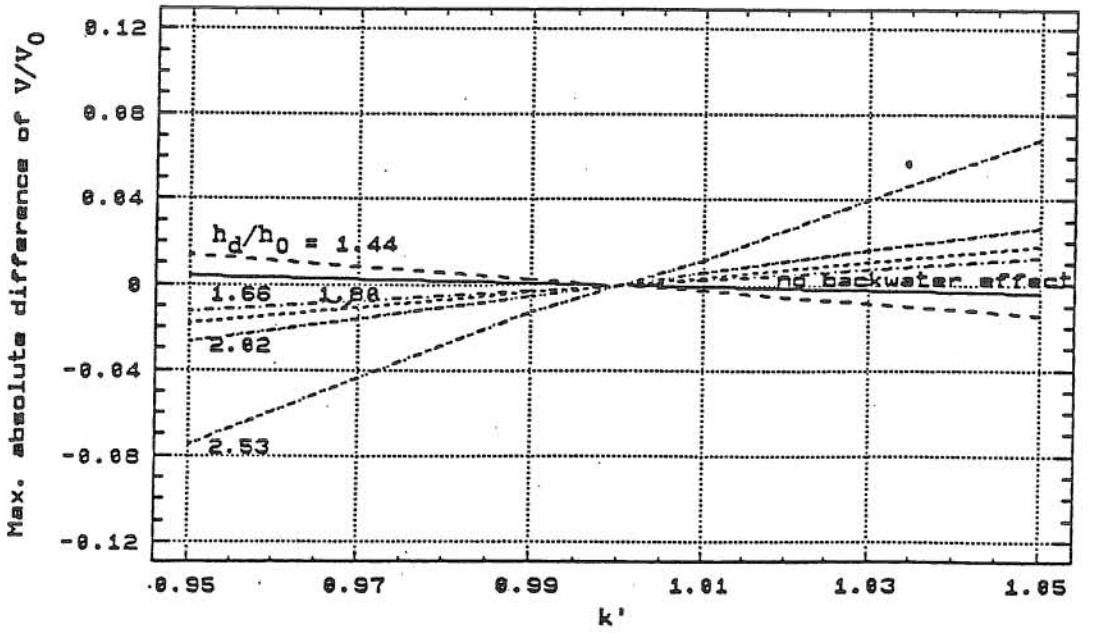

(a) Absolute Difference

Fig. 5.3 Variation of Maximum Solution Difference of V/V_0 with k and k' for $S_0 = 0.00019$

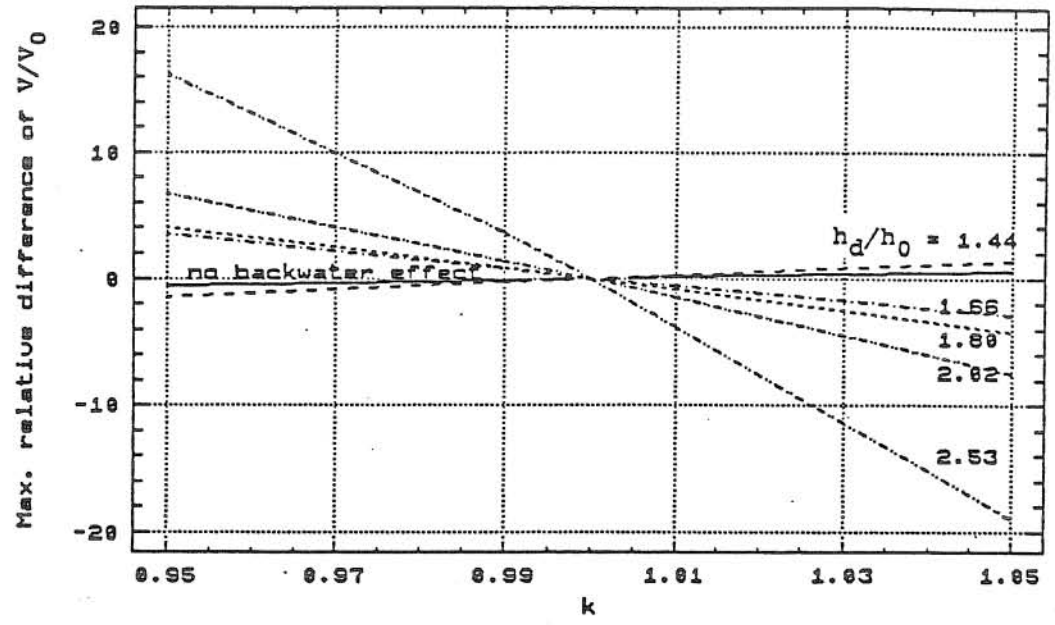

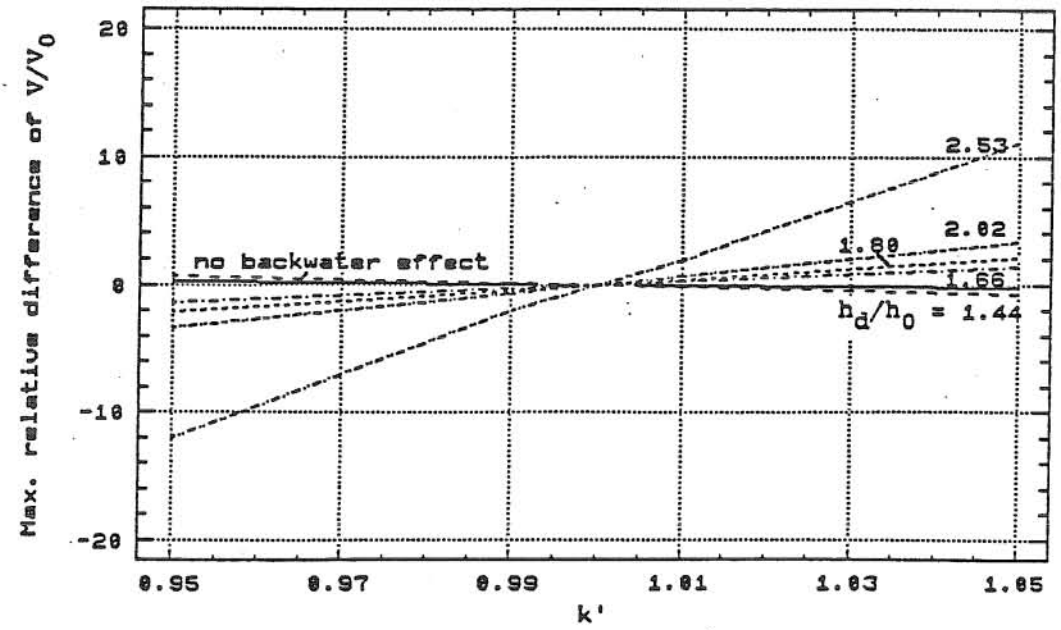

(b) Relative Difference

Fig. 5.3 (continued)

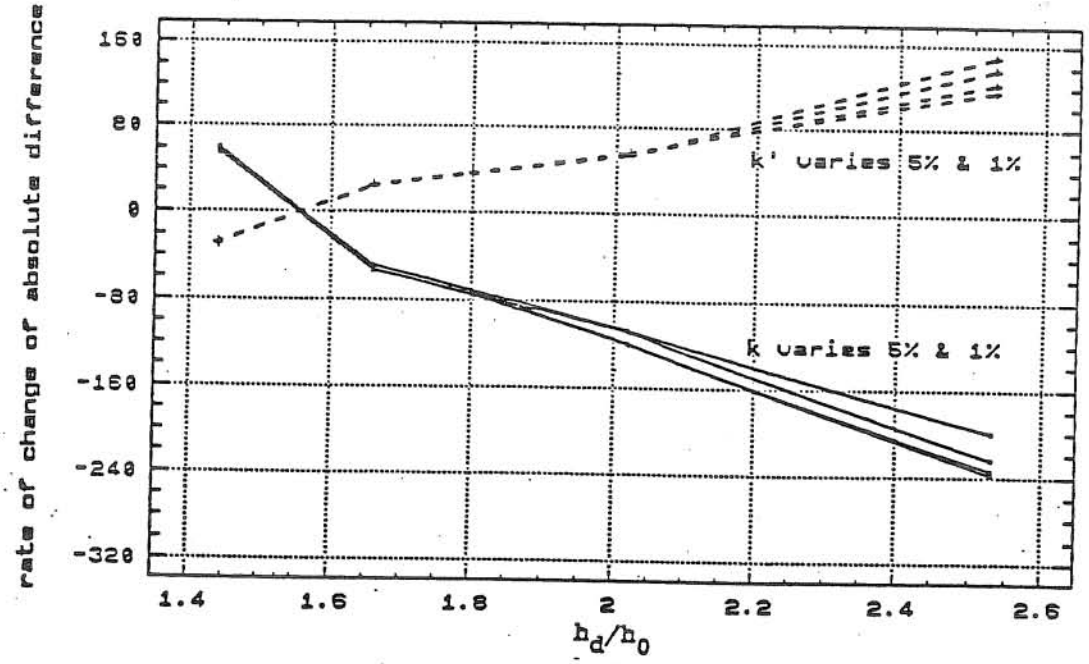

(a) Absolute Difference

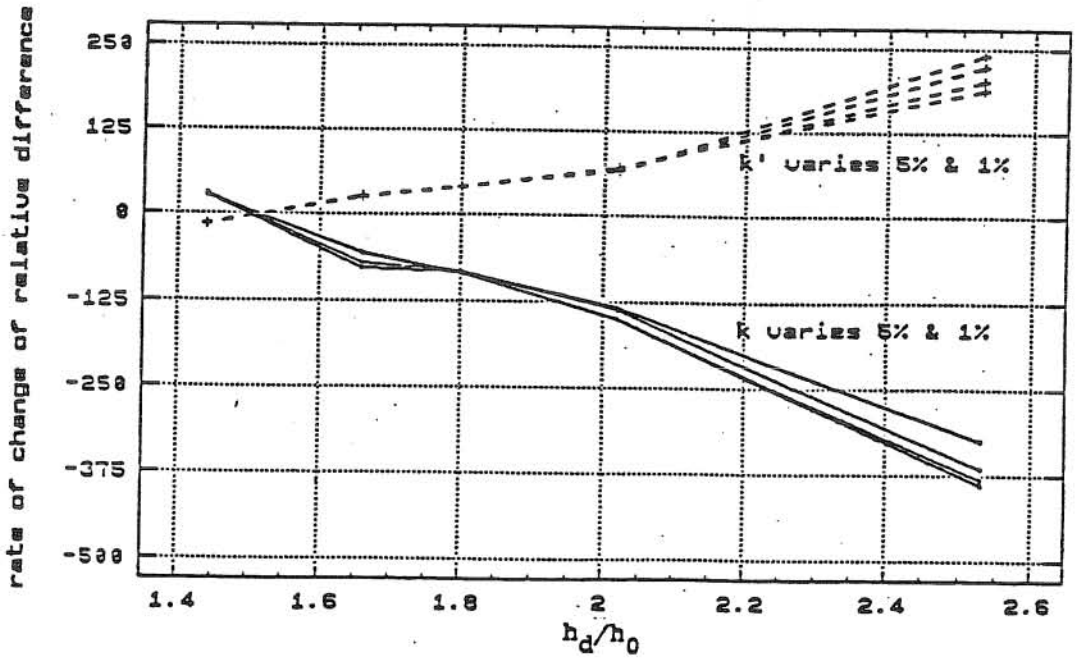

(b) Relative Difference

Fig. 5.4 Variation of Rate of Change of Maximum Solution Difference of V/V_0 with k and k'

the flow velocity, V, is more sensitive than on the flow depth, h, when the downstream water depth is large and the channel slope is small. In addition, these maximum absolute or relative solution differences of h/h_0 and V/V_0 for two extreme situations of nonhydrostatic pressure distribution (k = 0.95 and 1.05) are obviously much greater than those of near hydrostatic (k = 0.99 and 1.01). However, the average rates of change of MASD or MRSD of h/h_0 and V/V_0 with respect to k are approximately the same for S_0 = 0.00019 or 0.00095 with different downstream water depths, whether k varies 5% (from 1 to 0.95 or 1.05) or 1% (from 1 to 0.99 or 1.01).

In Tables 5.3 and 5.4, k' changes from 0.95 to 1.05 (i.e., k-k' from 0.05 to -0.05) while the values of ß and k are kept equal to unity for the range tested. The results show that the effect of k' on the solutions of h and V is qualitatively the same as for k, i.e., the impact of k' on the flow velocity is almost the same as on the flow depth for small downstream-boundary depth and large channel slope, but much greater than on the flow depth when the downstream-boundary depth becomes large and the channel slope is small. However, these maximum absolute or relative solution differences of h/h_0 and V/V_0 in Tables 5.3 and 5.4 are always roughly equal to half of the corresponding values in Tables 5.1 and 5.2, and the average rates of change of MASD or MRSD of nondimensional flow depth and flow velocity with respect to k' are also approximately half of those of k.

Therefore, the following six points can be concluded based on these tables and figures. First, the impact of k or k' on the

flow velocity, V, is greater than on the flow depth, h, when the downstream-boundary depth is large and the channel slope is small. Second, the impact of k on the solutions of the equations is about twice as large as that of k'. Third, the impacts of k and k' on the solutions are closely related to the downstream boundary condition. When there is no downstream backwater effect the impacts of k and k' on the solutions of the exact momentum and continuity equations are insignificant. With increasing downstream boundary water depth the impacts of k and k' on the solutions of the equations become more important and the Saint-Venant equations gradually become a less satisfactory approximation of the exact momentum equation. Fourth, in Tables 5.1 and 5.2 or Tables 5.3 and 5.4, it is shown that the impact of k or k' is channel-slope dependent. The impact is smaller for a steeper channel than for a milder one. Fifth, since the values of MASD or MRSD of h/h_0 and V/V_0 are very small as k is equal to 0.99 and 1.01, it is safe to assume that within this range the exact momentum and continuity equations can be replaced by the Saint-Venant equations. However, for the extreme nonhydrostatic pressure distributions (e.g., the cases of k = 0.95 and 1.05) such as the channels with sharply curved bed, the substitution using the Saint-Venant equations could create some errors. Finally, based on Figs. 5.1 and 5.3, a larger solution difference is related to k, the downstream-boundary depth and channel slope. As the channel slope is very small and the downstream water depth is very large, it is possible that there is a large error even though the value of k is close to unity, i.e., the pressure distribution is almost hydrostatic.

MASD and MRSD of the nondimensional flow depth, h/h_0, and velocity, V/V_0, for various channel slopes, downstream-boundary water depths and combinations of k and k' are presented in Tables 5.5 and 5.6. The two tables are based on $\beta = 1$ and only selected as representative to display the relationships between either k (or k') and the channel slope or k (or k') and the downstream boundary condition. If $\beta = 1.33$ or 2, the relationships among k (or k'), S_0 and h_d/h_0 are similar to those reflected in Tables 5.5 and 5.6 and they are not listed here.

From Tables 5.5 and 5.6, it is observed that for wide rectangular channels with identical channel slopes and downstream boundary conditions, but completely different combinations of k and k', the values of either MASD or MRSD of h/h_0 or V/V_0 are the same. For the coefficient values tested, there are three groups of coefficient combinations. The first is the case of $\beta = 1$, $k = 0.95$, $k' = 0.95$ and the case of $\beta = 1$, $k = 1$, $k' = 1.05$. The second is the case of $\beta = 1$, $k = 1$, $k' = 0.95$ and the case of $\beta = 1$, $k = 1.05$, $k' = 1.05$. The last is the case of $\beta = 1$, $k = 0.95$, $k' = 0.9$ and the case of $\beta = 1$, $k = 1.05$, $k' = 1.1$. In the last group, the meaning of zero value of either MASD or MRSD is that the solutions of the exact momentum and continuity equations and the approximate Saint-Venant equations are essentially the same, as has been mentioned previously.

This outcome indicates two facts. The first is that for a wide rectangular channel, although the flow conditions reflected by k and k' are different, the solutions of the exact momentum and continuity equations are the same in each group. The reason can

Table 5.5 Maximum Difference of h/h_0 between Solutions of Exact Momentum and Continuity Equations and Saint-Venant Equations

(a) Absolute Difference

ß = 1 Value of k & k'	h_d/h_0	Channel slope = 0.00019	0.00057	0.00095	0.00114
		Maximum absolute solution difference of h/h_0			
k=0.95, k'=1	1.44	0.0274	0.0129	0.0015	0.0010
	1.66	-0.0250	-0.0163	0.0017	0.0014
	1.80	-0.0361	-0.0269	0.0018	0.0014
	2.02	-0.0547	-0.0484	0.0022	0.0016
	2.53	-0.0874	-0.0780	-0.0066	0.0054
k=0.95, k'=0.95 & k=1, k'=1.05	1.44	0.0133	0.0066	0.0008	0.0006
	1.66	-0.0126	-0.0086	0.0009	0.0008
	1.80	-0.0181	-0.0140	0.0010	0.0009
	2.02	-0.0269	-0.0244	0.0015	0.0011
	2.53	-0.0467	-0.0419	-0.0047	0.0032
k=0.95, k'=0.9 & k=1.05, k'=1.1	1.44	0.0000	0.0000	0.0000	0.0000
	1.66	0.0000	0.0000	0.0000	0.0000
	1.80	0.0000	0.0000	0.0000	0.0000
	2.02	0.0000	0.0000	0.0000	0.0000
	2.53	0.0000	0.0000	0.0000	0.0000
k=1, k'=0.95 & k=1.05, k'=1.05	1.44	-0.0125	-0.0068	-0.0005	0.0004
	1.66	0.0130	0.0094	-0.0008	0.0003
	1.80	0.0182	0.0148	-0.0009	-0.0006
	2.02	0.0262	0.0249	0.0008	-0.0007
	2.53	0.0440	0.0390	0.0045	-0.0027
k=1.05, k'=1	1.44	-0.0243	-0.0137	-0.0013	0.0007
	1.66	0.0259	0.0197	-0.0019	0.0007
	1.80	0.0361	0.0305	-0.0019	0.0006
	2.02	0.0513	0.0494	0.0020	-0.0004
	2.53	0.0750	0.0724	0.0110	-0.0049

Table 5.5 (continued)

(b) Relative Difference

ß = 1 Value of k & k'	h_d/h_0	Channel slope = 0.00019	0.00057	0.00095	0.00114
		Maximum relative solution difference of h/h_0 in %			
k=0.95, k'=1	1.44	1.44	0.58	0.15	0.10
	1.66	-2.24	-1.57	0.16	0.13
	1.80	-3.13	-2.53	0.18	0.14
	2.02	-4.33	-4.25	0.22	0.16
	2.53	-6.03	-5.37	-0.51	0.53
k=0.95, k'=0.95 & k=1, k'=1.05	1.44	0.70	0.30	0.08	0.06
	1.66	-1.13	-0.83	0.09	0.08
	1.80	-1.55	-1.31	0.10	0.09
	2.02	-2.13	-2.14	0.15	0.11
	2.53	-3.23	-2.58	-0.47	0.32
k=0.95, k'=0.9 & k=1.05, k'=1.1	1.44	0.00	0.00	0.00	0.00
	1.66	0.00	0.00	0.00	0.00
	1.80	0.00	0.00	0.00	0.00
	2.02	0.00	0.00	0.00	0.00
	2.53	0.00	0.00	0.00	0.00
k=1, k'=0.95 & k=1.05, k'=1.05	1.44	-0.66	-0.30	-0.02	0.03
	1.66	1.16	0.91	-0.04	0.02
	1.80	1.57	1.39	-0.04	-0.06
	2.02	2.08	2.18	0.06	-0.07
	2.53	3.04	2.40	0.44	-0.27
k=1.05, k'=1	1.44	-1.27	-0.61	-0.06	0.07
	1.66	2.32	1.90	-0.08	0.07
	1.80	3.12	2.85	-0.09	0.06
	2.02	4.08	4.33	0.14	-0.02
	2.53	5.88	4.62	1.09	-0.49

Table 5.6 Maximum Difference of V/V_0 between Solutions of Exact Momentum and Continuity Equations and Saint-Venant Equations

(a) Absolute Difference

ß = 1 Value of k & k'	h_d/h_0	Channel slope = 0.00019	0.00057	0.00095	0.00114
		Maximum absolute solution difference of V/V_0			
k=0.95, k'=1	1.44	-0.0294	-0.0097	-0.0013	-0.0010
	1.66	0.0244	0.0156	-0.0013	-0.0009
	1.80	0.0353	0.0250	-0.0012	-0.0009
	2.02	0.0533	0.0395	-0.0012	-0.0009
	2.53	0.0998	0.0509	0.0064	-0.0046
k=0.95, k'=0.95 & k=1, k'=1.05	1.44	-0.0144	-0.0050	-0.0007	-0.0005
	1.66	0.0126	0.0081	-0.0006	-0.0004
	1.80	0.0182	0.0126	-0.0006	-0.0004
	2.02	0.0269	0.0194	-0.0006	-0.0004
	2.53	0.0686	0.0235	0.0051	-0.0027
k=0.95, k'=0.9 & k=1.05, k'=1.1	1.44	0.0000	0.0000	0.0000	0.0000
	1.66	0.0000	0.0000	0.0000	0.0000
	1.80	0.0000	0.0000	0.0000	0.0000
	2.02	0.0000	0.0000	0.0000	0.0000
	2.53	0.0000	0.0000	0.0000	0.0000
k=1, k'=0.95 & k=1.05, k'=1.05	1.44	0.0140	0.0051	0.0007	0.0006
	1.66	-0.0127	-0.0086	0.0006	0.0004
	1.80	-0.0184	-0.0128	0.0006	0.0004
	2.02	-0.0265	-0.0188	-0.0008	0.0004
	2.53	-0.0744	-0.0214	-0.0085	0.0028
k=1.05, k'=1	1.44	0.0275	0.0104	0.0013	0.0010
	1.66	-0.0262	-0.0177	0.0013	0.0009
	1.80	-0.0374	-0.0260	0.0013	0.0009
	2.02	-0.0602	-0.0374	-0.0019	0.0009
	2.53	-0.1169	-0.0413	-0.0101	0.0054

Table 5.6 (continued)

(b) Relative Difference

ß = 1 Value of k & k'	h_d/h_0	Channel slope = 0.00019	0.00057	0.00095	0.00114
		Maximum relative solution difference of V/V_0 in %			
k=0.95, k'=1	1.44	-1.46	-0.55	-0.08	-0.06
	1.66	3.53	1.61	-0.10	-0.07
	1.80	4.03	2.67	-0.10	-0.08
	2.02	6.67	4.50	-0.12	-0.09
	2.53	16.25	7.36	0.64	-0.46
k=0.95, k'=0.95 & k=1, k'=1.05	1.44	-0.72	-0.28	-0.04	-0.03
	1.66	1.37	0.84	-0.05	-0.03
	1.80	2.07	1.34	-0.05	-0.04
	2.02	3.36	2.21	-0.06	-0.04
	2.53	11.13	3.37	0.50	-0.27
k=0.95, k'=0.9 & k=1.05, k'=1.1	1.44	0.00	0.00	0.00	0.00
	1.66	0.00	0.00	0.00	0.00
	1.80	0.00	0.00	0.00	0.00
	2.02	0.00	0.00	0.00	0.00
	2.53	0.00	0.00	0.00	0.00
k=1, k'=0.95 & k=1.05, k'=1.05	1.44	0.70	0.29	0.04	0.04
	1.66	-1.38	-0.89	0.04	0.04
	1.80	-2.10	-1.37	0.04	0.04
	2.02	-3.31	-2.15	-0.06	0.04
	2.53	-12.06	-3.09	-0.86	0.28
k=1.05, k'=1	1.44	1.38	0.59	0.08	0.07
	1.66	-2.86	-1.83	0.08	0.07
	1.80	-4.27	-2.78	0.08	0.08
	2.02	-7.53	-4.26	-0.16	0.09
	2.53	-19.04	-5.97	-1.01	0.54

be found by inspecting Eq. (4.12). For a wide rectangular channel with $\beta = 1$, the coefficient of the term $\partial h_*/\partial x_*$ in Eq. (4.12) is $(2k - k')\cos\theta/F_0$. If the values of k and k' involved in each of the aforementioned three groups are substituted in the expression of $(2k - k')$, it is found that the values of $(2k - k')$ corresponding to the three groups are equal to 0.95, 1.05 and 1, respectively. This implies that for different combinations of k and k' as long as the value of $(2k - k')$ is equal to a certain value the solutions of the exact momentum and continuity equations are always the same. The second observation signifies that for wide rectangular channels, there is no difference between the solutions of the exact momentum and continuity equations and the Saint-Venant equations under certain flow conditions, namely, $\beta = 1$ and $(2k - k') = 1$. Under this condition, the Saint-Venant equations can safely replace the exact momentum and continuity equations without loosing accuracy. However, in reality, it is difficult to satisfy this condition because for viscous liquid in a channel, β is always greater than unity.

The impact of k on the solutions is approximately twice as large as that of k'. Therefore, k is an important coefficient for determining what kind of equations, i.e., the exact momentum and continuity equations or the Saint-Venant equations, can be used. It is obvious that for channels with extremely nonhydrostatic pressure distribution, small channel slope, and large downstream-boundary water depth, the difference between the solutions of the two sets of equations appears to be significant. For this condition, use of the exact momentum and continuity equations

provides more reliable results.

5.1.2. Impact of ß

The impact of the momentum correction coefficient ß on the solutions of the equations is presented in Tables 5.7 and 5.8, and also shown in Fig. 5.5 for an example with the channel slope, S_0 = 0.00019. Tables 5.7 and 5.8 are similar to Tables 5.1 and 5.2 and Tables 5.3 and 5.4, i.e., only ß varies while k and k' are kept equal to unity (as mentioned in section 5.1.1, varying ß alone is a fundamental study). The two tables and the figure demonstrate that as ß increases by 33%, from 1 to 1.33, and by 50%, from 1.33 to 2, respectively, the average rates of change of MASD or MRSD of h/h_0 and V/V_0 with respect to ß are very small for various downstream water depths. Therefore, the impact of ß on the solutions of the equations is much weaker than that of k or k'.

From Tables 5.7 and 5.8, it is similarly shown that, when there is no downstream backwater effect, the impact produced by changing the value of ß on the solutions becomes very small and can almost be completely ignored. When there is the downstream backwater effect the values of MASD or MRSD of h/h_0 or V/V_0 decrease with increasing downstream boundary water depth. This result is exactly opposite to that of k or k'. The reason is when the downstream water depth increases, the subcritical flow in a channel converts gradually from a less convectively decelerating condition to a more convectively decelerating one. From section 5.1.1, it seems that the solution difference is a function of the

Table 5.7 Impact of Momentum Correction Coefficient ß on Maximum Solution Difference of Flow Depth

(a) Absolute Difference

S_0=0.00019 k=1, k'=1	No backwater effect	h_d/h_0= 1.44	1.66	1.80	2.02	2.53
	Maximum absolute solution difference of h/h_0					
ß = 1	0.0000	0.0000	0.0000	0.0000	0.0000	0.0000
ß = 1.33	0.0009	0.0070	0.0043	0.0028	-0.0014	-0.0023
ß = 2	0.0028	0.0215	0.0133	0.0086	-0.0044	-0.0069
	Rate of change of solution difference with respect to ß in %					
ß varies 33% from 1 to 1.33	+0.2	+2	+1	+0.8	-0.4	-0.7
ß varies 50% from 1.33 to 2	+0.2	+2	+1	+0.9	-0.4	-0.7

(b) Relative Difference

S_0=0.00019 k=1, k'=1	No backwater effect	h_d/h_0= 1.44	1.66	1.80	2.02	2.53
	Maximum relative solution difference of h/h_0 in %					
ß = 1	0.00	0.00	0.00	0.00	0.00	0.00
ß = 1.33	0.08	0.36	0.22	0.14	-0.09	-0.12
ß = 2	0.23	1.11	0.67	0.42	-0.31	-0.35
	Rate of change of solution difference with respect to ß in %					
ß varies 33% from 1 to 1.33	+0.2	+1	+0.7	+0.4	-0.3	-0.4
ß varies 50% from 1.33 to 2	+0.2	+1	+0.7	+0.4	-0.3	-0.4

Table 5.8 Impact of ß on Maximum Solution Difference of Flow Velocity

(a) Absolute Difference

S_0=0.00019 k=1, k'=1	No backwater effect	1.44	1.66	h_d/h_0= 1.80	2.02	2.53
	Maximum absolute solution difference of V/V_0					
ß = 1	0.0000	0.0000	0.0000	0.0000	0.0000	0.0000
ß = 1.33	0.0023	-0.0085	-0.0054	-0.0038	0.0032	0.0035
ß = 2	0.0069	-0.0261	-0.0167	-0.0115	0.0096	0.0107
	Rate of change of solution difference with respect to ß in %					
ß varies 33% from 1 to 1.33	+1	-3	-2	-1	+1	+1
ß varies 50% from 1.33 to 2	+1	-3	-2	-1	+1	+1

(b) Relative Difference

S_0=0.00019 k=1, k'=1	No backwater effect	1.44	1.66	h_d/h_0= 1.80	2.02	2.53
	Maximum relative solution difference of V/V_0 in %					
ß = 1	0.00	0.00	0.00	0.00	0.00	0.00
ß = 1.33	0.16	-0.42	-0.28	-0.20	0.26	0.27
ß = 2	0.50	-1.29	-0.85	-0.60	0.80	0.81
	Rate of change of solution difference with respect to ß in %					
ß varies 33% from 1 to 1.33	+0.5	-1	-0.9	-0.6	+0.8	+0.8
ß varies 50% from 1.33 to 2	+0.7	+1	-0.9	-0.6	+0.8	+0.8

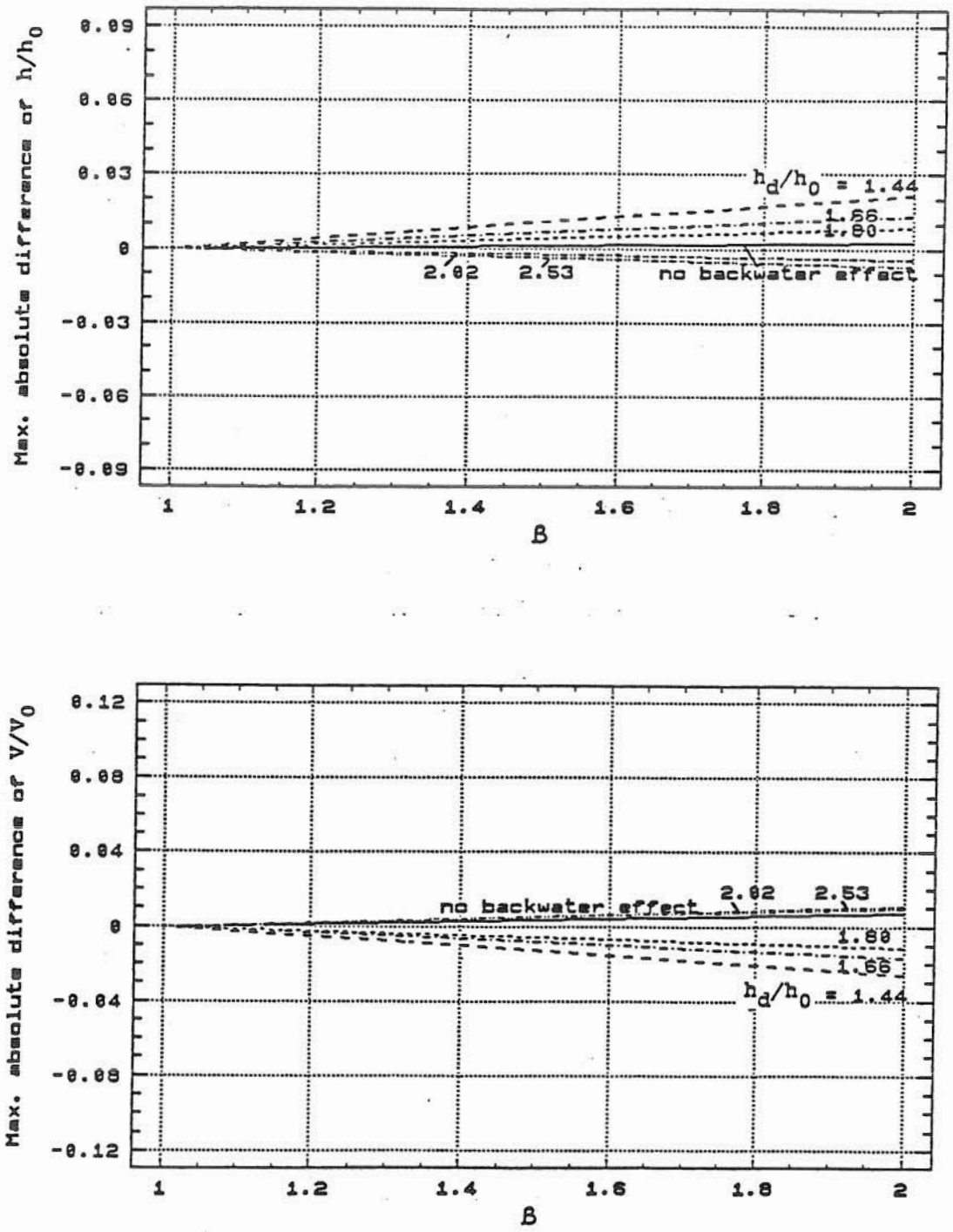

(a) Absolute Difference

Fig. 5.5 Variation of Maximum Solution Difference of h/h_0 and V/V_0 with β for $S_0 = 0.00019$

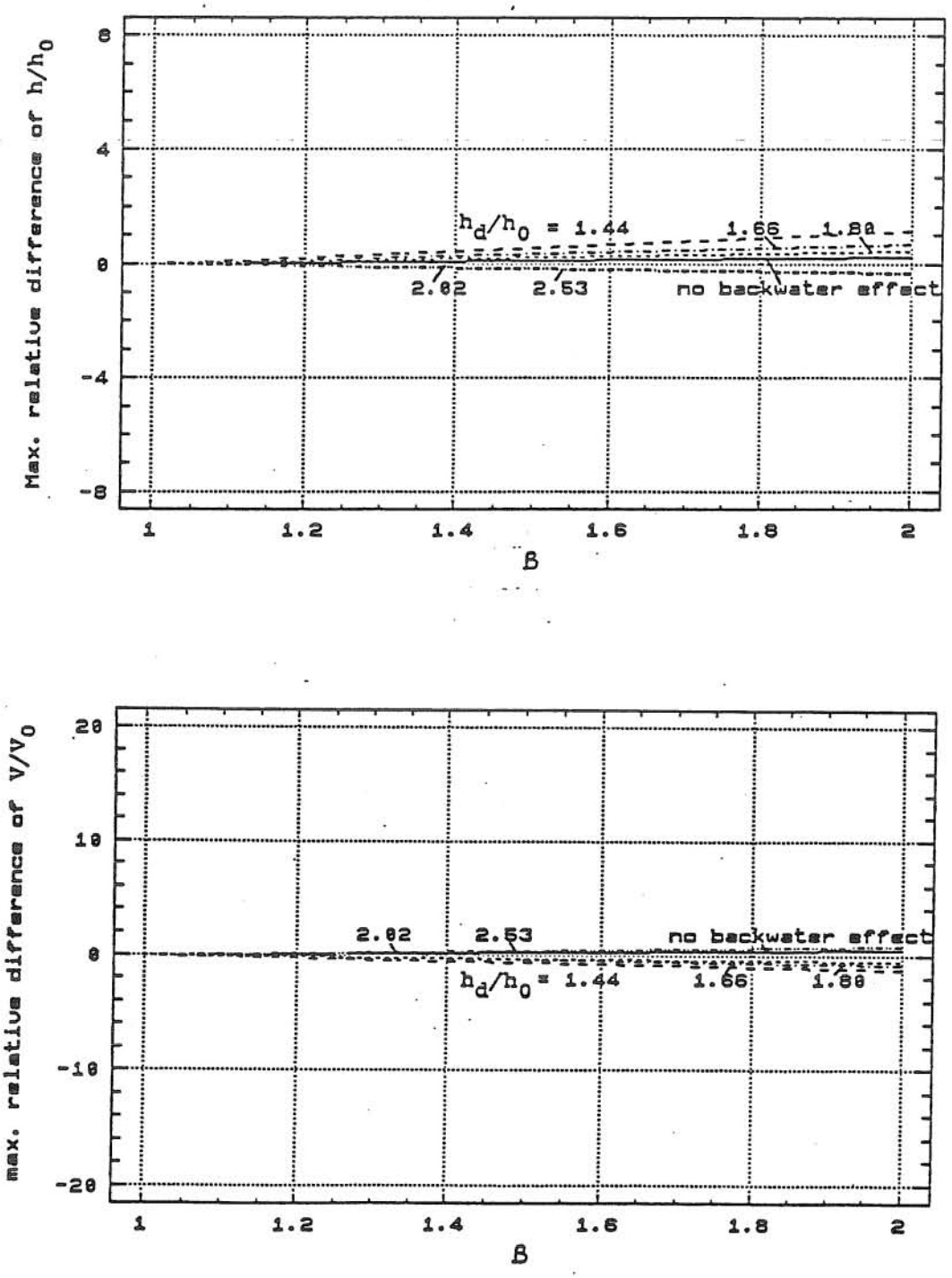

(b) Relative Difference

Fig. 5.5 (continued)

extent of the convective deceleration, i.e., the greater the extent of the convective deceleration (or the stronger the backwater effect), the larger the solution difference. However, ß is a momentum correction coefficient for a given channel, it is closely related to the convective acceleration, and its value decreases with flow deceleration. In other words, the impact of ß on the solutions is opposite to that of the convective deceleration. It is likely that the effect of ß on flow is stronger than that of the convective deceleration for the less convectively decelerating condition. Therefore, for ß, the solution difference increases with lowering downstream-boundary water depth. In addition, from Tables 5.7 and 5.8, it is obvious that similar to k and k', the impact of ß on the flow velocity is also greater than on the flow depth.

Of course, the impact of ß on the solutions of the equations exists, since the values of MASD or MRSD of the nondimensional flow depth, h/h_0, and flow velocity, V/V_0, become large with increasing values of ß as shown in Tables 5.7 and 5.8. In addition, when k is not equal to unity the combined impact of ß and k on the solutions of the equations is more significant. The results are listed in Tables 5.9 and 5.10. From the two tables, it is obvious that when k = 0.95 or 1.05, the values of MASD or MRSD of h/h_0 and V/V_0 increase greatly with increasing values of ß for any downstream water depth tested. Therefore, it can be concluded that in flow simulation, for channels having very mild slope, large downstream-boundary water depth, extremely nonhydrostatic pressure distribution and extremely nonuniform velocity distribution it is very necessary to select flow equations with caution.

Table 5.9 Combined Impact of ß and k on Maximum Solution Difference of Flow Depth

(a) Absolute Difference

S_0=0.00019 k'=1	1.44	1.66	h_d/h_0= 1.80	2.02	2.53
k=0.95	Maximum absolute solution difference of h/h_0				
ß = 1	0.0274	-0.0250	-0.0361	-0.0547	-0.0874
ß = 1.33	0.0347	0.0257	-0.0372	-0.0560	-0.0885
ß = 2	0.0502	0.0355	-0.0394	-0.0588	-0.0908
S_0=0.00019 k'=1	1.44	1.66	h_d/h_0= 1.80	2.02	2.53
k=1.05	Maximum absolute solution difference of h/h_0				
ß = 1	-0.0243	0.0259	0.0361	0.0513	0.0750
ß = 1.33	-0.0186	0.0251	0.0352	0.0503	0.0743
ß = 2	0.0137	0.0237	0.0332	0.0483	0.0729

(b) Relative Difference

S_0=0.00019 k'=1	1.44	1.66	h_d/h_0= 1.80	2.02	2.53
k=0.95	Maximum relative solution difference of h/h_0 in %				
ß = 1	1.44	-2.24	-3.13	-4.33	-6.03
ß = 1.33	1.81	1.31	-3.22	-4.44	-5.44
ß = 2	2.61	1.80	-3.41	-4.68	-5.58
S_0=0.00019 k'=1	1.44	1.66	h_d/h_0= 1.80	2.02	2.53
k=1.05	Maximum relative solution difference of h/h_0 in %				
ß = 1	-1.27	2.32	3.12	4.08	5.88
ß = 1.33	-1.00	2.26	3.04	3.98	4.58
ß = 2	1.08	2.10	2.85	3.82	4.49

Table 5.10 Combined Impact of ß and k on Maximum Solution Difference of Flow Velocity

(a) Absolute Difference

S_0=0.00019 k'=1	1.44	1.66	h_d/h_0= 1.80	2.02	2.53
k=0.95	Maximum absolute solution difference of V/V_0				
ß = 1	-0.0294	0.0244	0.0353	0.0533	0.0998
ß = 1.33	-0.0375	-0.0272	0.0366	0.0551	0.1009
ß = 2	-0.0553	-0.0385	0.0392	0.0586	0.1030
S_0=0.00019 k'=1	1.44	1.66	h_d/h_0= 1.80	2.02	2.53
k=1.05	Maximum absolute solution difference of V/V_0				
ß = 1	0.0275	-0.0262	-0.0374	-0.0602	-0.1169
ß = 1.33	0.0223	-0.0250	-0.0361	-0.0584	-0.1148
ß = 2	0.0214	-0.0224	-0.0333	-0.0548	-0.1105

(b) Relative Difference

S_0=0.00019 k'=1	1.44	1.66	h_d/h_0= 1.80	2.02	2.53
k=0.95	Maximum relative solution difference of V/V_0 in %				
ß = 1	-1.46	3.53	4.03	6.67	16.25
ß = 1.33	-1.85	-1.38	4.18	6.89	16.43
ß = 2	-2.72	-1.94	4.47	7.33	16.77
S_0=0.00019 k'=1	1.44	1.66	h_d/h_0= 1.80	2.02	2.53
k=1.05	Maximum relative solution difference of V/V_0 in %				
ß = 1	1.38	-2.86	-4.27	-7.53	-19.04
ß = 1.33	1.61	-2.72	-4.12	-7.31	-18.69
ß = 2	1.12	-2.43	-3.80	-6.86	-17.99

5.1.3. Impacts of Channel Slope and Downstream Boundary Condition

As discussed in sections 5.1.1 and 5.1.2, the values of MASD or MRSD of the nondimensional flow depth and flow velocity are related to the channel slope and downstream boundary condition. Therefore, it is necessary to recapitulate the impacts of the channel slope and downstream boundary condition on the solutions of the equations.

For various combinations of ß, k, k' and downstream water depth, the values of either MASD or MRSD of h/h_0 and V/V_0 always decrease with increasing values of the channel slope. Tables 5.11 and 5.12 illustrate this impact of S_0 on the solutions of the equations. For ß = 1 and h_d/h_0 = 1.80 with different combinations of k and k', the value of the channel slope is reduced only by 40% and 80%, respectively, but the values of MASD or MRSD of h/h_0 and V/V_0 increase sharply by several orders of magnitude. Therefore, it can be deduced that for channels with large bed slope the Saint-Venant equations can be safely applied to solve open channel problems. Without significant downstream backwater effect or for nearly uniform flow, the channel slope can be expressed as a function of the flow Froude number or Kinematic wave number; hence the steeper the channel slope, the greater the values of the Froude number, F_r, and kinematic wave number, κ. It can be further deduced that the Saint-Venant equations can replace the exact momentum and continuity equations under the condition of high flow Froude number or kinematic wave number. It is valuable to investigate in what ranges of Froude number and kinematic wave

Table 5.11 Impact of S_0 on Maximum Solution Difference of Flow Depth

(a) Absolute Difference

ß = 1 h_d/h_0=1.80	k=0.95 k'=1	k=1 k'=1.05	k=1 k'=0.95	k=1.05 k'=1
	Maximum absolute solution difference of h/h_0			
S0=0.00095	0.0018	0.0010	-0.0009	-0.0019
S0=0.00057	-0.0269	-0.0140	0.0148	0.0305
S0=0.00019	-0.0361	-0.0181	0.0182	0.0361
	Increased multiple of solution difference with respect to S_0			
S_0 is reduced by 40% from 0.00095 to 0.00057	15	14	16	16
S_0 is reduced by 80% from 0.00095 to 0.00019	20	18	20	19

(b) Relative Difference

ß = 1 h_d/h_0=1.80	k=0.95 k'=1	k=1 k'=1.05	k=1 k'=0.95	k=1.05 k'=1
	Maximum relative solution difference of h/h_0 in %			
S0=0.00095	0.18	0.10	-0.04	-0.09
S0=0.00057	-2.53	-1.31	1.39	2.85
S0=0.00019	-3.13	-1.55	1.57	3.12
	Increased multiple of solution difference with respect to S_0			
S_0 is reduced by 40% from 0.00095 to 0.00057	14	13	35	32
S_0 is reduced by 80% from 0.00095 to 0.00019	17	16	39	35

Table 5.12 Impact of S_0 on Maximum Solution Difference of Flow Velocity

(a) Absolute Difference

ß = 1 h_d/h_0=1.80	k=0.95 k'=1	k=1 k'=1.05	k=1 k'=0.95	k=1.05 k'=1
	Maximum absolute solution difference of V/V_0			
S0=0.00095	-0.0012	-0.0006	0.0006	0.0013
S0=0.00057	0.0250	0.0126	-0.0128	-0.0260
S0=0.00019	0.0353	0.0182	-0.0184	-0.0374
	Increased multiple of solution difference with respect to S_0			
S_0 is reduced by 40% from 0.00095 to 0.00057	21	21	21	20
S_0 is reduced by 80% from 0.00095 to 0.00019	29	30	30	29

(b) Relative Difference

ß = 1 h_d/h_0=1.80	k=0.95 k'=1	k=1 k'=1.05	k=1 k'=0.95	k=1.05 k'=1
	Maximum relative solution difference of V/V_0 in %			
S0=0.00095	-0.10	-0.05	0.04	0.08
S0=0.00057	2.67	1.34	-1.37	-2.78
S0=0.00019	4.03	2.07	-2.10	-4.27
	Increased multiple of solution difference with respect to S_0			
S_0 is reduced by 40% from 0.00095 to 0.00057	27	27	34	35
S_0 is reduced by 80% from 0.00095 to 0.00019	40	41	53	53

number the difference of the solutions between the exact momentum and continuity equations and the Saint-Venant equations can be ignored. From present results, if the initial steady-uniform-flow Froude number ($V_0/(gh_0)^{0.5}$) is greater than 0.2, the difference of the solutions of both sets of equations becomes very small.

The impact of the downstream boundary condition is presented in Tables 5.13 and 5.14 and also shown in Fig. 5.6. In order to describe the problem briefly and concisely only one combination of ß, k and k', i.e., ß = 1, k = 0.95 and k' = 1, is selected as an example and eight values of h_d/h_0 are chosen to study the change of the maximum solution difference as the downstream water depth varies. Two facts can be observed from Tables 5.13 and 5.14 and Fig. 5.6. One is that the values of MASD or MRSD of the nondimensional flow depth and flow velocity always increase with increasing values of h_d/h_0. It indicates the importance of the downstream boundary condition to the solutions. The other fact is that the influence of the downstream boundary condition on the MASD or MRSD of h/h_0 and V/V_0 is related to the channel slope. When the channel slope is small, the values of MASD or MRSD of h/h_0 and V/V_0 increase greatly with increasing h_d/h_0. But, when the channel slope becomes large the influence of the downstream boundary condition on the value of MASD or MRSD is reduced. Thus, indicating again that the channel slope is an important factor.

5.2. Rectangular and Trapezoidal Channels

The main difference between a wide rectangular channel and a rectangular channel is the width of the channel bottom, b, and the

Table 5.13 Impact of Downstream Boundary Condition on Maximum Solution Difference of Flow Depth

(a) Absolute Difference

ß = 1 Value of k & k'	h_d/h_0	Channel slope = 0.00019	0.00057	0.00095	0.00114
		Maximum absolute solution difference of h/h_0			
k=0.95, k'=1	1.44	0.0274	0.0129	0.0015	0.0010
	1.52	0.0255	0.0125	0.0015	0.0011
	1.59	0.0234	-0.0122	0.0017	0.0012
	1.66	-0.0250	-0.0163	0.0017	0.0014
	1.80	-0.0361	-0.0269	0.0018	0.0014
	2.02	-0.0547	-0.0484	0.0022	0.0016
	2.31	-0.0761	-0.0657	-0.0028	0.0019
	2.53	-0.0874	-0.0780	-0.0066	0.0054

(b) Relative Difference

ß = 1 Value of k & k'	h_d/h_0	Channel slope = 0.00019	0.00057	0.00095	0.00114
		Maximum relative solution difference of h/h_0 in %			
k=0.95, k'=1	1.44	1.44	0.58	0.15	0.10
	1.52	1.33	0.56	0.15	0.11
	1.59	1.21	-1.19	0.16	0.12
	1.66	-2.24	-1.57	0.16	0.13
	1.80	-3.13	-2.53	0.18	0.14
	2.02	-4.33	-4.25	0.22	0.16
	2.31	-5.23	-4.87	-0.18	0.19
	2.53	-6.03	-5.37	-0.51	0.53

Table 5.14 Impact of Downstream Boundary Condition on Maximum Solution Difference of Flow Velocity

(a) Absolute Difference

ß = 1 Value of k & k'	h_d/h_0	Channel slope = 0.00019	0.00057	0.00095	0.00114
		Maximum absolute solution difference of V/V_0			
k=0.95, k'=1	1.44	-0.0294	-0.0097	-0.0013	-0.0010
	1.52	-0.0271	-0.0094	-0.0013	-0.0010
	1.59	-0.0248	0.0121	-0.0013	-0.0009
	1.66	0.0244	0.0156	-0.0013	-0.0009
	1.80	0.0353	0.0250	-0.0012	-0.0009
	2.02	0.0533	0.0395	-0.0012	-0.0009
	2.31	0.0778	0.0500	0.0018	-0.0009
	2.53	0.0998	0.0509	0.0064	-0.0046

(b) Relative Difference

ß = 1 Value of k & k'	h_d/h_0	Channel slope = 0.00019	0.00057	0.00095	0.00114
		Maximum relative solution difference of V/V_0 in %			
k=0.95, k'=1	1.44	-1.46	-0.55	-0.08	-0.06
	1.52	-1.36	-0.53	-0.08	-0.06
	1.59	-1.25	1.24	-0.09	-0.06
	1.66	3.53	1.61	-0.10	-0.07
	1.80	4.03	2.67	-0.10	-0.08
	2.02	6.67	4.50	-0.12	-0.09
	2.31	11.25	6.45	0.13	-0.11
	2.53	16.25	7.36	0.64	-0.46

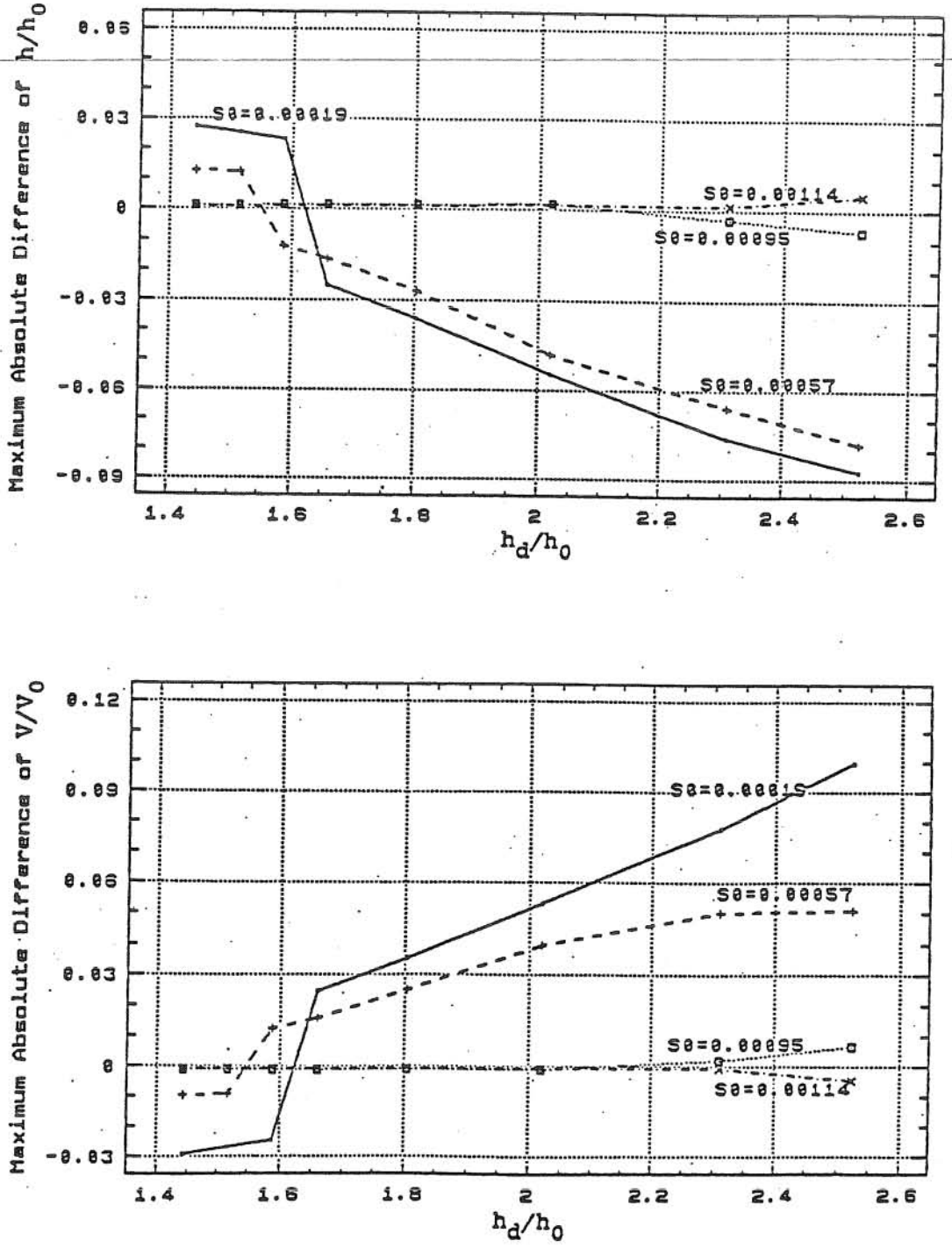

Fig. 5.6 Impact of Downstream Water Depth on Absolute Solution Difference of h/h_0 and V/V_0 for Case of $\beta = 1$, $k = 0.95$ and $k' = 1$

existence of the banks to slow down the flow. By examining the numerical solutions for various combinations of the coefficients, channel slope and downstream water depth, it has been found that for a rectangular channel the impact of the coefficient, ß, k or k' on the solutions of the equations is basically similar to that of a wide rectangular channel. Therefore, discussion of the impacts of the coefficients, ß, k and k', on the solutions for a rectangular channel are not repeated here, whereas, the impact of the channel bottom width, b, on the solutions of the equations is investigated in this section.

The impact of b on the solutions of the equations is presented in Tables 5.15 and 5.16. From the experience of investigating wide rectangular channels, the condition of S_0 = 0.00019, ß = 1, k = 0.95 and k' = 1 is selected as an example to explain the change of MASD or MRSD of h/h_0 or V/V_0 with increasing values of the channel bottom width, b, for various downstream water depths. Three values of b (5000 ft, 500 ft and 100 ft), i.e., b/h_0 = 360, 36 and 7, are considered as examples. From Tables 5.15 and 5.16, as b/h_0 decreases from 360 to 7, the values of MASD or MRSD of h/h_0 and V/V_0 vary only insignificantly. Thus, it is shown that for the range of width to depth ratio tested, the impact of the channel width b on the solutions is not significant.

A trapezoidal channel differs geometrically from a rectangular channel due to the side slope of the channel cross section, z. If the value of z is equal to zero, the trapezoidal channel becomes a rectangular channel. For reasons discussed previously, the impacts of the coefficients, ß, k and k', on the solutions of the

Table 5.15 Impact of Rectangular Channel Width b on Maximum Solution Difference of Flow Depth

(a) Absolute Difference

S_0=0.00019 ß=1 k'=1 k=0.95	h_d/h_0= 1.44	1.66	1.80	2.02	2.53
	Maximum absolute solution difference of h/h_0				
b/h_0=360	0.0274	-0.0250	-0.0361	-0.0547	-0.0874
b/h_0=36	0.0275	-0.0255	-0.0366	-0.0547	-0.0866
b/h_0=7	0.0277	-0.0271	-0.0378	-0.0547	-0.0843

(b) Relative Difference

S_0=0.00019 ß=1 k'=1 k=0.95	h_d/h_0= 1.44	1.66	1.80	2.02	2.53
	Maximum relative solution difference of h/h_0 in %				
b/h_0=360	1.44	-2.24	-3.13	-4.33	-6.03
b/h_0=36	1.45	-2.28	-3.13	-4.31	-5.31
b/h_0=7	1.45	-2.38	-3.18	-4.23	-5.09

Table 5.16 Impact of Rectangular Channel Width b on Maximum Solution Difference of Flow Velocity

(a) Absolute Difference

S_0=0.00019 ß=1 k'=1 k=0.95	h_d/h_0= 1.44	1.66	1.80	2.02	2.53
	Maximum absolute solution difference of V/V_0				
b/h_0=360	-0.0294	0.0244	0.0353	0.0533	0.0998
b/h_0=36	-0.0288	0.0255	0.0354	0.0532	0.0996
b/h_0=7	-0.0269	0.0265	0.0357	0.0520	0.0949

(b) Relative Difference

S_0=0.00019 ß=1 k'=1 k=0.95	h_d/h_0= 1.44	1.66	1.80	2.02	2.53
	Maximum relative solution difference of V/V_0 in %				
b/h_0=360	-1.46	3.53	4.03	6.67	16.25
b/h_0=36	-1.48	3.71	4.06	6.71	16.38
b/h_0=7	-1.54	3.90	4.17	6.72	16.49

exact momentum and continuity equations for trapezoidal channels are not repeated in this section. The investigation here is focused on the impact of channel side slope, z, on the solutions of the equations.

Tables 5.17 and 5.18 demonstrate the impact of z on the solutions of the flow equations. Based on the experience of investigating wide rectangular channels, a typical condition (S_0 = 0.00019, β = 1, k = 0.95, k' = 1) and two different values of the channel bottom width, b = 5000 ft and 100 ft (i.e., b/h_0 = 360 and 7), are considered as examples. From the top portions of Tables 5.17 and 5.18, it is shown that if the width to depth ratio of the channel bottom is large, increase of the channel side slope does not significantly affect the solutions of the equations. However, if the width to depth ratio of the channel bottom is small and the downstream-boundary water depth becomes large, a change of the channel side slope produces an important impact on the solutions of the equations, especially on the flow velocity. This result is displayed clearly in the bottom portions of Tables 5.17 and 5.18. For a given b/h_0, the larger the value of z, the more the change of the flow area A for a change in the depth of the unsteady nonuniform flow.

Therefore, it is concluded that in determining which equations (the exact momentum and continuity equations or the Saint-Venant equations) are reliable for solving an open channel problem, the side slope and bottom width to depth ratio of the trapezoidal channel should be considered as contributing factors.

Table 5.17 Impact of Side Slope z on Maximum Solution Difference of Flow Depth

(a) Absolute Difference

S_0=0.00019 ß=1 k=0.95, k'=1 b/h_0=360	h_d/h_0= 1.44	1.66	1.80	2.02	2.53
	Maximum absolute solution difference of h/h_0				
z=0	0.0274	-0.0250	-0.0361	-0.0547	-0.0874
z=1	0.0275	-0.0250	-0.0362	-0.0548	-0.0877
z=4	0.0277	-0.0250	-0.0362	-0.0551	-0.0888
S_0=0.00019 ß=1 k=0.95, k'=1 b/h_0=7	h_d/h_0= 1.44	1.66	1.80	2.02	2.53
	Maximum absolute solution difference of h/h_0				
z=0	0.0267	-0.0266	-0.0378	-0.0547	-0.0843
z=1	0.0309	-0.0271	-0.0388	-0.0595	-0.0979
z=4	0.0352	-0.0304	-0.0402	-0.0668	-0.1177

(b) Relative Difference

S_0=0.00019 ß=1 k=0.95, k'=1 b/h_0=360	h_d/h_0= 1.44	1.66	1.80	2.02	2.53
	Maximum relative solution difference of h/h_0 in %				
z=0	1.44	-2.24	-3.13	-4.33	-6.03
z=1	1.44	-2.24	-3.13	-4.34	-6.40
z=4	1.45	-2.24	-3.14	-4.38	-6.47
S_0=0.00019 ß=1 k=0.95, k'=1 b/h_0=7	h_d/h_0= 1.44	1.66	1.80	2.02	2.53
	Maximum relative solution difference of h/h_0 in %				
z=0	1.45	-2.38	-3.18	-4.23	-5.09
z=1	1.62	-2.39	-3.36	-4.72	-6.04
z=4	1.80	-2.53	-3.57	-5.45	-7.39

Table 5.18 Impact of Side Slope z on Maximum Solution Difference of Flow Velocity

(a) Absolute Difference

S_0=0.00019 ß=1 k=0.95, k'=1 b/h_0=360	h_d/h_0= 1.44	1.66	1.80	2.02	2.53
	Maximum absolute solution difference of V/V_0				
z=0	-0.0294	0.0244	0.0353	0.0533	0.0998
z=1	-0.0296	0.0245	0.0354	0.0535	0.1002
z=4	-0.0303	0.0245	0.0357	0.0540	0.1014
S_0=0.00019 ß=1 k=0.95, k'=1 b/h_0=7	h_d/h_0= 1.44	1.66	1.80	2.02	2.53
	Maximum absolute solution difference of V/V_0				
z=0	-0.0269	0.0265	0.0357	0.0520	0.0949
z=1	-0.0351	0.0266	0.0396	0.0609	0.1150
z=4	-0.0459	0.0305	0.0459	0.0761	0.1440

(b) Relative Difference

S_0=0.00019 ß=1 k=0.95, k'=1 b/h_0=360	h_d/h_0= 1.44	1.66	1.80	2.02	2.53
	Maximum relative solution difference of V/V_0 in %				
z=0	-1.46	3.53	4.03	6.67	16.25
z=1	-1.47	3.53	4.04	6.69	16.31
z=4	-1.49	3.54	4.07	6.75	16.49
S_0=0.00019 ß=1 k=0.95, k'=1 b/h_0=7	h_d/h_0= 1.44	1.66	1.80	2.02	2.53
	Maximum relative solution difference of V/V_0 in %				
z=0	-1.54	3.90	4.17	6.72	16.38
z=1	-1.89	3.99	4.58	7.81	19.98
z=4	-2.46	4.34	5.28	9.80	25.89

In addition, it should be mentioned that for rectangular channels, the values of either MASD or MRSD of h/h_0 or V/V_0 are the same for certain combinations of k and k'. However, this regularity disappears for trapezoidal channels, i.e., the values of either MASD or MRSD of h/h_0 or V/V_0 for each combination of k and k' are different, although the difference is not very large. Table 5.19 for $\beta = 1$, $S_0 = 0.00019$ and $h_d/h_0 = 2.53$ is selected as an example to display the difference of MASD or MRSD of the nondimensional flow depth between the rectangular and trapezoidal channels. For trapezoidal channels, the solutions of the exact momentum and continuity equations are definitely different if one of the three coefficients, β, k and k', is varied.

As to the effect of an arbitrary cross-sectional shape on the solutions of the equations, a key point is how to express the cross-sectional geometry functions, i.e., various G functions mentioned in Chapter 4. If these G functions of an arbitrary cross-sectional shape can be found, the exact momentum and continuity equations can be solved, and the effect of the arbitrary shape on the solutions can be obtained by comparing the solutions of the exact momentum and continuity equations with those of the Saint-Venant equations. Generally speaking, it is easy to represent G functions for regular shapes, for example, rectangle, trapezoid, triangle, circle, parabola and so on, but it is difficult to find the G functions for an arbitrary irregular shape. One method to solve this problem is to use an approximation. Since the G functions are a function of nondimensional flow depth, h_* ($h_* = h/h_0$), graphs reflecting the relationships between each G

Table 5.19 Comparison of Maximum Solution Difference of Flow Depth for Different Channel Shapes

(a) Absolute Difference

ß = 1		S_0 = 0.00019, b/h_0 = 7	
Value of k & k'	h_d/h_0	Rectangular channel	Trapezoidal channel (z=1)
		Maximum absolute solution difference of h/h_0	
k=0.95, k'=0.95	2.53	-0.0467	-0.0421
k=1, k'=1.05		-0.0467	-0.0517
k=0.95, k'=0.9	2.53	0.0000	0.0089
k=1.05, k'=1.1		0.0000	-0.0090
k=1, k'=0.95	2.53	0.0440	0.0474
k=1.05, k'=1.05		0.0440	0.0391

(b) Relative Difference

ß = 1		S_0 = 0.00019, b/h_0 = 7	
Value of k & k'	h_d/h_0	Rectangular channel	Trapezoidal channel (z=1)
		Maximum relative solution difference of h/h_0 in %	
k=0.95, k'=0.95	2.53	-3.23	-2.59
k=1, k'=1.05		-3.23	-3.19
k=0.95, k'=0.9	2.53	0.00	0.55
k=1.05, k'=1.1		0.00	-0.56
k=1, k'=0.95	2.53	3.04	2.93
k=1.05, k'=1.05		3.04	2.41

function and h_* for various regular shapes can be made. The unknown relationships between each G function of an arbitrary shape and h_* can be estimated using these graphs. Figures 5.7 through 5.11 are graphs expressing the relationships between G_1, G_2, G_3, G_4, G_5 and h_* for rectangular and trapezoidal channels (the width to depth ratio of channel bottom, b/h_0, is equal to 7 and the side slope, z, is equal to 0, 1, 2 or 4), respectively. For an arbitrary cross-sectional shape, the G functions can be roughly assessed by utilizing the known family of curves. Figures 5.7 through 5.11 are given here as a demonstration. More curves for different regular shapes are necessary, so that these graphs can be employed.

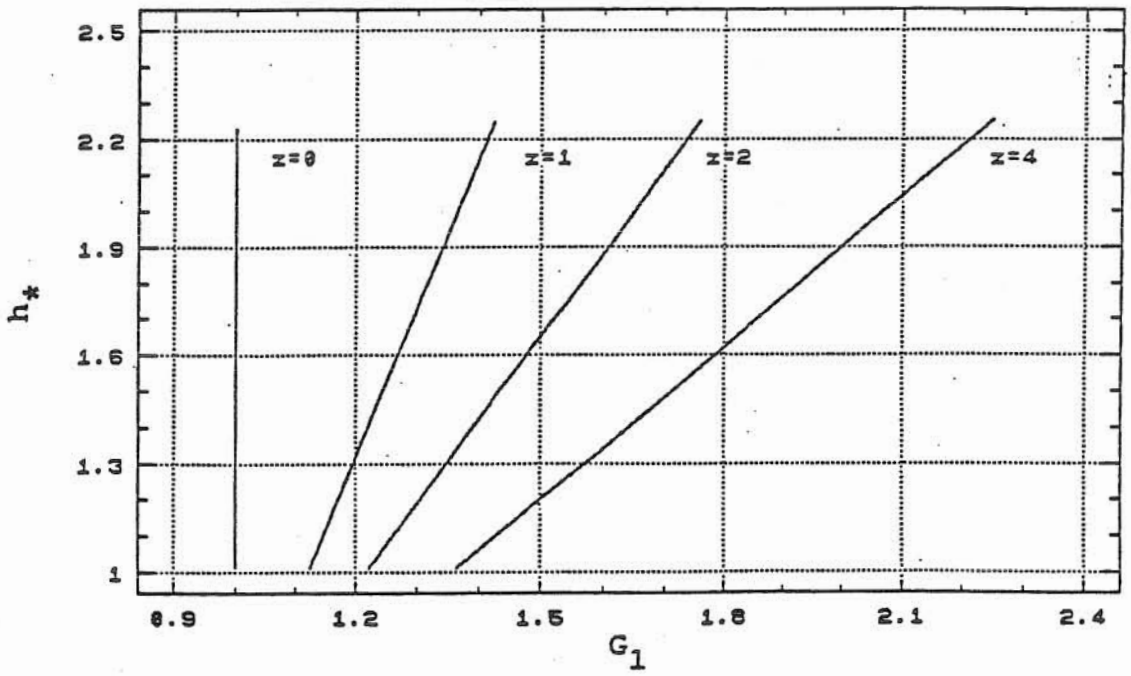

Fig. 5.7 Geometry Function G_1 vs. h_* for Trapezoidal Channels with $b/h_0 = 7$

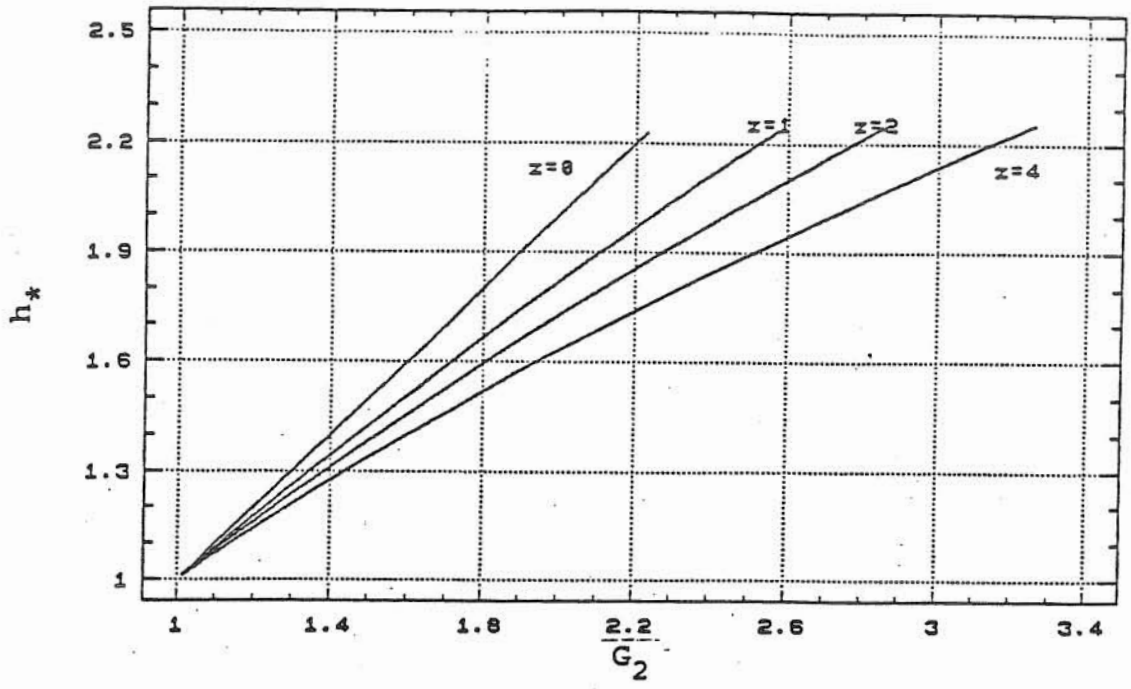

Fig. 5.8 Geometry Function G_2 vs. h_* for Trapezoidal Channels with $b/h_0 = 7$

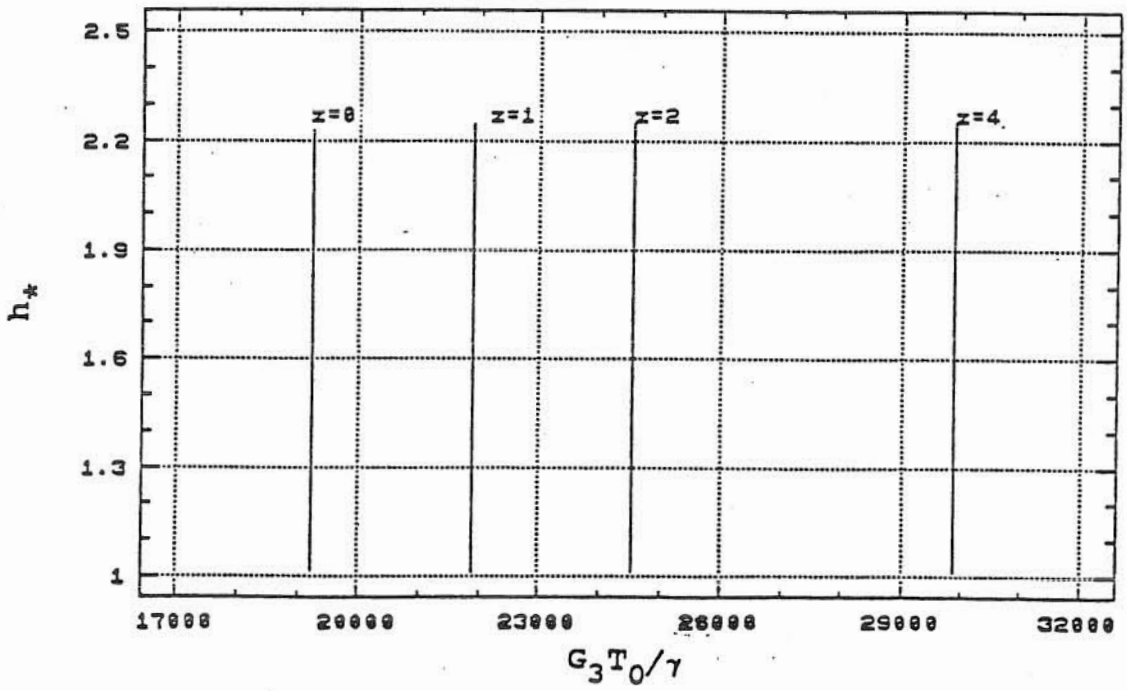

Fig. 5.9 Geometry Function G_3 vs. h_* for Trapezoidal Channels with $b/h_0 = 7$

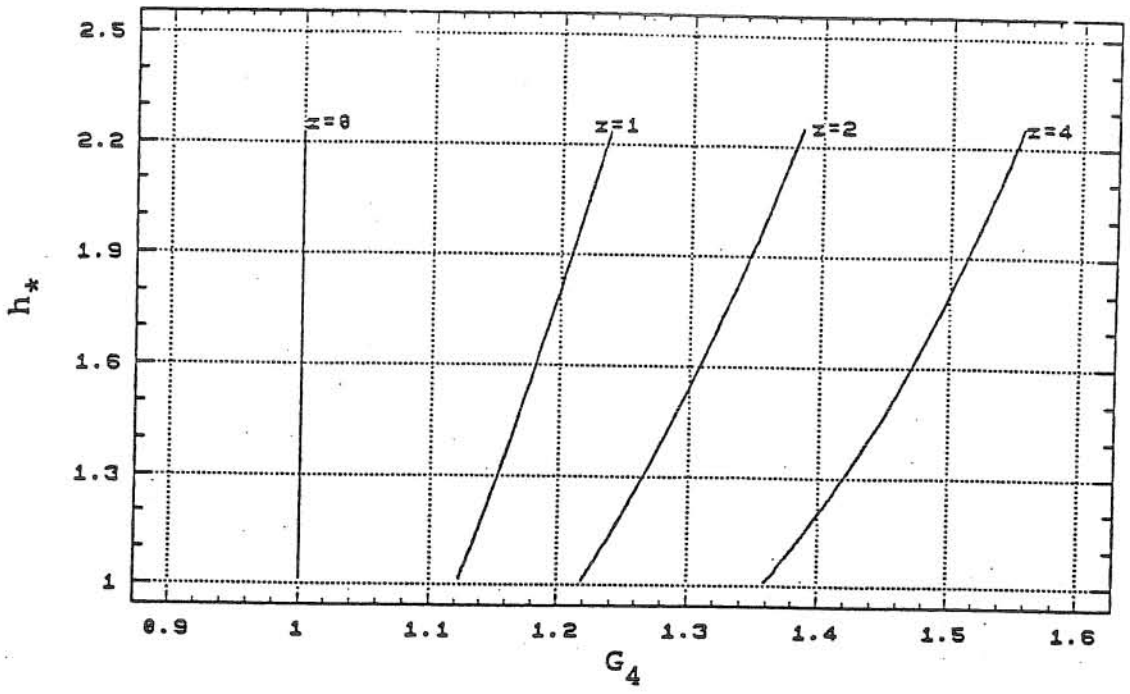

Fig. 5.10 Geometry Function G_4 vs. h_* for Trapezoidal Channels with $b/h_0 = 7$

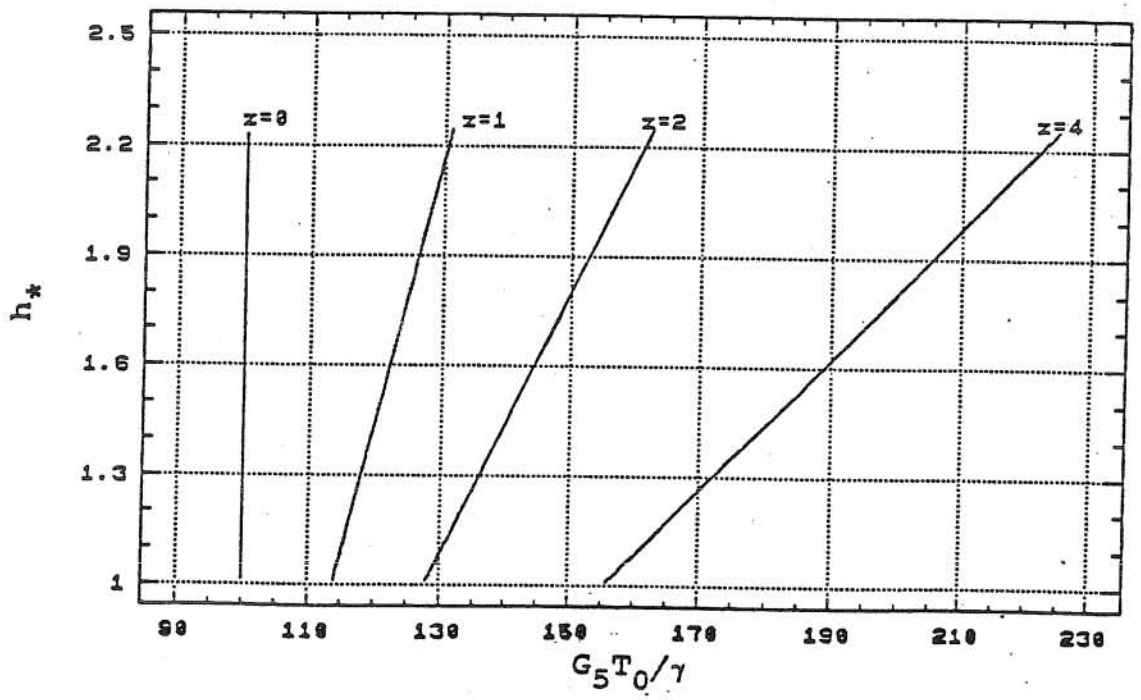

Fig. 5.11 Geometry Function G_5 vs. h_* for Trapezoidal Channels with $b/h_0 = 7$

5.3. Situation of Accelerating Type Water Surface Profiles

It is interesting to investigate if the effects of the coefficients and terms of the exact momentum equation for convectively accelerating and decelerating type water surface profiles are similar. The results reported in the preceding two sections are for the cases with $h_d/h_0 > 1$, i.e., at least initially the flow is convectively decelerating, $\partial h/\partial x > 0$, similar to the M1 (or S1) type backwater curve of steady flow. Discussed in this section are the results of convectively accelerating flow with $h_d/h_0 < 1$ and $\partial h/\partial x < 0$, similar to the M2 type backwater curve of steady flow.

For unsteady flow, the convectively accelerating type water surface profile occurs for the following cases: (a) The elevation of the normal depth of the flow in a mild-slope channel, which is a function of time, is greater than the elevation of the water surface at the downstream end of the channel, e.g., in a reservoir or a lake. (b) The subcritical flow depth decreases along a channel because of the enlargement of cross section at the downstream end. (c) Under certain situations, the flood flow of the initially decelerating M1-type water surface profile may temporally change to the M2 type convectively accelerating profile. This process is not discussed here.

According to experiences gained from investigation of the initially decelerating M1-type water surface profiles, the study of importance of the coefficients, ß, k and k', in the exact momentum equation to the solutions of the equations for convectively accelerating type profiles only focuses on some special

conditions, for example, wide rectangular channel, very mild channel slope, and consideration of changes of k and ß.

Tables 5.20 through 5.23 demonstrate the values of MASD or MRSD of nondimensional flow depth, h/h_0, and flow velocity, V/V_0, for $S_0 = 0.00019$, ß = 1, 1.33 and 2, k = 0.95 and 1.05, k' = 1, with various selected downstream water depths. From the four tables, it is observed that the values of MASD or MRSD of h/h_0 and V/V_0 for various values of k and ß increase with lowering the values of the downstream-boundary water depth, and they asymptotically approach a certain constant. This is because for a convectively accelerating type profile, there is a terminal depth, i.e., the critical depth, at the downstream end. Therefore, by lowering the downstream depth and gradually approaching the critical depth, the solution difference approaches a certain value. This result is opposite to that of the convectively decelerating type profiles for which the solution difference is backwater effect dependent. For a water syrface profile of the convectively decelerating type, the backwater effect increases with increasing downstream depth. Thus, the solution difference also increases with increasing downstream water depth. However, for a convectively accelerating profile, the backwater effect increases with lowering downstream depth.

Furthermore, by comparing Tables 5.20 and 5.21 with Tables 5.1 and 5.2, and Tables 5.22 and 5.23 with Tables 5.7 and 5.8, respectively, it is found that for convectively decelerating type profiles, the values of MASD or MRSD of h/h_0 and V/V_0 corresponding to various values of k are always greater than those for convectively accelerating type profiles, but for various values of ß the

Table 5.20 Impact of Pressure Correction Coefficient k on Maximum Solution Difference of h/h_0 for Flow with Accelerating Type Water Surface Profiles

(a) Absolute Difference

S_0=0.00019 ß=1, k'=1	h_d/h_0= 0.31	0.50	0.70	0.80	1.00
	Maximum absolute solution difference of h/h_0				
k = 0.95	0.0456	0.0456	0.0456	0.0437	0.0368
k = 1	0.0000	0.0000	0.0000	0.0000	0.0000
k = 1.05	-0.0404	-0.0404	-0.0404	-0.0387	-0.0330
	Rate of change of solution difference with respect to k in %				
k varies 5% (0.95 to 1)	-91	-91	-91	-87	-74
k varies 5% (1 to 1.05)	-81	-81	-81	-77	-66

(b) Relative Difference

S_0=0.00019 ß=1, k'=1	h_d/h_0= 0.31	0.50	0.70	0.80	1.00
	Maximum relative solution difference of h/h_0 in %				
k = 0.95	2.37	2.37	2.37	2.29	1.98
k = 1	0.00	0.00	0.00	0.00	0.00
k = 1.05	-2.11	-2.11	-2.11	-2.03	-1.78
	Rate of change of solution difference with respect to k in %				
k varies 5% (0.95 to 1)	-47	-47	-47	-46	-40
k varies 5% (1 to 1.05)	-42	-42	-42	-41	-36

Table 5.21 Impact of Pressure Correction Coefficient k on Maximum Solution Difference of V/V_0 for Flow with Accelerating Type Water Surface Profiles

(a) Absolute Difference

S_0=0.00019 ß=1, k'=1	h_d/h_0= 0.31	0.50	0.70	0.80	1.00
	Maximum absolute solution difference of V/V_0				
k = 0.95	-0.0468	-0.0469	-0.0471	-0.0441	-0.0393
k = 1	0.0000	0.0000	0.0000	0.0000	0.0000
k = 1.05	0.0439	0.0439	0.0440	0.0414	0.0372
	Rate of change of solution difference with respect to k in %				
k varies 5% (0.95 to 1)	+94	+94	+94	+88	+79
k varies 5% (1 to 1.05)	+88	+88	+88	+83	+74

(b) Relative Difference

S_0=0.00019 ß=1, k'=1	h_d/h_0= 0.31	0.50	0.70	0.80	1.00
	Maximum relative solution difference of V/V_0 in %				
k = 0.95	-2.38	-2.38	-2.38	-2.19	-1.93
k = 1	0.00	0.00	0.00	0.00	0.00
k = 1.05	2.25	2.25	2.25	2.06	1.82
	Rate of change of solution difference with respect to k in %				
k varies 5% (0.95 to 1)	+48	+48	+48	+44	+39
k varies 5% (1 to 1.05)	+45	+45	+45	+41	+36

Table 5.22 Impact of Momentum Correction Coefficient ß on Maximum Solution Difference of h/h_0 for Flow with Accelerating Type Water Surface Profiles

(a) Absolute Difference

S_0=0.00019 k=1, k'=1	h_d/h_0= 0.31	0.50	0.70	0.80	1.00
	Maximum absolute solution difference of h/h_0				
ß = 1	0.0000	0.0000	0.0000	0.0000	0.0000
ß = 1.33	0.0323	0.0323	0.0324	0.0276	0.0155
ß = 2.00	0.1106	0.1106	0.1108	0.0927	0.0489
	Rate of change of solution difference with respect to ß in %				
ß varies 33% (1 to 1.33)	10	10	10	8	5
ß varies 100% (1 to 2.00)	11	11	11	9	5

(b) Relative Difference

S_0=0.00019 k=1, k'=1	h_d/h_0= 0.31	0.50	0.70	0.80	1.00
	Maximum relative solution difference of h/h_0 in %				
ß = 1	0.00	0.00	0.00	0.00	0.00
ß = 1.33	1.65	1.65	1.66	1.43	0.81
ß = 2.00	5.66	5.66	5.67	4.78	2.57
	Rate of change of solution difference with respect to ß in %				
ß varies 33% (1 to 1.33)	5	5	5	4	2
ß varies 100% (1 to 2.00)	6	6	6	5	3

Table 5.23 Impact of Momentum Correction Coefficient ß on Maximum Solution Difference of V/V_0 for Flow with Accelerating Type Water Surface Profiles

(a) Absolute Difference

S_0=0.00019 k=1, k'=1	h_d/h_0= 0.31	0.50	0.70	0.80	1.00
	Maximum absolute solution difference of V/V_0				
ß = 1	0.0000	0.0000	0.0000	0.0000	0.0000
ß = 1.33	-0.0339	-0.0339	-0.0339	-0.0299	-0.0179
ß = 2.00	-0.1113	-0.1113	-0.1111	-0.0969	-0.0557
	Rate of change of solution difference with respect to ß in %				
ß varies 33% (1 to 1.33)	-10	-10	-10	-9	-5
ß varies 100% (1 to 2.00)	-11	-11	-11	-10	-6

(b) Relative Difference

S_0=0.00019 k=1, k'=1	h_d/h_0= 0.31	0.50	0.70	0.80	1.00
	Maximum relative solution difference of V/V_0 in %				
ß = 1	0.00	0.00	0.00	0.00	0.00
ß = 1.33	-1.70	-1.70	-1.69	-1.48	-0.87
ß = 2.00	-5.56	-5.56	-5.55	-4.81	-2.71
	Rate of change of solution difference with respect to ß in %				
ß varies 33% (1 to 1.33)	-5	-5	-5	-4	-3
ß varies 100% (1 to 2.00)	-6	-6	-6	-5	-3

results become opposite. This means that the impact of k on the solutions for the convectively accelerating type profiles is smaller than that for the convectively decelerating type profiles, but the impact of ß on solutions for the former becomes larger than for the latter. However, by comparing Tables 5.20 and 5.21 with Tables 5.22 and 5.23 it is obvious that for convectively accelerating type profiles the impact of k on the solutions of the equations is also greater than that of ß. Thus, it can be further concluded that for convectively accelerating type profiles, the difference between the solutions of the exact momentum and continuity equations and the Saint-Venant equations due to the variations of the coefficients, ß and k, is also relatively not as significant as for the convectively decelerating type water surface profiles.

5.4. Situation of Time-varying Downstream Boundary Water Depth

In section 5.1 the downstream boundary condition is assumed to have a constant water depth for the sake of simplicity in discussion. In nature the downstream depth often changes with time. Based on discussions in previous sections, for the sake of brevity without losing generality, the effect of time-varying downstream-boundary depth on the solutions of the equations is investigated only for one coefficient combination (ß = 1, k = 0.95 and k' = 1) and one channel slope (S_0 = 0.00019) of a wide rectangular channel. As depicted in section 4.4, four typical situations of time-varying downstream depth are considered here: (a) The depth hydrograph at the downstream boundary is identical

with that at the upstream boundary, i.e., the same period and amplitude. (b) The period of the depth hydrograph at the downstream boundary is the same as that at the upstream boundary, but the amplitude of the former is larger than the latter, either twice or one and a half times. (c) Similar to (b), but the amplitude of the former is smaller than the latter, either one half or two thirds. (d) The depth hydrograph at the downstream boundary is the same as that at the upstream boundary in both the period and amplitude, but the two depth hydrographs are in reverse. The results tested are presented in Table 5.24.

From Table 5.24, it is observed that the difference between the solutions of the exact momentum and continuity equations and the Saint-Venant equations increases with enlarging the amplitude difference of the depth hydrograph between upstream and downstream. When the depth hydrograph at the downstream boundary is the same as that at the upstream (i.e., no backwater effect), there are insignificant solution differences. When the variation of the water depth at the downstream boundary is greater than that at the upstream, the flow profile is the convectively decelerating type, and the larger the variation of the flow depth at the downstream, the more important the backwater effect, thus, the difference between the solutions of the two sets of equations becomes large. When the variation of the depth at the downstream boundary is smaller than that at the upstream, the flow profile is the convectively accelerating type. At this time, the solution difference increases with lowering downstream-boundary water depth. These results are basically in accord with those obtained from the condition of a constant downstream water depth for the convectively

Table 5.24 Impact of Time-varying Downstream Water Depth on Maximum Solution Difference of Flow Depth and Flow Velocity

(a) Absolute Difference

	Comparison of stage hydrograph at downstream with that at upstream					
	Reverse	Twice	One and half	Equal	Two thirds	Half
	Maximum absolute solution difference of h/h_0					
S_0=0.00019 ß=1 k'=1 k=0.95	-0.0678	-0.1284	-0.0666	-0.0161	0.0297	0.0362
	Maximum absolute solution difference of V/V_0					
	0.0759	0.0942	0.0430	0.0094	-0.0271	-0.0367

(b) Relative Difference

	Comparison of stage hydrograph at downstream with that at upstream					
	Reverse	Twice	One and half	Equal	Two thirds	Half
	Maximum relative solution difference of h/h_0 in %					
S_0=0.00019 ß=1 k'=1 k=0.95	-4.90	-4.79	-3.15	-1.12	1.73	2.04
	Maximum relative solution difference of V/V_0 in %					
	10.80	6.82	4.60	1.05	-1.34	-1.79

decelerating and accelerating profiles. In addition, it is shown that there is a maximum relative solution difference of either flow depth, h, or velocity, V, when the two depth hydrographs at the downstream and upstream are reversed. This result implies that if the depth hydrographs at the downstream and upstream are not synchronous (this situation may be more common in nature), the difference of the solutions of the two sets of equations are significant.

5.5. Further Remarks

From previous discussions, it can be summarized that the order of importance of the coefficients involved in the exact momentum equation is k first, then k', and ß last. The importance of ß, k or k' to the solutions of the equations is greatly influenced by the channel slope and the downstream-boundary water depth. For channels with very small slope and large downstream backwater effect (i.e., the more convectively decelerating or accelerating subcritical flow), the further the value of k departs from unity and the larger the value of ß (i.e., the more nonhydrostatic pressure distribution and nonuniform velocity distribution), the larger the difference between the solutions of the exact momentum and continuity equations and the Saint-Venant equations.

6. CONTRIBUTIONS OF TERMS INVOLVED IN EXACT MOMENTUM EQUATION

There are five terms, in addition to the $\partial T/\partial x$ term, in the exact momentum equation, namely, the local acceleration, convective acceleration, pressure, friction slope, and channel slope. As described in section 4.4, contributions of these terms to the solutions of the equations are investigated in two aspects. One is to study the magnitudes of these terms at different times and positions of simulation for various values of ß, k and k' without backwater effect. The other is to study the same terms with downstream backwater effect. Similar to Chapter 5, the investigation is first focused on wide rectangular channels with convectively decelerating type water surface profiles. Next, channels with other cross-sectional shapes and, finally, the convectively accelerating type profiles are briefly studied.

6.1. Wide Rectangular Channel

6.1.1. No Backwater Effect

As described in section 4, the case of unsteady flow without considering the downstream backwater effect is simulated through using a very long channel and using the result only up to x = L = 54 miles. In order to concisely analyze the effect of the five main terms in the exact momentum equation for various values of ß, k and k', the situation with ß = 1, k = k' = 1, and two extreme situations, ß = 2, k = 1.05, k' = 1 and ß = 2, k = 0.95, k' = 1 (ß assumes the largest value tested while k assumes the largest and smallest values), for only one channel slope, S_0 = 0.00019, are

selected as examples. The nondimensional solution values of these terms and their ratios in the absolute value at different times and channel cross-sectional positions from the channel upstream entrance, x/L = 0, 10/27, 5/9, 20/27, 25/27 and 1 (L is the channel length investigated and it is equal to 54 miles), are presented in Appendices A, B and C for the case of no backwater effect, and also shown in Figs. 6.1, 6.2 and 6.3. In addition, Table 6.1 demonstrates the time-average ratios in the absolute value between these terms, namely, the local acceleration and the convective acceleration terms, respectively, versus the pressure term, the sum of the two acceleration terms versus the pressure term, and the pressure term versus the friction slope and the difference between the friction and channel slopes, respectively.

From these tables and figures, it is obvious that the most important terms are the friction and channel slopes. The sum of the local and convective acceleration terms is less than 8% of the pressure term, and the pressure term is approximately 7% of the friction slope. Therefore, without downstream backwater effect the two inertia terms and the pressure term can often be neglected as compared to either the friction slope or channel slope, i.e., the kinematic wave model is applicable. However, it is cautioned that this observation is valid only for the calculation of the flow variables at a particular location or cross section. To calculate the variation of a nonuniform flow along a channel, such as the water surface profile variation, $\partial h/\partial x$, the pressure and inertia terms should be compared with the combination of the friction and channel slopes. From Table 6.1, because the ratio between the

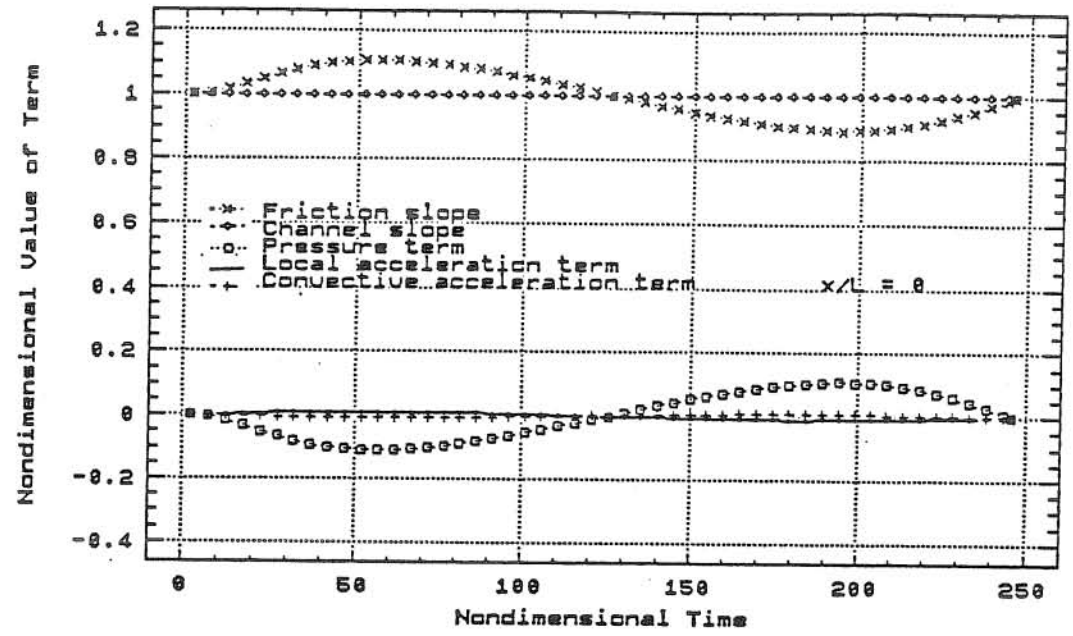

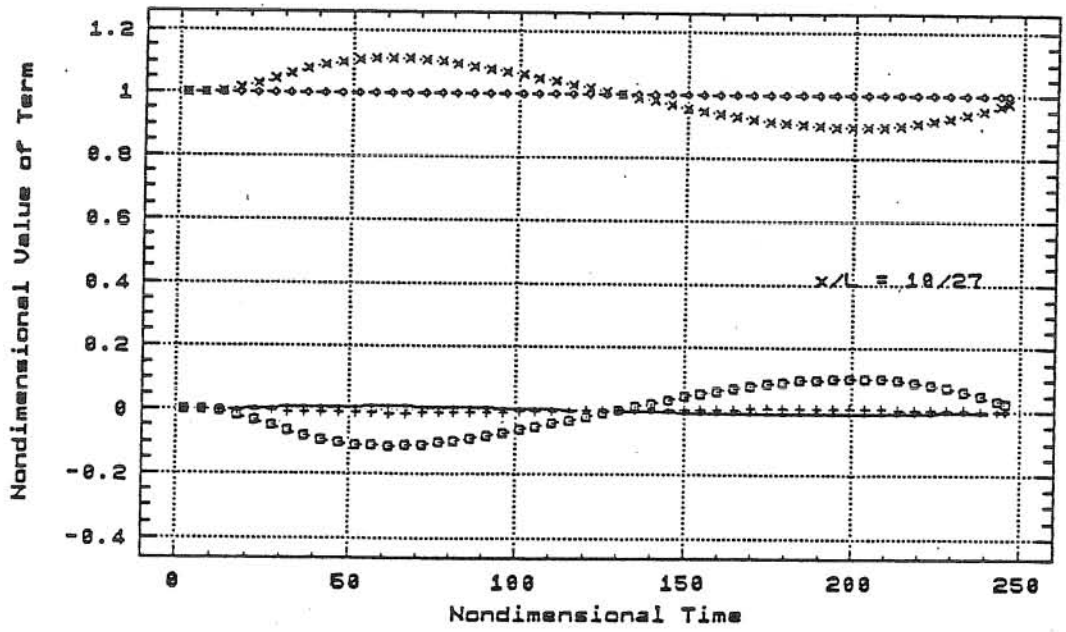

(a) Sections 0 and 10/27

Fig. 6.1 Nondimensional Values of Terms for $\beta = 1$, $k = k' = 1$, $S_0 = 0.00019$ and No Backwater Effect

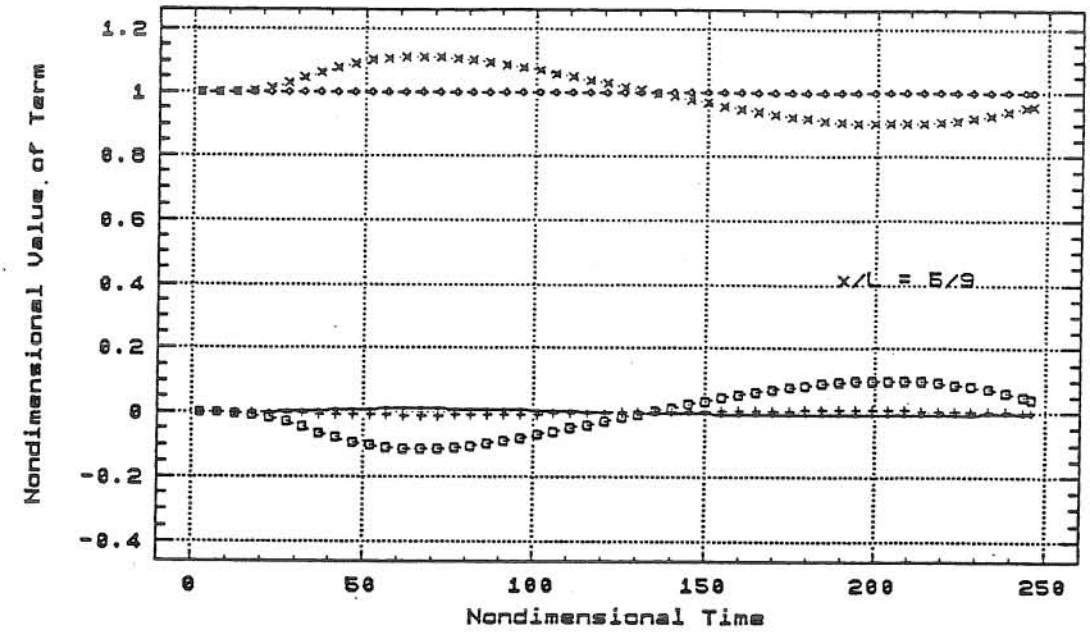

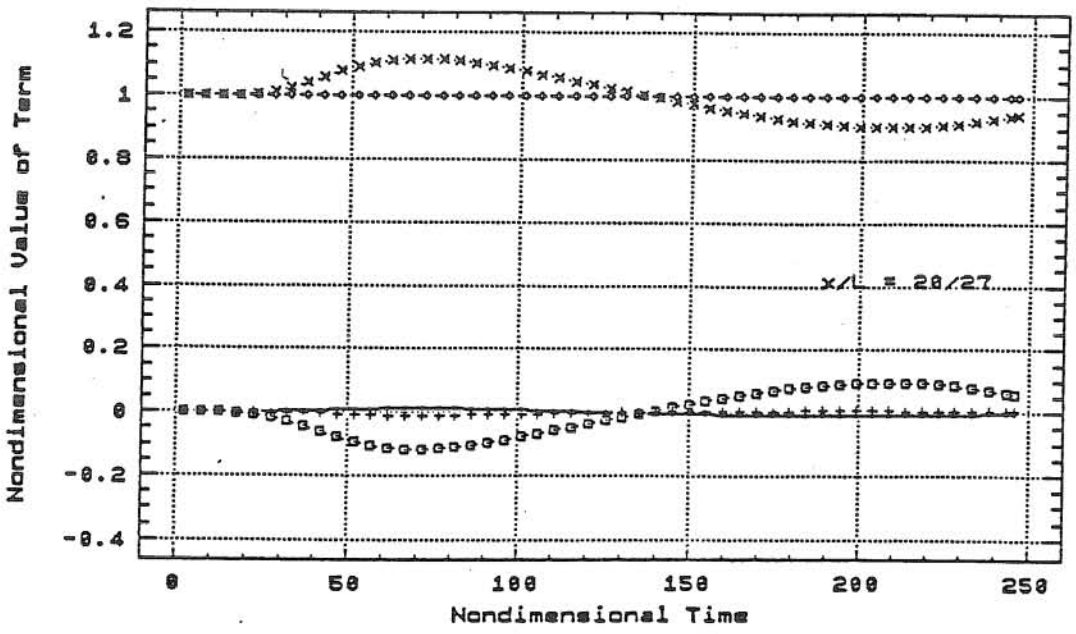

(b) Sections 5/9 and 20/27

Fig. 6.1 (continued)

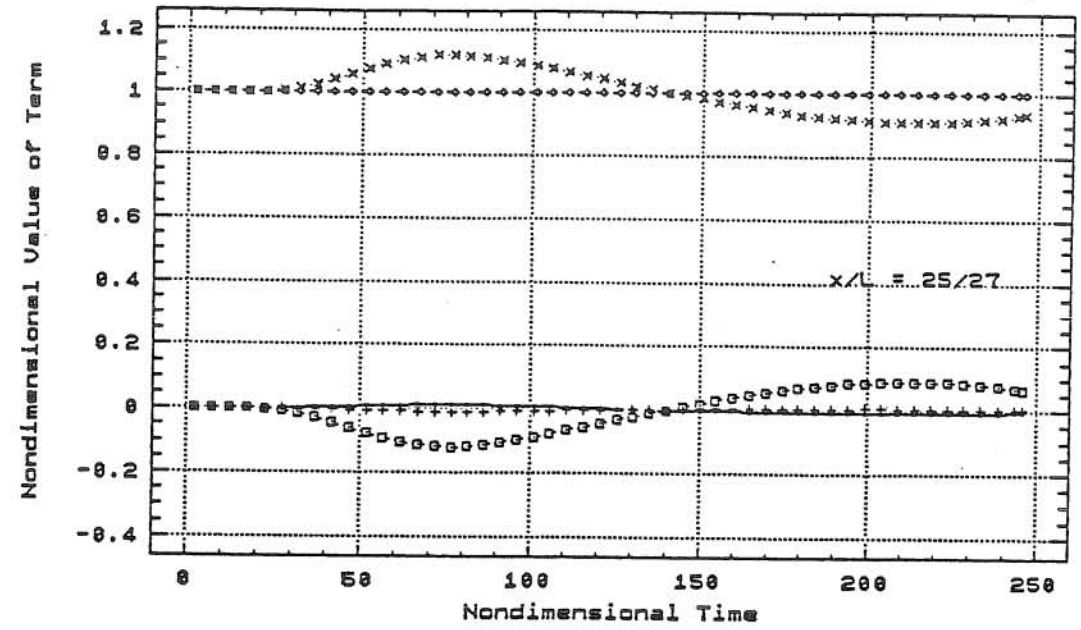

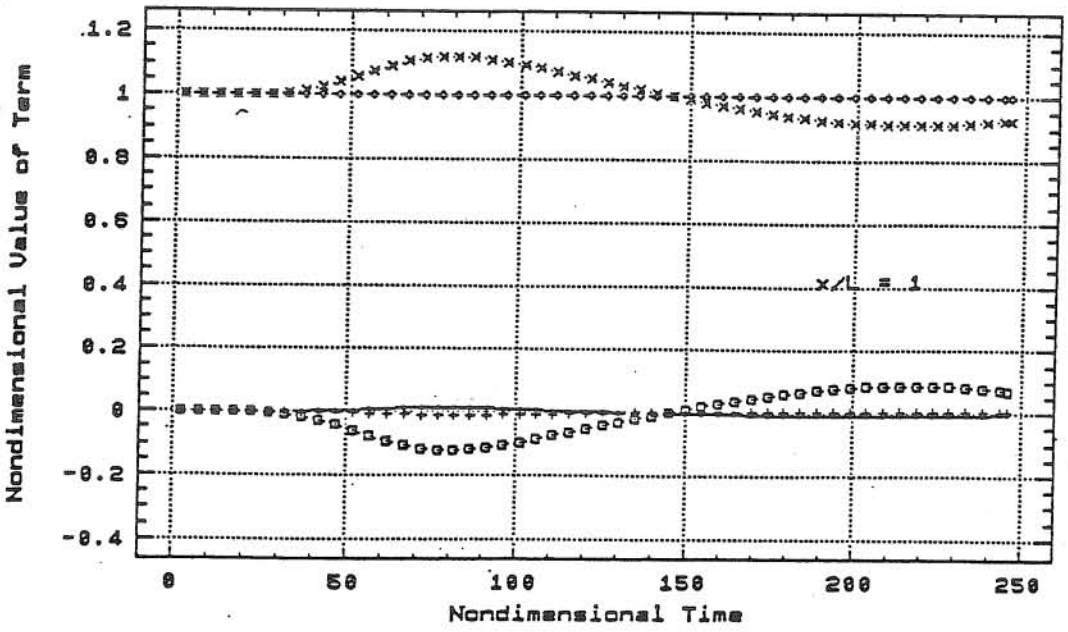

(c) Sections 25/27 and 1

Fig. 6.1 (continued)

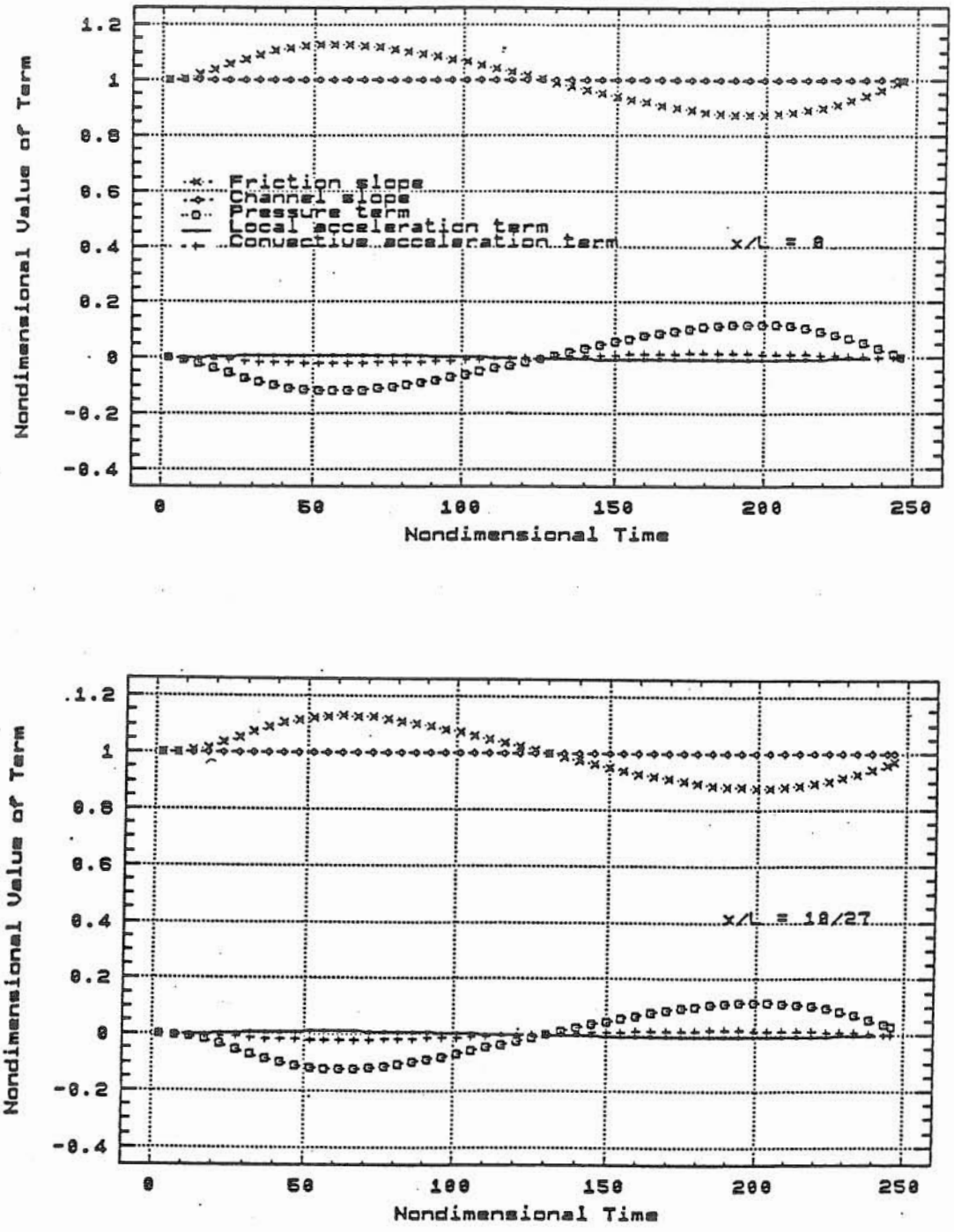

(a) Sections 0 and 10/27

Fig. 6.2 Nondimensional Values of Terms for $\beta = 2$, $k = 1.05$, $k' = 1$, $S_0 = 0.00019$ and No Backwater Effect

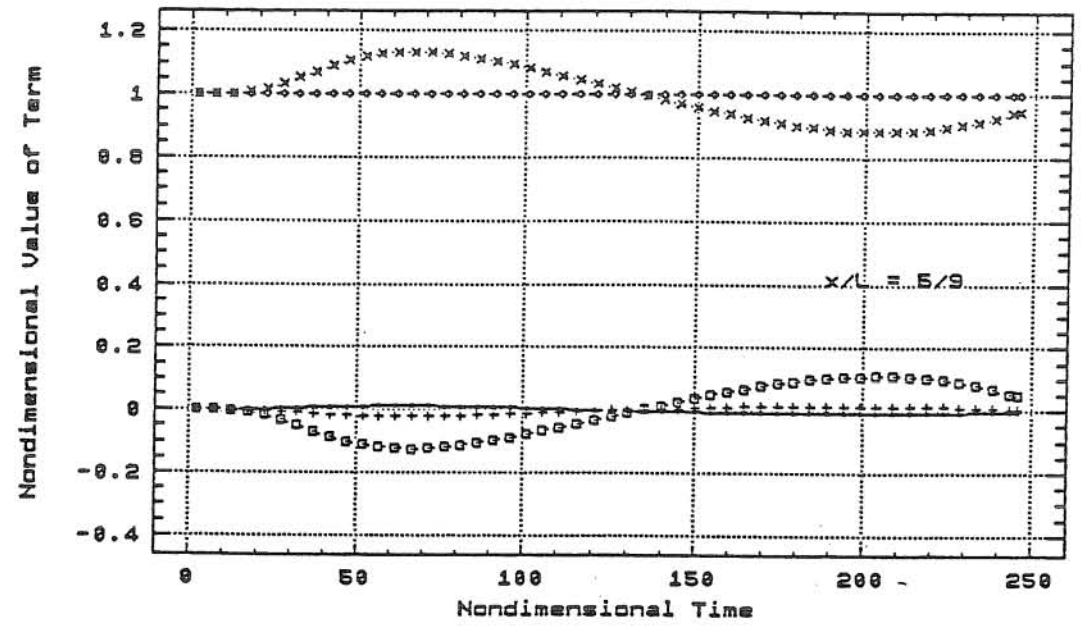

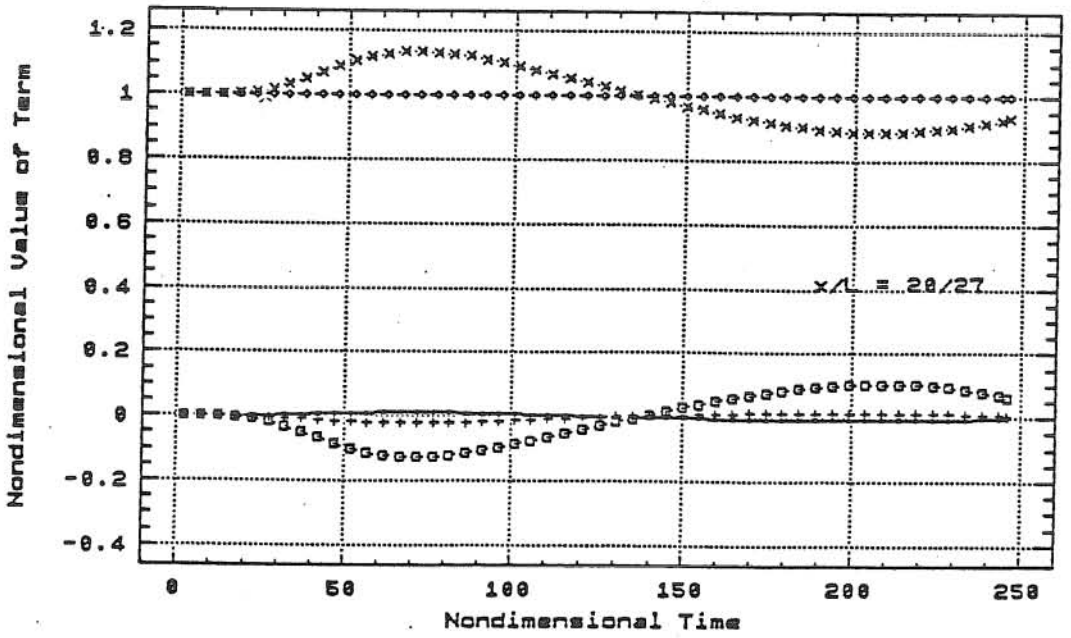

(b) Sections 5/9 and 20/27

Fig. 6.2 (continued)

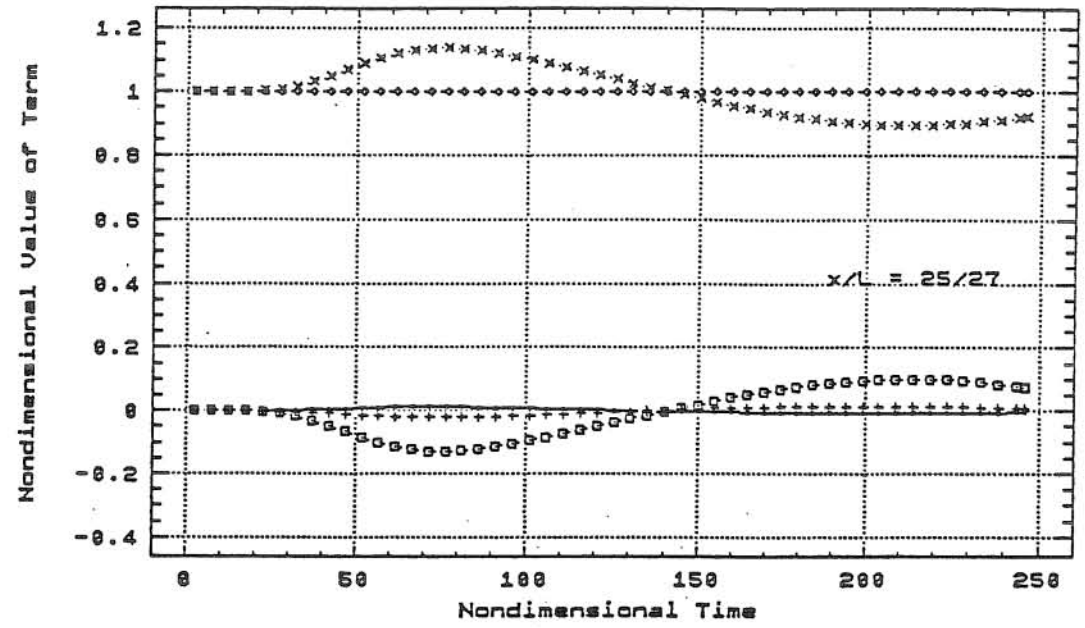

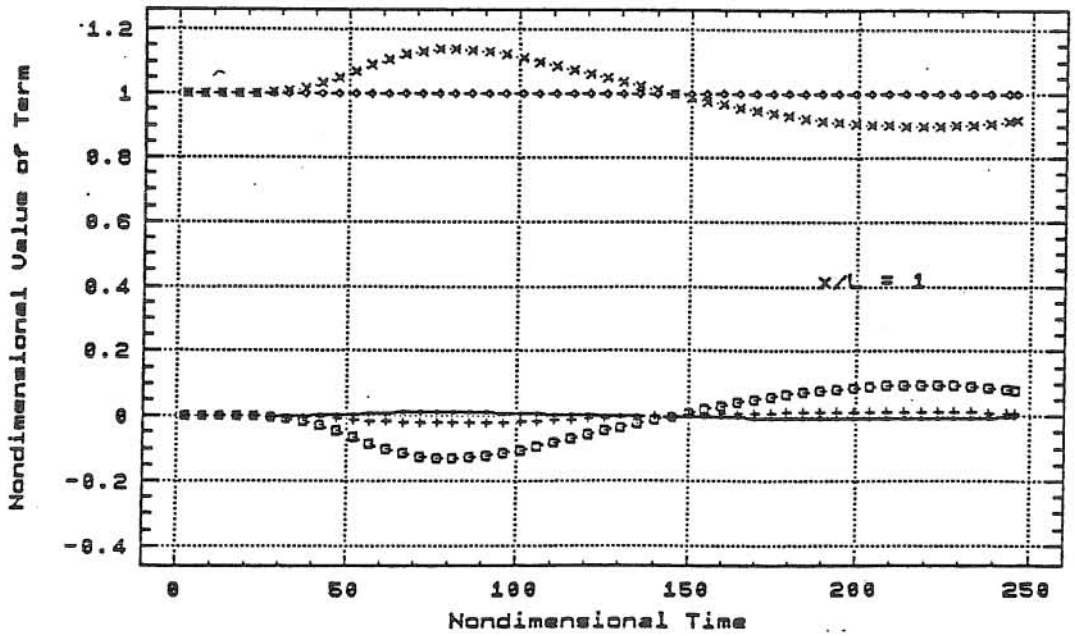

(c) Sections 25/27 and 1

Fig. 6.2 (continued)

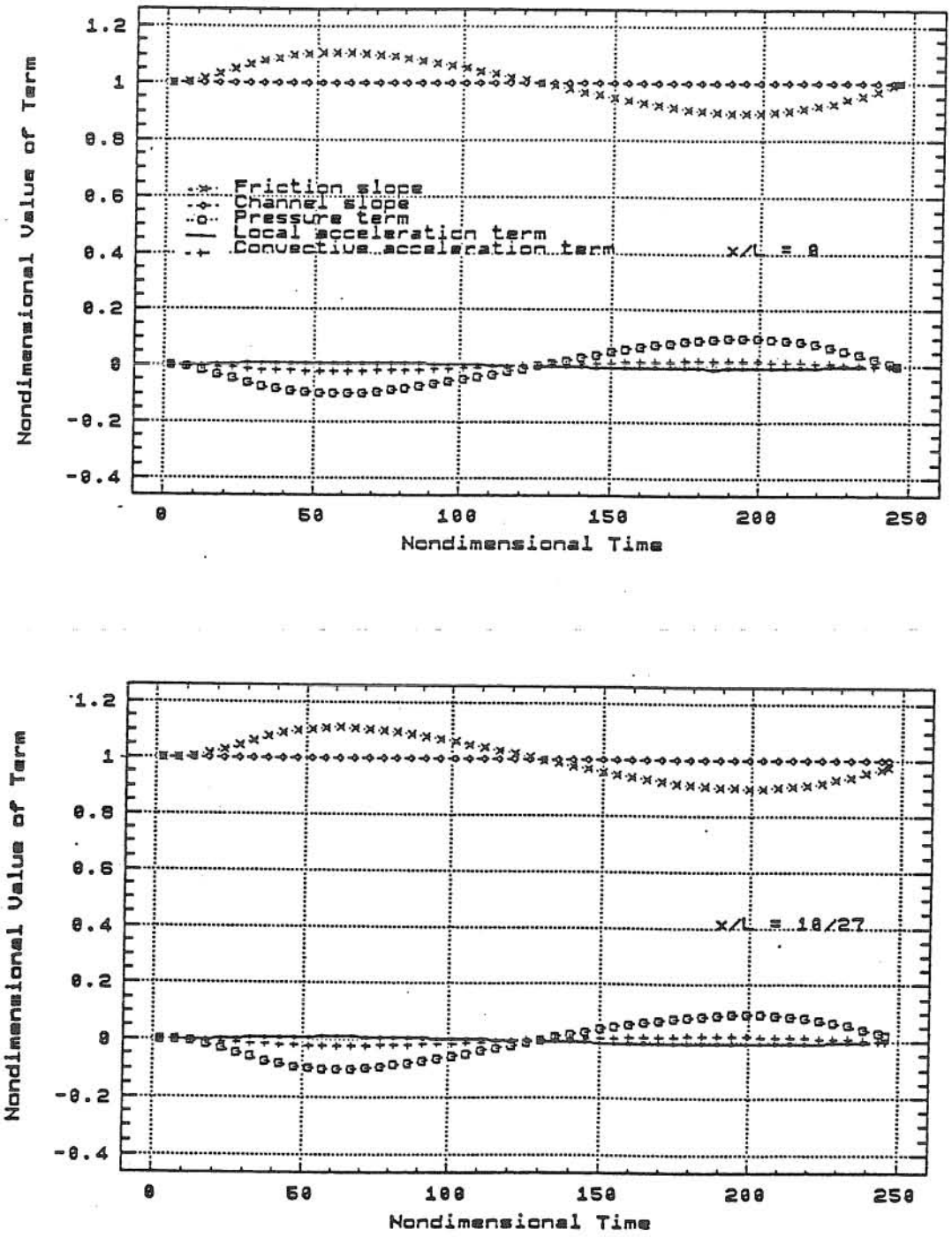

(a) Sections 0 and 10/27

Fig. 6.3 Nondimensional Values of Terms for $\beta = 2$, $k = 0.95$, $k' = 1$, $S_0 = 0.00019$ and No Backwater Effect

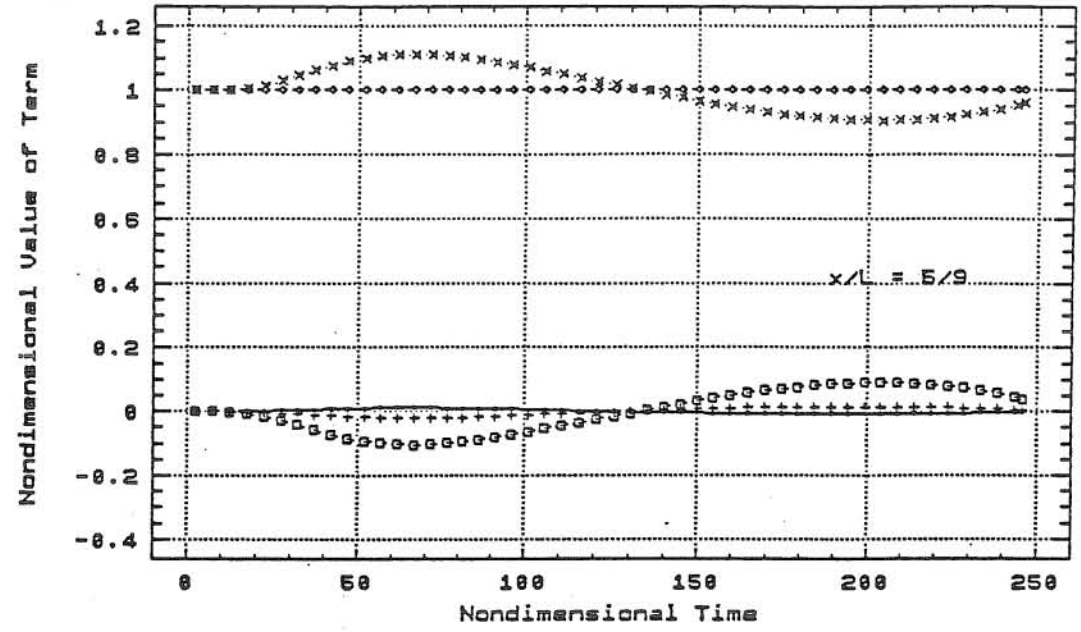

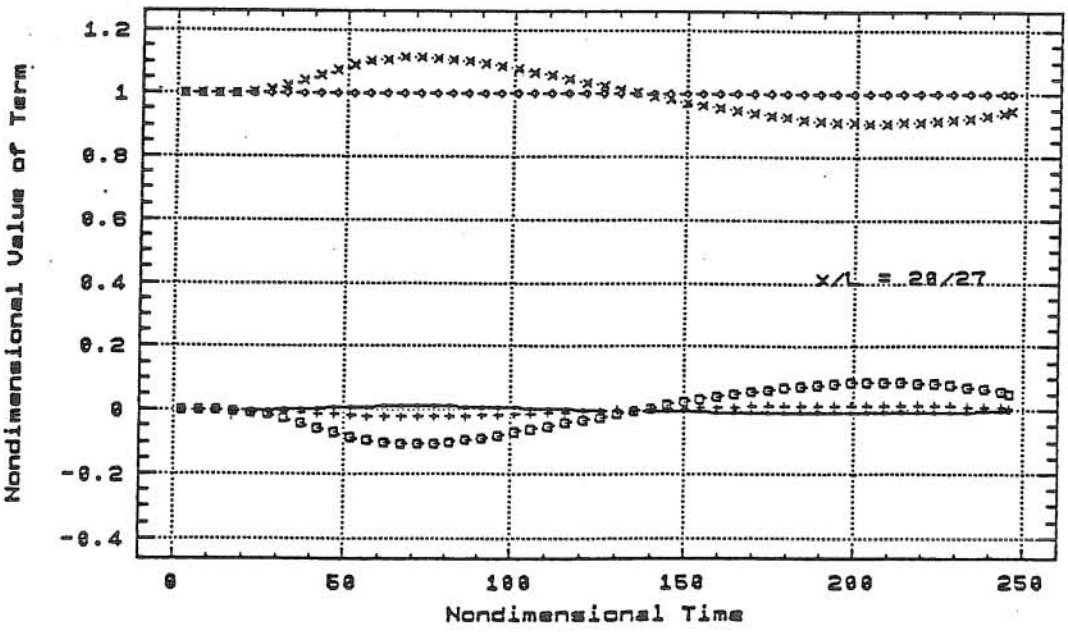

(b) Sections 5/9 and 20/27

Fig. 6.3 (continued)

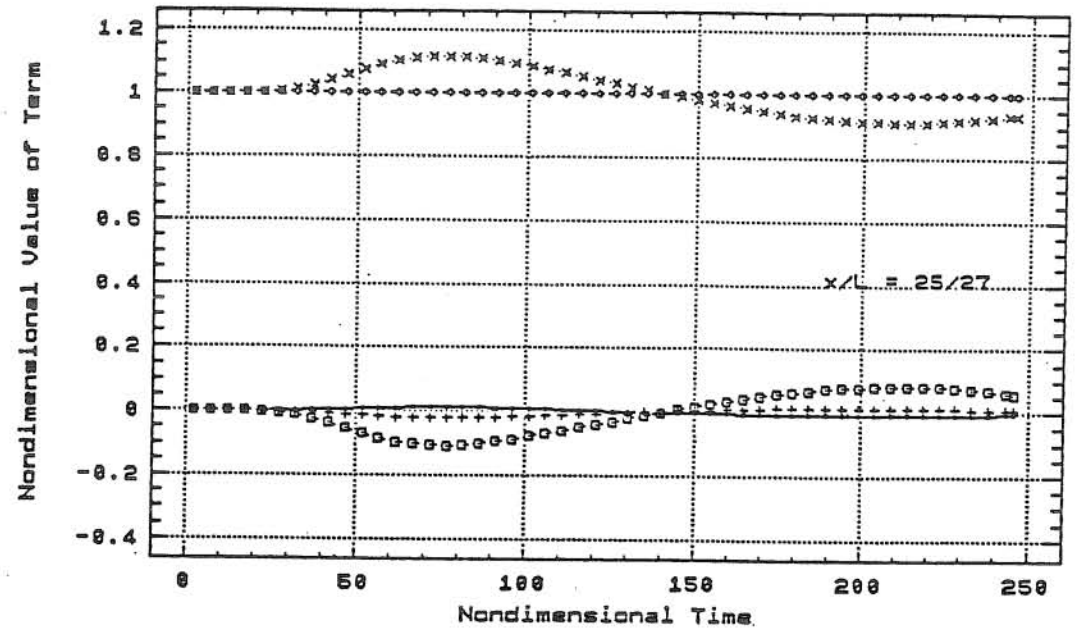

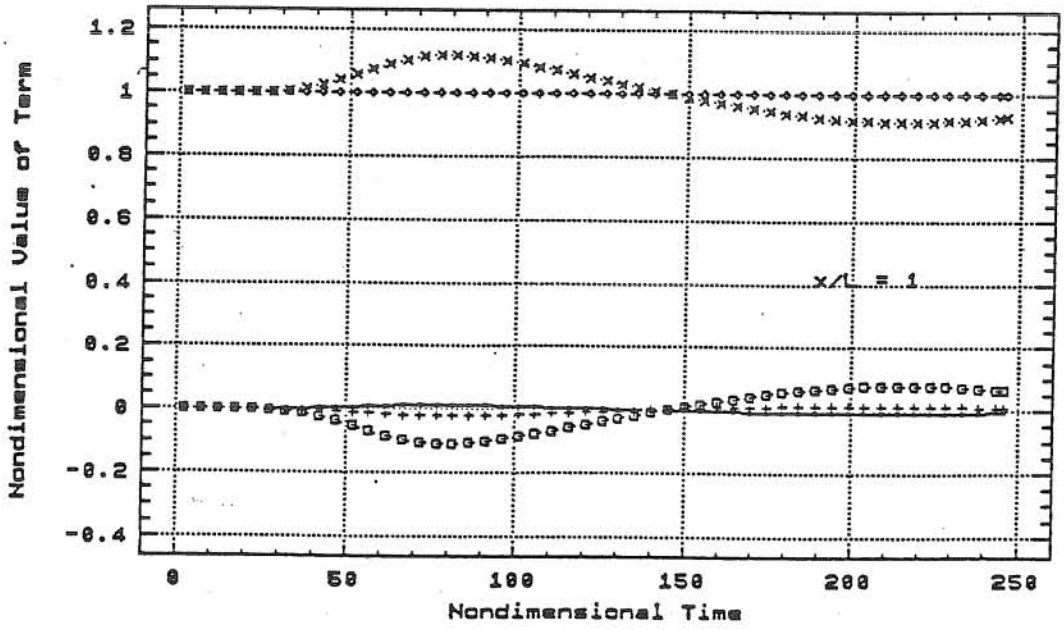

(c) Sections 25/27 and 1

Fig. 6.3 (continued)

Table 6.1 Time-average Ratios between Terms in Exact Momentum Equation for Case of no Backwater Effect

No backwater effect	Location of cross section	Ratio in absolute value: Local accele. vs. Pressure	Convective accele. vs. Pressure	Sum of two accele. vs. Pressure	Pressure vs. Friction slope	Pressure vs. $(S_f - S_0)$
	0	0.09	0.08	0.02	0.07	1.01
ß = 1	10/27	0.10	0.08	0.02	0.07	1.02
k = 1	5/9	0.11	0.09	0.02	0.07	1.02
k' = 1	20/27	0.10	0.09	0.02	0.07	1.02
	25/27	0.11	0.09	0.02	0.06	1.02
	1	0.10	0.09	0.02	0.06	1.02
	0	0.09	0.15	0.07	0.08	0.94
ß = 2	10/27	0.09	0.16	0.06	0.08	0.94
k = 1.05	5/9	0.10	0.16	0.06	0.07	0.94
k' = 1	20/27	0.10	0.17	0.07	0.07	0.94
	25/27	0.10	0.16	0.06	0.07	0.94
	1	0.10	0.15	0.07	0.07	0.93
	0	0.10	0.18	0.08	0.07	0.93
ß = 2	10/27	0.11	0.19	0.08	0.06	0.93
k = 0.95	5/9	0.11	0.19	0.08	0.06	0.93
k' = 1	20/27	0.11	0.19	0.08	0.06	0.93
	25/27	0.12	0.19	0.08	0.06	0.93
	1	0.12	0.19	0.08	0.06	0.93

pressure term and $(S_f - S_0)$ for various situations investigated is always in the order of one, it is implied that the pressure term is no longer negligible. In other words, the advantage of using the noninertia model which is simpler than the full dynamic wave model and more accurate than the kinematic wave model is indicated.

The values of the convective acceleration term and pressure term for the case of ß = 2 and k = 1.05 increase from those for the reference condition of ß = 1 and k = 1. However, the change

is not significant. By comparing Appendix B with Appendix A and referring to Table 6.1, it is shown that the nondimensional value of the convective acceleration term and the ratio between it and the pressure term in the case of ß = 2 and k = 1.05 are about twice as large as that of the case of ß = 1 and k = 1, but the former term is still much smaller than the latter (more than an order of magnitude). The nondimensional value of the pressure term and the ratio between it and the friction slope increase only slightly in the case of ß = 2 and k = 1.05. Furthermore, the other ratios between these terms in the case of ß = 2 and k = 1.05 are almost the same as those for the case of ß = 1 and k = 1. For another extreme case of ß = 2 and k = 0.95, if the results given in Appendix C are compared with those in Appendix A, it is also apparent that the convective acceleration term is approximately twice as large as that of the reference condition of ß = 1 and k = 1, and the pressure term is reduced, but only slightly from the reference case. From Table 6.1, the same conclusions can be obtained.

6.1.2. With Downstream Backwater Effect

Similar to the situation without downstream backwater effect discussed in section 6.1.1, only three situations (ß = 1, k = k' = 1; ß = 2, k = 1.05, k' = 1 and ß = 2, k = 0.95, k' = 1) are selected to illustrate the influence of the five main terms on the unsteady nonuniform flow with downstream backwater effect. The downstream boundary condition is tested by using three constant downstream water depths, i.e., h_d/h_0 = 1.44, 1.80 and 2.53,

respectively. The results are shown in Figs. 6.4 through 6.12 and also summarized in Appendices D, E and F. Similar to Table 6.1, the time-average ratios in the absolute value between these terms for the aforementioned three situations with different downstream water depths are presented in Table 6.2.

By comparing Appendix D with Appendix A or Figs. 6.4 through 6.6 with Fig. 6.1 and examining Table 6.2, it is shown that if there is a downstream backwater condition the pressure term becomes very significant. Its magnitude may be equal to or greater than that of the friction slope at the cross sections near the downstream boundary. As the nondimensional downstream depth, h_d/h_0, increases from 1.44 to 2.53, the ratio between the pressure term and the friction slope increases sharply, and the cross section where the pressure term becomes important (i.e., the ratio between it and the friction slope reaches greater than 20%) moves farther and farther upstream. For example, this position is at $x/L = 25/27$ for $h_d/h_0 = 1.44$, and it is at $x/L = 5/9$ for $h_d/h_0 = 2.53$ (see Figs. 6.4 through 6.6 and Table 6.2). Thus, the pressure term cannot be ignored when the downstream backwater effect exists. Because the pressure term becomes significant and the sum of two acceleration terms is much smaller than the magnitude of the pressure term (it can be seen from Table 6.2 that the ratio between the sum of inertia terms and the pressure term is less than 6% for the case of $\beta = 1$, $k = k' = 1$ with $h_d/h_0 = 1.44$, 1.80 and 2.53, less than 9% for the cases of $\beta = 2$, $k = 1.05$, $k' = 1$ and $\beta = 2$, $k = 0.95$, $k' = 1$ with $h_d/h_0 = 1.80$ and 2.53, and less than 17% for the cases of $\beta = 2$, $k = 1.05$, $k' = 1$ and $\beta = 2$, $k = 0.95$, $k' = 1$

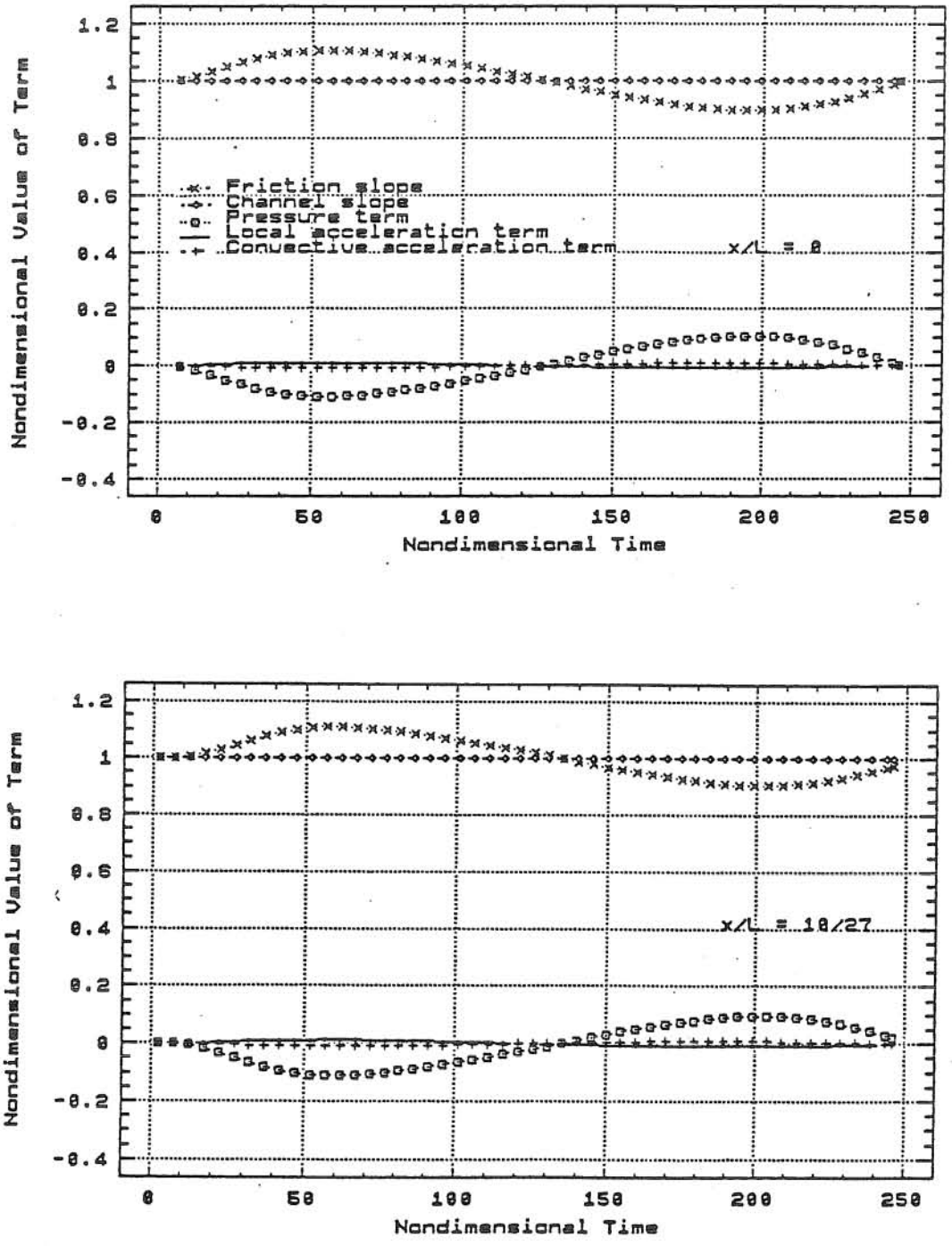

(a) Sections 0 and 10/27

Fig. 6.4 Nondimensional Values of Terms for $\beta = 1$, $k = k' = 1$, $S_0 = 0.00019$ and $h_d/h_0 = 1.44$

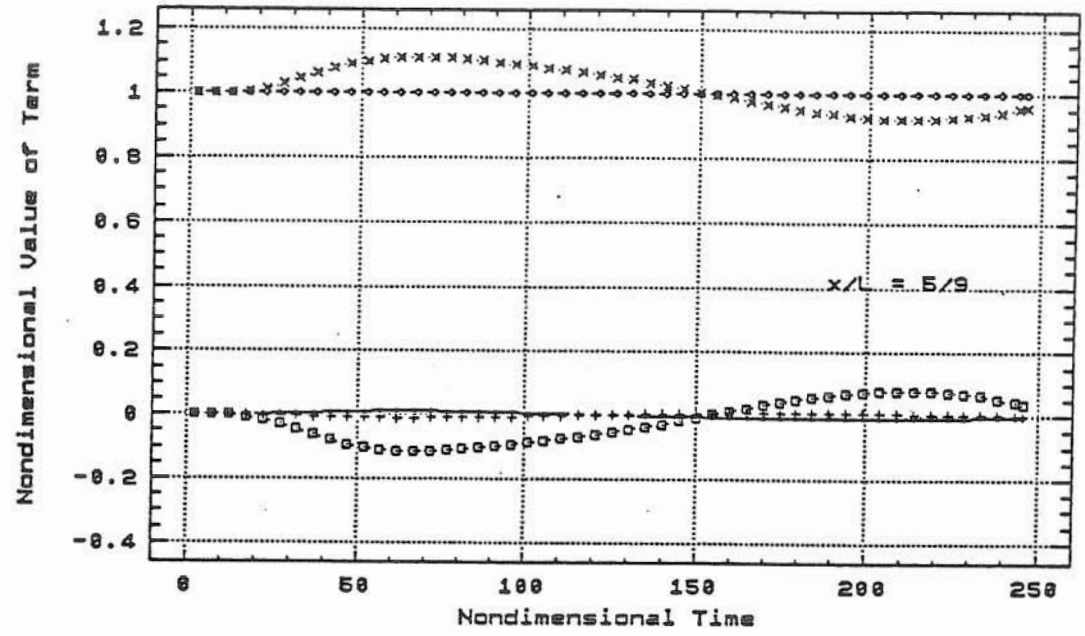

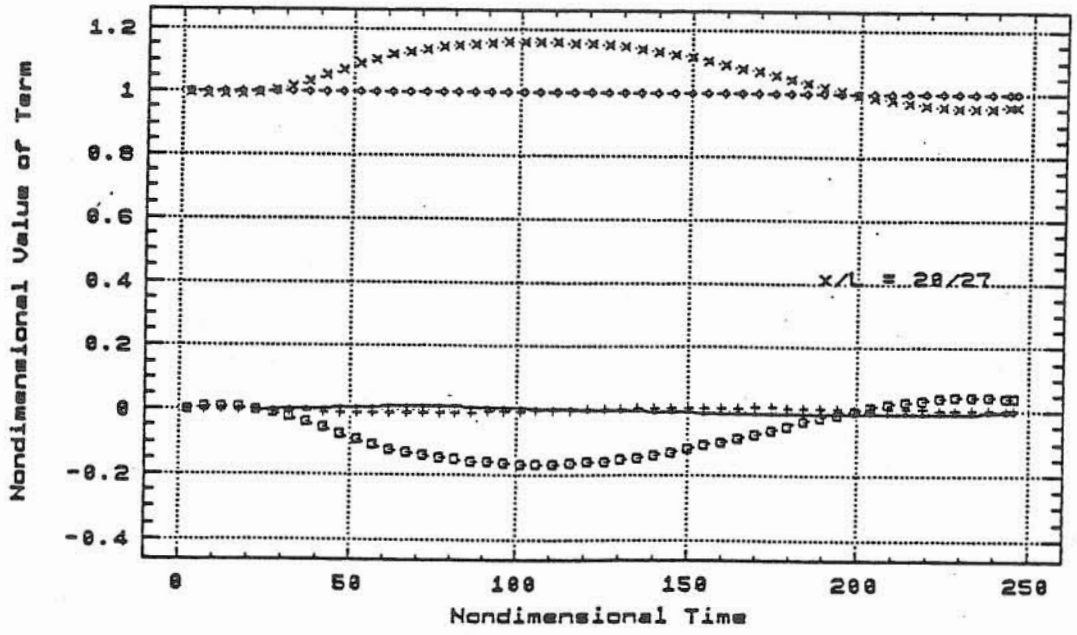

(b) Sections 5/9 and 20/27

Fig. 6.4 (continued)

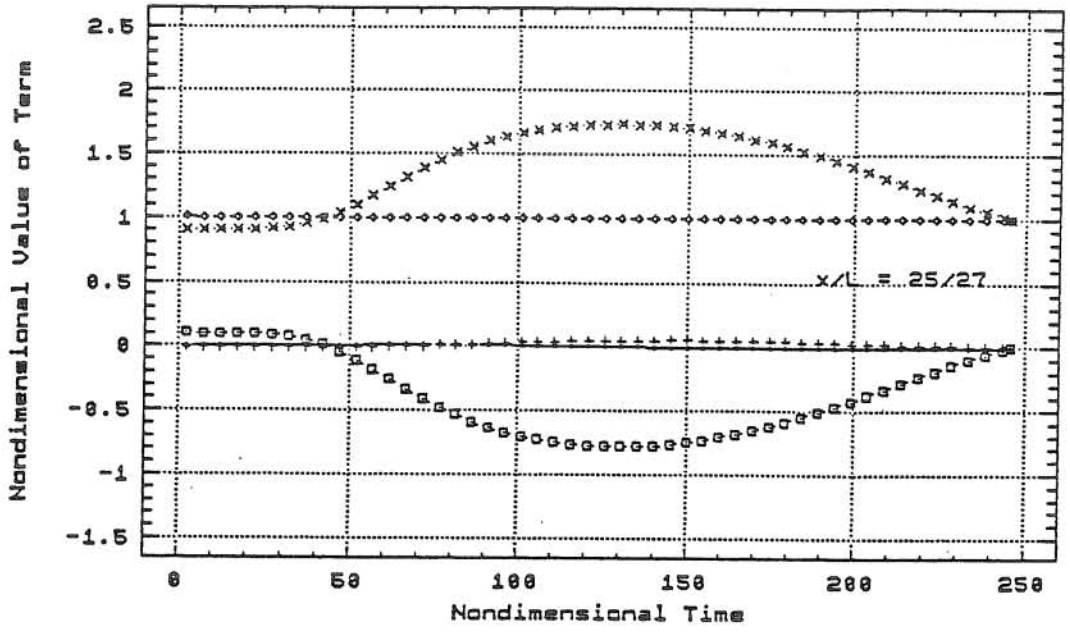

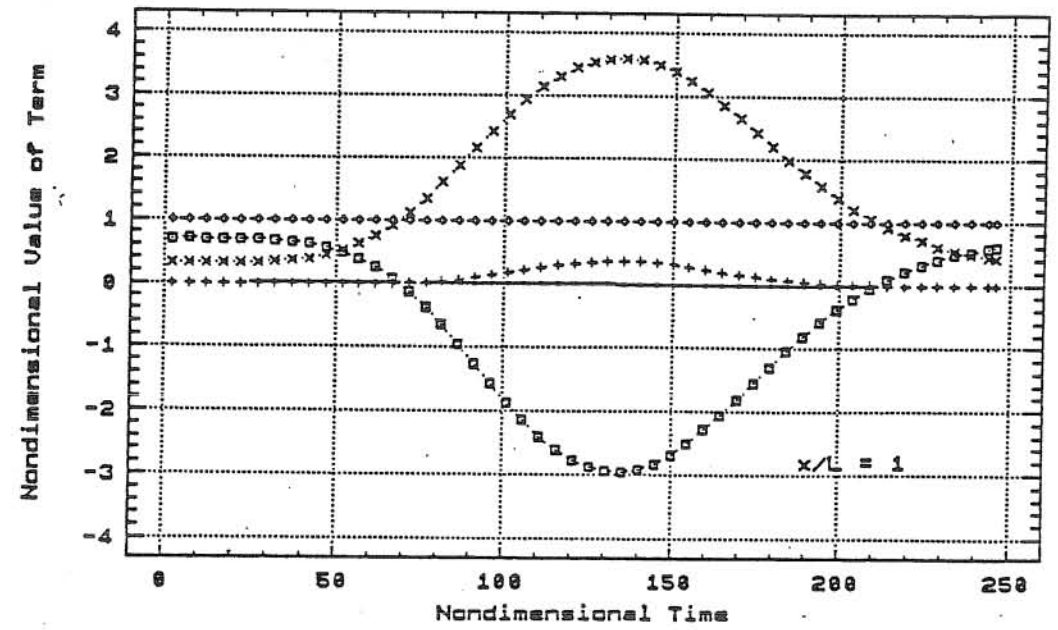

(c) Sections 25/27 and 1

Fig. 6.4 (continued)

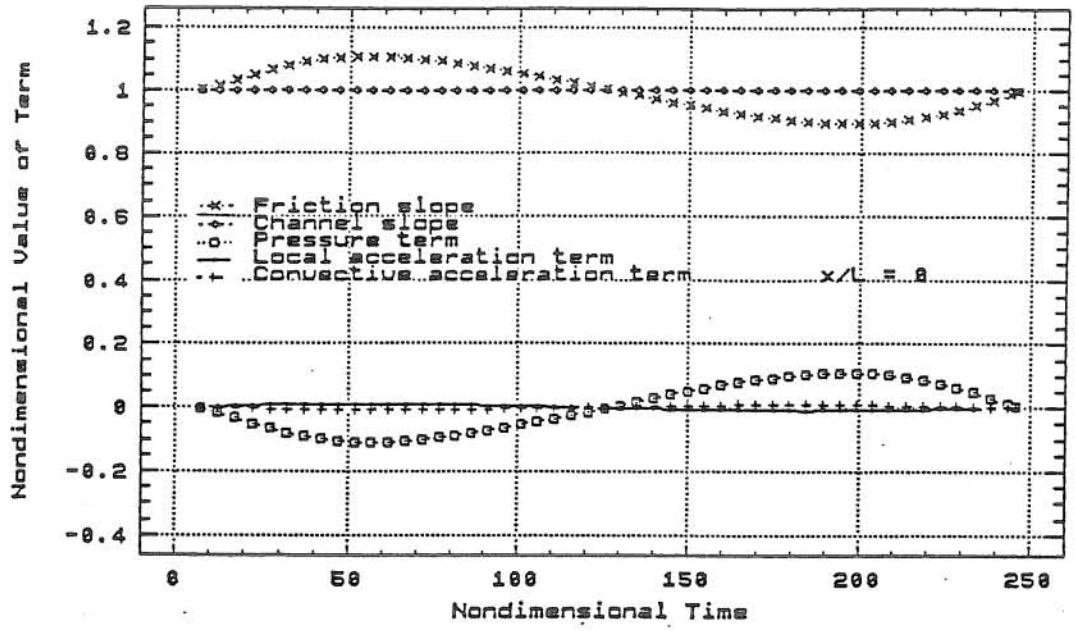

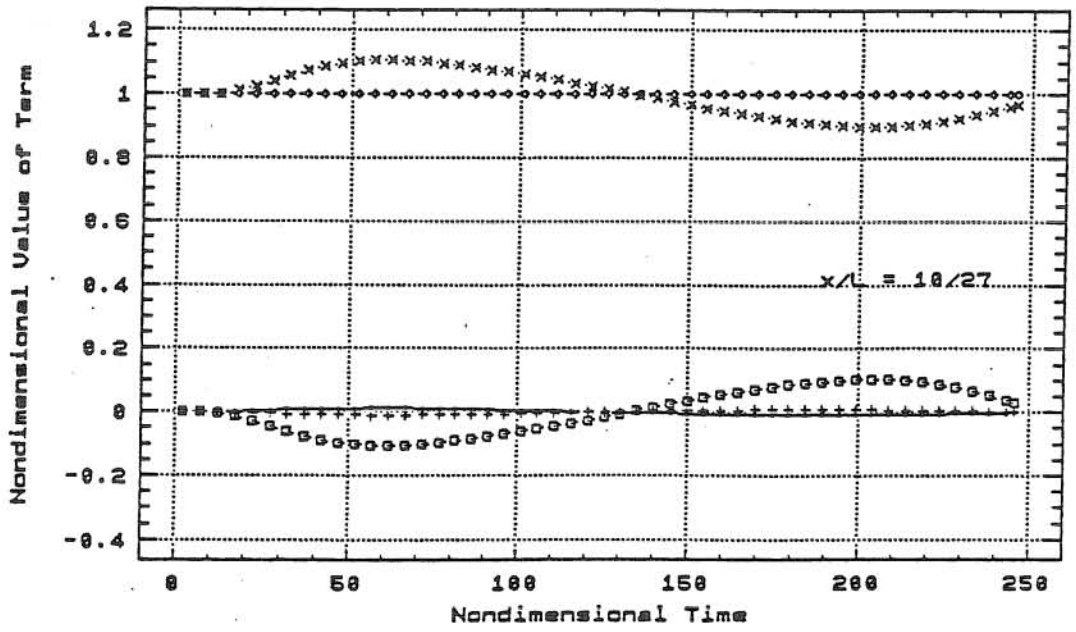

(a) Sections 0 and 10/27

Fig. 6.5 Nondimensional Values of Terms for $\beta = 1$, $k = k' = 1$, $S_0 = 0.00019$ and $h_d/h_0 = 1.80$

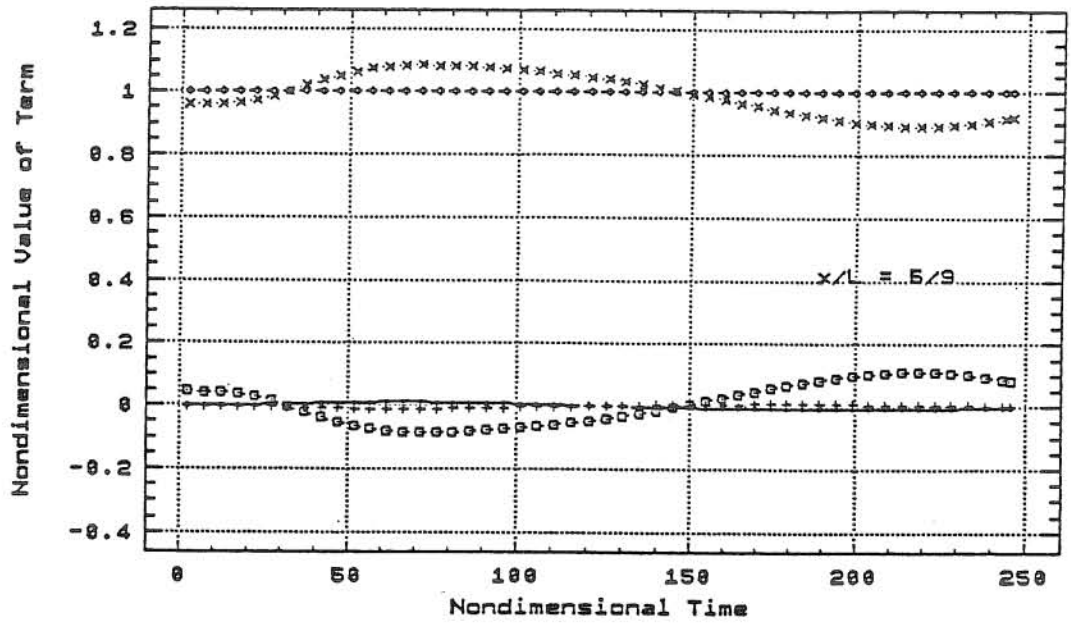

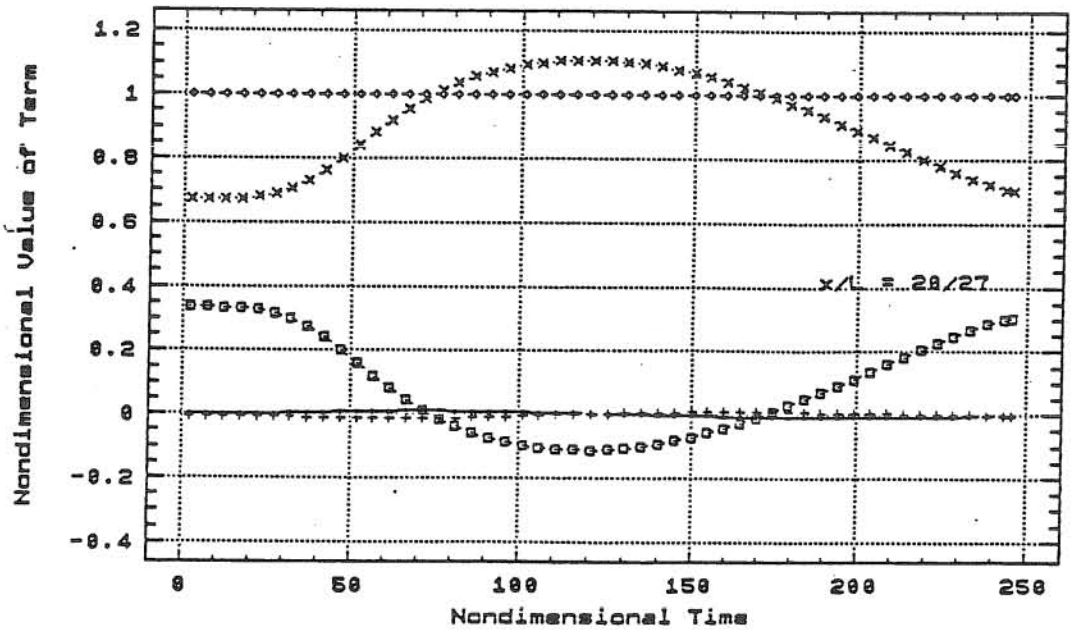

(b) Sections 5/9 and 20/27

Fig. 6.5 (continued)

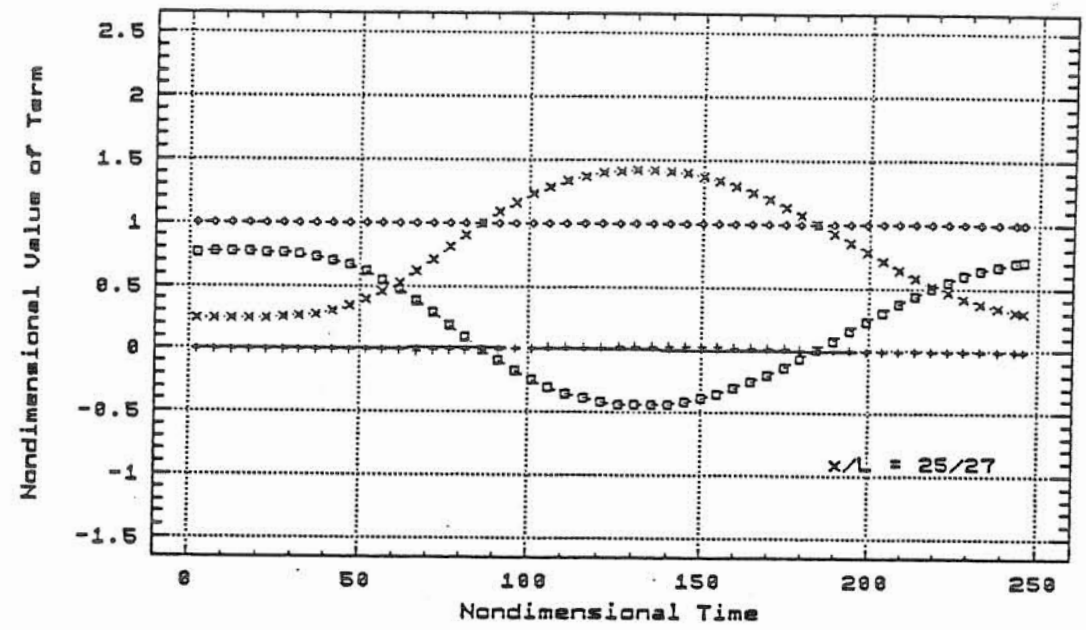

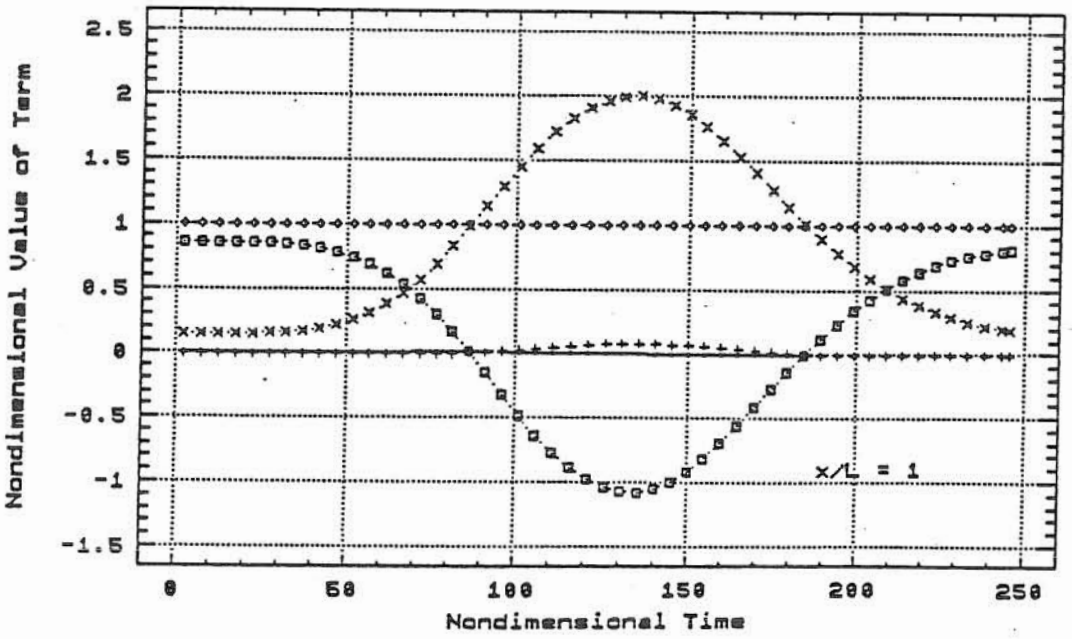

(c) Sections 25/27 and 1

Fig. 6.5 (continued)

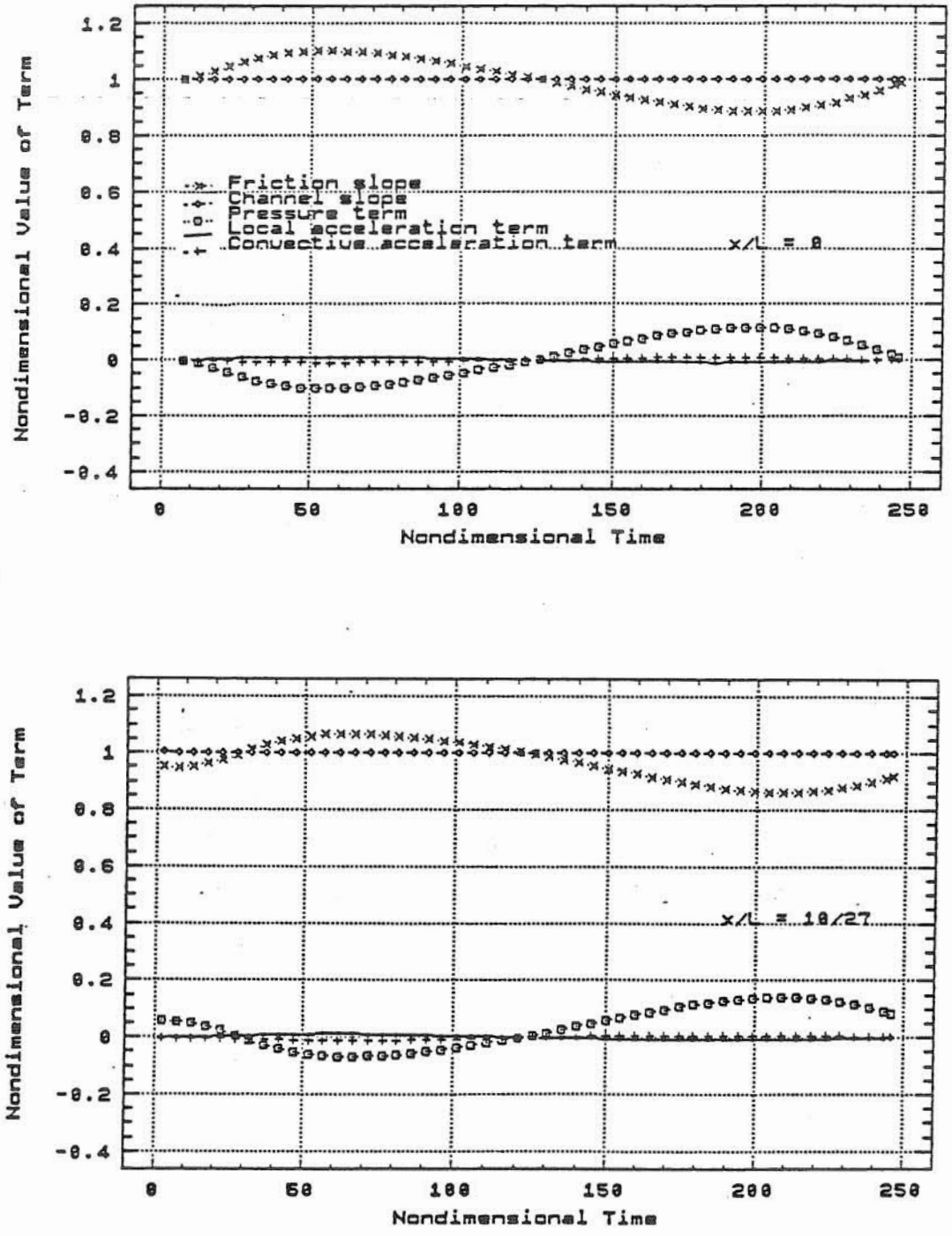

(a) Sections 0 and 10/27

Fig. 6.6 Nondimensional Values of Terms for $\beta = 1$, $k = k' = 1$, $S_0 = 0.00019$ and $h_d/h_0 = 2.53$

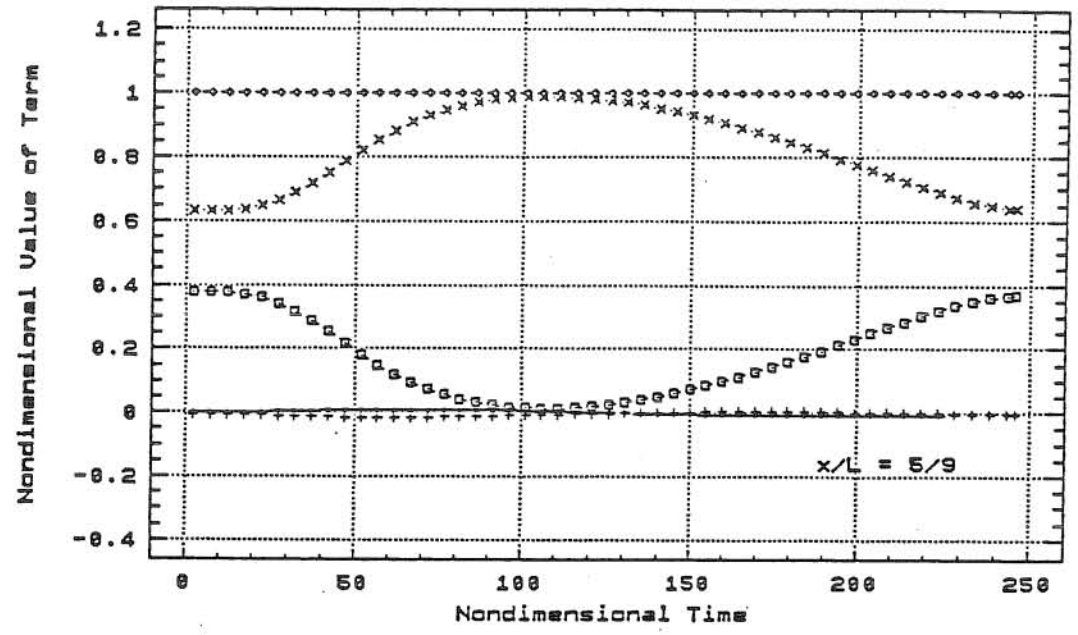

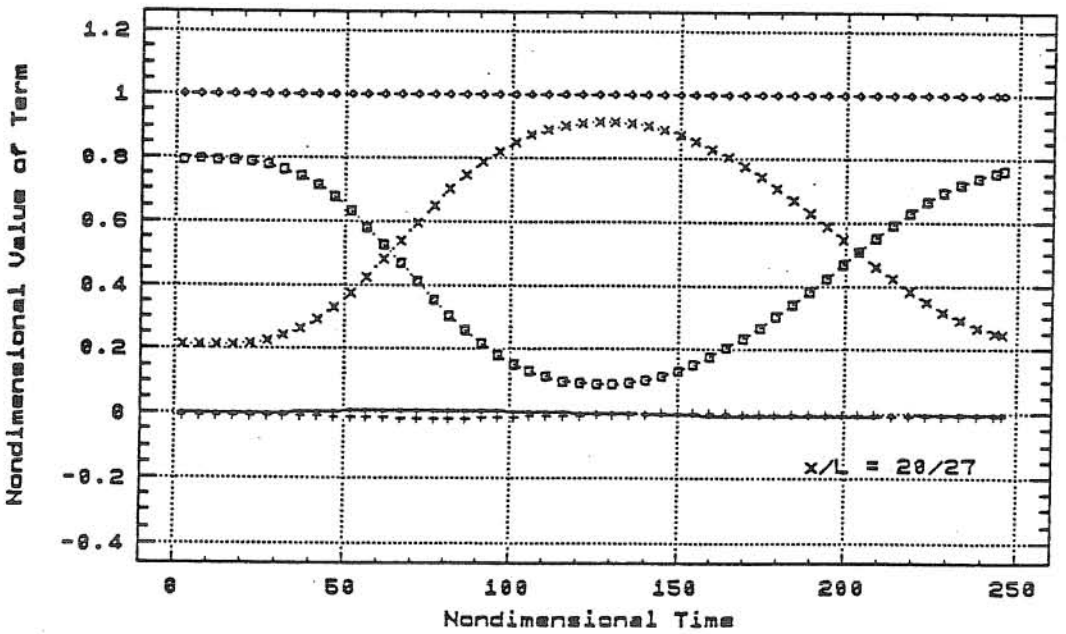

(b) Sections 5/9 and 20/27

Fig. 6.6 (continued)

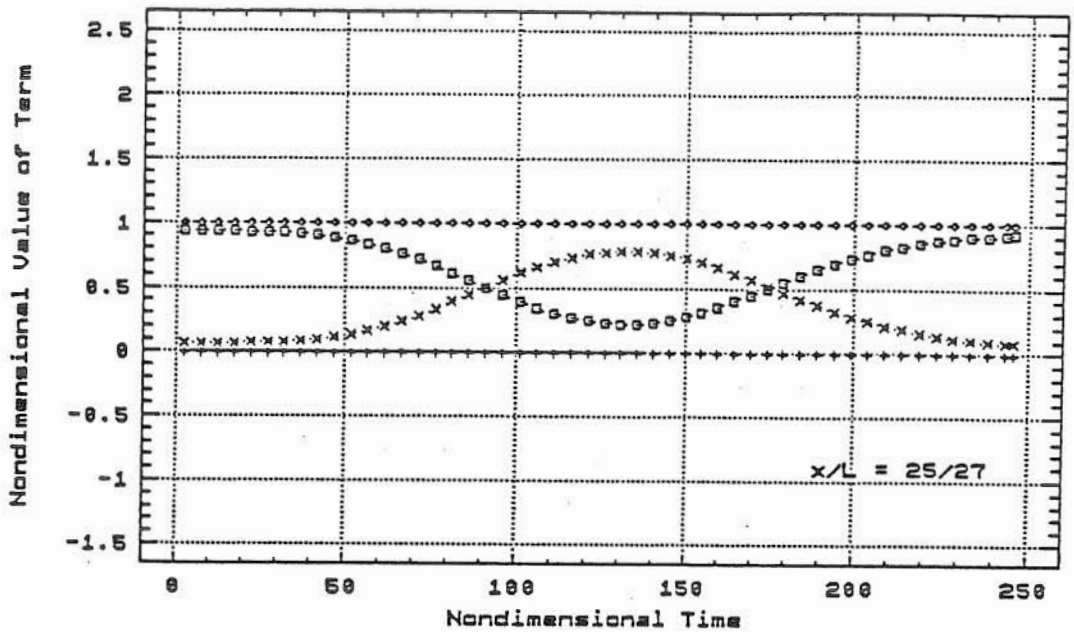

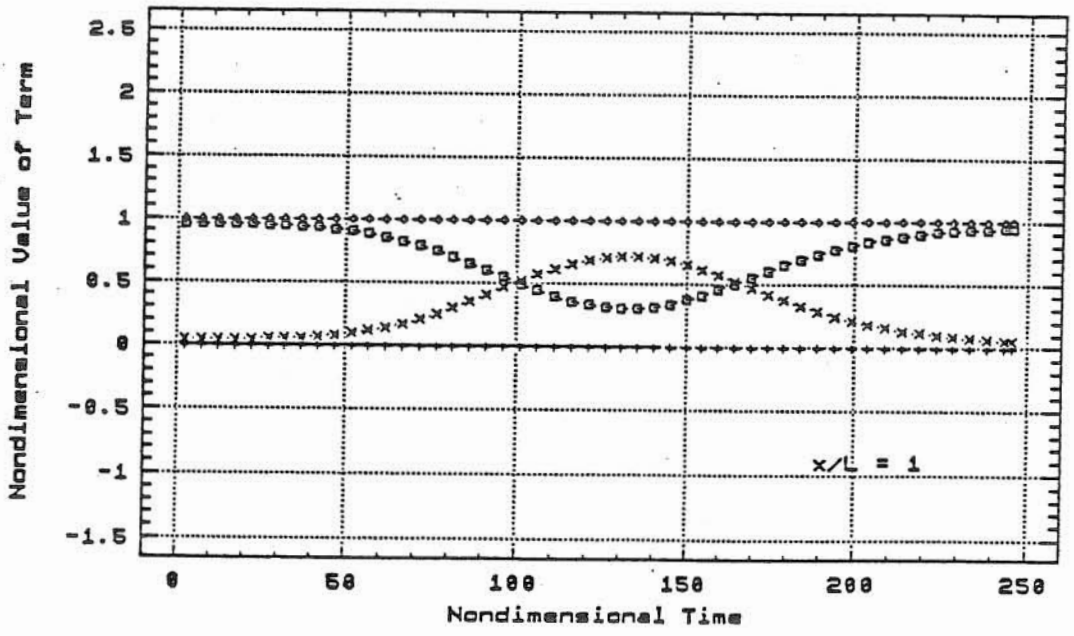

(c) Sections 25/27 and 1

Fig. 6.6 (continued)

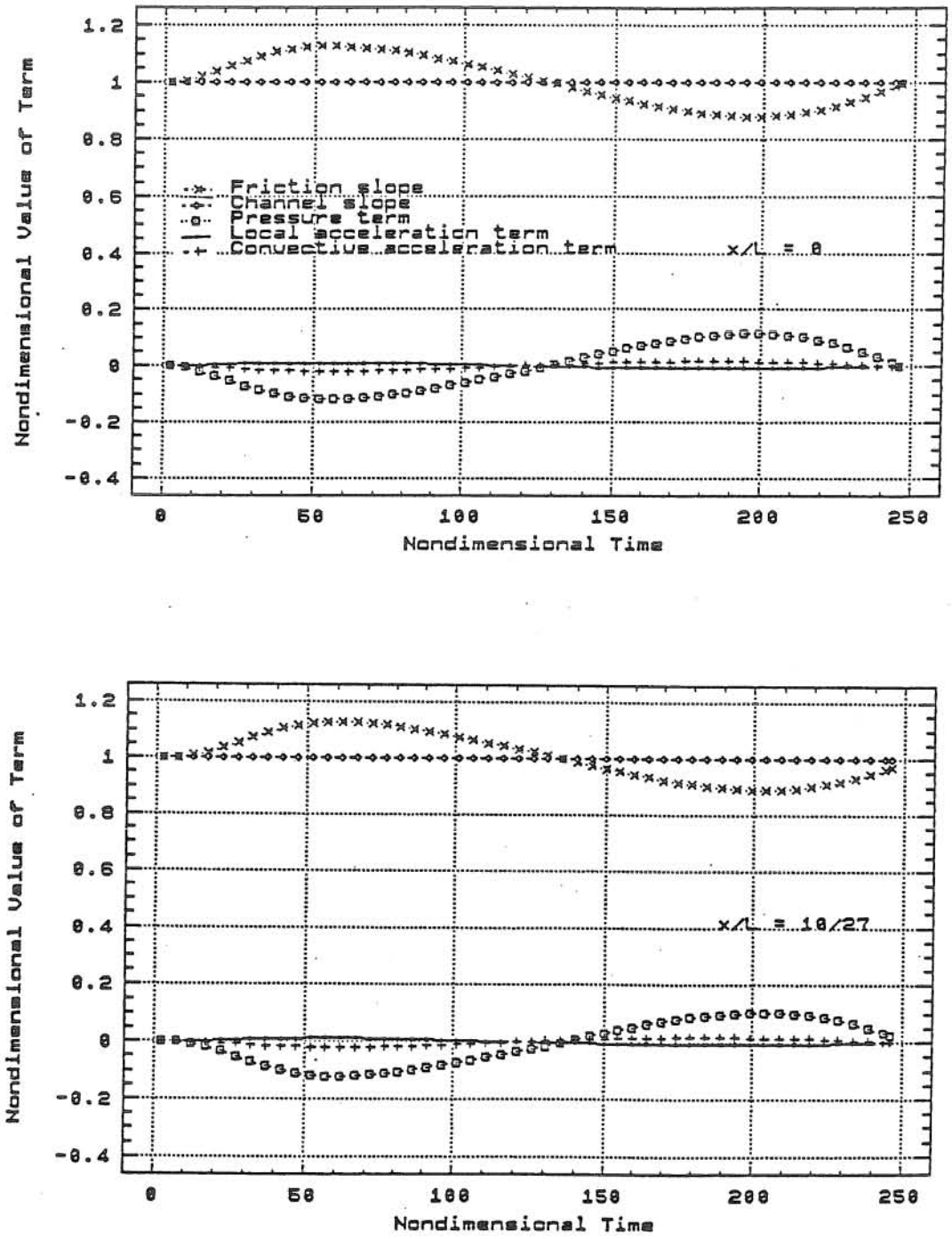

(a) Sections 0 and 10/27

Fig. 6.7 Nondimensional Values of Terms for $\beta = 2$, $k = 1.05$, $k' = 1$, $S_0 = 0.00019$ and $h_d/h_0 = 1.44$

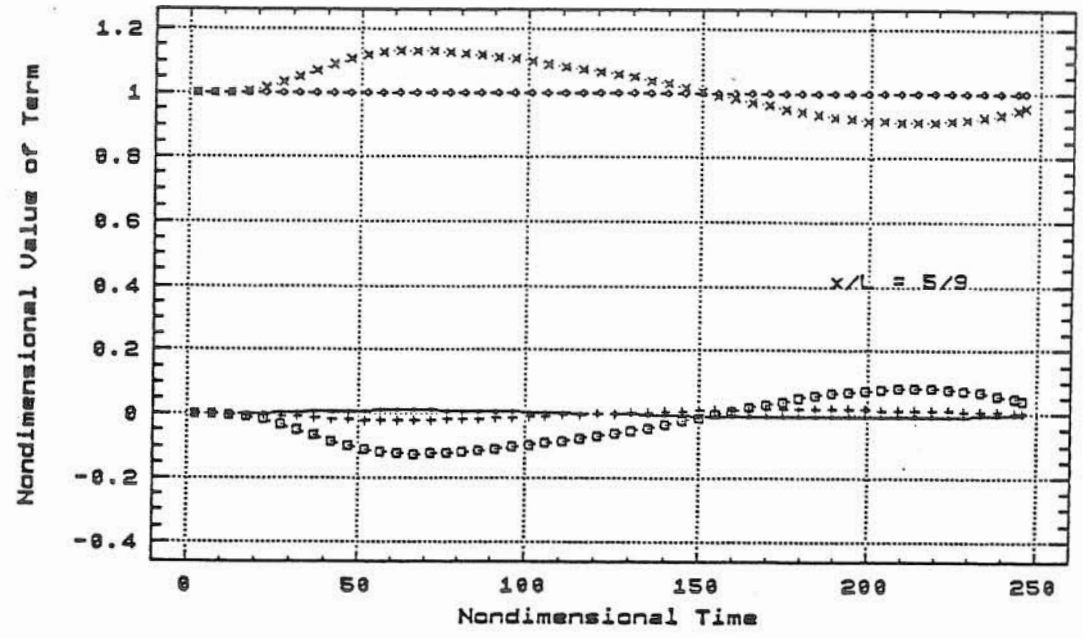

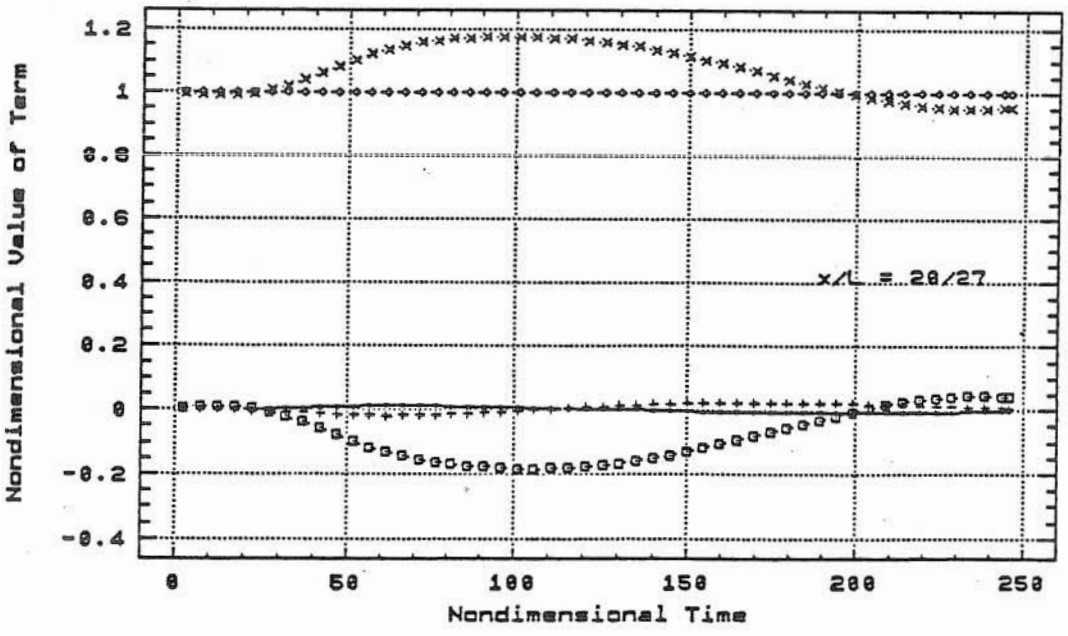

(b) Sections 5/9 and 20/27

Fig. 6.7 (continued)

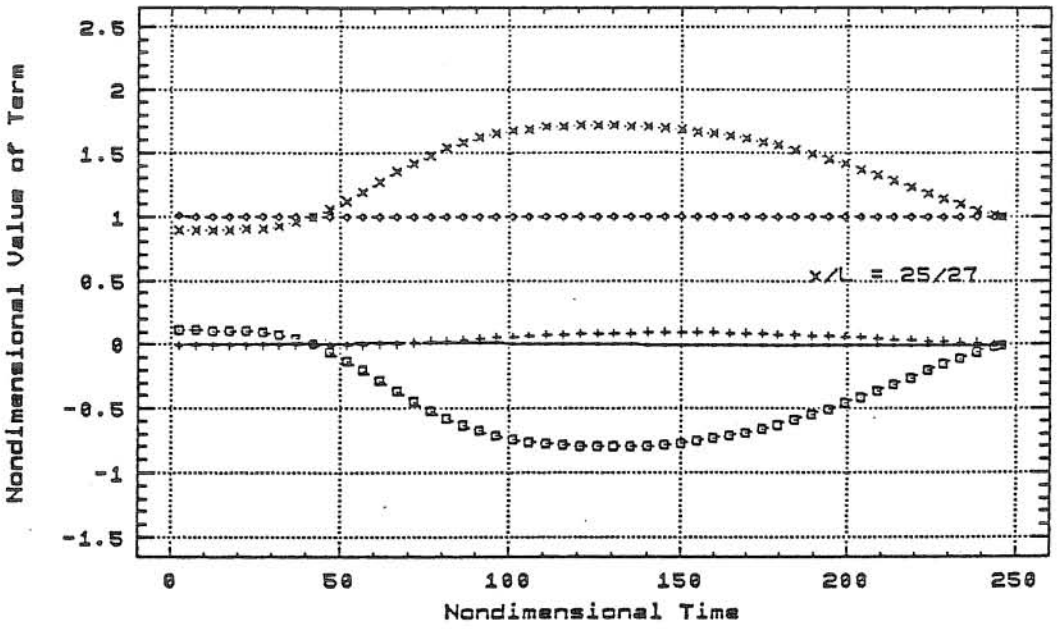

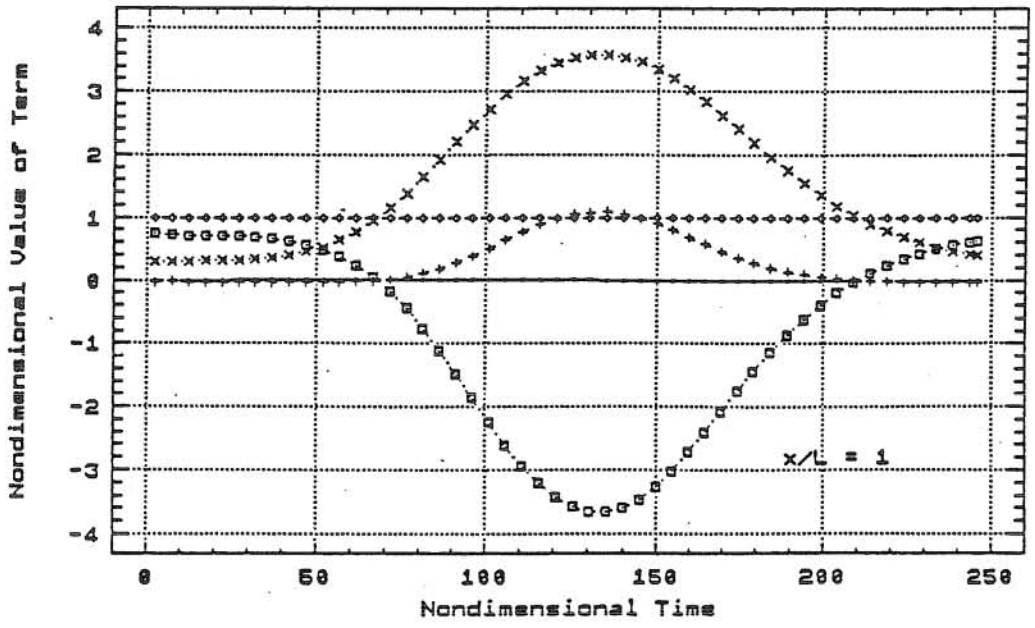

(c) Sections 25/27 and 1

Fig. 6.7 (continued)

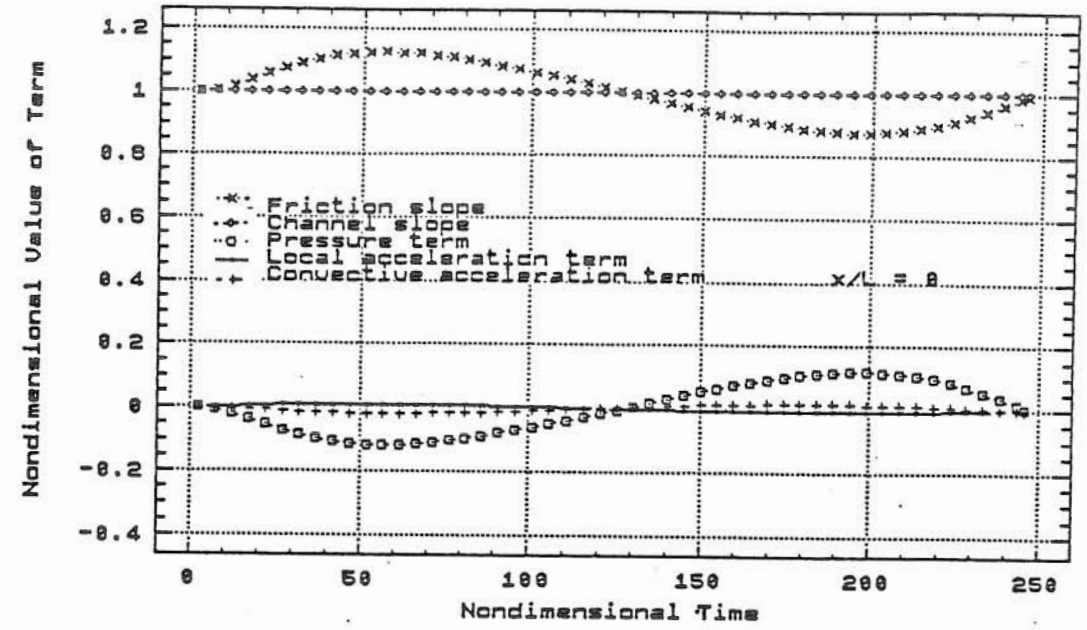

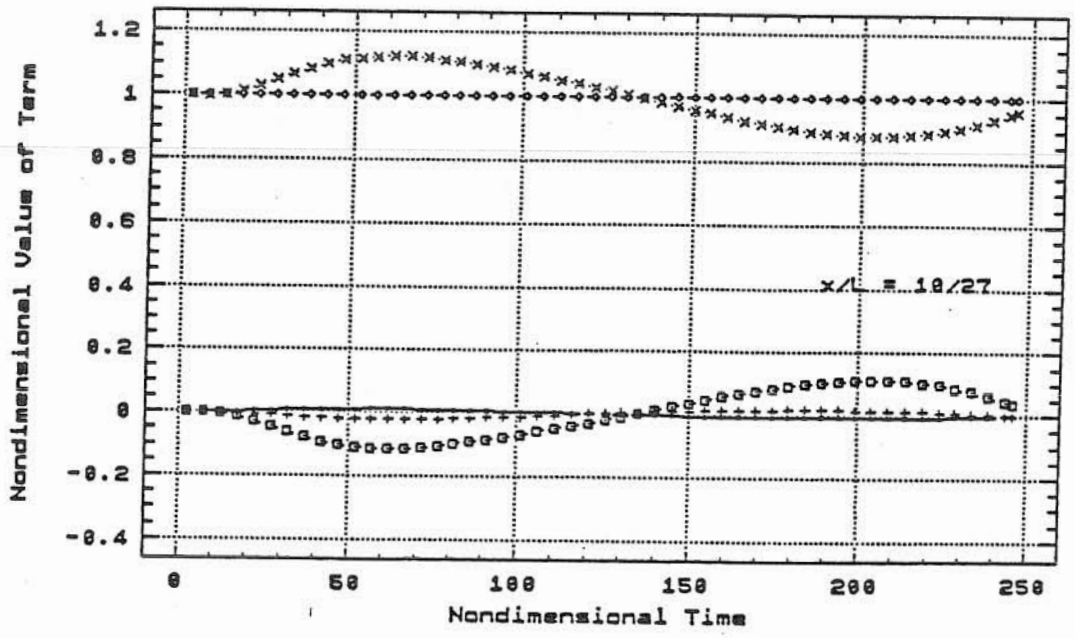

(a) Sections 0 and 10/27

Fig. 6.8 Nondimensional Values of Terms for $\beta = 2$, $k = 1.05$, $k' = 1$, $S_0 = 0.00019$ and $h_d/h_0 = 1.80$

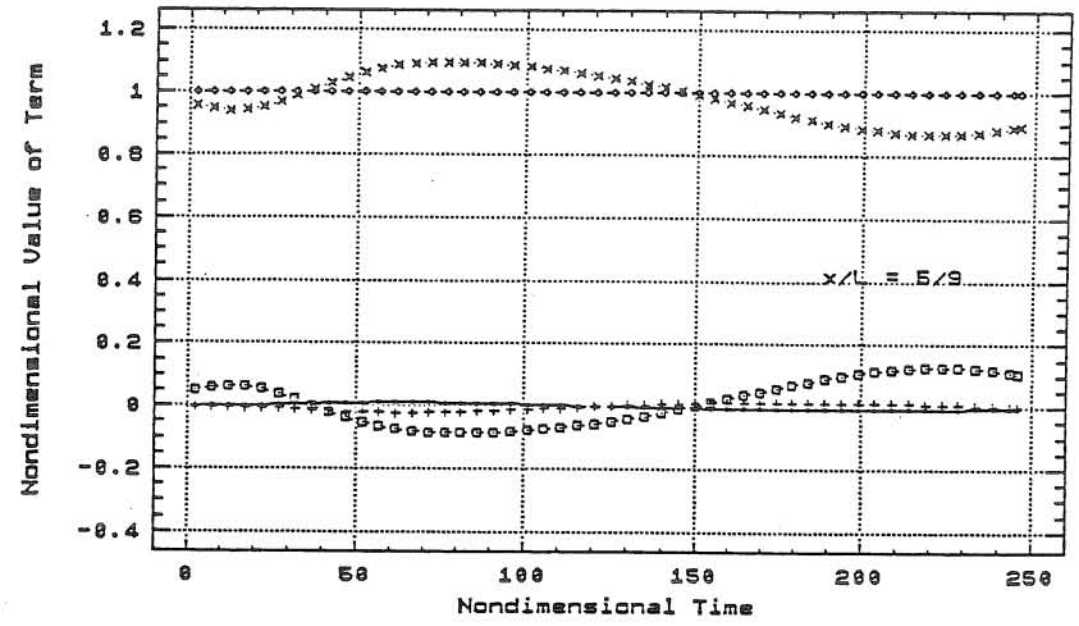

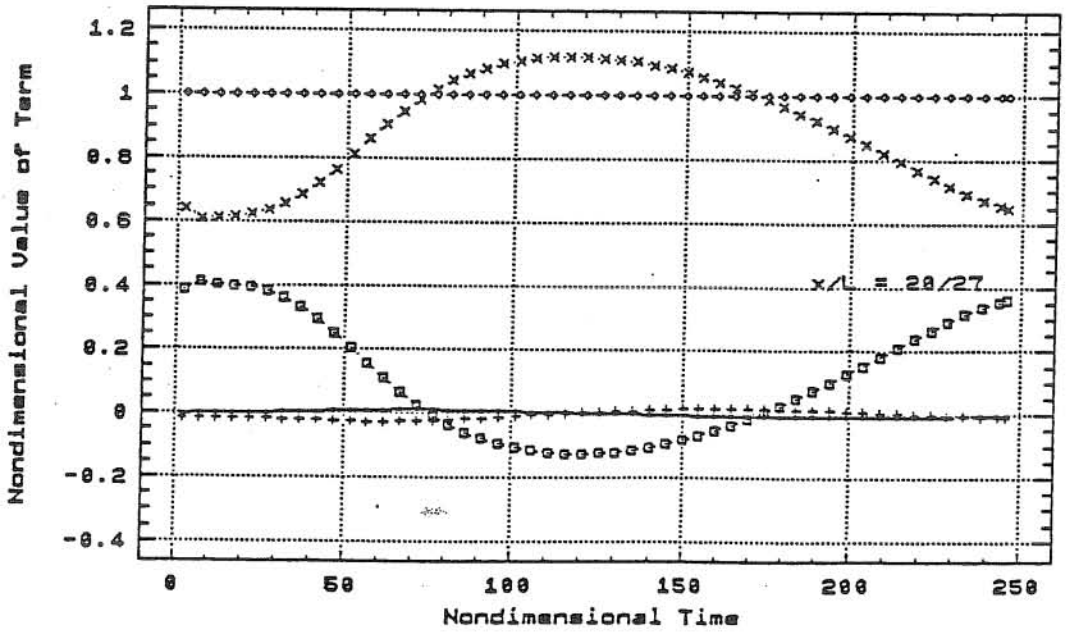

(b) Sections 5/9 and 20/27

Fig. 6.8 (continued)

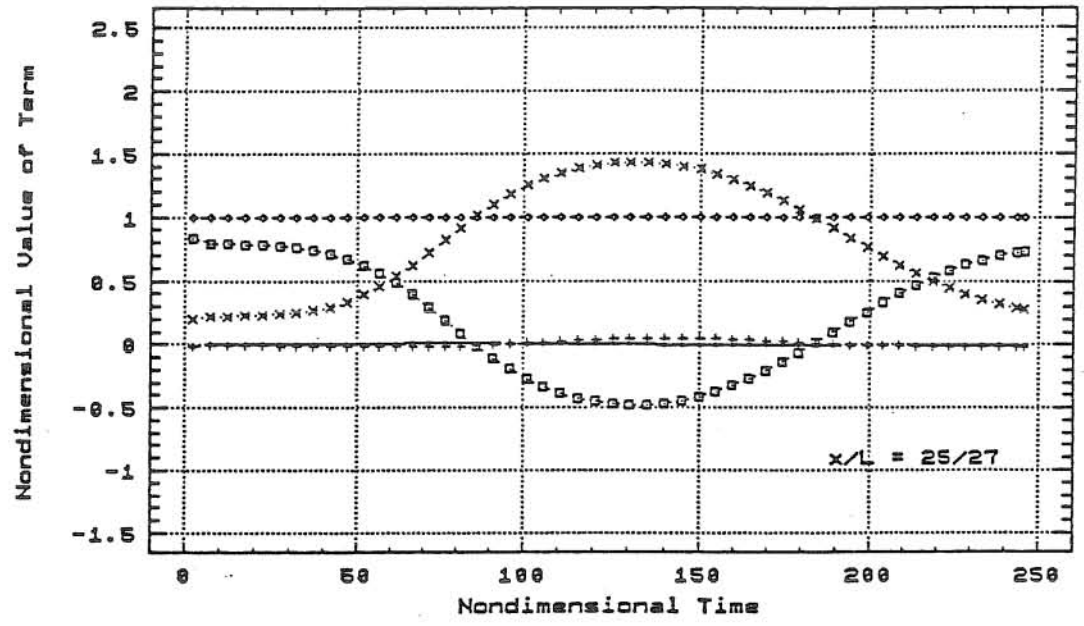

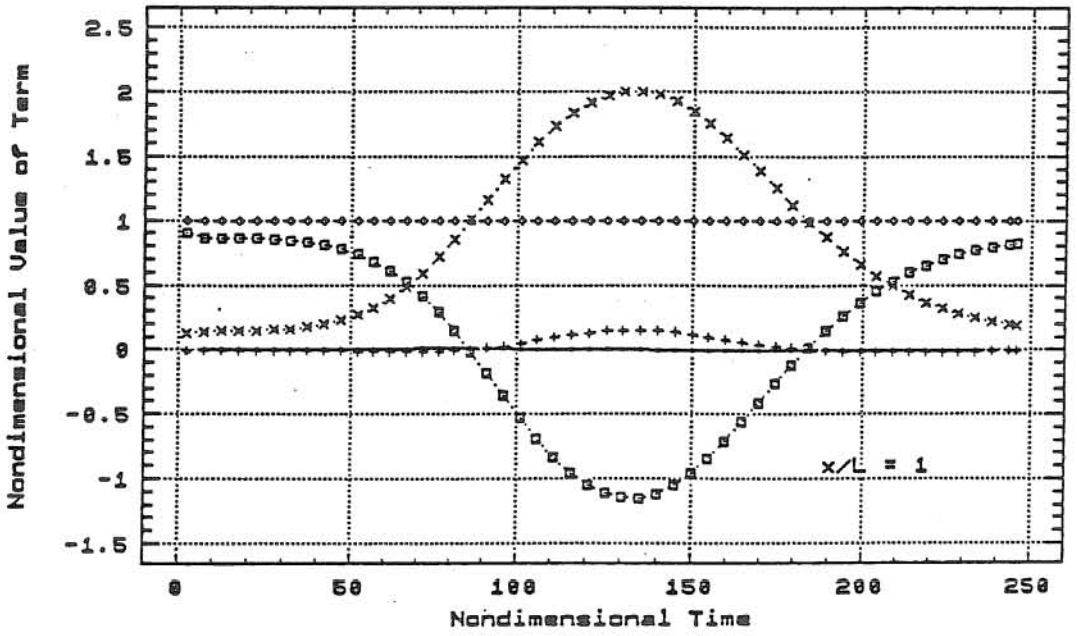

(c) Sections 25/27 and 1

Fig. 6.8 (continued)

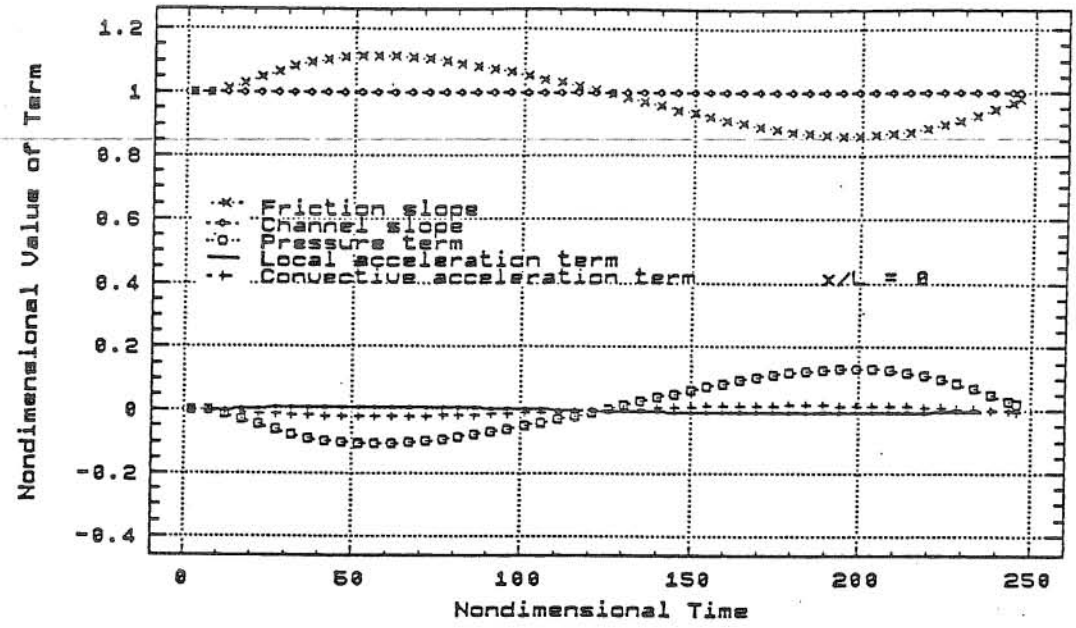

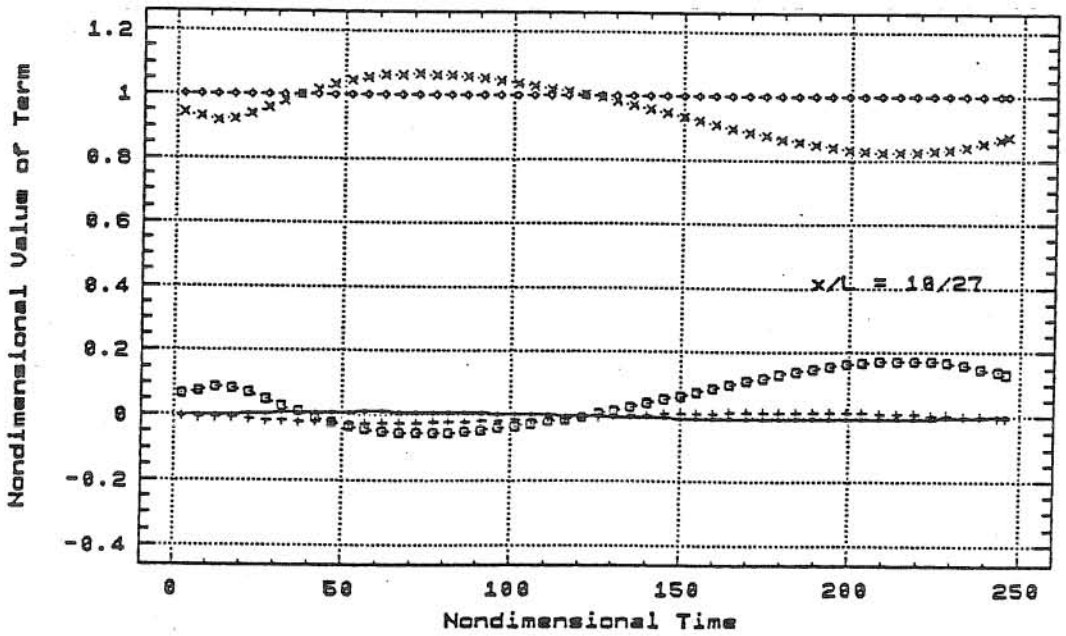

(a) Sections 0 and 10/27

Fig. 6.9 Nondimensional Values of Terms for $\beta = 2$, $k = 1.05$, $k' = 1$, $S_0 = 0.00019$ and $h_d/h_0 = 2.53$

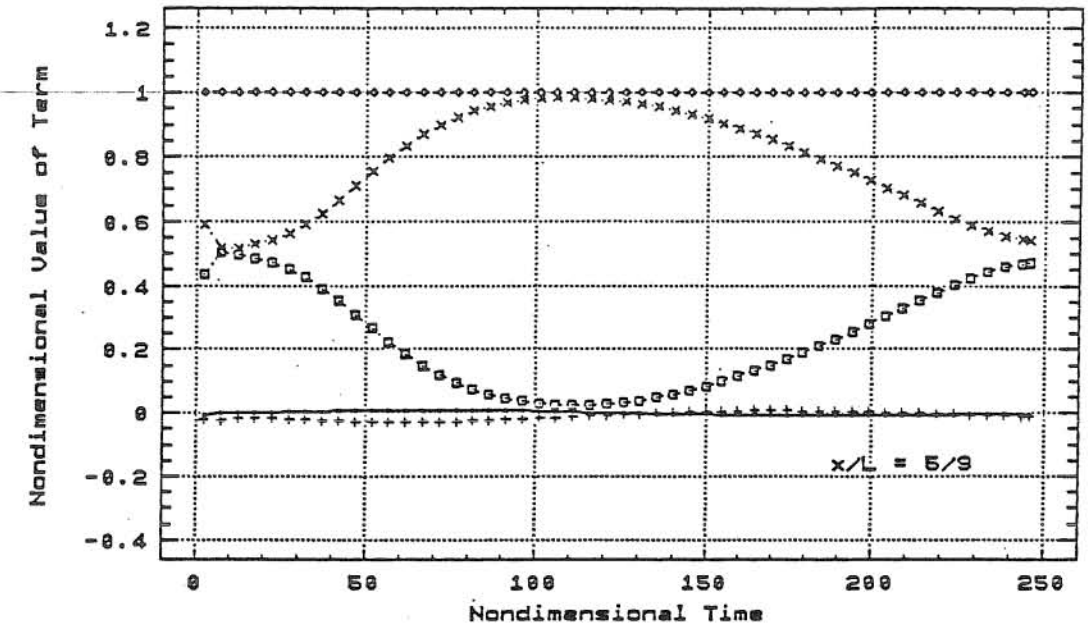

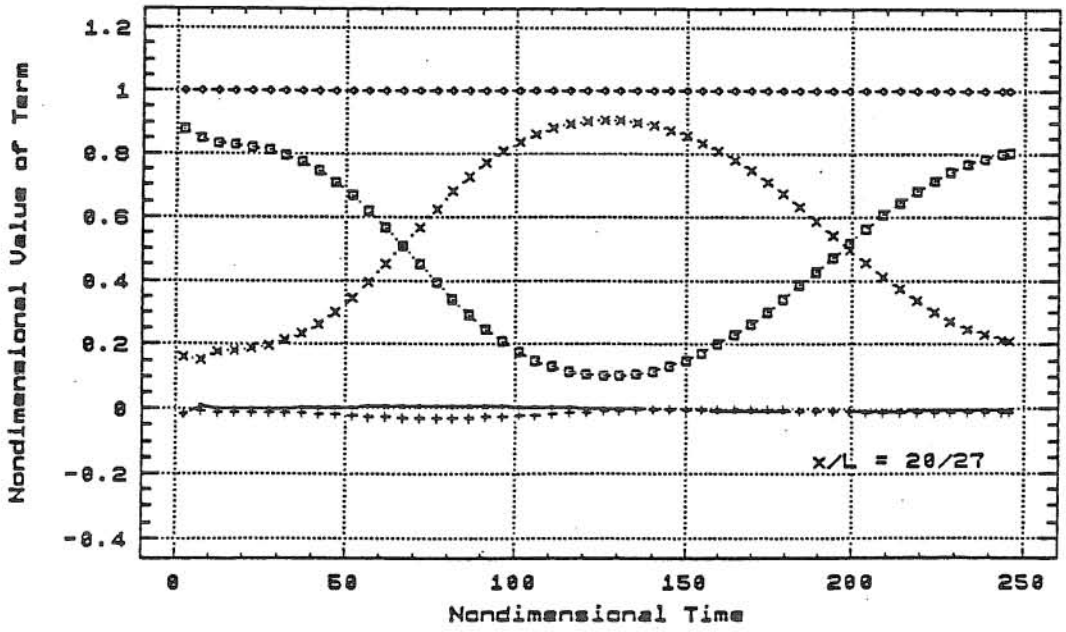

(b) Sections 5/9 and 20/27

Fig. 6.9 (continued)

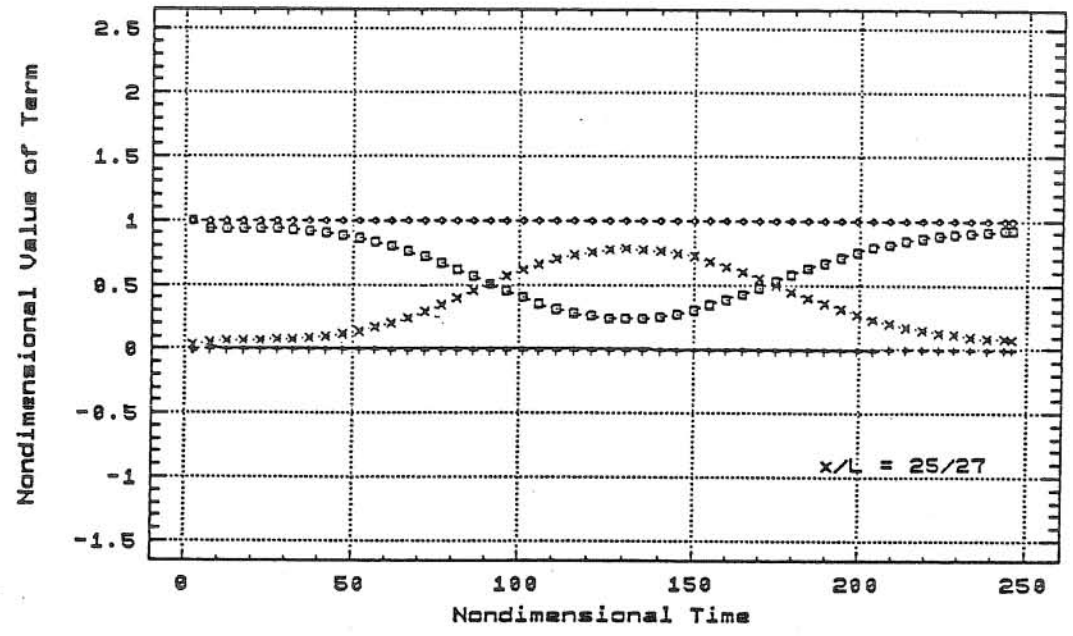

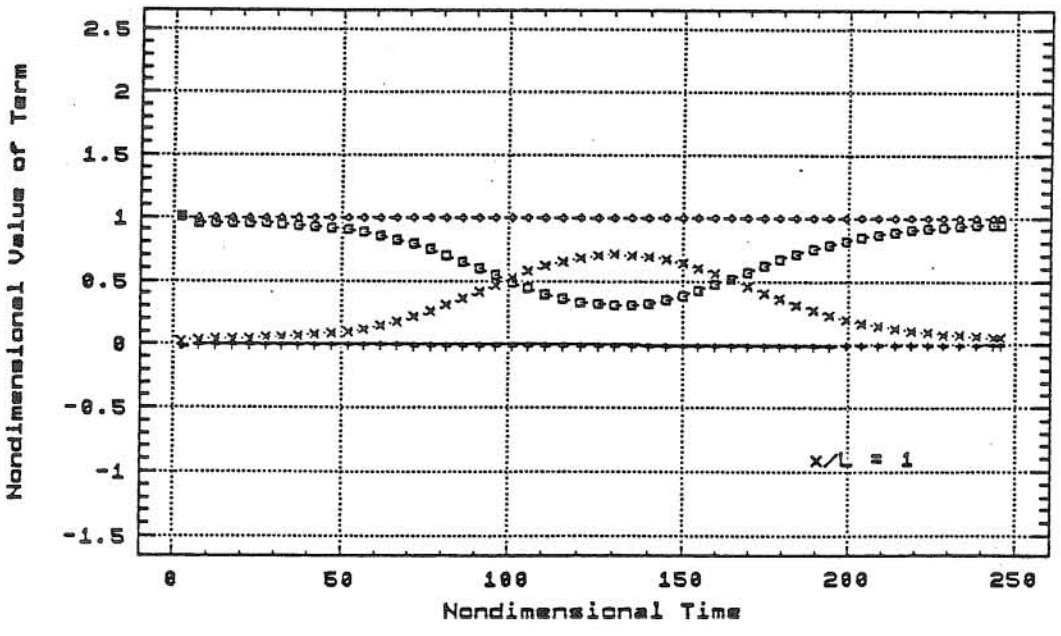

(c) Sections 25/27 and 1

Fig. 6.9 (continued)

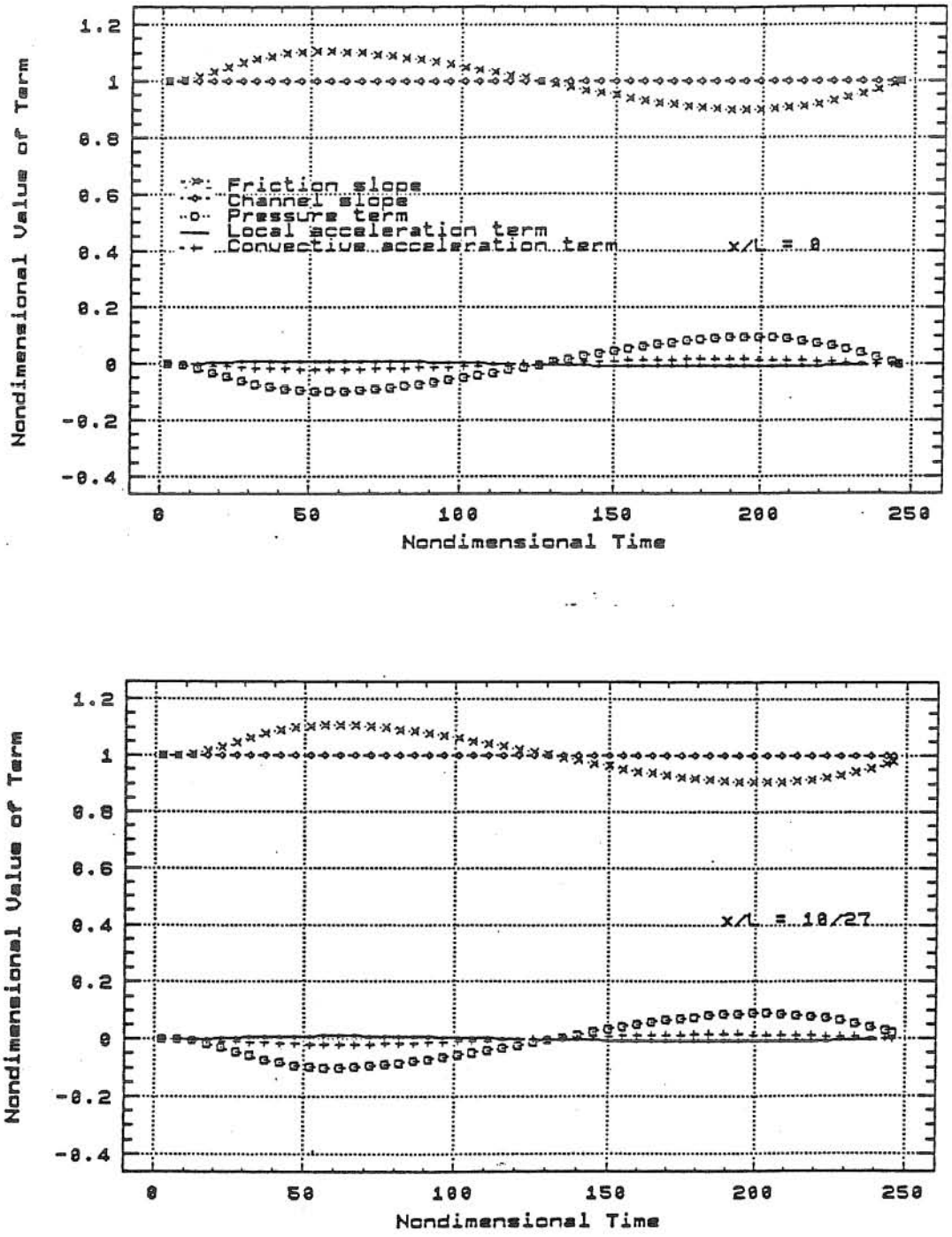

(a) Sections 0 and 10/27

Fig. 6.10 Nondimensional Values of Terms for $\beta = 2$, $k = 0.95$, $k' = 1$, $S_0 = 0.00019$ and $h_d/h_0 = 1.44$

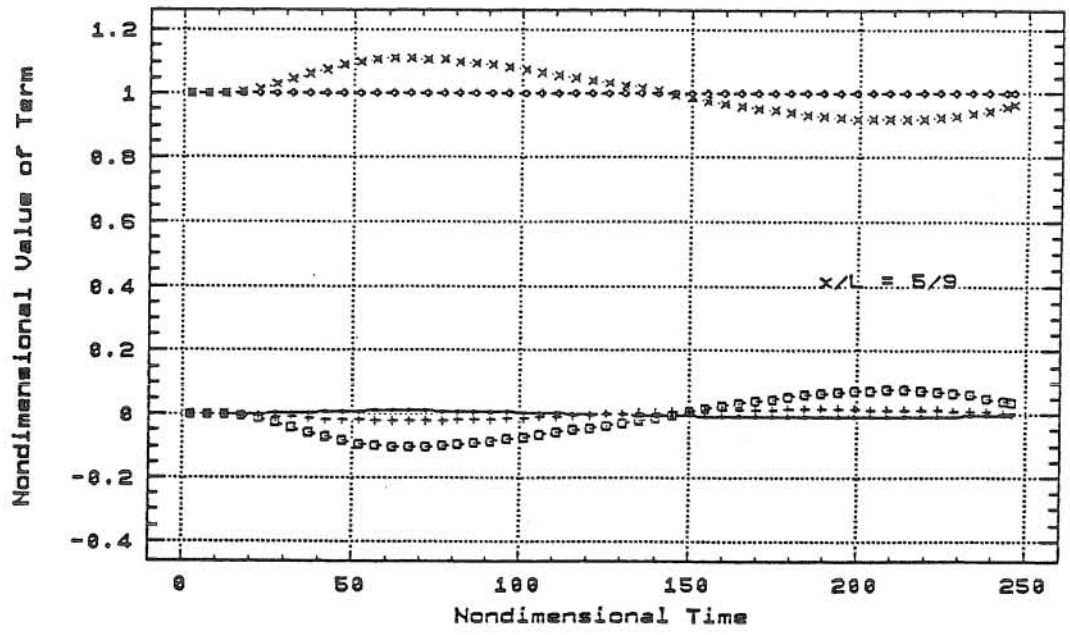

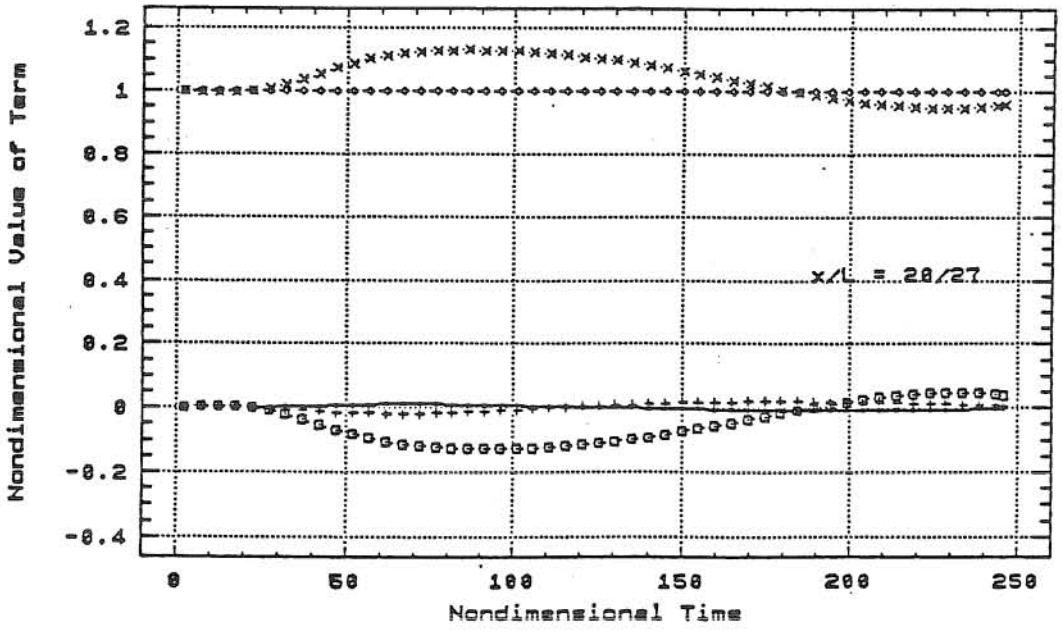

(b) Sections 5/9 and 20/27

Fig. 6.10 (continued)

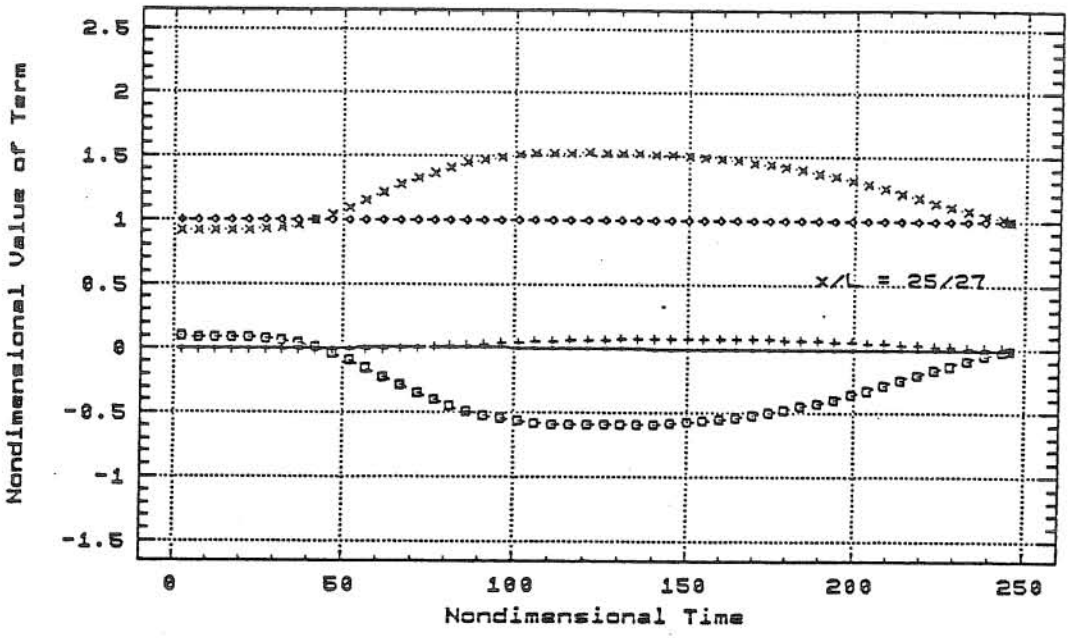

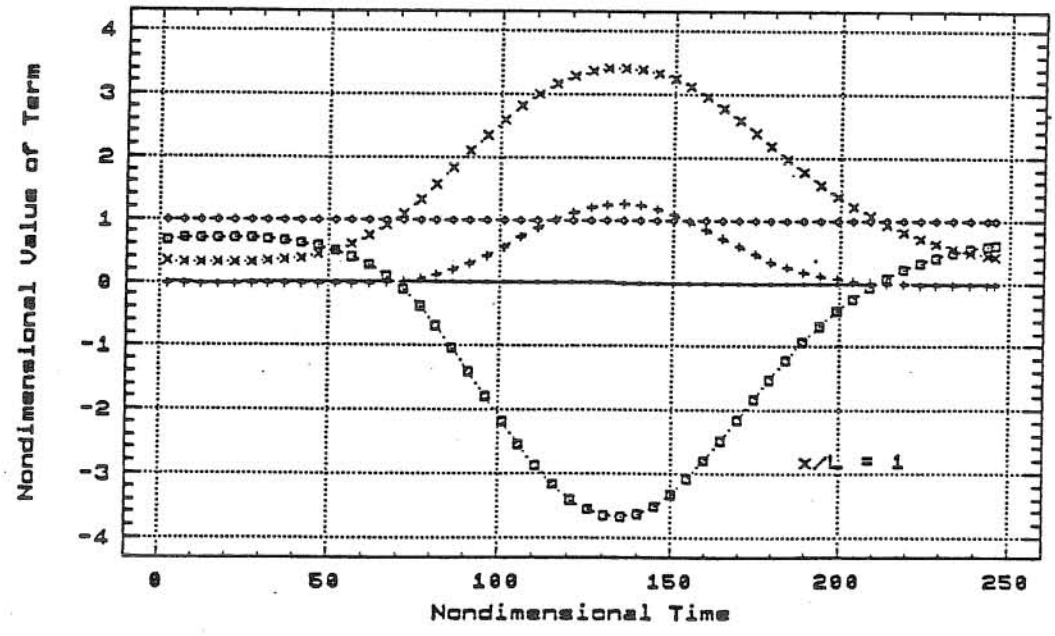

(c) Sections 25/27 and 1

Fig. 6.10 (continued)

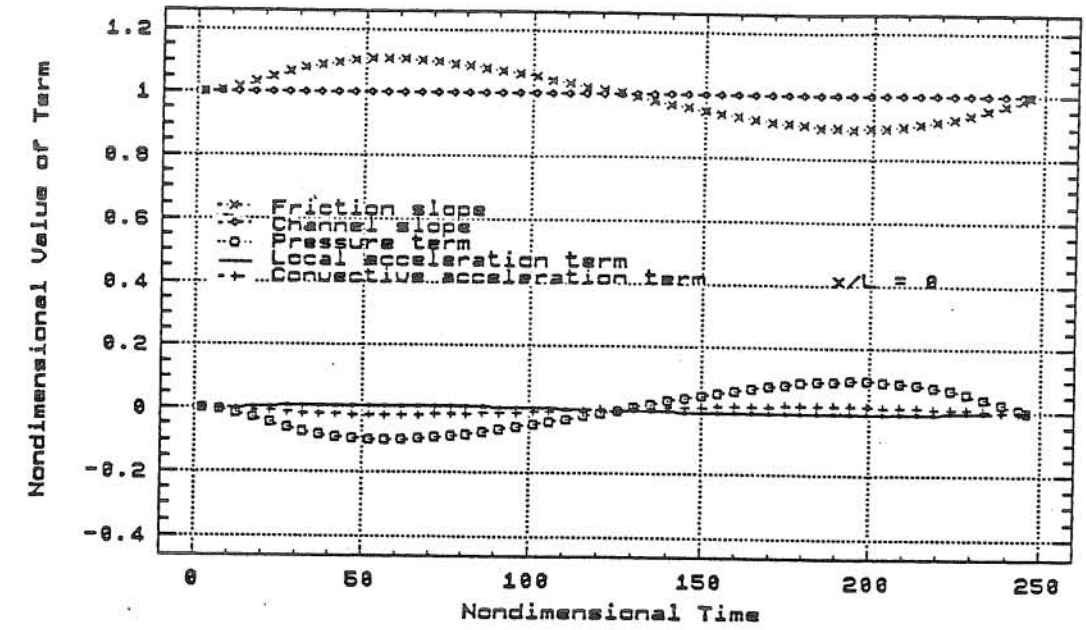

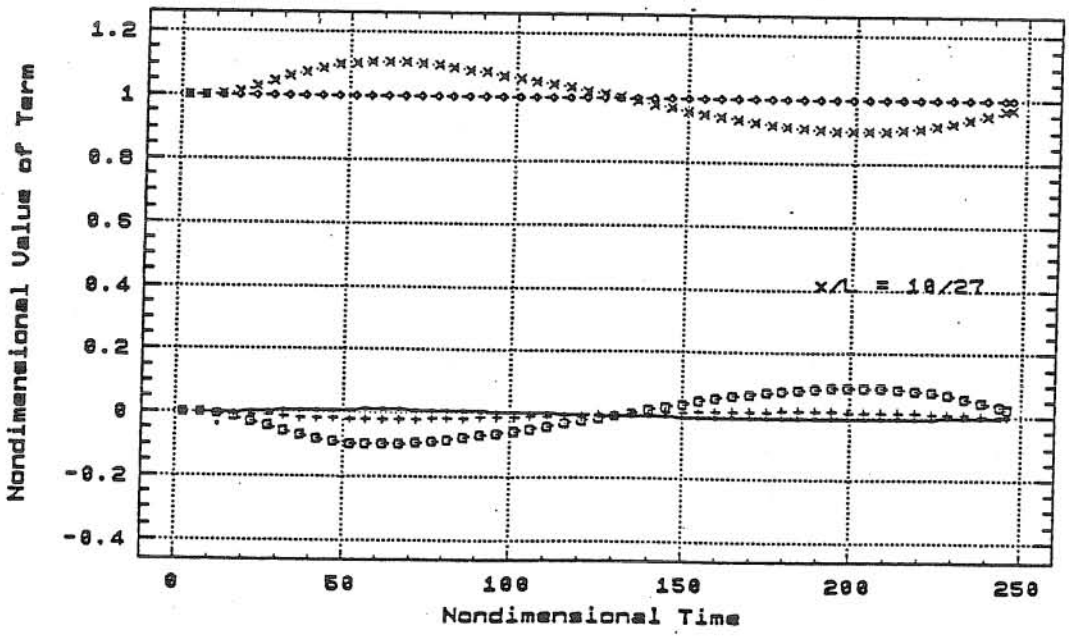

(a) Sections 0 and 10/27

Fig. 6.11 Nondimensional Values of Terms for $\beta = 2$, $k = 0.95$, $k' = 1$, $S_0 = 0.00019$ and $h_d/h_0 = 1.80$

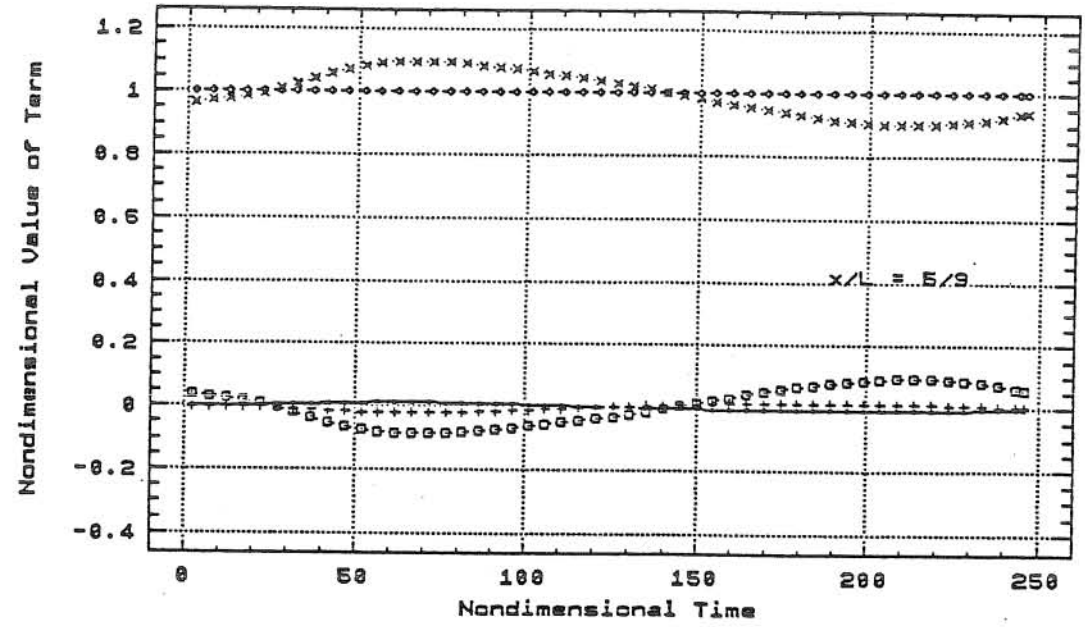

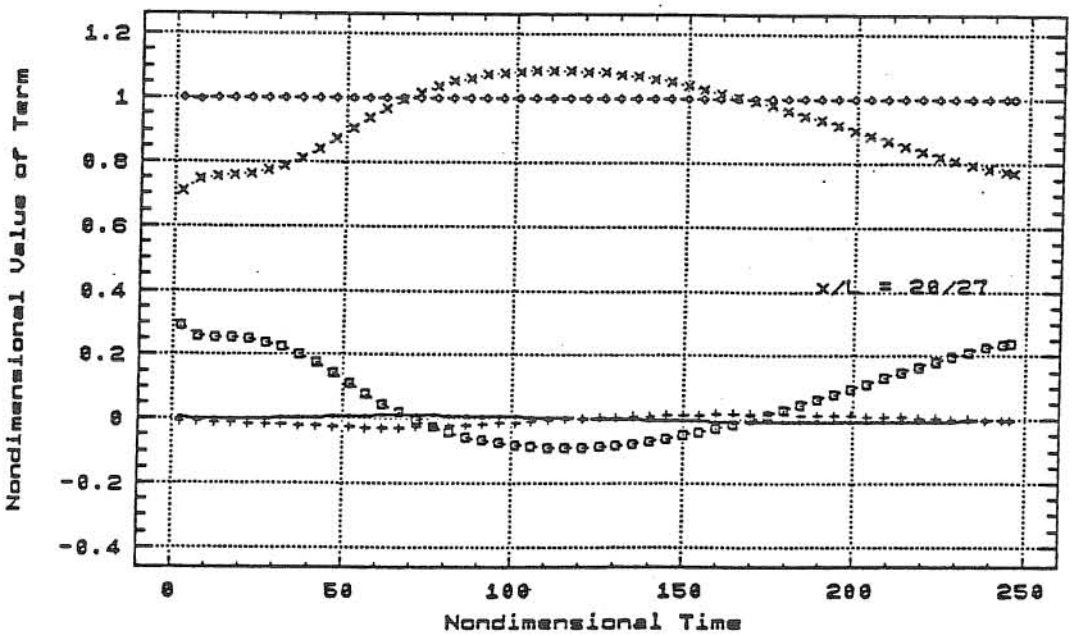

(b) Sections 5/9 and 20/27

Fig. 6.11 (continued)

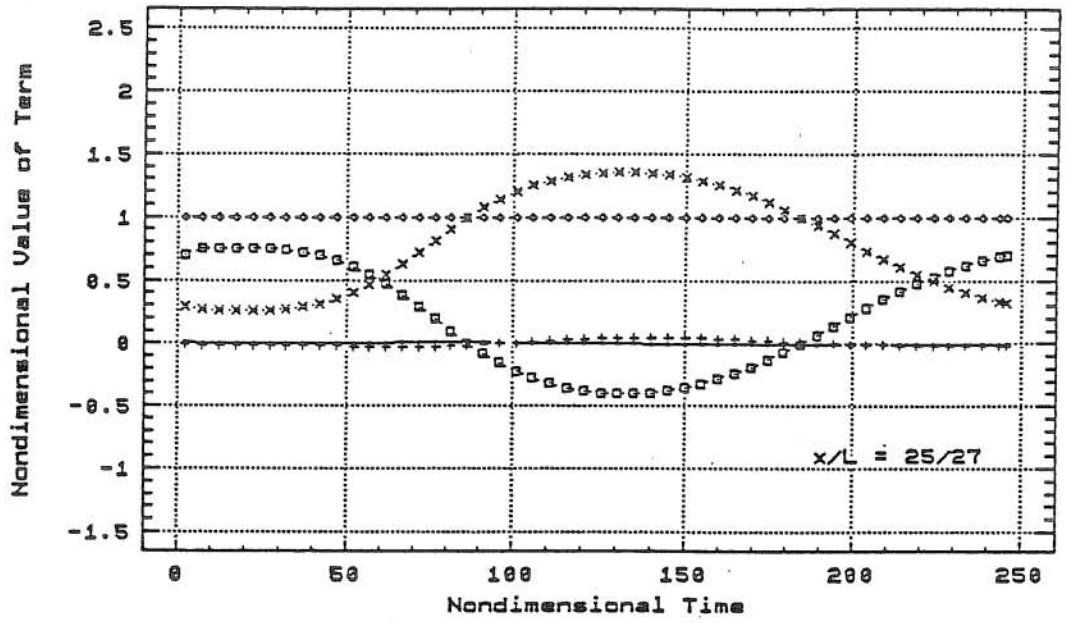

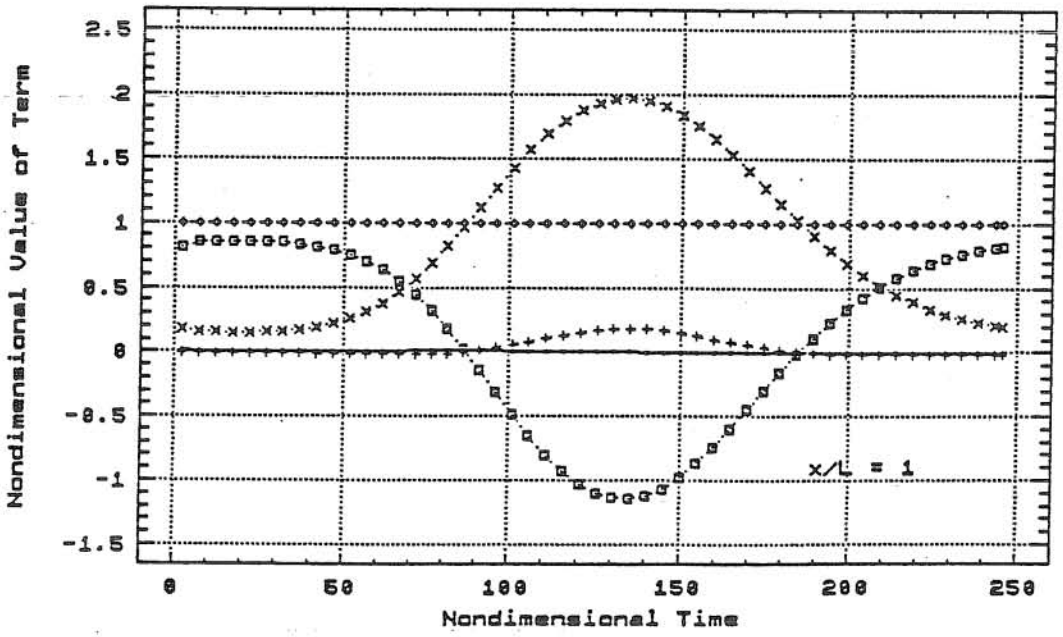

(c) Sections 25/27 and 1

Fig. 6.11 (continued)

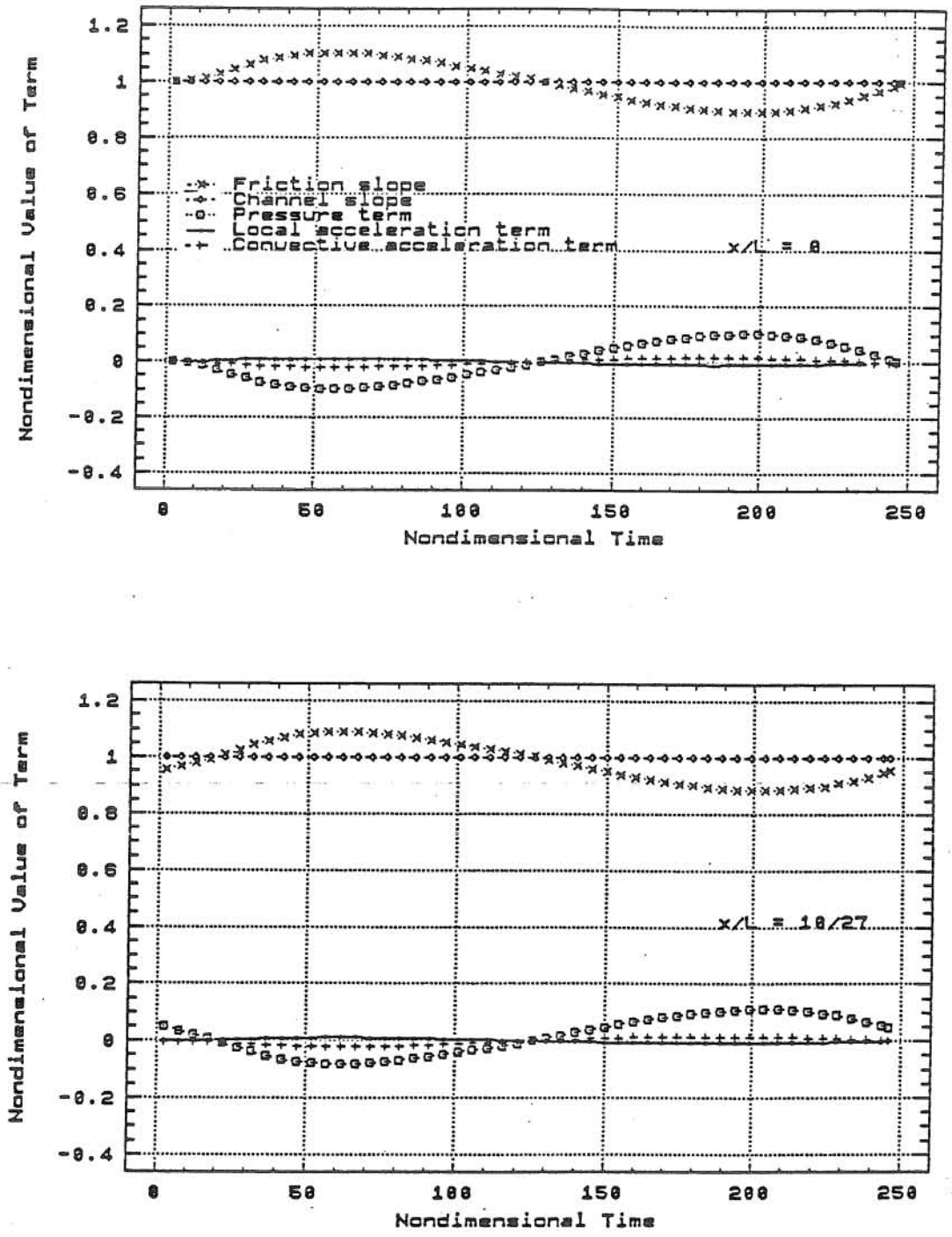

(a) Sections 0 and 10/27

Fig. 6.12 Nondimensional Values of Terms for $\beta = 2$, $k = 0.95$, $k' = 1$, $S_0 = 0.00019$ and $h_d/h_0 = 2.53$

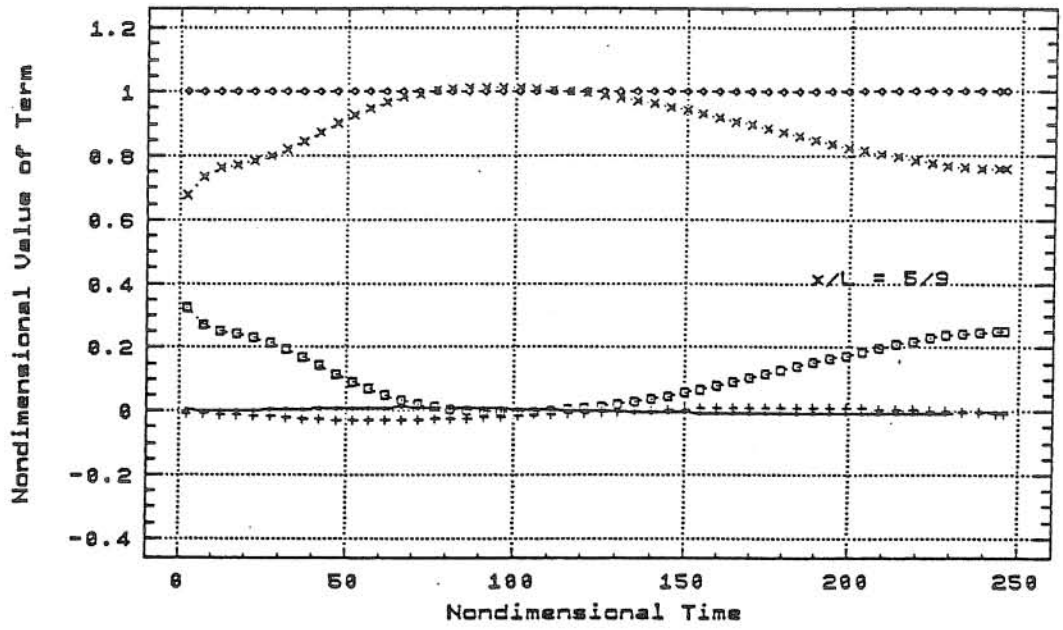

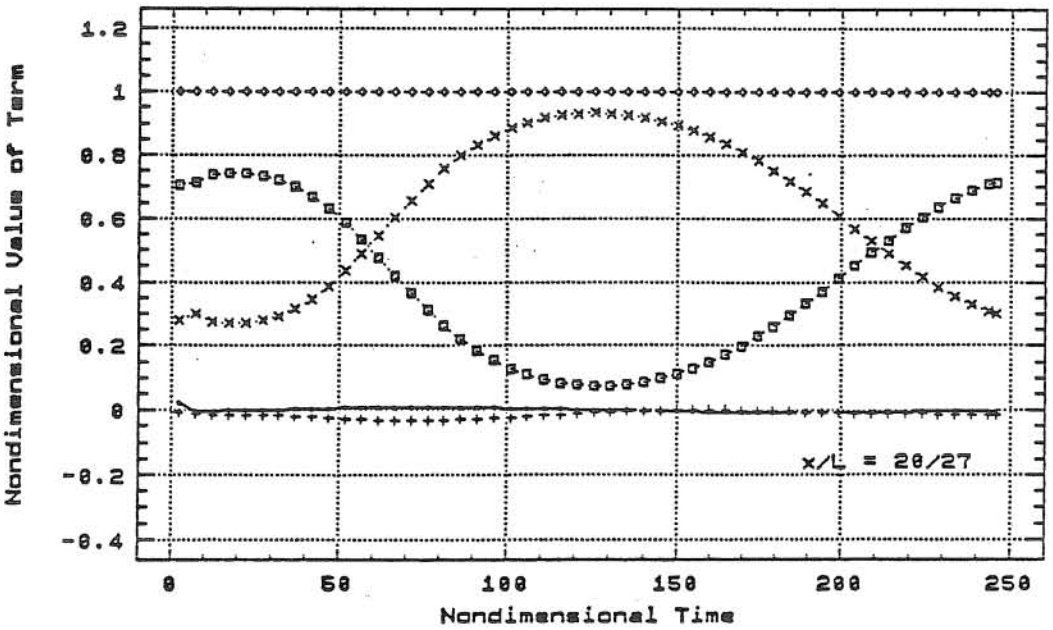

(b) Sections 5/9 and 20/27

Fig. 6.12 (continued)

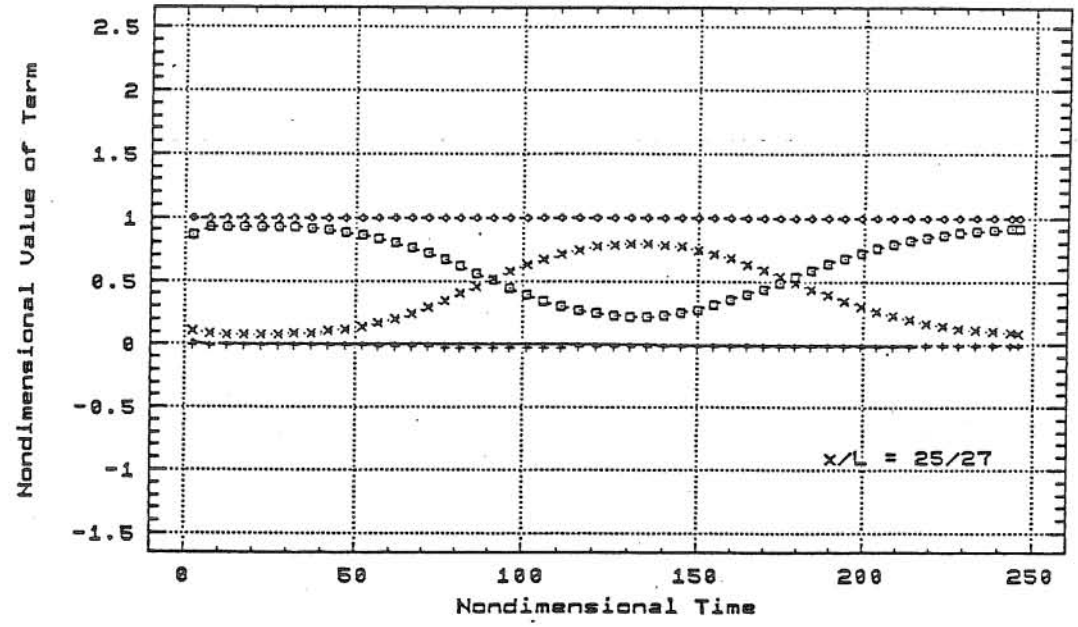

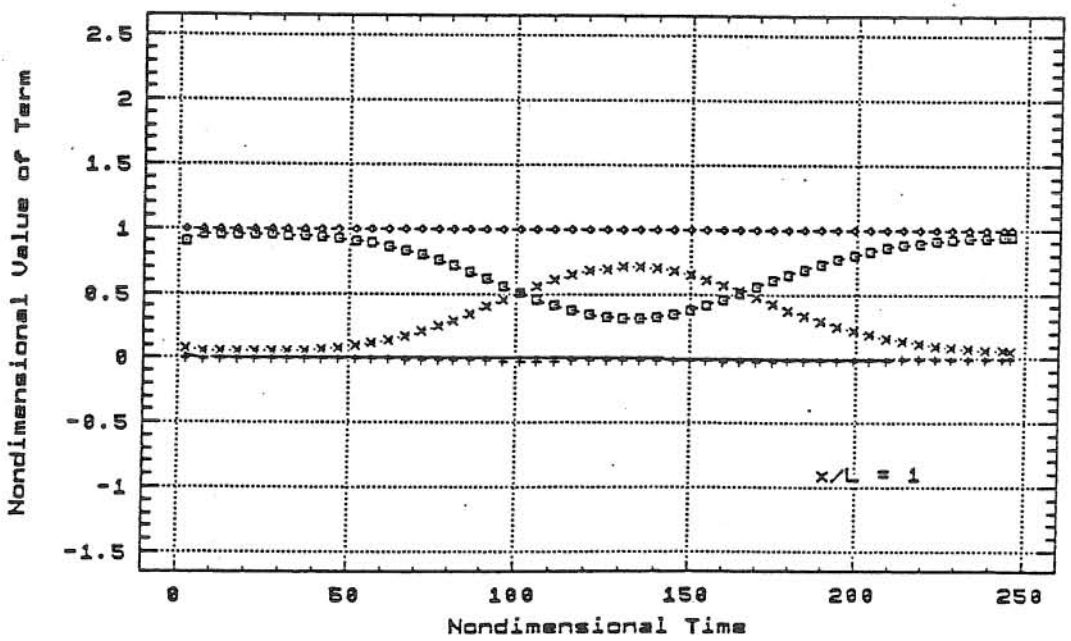

(c) Sections 25/27 and 1

Fig. 6.12 (continued)

Table 6.2 Time-average Ratios between Terms in Exact Momentum Equation for Cases with Backwater Effect

	Location of cross section	Ratio in absolute value: Local accele. vs. Pressure	Convective accele. vs. Pressure	Sum of two accele. vs. Pressure	Pressure vs. Friction slope	Pressure vs. (S_f-S_0)
		$h_d/h_0 = 1.44$				
	0	0.10	0.08	0.02	0.07	1.01
ß = 1	10/27	0.11	0.09	0.02	0.07	1.02
k = 1	5/9	0.11	0.10	0.02	0.06	1.02
k' = 1	20/27	0.10	0.10	0.03	0.08	1.03
	25/27	0.02	0.05	0.05	0.29	1.05
	1	0.01	0.06	0.06	0.94	1.06
	0	0.09	0.15	0.06	0.08	0.94
ß = 2	10/27	0.09	0.15	0.06	0.08	0.95
k = 1.05	5/9	0.09	0.17	0.08	0.07	0.97
k' = 1	20/27	0.08	0.16	0.10	0.09	1.05
	25/27	0.02	0.09	0.09	0.31	1.09
	1	0.02	0.15	0.15	0.95	1.18
	0	0.10	0.18	0.08	0.07	0.93
ß = 2	10/27	0.11	0.18	0.07	0.07	0.93
k = 0.95	5/9	0.11	0.18	0.08	0.06	0.94
k' = 1	20/27	0.09	0.18	0.10	0.07	1.04
	25/27	0.02	0.11	0.10	0.26	1.11
	1	0.02	0.17	0.17	0.95	1.23
		$h_d/h_0 = 1.80$				
	0	0.10	0.08	0.02	0.07	1.01
ß = 1	10/27	0.10	0.09	0.02	0.07	1.02
k = 1	5/9	0.10	0.10	0.02	0.07	1.02
k' = 1	20/27	0.05	0.05	0.03	0.20	1.03
	25/27	0.02	0.03	0.03	1.01	1.03
	1	0.01	0.03	0.03	1.79	1.03
	0	0.09	0.16	0.07	0.08	0.94
ß = 2	10/27	0.09	0.16	0.08	0.08	0.96
k = 1.05	5/9	0.09	0.16	0.08	0.08	0.98
k' = 1	20/27	0.05	0.10	0.06	0.25	1.05
	25/27	0.02	0.06	0.05	1.09	1.06
	1	0.01	0.06	0.06	1.86	1.06
	0	0.11	0.18	0.08	0.07	0.93
ß = 2	10/27	0.11	0.18	0.08	0.07	0.95
k = 0.95	5/9	0.10	0.18	0.08	0.06	0.95
k' = 1	20/27	0.06	0.12	0.07	0.15	1.04
	25/27	0.03	0.07	0.06	0.92	1.07
	1	0.01	0.07	0.07	1.76	1.08

Table 6.2 (continued)

		h_d/h_0 = 2.53				
	0	0.10	0.09	0.02	0.07	1.02
ß = 1	10/27	0.11	0.11	0.03	0.08	1.01
k = 1	5/9	0.05	0.05	0.03	0.27	1.03
k' = 1	20/27	0.02	0.02	0.02	1.20	1.02
	25/27	0.01	0.01	0.01	4.19	1.01
	1	0.01	0.01	0.01	6.31	1.01
	0	0.09	0.17	0.08	0.08	0.96
ß = 2	10/27	0.09	0.17	0.09	0.10	0.97
k = 1.05	5/9	0.04	0.09	0.06	0.36	1.08
k' = 1	20/27	0.02	0.04	0.04	1.49	1.04
	25/27	0.01	0.03	0.03	4.71	1.03
	1	0.01	0.02	0.02	6.86	1.02
	0	0.10	0.18	0.08	0.07	0.93
ß = 2	10/27	0.11	0.20	0.09	0.07	0.93
k = 0.95	5/9	0.05	0.11	0.06	0.18	1.08
k' = 1	20/27	0.02	0.05	0.05	0.91	1.06
	25/27	0.01	0.03	0.03	3.78	1.03
	1	0.01	0.03	0.03	5.97	1.03

with h_d/h_0 = 1.44) the two inertia terms can be ignored and the noninertia model is a good model to solve flood routing problems.

By comparing Figs. 6.7 through 6.9 or Figs. 6.10 through 6.12 with Figs. 6.4 through 6.6, or Appendix E or F with Appendix D and inspecting Table 6.2, it is obvious that the relative importance of most of the terms is unaffected by the variation of the values of ß and k tested. The pressure term for the cases of ß = 2, k = 1.05 and 0.95, k' = 1 has a small change, but the change as compared to the reference case of ß = 1 and k = k' = 1 appears to be insignificant. The most important effect is the change of magnitude of the convective acceleration term resulting from variation of the value of ß. For various values of h_d/h_0, the nondimensional magnitude of the convective acceleration term and

the ratio between it and the pressure term for the case of $\beta = 2$, $k = 1.05$ or $\beta = 2$, $k = 0.95$ become about twice as large as those for the case of $\beta = 1$ and $k = 1$.

In addition, the importance of the convective acceleration term is also influenced by the downstream water depth. For the case of $h_d/h_0 = 1.44$ where the downstream backwater depth is relatively small, the nondimensional magnitude of the convective acceleration term at the cross sections near the downstream boundary ($x/L = 25/27$ and 1) for various coefficient combinations investigated appears to be larger than that for $h_d/h_0 = 1.80$ and 2.53 (see Figs. 6.7 (c) and 6.10 (c) and Table 6.2). At the cross sections, the ratio between the convective acceleration term and the pressure term for $h_d/h_0 = 1.44$ reaches approximately 5% to 17%. However, for $h_d/h_0 = 1.80$ and 2.53, the ratio is only 1% to 7%. This is because with lowering downstream-boundary water depth the unsteady flow entering the channel gradually converts from a convectively less accelerating nonuniform subcritical flow to a convectively more accelerating one; thus, the convective acceleration term gradually becomes more significant.

On the basis of the above discussions, the effect of β on the convective acceleration term implies that using the Saint-Venant equations with $\beta = 1$ as a simplification of the exact momentum and continuity equations could produce significant error if the actual distribution of the flow velocity is extremely nonuniform, i.e., when the value of β is large. The reason is that the value of the convective acceleration term increases and is no longer unimportant whereas from the Saint-Venant equations with β

= 1 the convective acceleration term appears to be insignificant. Therefore, for the extreme situation of large ß (ß approaches 2) with small downstream depth (consider the influence of the downstream boundary condition on the convective acceleration term), the quasi-steady dynamic wave may be a more appropriate model than the noninertia model. Whereas in most other cases with significant downstream backwater effect, i.e., the convectively decelerating subcritical flow dominates, the noninertia model is adequate. Thus, it has been demonstrated that depending on the values of the coefficients used, different approximations of the exact momentum equation or models should be selected for simulation of an unsteady flow problem.

6.1.3. Internal Stress Term

As described in section 2.3.6, the magnitude of the internal stress term, $\partial T/\partial x$, generally is assumed small. In order to investigate its impact, its values to be tested are estimated by referring to the magnitudes of the terms of local acceleration, convective acceleration, pressure and friction slope. According to the simulated results discussed in sections 6.1.1 and 6.1.2, the nondimensional values of the two inertia terms are on the order of 0.01 and those of the pressure and friction slope terms from 0.1 to 1.0. Hence, the tested values of the nondimensional internal stress term (with a coefficient, $T_0/\gamma A_0 h_0 F_0^2$) are chosen as 0.01, 0.1, 0.5, 0.75 and 1.0, respectively. If the impact of the $\partial T/\partial x$ term on the solutions of the equations is small under this extreme range of conditions of $\partial T/\partial x$, the common practice of ignoring this

term is justifiable.

Only two situations, one with $\beta = 1$, $k = 0.95$ and $k' = 1$ and the other one with $\beta = 1$, $k = 1$ and $k' = 1$ (case of the Saint-Venant equations), are simulated for the 54-mile channel with the channel slope, $S_0 = 0.00019$, and the downstream boundary condition, $h_d/h_0 = 1.80$. The flow equations with and without the internal stress term, $\partial T/\partial x$, are tested. A comparison of the maximum absolute or relative differences of the solutions of h/h_0 and V/V_0, with and without the internal stress term in the equations, is demonstrated in Table 6.3. From this table, it is obvious that even as the nondimensional value of the $\partial T/\partial x$ term approaches unity, i.e., nearly the magnitude of the friction slope, the maximum relative differences of the solutions of the nondimensional flow depth and flow velocity with and without the $\partial T/\partial x$ term are no more than 5%. Usually the magnitude of the internal stress term is much smaller and, hence, the effect of this term on the solutions of the flow equations is insignificant and negligible.

6.1.4. Rate of Spatial Change of β and k

Usually spatial changes of the velocity and pressure distributions of the flow are not rapid and, hence, the spatial rates, $\partial\beta/\partial x$ and $\partial k/\partial x$, are small and negligible. Similar to section 6.1.3, the impacts of $\partial\beta/\partial x$ and $\partial k/\partial x$ on the solutions of the flow equations are investigated by giving them some nondimensional testing values, for example, 0.01, 0.1, 0.5, 0.75 and 1.0, and by examining the results. The simulation results are presented in Table 6.4. From this table, it can be seen that if

Table 6.3 Impact of Internal Stress Term on Maximum Solution Difference of h/h_0 or V/V_0

(a) Absolute Difference

$S_0 = 0.00019$, $h_d/h_0 = 1.80$		Nondimensional value of internal stress term 0.01	0.1	0.5	0.75	1.00
		Maximum absolute solution difference				
ß = 1, k = 0.95, k' = 1	for h/h0	-0.0003	-0.0027	-0.0129	-0.0191	-0.0250
	for V/V0	0.0009	0.0091	0.0450	0.0671	0.0891
ß = 1, k = 1, k' = 1	for h/h0	-0.0003	-0.0029	-0.0141	-0.0208	-0.0273
	for V/V0	0.0009	0.0090	0.0447	0.0667	0.0886

(b) Relative Difference

$S_0 = 0.00019$, $h_d/h_0 = 1.80$		nondimensional value of internal stress term 0.01	0.1	0.5	0.75	1.00
		maximum relative solution difference in %				
ß = 1, k = 0.95, k' = 1	for h/h0	-0.02	-0.23	-1.10	-1.63	-2.14
	for V/V0	0.04	0.42	2.08	3.11	4.13
ß = 1, k = 1, k' = 1	for h/h0	-0.02	-0.24	-1.18	-1.73	-2.28
	for V/V0	0.04	0.41	2.07	3.08	4.10

Table 6.4 Impact of $\partial ß/\partial x$ or $\partial k/\partial x$ on Maximum Solution Difference of h/h_0 or V/V_0

(a) Absolute Difference

$S_0 = 0.00019$, $h_d/h_0 = 1.80$		Nondimensional value of rate of spatial change of ß or k: 0.01	0.1	0.5	0.75	1.00
		Maximum absolute solution difference				
ß = 1, k = 0.95, k' = 1	for h/h0	0.0003	0.0027	0.0141	0.0214	0.0291
	for V/V0	-0.0009	-0.0091	-0.0459	-0.0691	-0.0925
ß = 1, k = 1, k' = 1	for h/h0	0.0003	0.0029	0.0149	0.0228	0.0308
	for V/V0	-0.0009	-0.0090	-0.0454	-0.0684	-0.0917

(b) Relative Difference

$S_0 = 0.00019$, $h_d/h_0 = 1.80$		Nondimensional value of rate of spatial change of ß or k: 0.01	0.1	0.5	0.75	1.00
		Maximum relative solution difference in %				
ß = 1, k = 0.95, k' = 1	for h/h0	0.02	0.23	1.20	1.83	2.49
	for V/V0	-0.04	-0.42	-2.12	-3.20	-4.28
ß = 1, k = 1, k' = 1	for h/h0	0.02	0.24	1.25	1.90	2.57
	for V/V0	-0.04	-0.42	-2.09	-3.15	-4.23

the spatial change of the velocity or pressure distribution is small, the maximum absolute and relative differences between the solutions of the exact momentum and continuity equations (or the Saint-Venant equations) with and without considering $\partial\beta/\partial x$ or $\partial k/\partial x$ are not very large. This proves that for most flow conditions the two rates of spatial change of β and k can be ignored. But, if the velocity or pressure distribution has a rapid change along the x direction, such as an abrupt contraction or expansion of a channel, the values of $\partial\beta/\partial x$ and $\partial k/\partial x$ may become very large (i.e., much greater than the values tested), and the effects of the two rates of spatial change of β and k on the solutions should be carefully evaluated. Otherwise the accuracy of the solutions of the equations could be in doubt.

6.2. Rectangular and Trapezoidal Channels

From the preceding sections, the investigation of the momentum equation for flow in an infinitely wide channel provides a basic understanding of the relative contributions of the terms in the equation. The influence of the channel cross-sectional shape on the contributions of the terms is further studied herewith by considering prismatic channels with rectangular and trapezoidal shapes. For rectangular channels, one case with the channel width, b = 100 ft (i.e., $b/h_0 = 7$) is investigated. For trapezoidal channels, only the case with the side slope, z = 4, and the channel bottom width, b = 100 ft (i.e., $b/h_0 = 7$) is tested as an example. In addition, in this analysis, the situation of $\beta = 1$, $k = 1$, k'

= 1, S_0 = 0.00019 and h_d/h_0 = 1.80 is used. These results are summarized in Appendices G and H, respectively.

By comparing Appendix G with the corresponding portions in Appendix D, it can be seen that the nondimensional values of the terms and the ratios between them for a rectangular channel are almost the same as those for the wide rectangular channel. This means that for a rectangular channel beyond the tested width to depth ratio, b/h_0 = 7, the channel width has no significant influence on the relative contributions of the terms in the exact momentum equation. For the situations of the width to depth ratio less than 7, the influence of the channel width on the contributions of the terms should be further investigated in the future.

By comparing Appendix H with Appendix G, it can be observed that the nondimensional values of the terms and the ratios between them for trapezoidal channels are almost the same as those of rectangular channels. Thus, for this tested case, i.e., z = 4 and b/h_0 = 7, the side slope, z, seems to be not an important variable for the relative contributions of the terms in the exact momentum equation. However, for other cases of the value of z greater than 4, it would be valuable to further investigate the influence of z on the contributions of the terms.

6.3. Situation of Accelerating Type Water Surface Profiles

The water surface profiles investigated in section 6.1 are characterized by an initially convectively decelerating subcritical flow when the flood enters the channel. Likewise, the convectively accelerating type subcritical flow is simulated herein for

three typical cases, namely, $\beta = 1$, $k = k' = 1$; $\beta = 2$, $k = 1.05$, $k' = 1$ and $\beta = 2$, $k = 0.95$, $k' = 1$, for unsteady flow in a very wide channel with a channel slope, $S_0 = 0.00019$, in order to test the contributions of the terms in the exact momentum equation to the solutions of the equations. The nondimensional downstream water depth, $h_d/h_0 = 0.7$, is selected as the downstream boundary condition. The results are presented in Appendices I, J and K, and the time-average ratios in the absolute value between these terms in the exact momentum equation are listed in Table 6.5.

Table 6.5 Time-average Ratios between Terms in Exact Momentum Equation for Case of Convectively Accelerating Type Water Surface Profiles

$h_d/h_0 = 0.7$ for convectively accelerating type profiles	Location of cross section	Ratio in absolute value				
		Local accele. vs. Pressure	Convective accele. vs. Pressure	Sum of two accele. vs. Pressure	Pressure vs. Friction slope	Pressure vs. (S_f-S_0)
	0	0.10	0.08	0.02	0.07	1.01
$\beta = 1$	10/27	0.10	0.08	0.01	0.07	1.01
$k = 1$	5/9	0.10	0.08	0.02	0.07	1.02
$k' = 1$	20/27	0.07	0.07	0.04	0.09	1.04
	25/27	0.01	0.05	0.05	0.31	1.05
	1	0.00	0.20	0.20	1.03	1.26
	0	0.09	0.15	0.06	0.08	0.94
$\beta = 2$	10/27	0.09	0.16	0.06	0.08	0.95
$k = 1.05$	5/9	0.09	0.16	0.07	0.07	0.96
$k' = 1$	20/27	0.06	0.12	0.07	0.09	1.05
	25/27	0.01	0.08	0.08	0.30	1.09
	1	0.00	0.34	0.34	1.31	1.59
	0	0.11	0.18	0.07	0.07	0.93
$\beta = 2$	10/27	0.11	0.18	0.07	0.06	0.93
$k = 0.95$	5/9	0.11	0.18	0.07	0.06	0.94
$k' = 1$	20/27	0.08	0.15	0.08	0.06	1.00
	25/27	0.02	0.09	0.09	0.21	1.10
	1	0.00	0.37	0.37	1.38	1.71

By comparing Appendices I through K and Table 6.5 with the results of the convectively decelerating type profiles given in Appendices A through F and Tables 6.1 and 6.2, two observations are made. One is that the influences of the coefficients, ß and k, on the contributions of the terms for the convectively accelerating type profiles are similar to that for the convectively decelerating ones. For example, for the case of ß = 2, k = 1.05 or 0.95 the nondimensional magnitude of the convective acceleration term is about twice as large as that for the case of ß = 1, k = 1. The nondimensional magnitude of the pressure term increases or decreases only slightly when compared to that of k = 1. The other observation is that there are some differences in the magnitudes of the terms and their ratios between the convectively accelerating and decelerating type profiles. First, for the convectively accelerating type profiles, at the cross sections near the downstream boundary the nondimensional value of the convective acceleration term is much larger than that of the convectively decelerating type profiles. It is approximately 20% to 37% of the pressure term for the various cases investigated. This implies that the convective acceleration term becomes more important for the convectively accelerating type profiles. Second, based on the values of the ratio between the pressure term and friction slope for the convectively accelerating type profiles, the pressure term is also important and cannot be disregarded, whereas the magnitude of this ratio is less than that of the convectively decelerating type profiles. Therefore, for convectively accelerating type profiles, because of the importance of the convective acceleration

term and pressure term, the quasi-steady dynamic wave may be a more appropriate model than the noninertia model for solving an open channel problem with the convectively accelerating type water surface profiles.

6.4. Further Remarks

From previous sections, it is summarized that the relative contributions of the terms in the exact momentum equation are closely related to the downstream boundary condition, slightly influenced by the variations of the coefficients, ß and k, and probably insensitive to the cross-sectional shape of prismatic channels (based on present tested cases).

The downstream boundary condition has an important effect on the contributions of the terms. For channels with small slope and without downstream backwater effect, the most important terms are the friction slope and channel slope, and other terms can be ignored. On the other hand, nonuniform flow with convectively decelerating type profiles, because of the backwater effect the pressure term becomes significant. In addition, under this decelerating situation, by lowering downstream-boundary water depth, the subcritical flow gradually converts from a more convectively decelerating condition to a less convectively decelerating one, the contribution of the convective acceleration term increases. For nonuniform flow with the convectively accelerating profiles, the pressure term is also important, and since the convectively accelerating subcritical flow is dominant, the contribution of the convective acceleration term increases greatly.

Among the coefficients, ß, k and k', the variation of ß is related to the contribution of the convective acceleration term. When the value of ß is large, i.e., the distribution of flow velocity is excessively nonuniform in a cross section, the contribution of the convective acceleration term increases.

7. SOLUTIONS OF EXACT MOMENTUM AND CONTINUITY EQUATIONS IN Q-h FORM

As depicted in section 4.1, the exact momentum and continuity equations in the form of V and h and in the form of Q and h have the same mathematical properties. However, the numerical solutions for the flow depth which is a common dependent variable included in both forms of the equations may not be identical because the other dependent variable used in the equations is different. Therefore, the difference of the numerical solutions between the two forms of the exact momentum and continuity equations is investigated in this chapter. In addition, in order to test the sensitivity of the discharge and flow depth to the use of different equations (the exact momentum and continuity equations and the Saint-Venant equations) the solution differences of the nondimensional discharge and flow depth between the exact momentum and continuity equations in the form of Q and h and the Saint-Venant equations in the form of Q and h are also studied.

7.1. Difference between Solutions of Two Forms of Exact Momentum and Continuity Equations

For simplicity and convenience, among all the differences of flow depths at different times and locations given in the solutions of the exact momentum and continuity equations in the V-h form and Q-h form, only the maximum difference is used as a reference for discussion. The maximum absolute and relative solution differences are designated as MASDVHQH and MRSDVHQH, respectively. Similar to Chapter 5, variations of MASDVHQH and MRSDVHQH are investigated for

various flow and downstream boundary conditions. Five coefficient combinations, $\beta = 1$, $k = k' = 1$; $\beta = 1$, $k = 1.05$, $k' = 1$; $\beta = 1$, $k = 0.95$, $k' = 1$; $\beta = 1.33$, $k = 0.95$ $k' = 1$ and $\beta = 2$, $k = 0.95$, $k' = 1$, and three downstream water depths, $h_d/h_0 = 1.44$, 1.80 and 2.53, for a wide rectangular channel and a trapezoidal channel with channel slope, $S_0 = 0.00019$, are investigated and the results are summarized in Tables 7.1 and 7.2, respectively.

From Table 7.1, it is shown that the difference between the solutions of the two forms of the exact momentum and continuity equations for various situations considered is not very large. This means that for wide rectangular channels, both forms of the equations can be selected to solve flood routing problems without significant errors in the solutions of the flow depth, h.

Furthermore, two points are observed from Table 7.1. One is that the magnitudes of MASDVHQH and MRSDVHQH are almost unchanged with increasing β from 1 to 2, and have only a small variation with decreasing k from 1.05 to 0.95. In other words, varying these coefficients, β and k, does not generate a significant impact on the difference between the solutions of the two forms of the equations. Thus, for wide rectangular channels, whatever the variations of β and k, the solutions of flow depth, h, obtained from the exact momentum and continuity equations in the V-h form or in the Q-h form are almost the same. The other point is that the smaller the downstream water depth, the larger the difference between the solutions of the two forms of the equations. Therefore, it should be noted that if the downstream water depth is small, namely, the condition of the convectively less decelerating

Table 7.1 Maximum Difference of h/h_0 between Two Forms of Exact Momentum and Continuity Equations for Wide Rectangular Channel

(a) Absolute Difference

S_0=0.00019 k' = 1	h_d/h_0= 1.44	1.80	2.53
	Maximum absolute solution difference of h/h_0		
ß=1 k=1.05	-0.0229	-0.0078	0.0067
ß=1 k=0.95	-0.0093	-0.0092	-0.0077
ß=1.33 k=0.95	-0.0093	-0.0092	0.0083
ß=2 k=0.95	-0.0093	-0.0092	0.0083

(b) Relative Difference

S_0=0.00019 k' = 1	h_d/h_0= 1.44	1.80	2.53
	Maximum relative solution difference of h/h_0 in %		
ß=1 k=1.05	-1.19	-0.55	0.47
ß=1 k=0.95	-0.71	-0.64	-0.49
ß=1.33 k=0.95	-0.71	-0.64	0.66
ß=2 k=0.95	-0.71	-0.64	0.67

Table 7.2 Maximum Difference of h/h_0 between Two Forms of Exact Momentum and Continuity Equations for Trapezoidal Channel

(a) Absolute Difference

S_0=0.00019 ß=1 k=0.95 k'=1	h_d/h_0= 1.44	1.66	1.80	2.02	2.53
	Maximum absolute solution difference of h/h_0				
z=0 b/h_0=36	-0.0093	-0.0093	-0.0092	-0.0085	-0.0077
z=4 b/h_0=7	-0.0144	-0.0144	-0.0144	-0.0138	0.0132

(b) Relative Difference

S_0=0.00019 ß=1 k=0.95 k'=1	h_d/h_0= 1.44	1.66	1.80	2.02	2.53
	Maximum relative solution difference of h/h_0 in %				
z=0 b/h_0=36	-0.71	-0.68	-0.64	-0.55	-0.49
z=4 b/h_0=7	-1.03	-1.02	-0.96	-0.86	1.02

subcritical flow, using the two forms of the exact momentum and continuity equations to solve the same open channel problem could lead to appreciable different solutions of flow depth.

For trapezoidal channels, Table 7.2 demonstrates that the magnitudes of MASDVHQH and MRSDVHQH increase with changing channel shape from a wide rectangular one to a trapezoidal one. However, the solution differences on the flow depth, h, between the two forms of the exact momentum and continuity equations are also insignificant based on the results investigated. Thus, for trapezoidal channels, both forms of the equations can be used to calculate the flow depth.

7.2. Difference between Solutions of Exact Momentum and Continuity Equations in Q-h Form and Saint-Venant Equations in Q-h Form

The solution differences of flow depth, h, or discharge, Q, between the exact momentum and continuity equations in the Q-h form and the Saint-Venant equations in the Q-h form at various distance-time increments are computed and only the maximum absolute and relative differences of Q/Q_0 or h/h_0 are used for discussion. Again, the four different coefficient combinations and three different downstream depths considered in section 7.1 are investigated for a wide rectangular channel with channel slope S_0 = 0.00019. The results are presented in Tables 7.3 and 7.4. In addition, in order to further display the distinction between the two different forms of the exact momentum and continuity equations, the maximum absolute and relative solution differences of V/V_0 or h/h_0 between the exact momentum and continuity equations in the V-

Table 7.3 Maximum Difference of h/h_0 between Exact Momentum and Continuity Equations and Saint-Venant Equations in Q-h or V-h Form For Rectangular Channel

(a) Absolute Difference

	Q-h form			V-h form		
S_0=0.00019 k' = 1	h_d/h_0= 1.44	1.80	2.53	1.44	1.80	2.53
	Maximum absolute solution difference of h/h_0					
ß=1 k=0.95	0.0271	-0.0362	-0.0875	0.0274	-0.0361	-0.0874
ß=1 k=1.05	-0.0241	0.0360	0.0749	-0.0243	0.0361	0.0750
ß=1.33 k=0.95	0.0344	-0.0373	-0.0886	0.0347	-0.0372	-0.0885
ß=2 k=0.95	0.0498	-0.0396	-0.0909	0.0502	-0.0394	-0.0908

(b) Relative Difference

	Q-h form			V-h form		
S_0=0.00019 k' = 1	h_d/h_0= 1.44	1.80	2.53	1.44	1.80	2.53
	Maximum relative solution difference of h/h_0 in %					
ß=1 k=0.95	1.42	-3.13	-5.39	1.44	-3.13	-5.37
ß=1 k=1.05	-1.26	3.12	4.61	-1.27	3.12	4.62
ß=1.33 k=0.95	1.79	-3.22	-5.46	1.81	-3.22	-5.44
ß=2 k=0.95	2.59	-3.44	-5.60	2.61	-3.41	-5.58

Table 7.4 Maximum Difference of Q/Q_0 and V/V_0 between Exact Momentum and Continuity Equations and Saint-Venant Equations in Q-h or V-h Form for Rectangular Channel

(a) Absolute Difference

	Q-h form			V-h form		
S_0=0.00019 k' = 1	h_d/h_0= 1.44	1.80	2.53	1.44	1.80	2.53
	Maximum absolute solution difference Q/Q_0			V/V_0		
ß=1 k=0.95	-0.0240	-0.0271	-0.0352	-0.0294	0.0353	0.0998
ß=1 k=1.05	0.0236	0.0265	0.0335	0.0275	-0.0374	-0.1169
ß=1.33 k=0.95	-0.0219	-0.0241	-0.0310	-0.0375	0.0366	0.1009
ß=2 k=0.95	-0.0192	-0.0190	0.0249	-0.0553	0.0392	0.1030

(b) Relative Difference

	Q-h form			V-h form		
S_0=0.00019 k' = 1	h_d/h_0= 1.44	1.80	2.53	1.44	1.80	2.53
	Maximum relative solution difference in % Q/Q_0			V/V_0		
ß=1 k=0.95	-1.03	-1.19	-1.63	-1.46	4.03	16.25
ß=1 k=1.05	1.01	1.17	1.55	1.38	-4.27	-19.04
ß=1.33 k=0.95	-0.85	-1.01	-1.44	-1.85	4.18	16.43
ß=2 k=0.95	-0.65	-0.62	1.27	-2.72	4.47	16.77

h form and the Saint-Venant equations in the V-h form are also presented in Tables 7.3 and 7.4.

From Table 7.3, it is obvious that the maximum absolute and relative solution differences of the nondimensional flow depth, h/h_0, between the exact momentum and continuity equations in the Q-h form and the Saint-Venant equations in the Q-h form are almost the same as those between the two sets of equations in the V-h form. This indicates again that the two different forms of the exact momentum and continuity equations can be used to solve the flow depth, h, in open channel problems without significant errors.

By comparing Table 7.3 with Table 7.4, it is observed that the magnitudes of the maximum absolute and relative solution differences of the nondimensional discharge, Q/Q_0, are smaller than those of the nondimensional flow depth, h/h_0, and both of the magnitudes of the solution differences for Q/Q_0 and h/h_0 are much smaller than those of the nondimensional velocity, V/V_0, especially when the downstream water depth is large (the condition of the subcritical flow with the large convective deceleration). This means that the flow velocity, V, is much more sensitive than the flow depth, h, and discharge, Q, for using different equations, i.e., the exact momentum and continuity equations or the Saint-Venant equations. Therefore, for open channel problems, if the discharge is considered as a solution, both the exact momentum and continuity equations and the Saint-Venant equations can be selected, but if the flow velocity is required the selection of the equations must be done carefully.

Furthermore, it is found from numerous calculations that the impact of each of the coefficients on the solutions of the equations and the relative contributions of each of the terms in the exact momentum equation in the form of Q and h are almost the same as those of the exact momentum equation in the form of V and h. Thus, the results investigated on the effect of the coefficients using the Q-h form are not presented here to avoid repetition.

8. EVALUATION ON IMPORTANCE OF COEFFICIENTS AND CONTRIBUTIONS OF TERMS

In preceding chapters, the importance of the coefficients, ß, k and k', and the relative contributions of the terms in the exact momentum equation are analyzed. To show the validity of the results obtained, it is essential to evaluate them by using certain theoretical methods and to compare them with those obtained by other investigators. In this chapter, the theory of linear stability applied by Ponce and Simons (1977) will be extended to evaluate the results on the importance of the coefficients. In addition, the results of the contributions of the terms obtained in this study will be evaluated with a method used by Price (1985).

8.1. Evaluation of Importance of Coefficients by Using Theory of Linear Stability

The exact momentum and continuity equations in the form of V and h for a wide rectangular channel without considering the internal stresses and two rates of spatial change of ß and k can be written as

$$\frac{\partial h}{\partial t} + h\frac{\partial V}{\partial x} + V\frac{\partial h}{\partial x} = 0 \tag{8.1}$$

$$\frac{1}{g}\frac{\partial V}{\partial t} + (2\beta-1)\frac{V}{g}\frac{\partial V}{\partial x} + \left[2k-k'+(\beta-1)\frac{V^2}{gh}\right]\frac{\partial h}{\partial x} + (S_f-S_0) = 0 \tag{8.2}$$

The friction and channel slopes, S_f and S_0, are written as

$$S_f = \frac{V^2}{C^2 h} = \frac{n^2 V^2}{2.21\ h^{3/4}} \tag{8.3}$$

$$S_0 = \frac{V_0^2}{C_0^2 h_0} = \frac{n_0^2 V_0^2}{2.21\ h_0^{3/4}} \tag{8.4}$$

in which C is the Chezy factor, n is the Manning factor, C_0 and n_0 are Chezy and Manning factors under the steady uniform flow, h_0 and V_0 are the steady uniform flow depth and velocity, respectively.

According to the theory of linear stability, the exact momentum and continuity equations must satisfy the unperturbed flow for which $V = V_0$ and $h = h_0$; as well as the perturbed flow for which $V = V_0 + V'$ and $h = h_0 + h'$. The V' or h' represents a perturbation to the steady uniform flow and is assumed to be small. In reality, the small perturbation is often impossible because a flood entering a channel will produce a large variation in the flow depth or velocity. Therefore, a small perturbation to the steady uniform flow is only hypothetical.

Substituting the perturbed variables into Eqs. (8.1) and (8.2), neglecting all the quadratic terms (because of higher order of magnitude), assuming the Chezy C, or Manning n, to be constant, and linearizing the two equations yield

$$\frac{\partial h'}{\partial t} + h_0 \frac{\partial V'}{\partial x} + V_0 \frac{\partial h'}{\partial x} = 0 \tag{8.5}$$

$$\frac{a_1}{g}\frac{\partial V'}{\partial t} + (2\beta-1)\frac{a_2 V_0}{g}\frac{\partial V'}{\partial x} + a_3\left[2k-k'+(\beta-1)\frac{V_0^2}{gh_0}\right]\frac{\partial h'}{\partial x}$$

$$+ a_4 S_0\left(2\frac{V'}{V_0} - f_c\frac{h'}{h_0}\right) = 0 \qquad (8.6)$$

in which f_c is a coefficient (it is equal to unity if the Chezy formula is used or 4/3 if the Manning formula is used), and a_1, a_2, a_3 and a_4 are integers that can only take values of 0 and 1. The purpose of introducing them is to clearly describe the various wave models.

The solutions of h' and V' can be postulated as

$$\frac{h'}{h_0} = h_{**}\exp[i(\sigma_* x_* - \Omega_* t_*)] \qquad (8.7)$$

$$\frac{V'}{V_0} = V_{**}\exp[i(\sigma_* x_* - \Omega_* t_*)] \qquad (8.8)$$

in which h_{**} is a dimensionless depth amplitude function, V_{**} is a dimensionless velocity amplitude function, σ_* is a dimensionless wave number, $\Omega_* = \Omega_{*r} + i\Omega_{*i}$ is a dimensionless complex propagation factor, Ω_{*r} and Ω_{*i} are the real and imaginary parts of the propagation factor, t_* and x_* are dimensionless space and time such that

$$\sigma_* = \frac{2\pi}{L_w} L_0 \qquad (8.9)$$

$$\Omega_{*r} = \frac{2\pi}{T_r}\frac{L_0}{V_0} \qquad (8.10)$$

$$\Omega_{*i} = \text{amplitude propagation factor} \tag{8.11}$$

$$x_* = \frac{x}{L_0} \tag{8.12}$$

$$t_* = \frac{tV_0}{L_0} \tag{8.13}$$

in which L_w is the wavelength of the disturbance, T_r is the period, L_0 is the reference length and it is defined as $L_0 = h_0/S_0$. Substituting the two expressions of h' and V' (Eqs. (8.7) and (8.8)) into the linearized Eqs. (8.5) and (8.6) yields:

$$\sigma_* V_{**} + (\sigma_* - \Omega_*)h_{**} = 0 \tag{8.14}$$

$$[2a_4 + (2\beta - 1)iF_0^2 a_2\sigma_* - iF_0^2 a_1\Omega_*]V_{**}$$

$$+ \{[2k - k' + (\beta - 1)F_0^2]ia_3\sigma_* - f_c a_4\}h_{**} = 0 \tag{8.15}$$

in which $F_0^2 = V_0^2/gh_0$

Mathematically, the solution of the homogeneous system of the two linear equations of unknowns V_{**} and h_{**} is nontrivial. The determinant of the coefficient matrix of the two equations must vanish. Therefore, the characteristic equation of Eqs. (8.14) and (8.15) is

$$ia_1\Omega_*^2F_0^2 - i\sigma_*^2\{[2k-k'+(\beta-1)F_0^2]a_3 - (2\beta-1)a_2F_0^2\}$$

$$+ (2+f_c)a_4\sigma_* - 2a_4\Omega_* - i\sigma_*\Omega_*[a_1+(2\beta-1)a_2]F_0^2 = 0 \tag{8.16}$$

If the values of β, k and k' are taken as equal to unity, and the Chezy formula is used, i.e., $f_c = 1$, Eqs. (8.15) and (8.16) become those derived by Ponce and Simons (1977) as follows

$$[2a_4 + iF_0^2(a_2\sigma_* - a_1\Omega_*)]V_{**} + (ia_3\sigma_* - a_4)h_{**} = 0 \qquad (8.17)$$

$$ia_1\Omega_*^2F_0^2 - i\sigma_*^2(a_3 - a_2F_0^2)$$

$$+ 3a_4\sigma_* - 2a_4\Omega_* - i\sigma_*\Omega_*(a_1 + a_2)F_0^2 = 0 \qquad (8.18)$$

Based on the suggestion of Ponce and Simons, the dimensionless celerity of the disturbance and the logarithmic decrement are respectively defined as

$$c_* = \frac{\Omega_{*r}}{\sigma_*} = \frac{L_w}{T_rV_0} \qquad (8.19)$$

$$\delta = 2\pi \frac{\Omega_{*i}}{|\Omega_{*r}|} = \frac{\Omega_{*i}T_r|V_0|S_0}{h_0} \qquad (8.20)$$

Thus, the magnitudes of the celerity and logarithmic decrement of the various approximate wave models can be determined. In addition, because the celerity and logarithmic decrement are functions of the coefficients, ß, k and k', the importance of the coefficients to the solutions of the equations can be detected by observing the variation of the magnitudes of the celerity and logarithmic decrement with the values of ß, k and k'.

(a) Kinematic wave model

Because the inertia and pressure terms are neglected in the kinematic wave model, in Eq. (8.16) $a_1 = a_2 = a_3 = 0$ and $a_4 = 1$, which yields

$$(2+f_c)\sigma_* - 2\Omega_* = 0 \qquad (8.21)$$

Accordingly, $\Omega_{*r} = \Omega_*$ and $\Omega_{*i} = 0$. Hence, the dimensionless celerity of the kinematic wave is

$$c_{*k} = \frac{\Omega_{*r}}{\sigma_*} = \frac{(2+f_c)}{2} \tag{8.22}$$

and the logarithmic decrement is

$$\delta_k = 2\pi \frac{\Omega_{*i}}{\Omega_{*r}} = 0 \tag{8.23}$$

(b) Noninertia model

In the noninertia model, only the inertia terms are neglected, i.e., $a_1 = a_2 = 0$ and $a_3 = a_4 = 1$, Eq. (8.16) becomes

$$- i\sigma_*^2[2k-k'+(\beta-1)F_0^2] + (2+f_c)\sigma_* - 2\Omega_* = 0 \tag{8.24}$$

Thus, the celerity of the noninertia wave is

$$c_{*n} = \frac{\Omega_{*r}}{\sigma_*} = \frac{(2+f_c)}{2} \tag{8.25}$$

and the logarithmic decrement of the noninertia wave is

$$\delta_n = 2\pi \frac{\Omega_{*i}}{\Omega_{*r}} = -2\pi[\frac{\sigma_*}{(2+f_c)}][2k-k'+(\beta-1)F_0^2] \tag{8.26}$$

(c) Dynamic wave model

In the dynamic wave model, all terms are considered. Therefore, Eq. (8.16) with $a_1 = a_2 = a_3 = a_4 = 1$ leads to

$$F_0^2\Omega_*^2 - 2(\beta\sigma_*F_0^2 - i)\Omega_* - [(2k-k'-\beta F_0^2)\sigma_*^2 + (2+f_c)\sigma_* i] = 0 \tag{8.27}$$

Thus, there are two wave propagations: One travels downstream and it is defined as 'Primary wave' with celerity, c_{*d1}, and logarithmic decrement, δ_1. The other called 'secondary wave' with celerity, c_{*d2}, and logarithmic decrement, δ_2, travels upstream. The celerity and attenuation functions are given by

$$c_{*d1} = 1 + CC^{1/2} \tag{8.28}$$

$$\delta_{d1} = -2\pi \frac{E - EE}{|1 + CC^{1/2}|} \tag{8.29}$$

$$c_{*d2} = 1 - CC^{1/2} \tag{8.30}$$

$$\delta_{d2} = -2\pi \frac{E + EE}{|1 - CC^{1/2}|} \tag{8.31}$$

in which $E = \frac{1}{\sigma_* F_0^2}$ (8.32)

$$CC = \frac{1}{2}\{AA^2 + [(2+f_c) - 2\beta]^2 \frac{1}{\sigma_*^2 F_0^4}\}^{1/2} + \frac{1}{2} AA \tag{8.33}$$

$$AA = (\beta^2 - \beta) + \frac{(2k - k')}{F_0^2} - \frac{1}{\sigma_*^2 F_0^4} \tag{8.34}$$

$$EE = (CC - AA)^{1/2} \tag{8.35}$$

If the values of β, k and k' are equal to unity and the Chezy formula is used, the above expressions of AA and CC become those obtained by Ponce and Simons (1977) as follows

$$CC = \frac{1}{2}[AA^2 + \frac{1}{\sigma_*^2 F_0^4}]^{1/2} + \frac{1}{2} AA \tag{8.36}$$

$$AA = \frac{1}{F_0^2} - \frac{1}{\sigma_*^2 F_0^4} \tag{8.37}$$

In order to explicitly display the results derived, a summary of the propagation characteristics of the various approximations is given in Table 8.1, in which the celerity is the relative celerity, c_{*r}, and it is defined as $(c_* - 1)$.

Table 8.1 A Comparison of Propagation Characteristics of Shallow Water Waves in Open Channel

Type of approximation	Relative celerity c_{*r}	Logarithmic decrement δ
	Results based on exact momentum equation	
Kinematic wave	$f_c/2$	0
Noninertia	$f_c/2$	$-2\pi[\sigma_*/(2+f_c)][2k-k'+(\beta-1)F_0^2]$
Dynamic Primary wave	$+CC^{1/2}$	$-2\pi[E-(CC-AA)^{1/2}]/\lvert 1+CC^{1/2}\rvert$
Secondary wave	$-CC^{1/2}$	$-2\pi[E+(CC-AA)^{1/2}]/\lvert 1-CC^{1/2}\rvert$
Note: $CC = (1/2)\{AA^2+[(2+f_c)-2\beta]^2E^2\}^{1/2}+(1/2)AA$; $E = 1/\sigma_*F_0^2$; $AA = (\beta^2-\beta)+[(2k-k')/F_0^2]-E^2$; $f_c = 1$ for Chezy formula and $f_c = 4/3$ for Manning formula		
	Ponce's results based on Saint-Venant equations	
Kinematic wave	1/2	0
Noninertia	1/2	$-2\pi(\sigma_*/3)$
Dynamic Primary wave	$+CC^{1/2}$	$-2\pi[E-(CC-AA)^{1/2}]/\lvert 1+CC^{1/2}\rvert$
Secondary wave	$-CC^{1/2}$	$-2\pi[E+(CC-AA)^{1/2}]/\lvert 1-CC^{1/2}\rvert$
Note: $CC = (1/2)(AA^2+E^2)^{1/2}+(1/2)AA$; $AA = (1/F_0^2)-E^2$		

From Table 8.1, two points are observed. One is that if the values of ß, k and k' are not equal to unity, the variations of the coefficients do not influence the kinematic wave model, nor the relative celerity of the noninertia model; but they affect dynamic wave model and the logarithmic decrement of the noninertia model. The other is that for the special case of ß, k and k' being taken as unity and the Chezy formula is used, the results become those of Ponce and Simons (1977).

In order to evaluate the results of the importance of the coefficients obtained in Chapter 5, seven combinations of the coefficients are selected as examples: (a) ß = 1, k = k' = 1 (case of the Saint-Venant equations); (b) ß = 1.33, k = k' = 1; (c) ß = 2, k = k' = 1; (d) ß = 1, k = 1.05, k' = 1; (e) ß = 1, k = 0.95, k' = 1; (f) ß = 1, k = 1, k' = 1.05; (g) ß = 1, k = 1, k' = 0.95, and for simplicity and convenience, only the variation of the relative celerity with the combinations of the coefficients is analyzed. The dimensionless relative celerity, c_{*r}, versus dimensionless wave number, σ_*, with the situation of $f_c = 1$ (the Chezy formula with $f_c = 1$ is selected as an example here, the results considering the Manning formula with $f_c = 4/3$ are similar) is shown in Figs. 8.1 (a) through (e), respectively, for the first five cases. Furthermore, the variation of the dimensionless relative celerity with dimensionless wave number for F_0 (Froude number based on V_0 and h_0) ranging from 0.01 to 1 is listed in Tables 8.2 (a) through (g). These tables include all seven cases considered. The reason for considering the Froude number to be less than unity is that the exact momentum and continuity equations do

not contain terms explicitly accounting for the occurrence of the pulsating flow for supercritical flows.

In order to display the impacts of the coefficients, ß, k and k', on the relative celerity, the rates of change of the relative difference of the relative celerity with respect to ß, k and k' are listed in Tables 8.3 (a) through (f), respectively. The relative difference is defined as the difference between the relative celerity of a specified combination of the coefficients and that of the reference case (ß = 1, k = k' = 1) divided by the value of the latter.

From Fig. 8.1 and Tables 8.2 and 8.3, the impacts of the coefficients in the exact momentum equation on the solutions of the equations for the subcritical flow condition are verified to be in accordance with those obtained in Chapter 5.

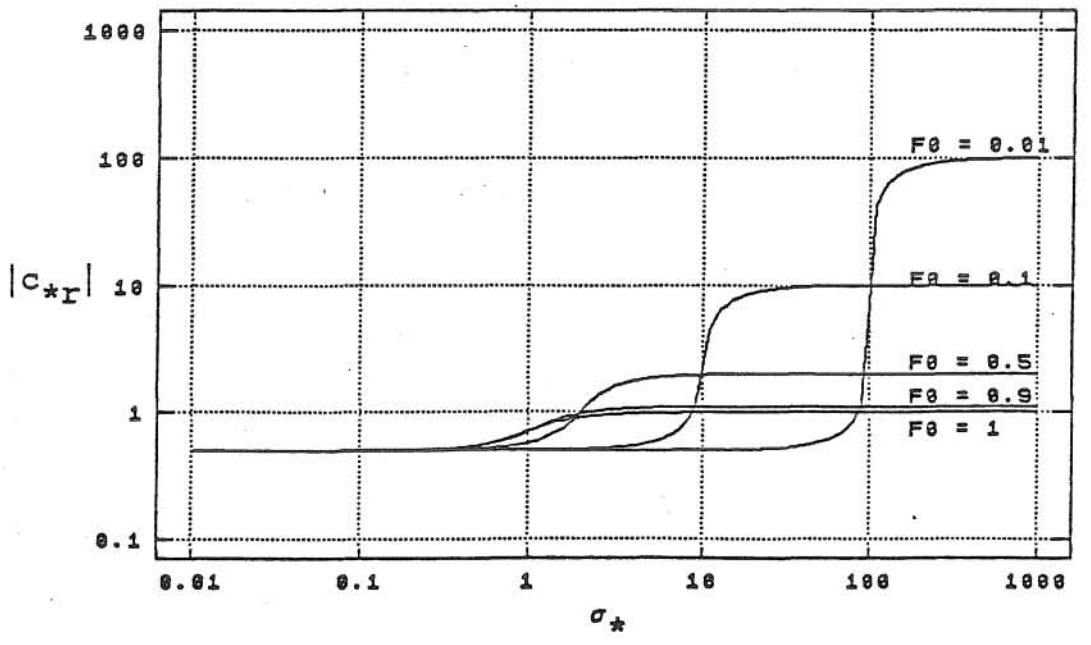

(a) ß = 1, k = k' = 1

Fig. 8.1 Dimensionless Relative Celerity c_{*r} versus Dimensionless Wave Number σ_* for Froude Number F_0 from 0.01 to 1

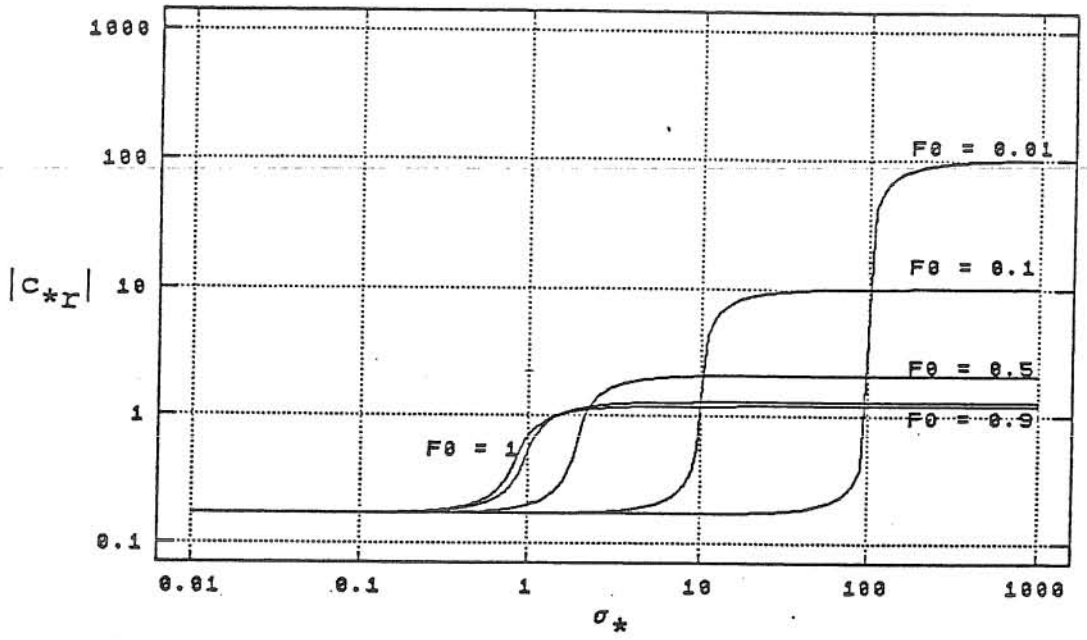

(b) $\beta = 1.33$, $k = k' = 1$

Fig. 8.1 (continued)

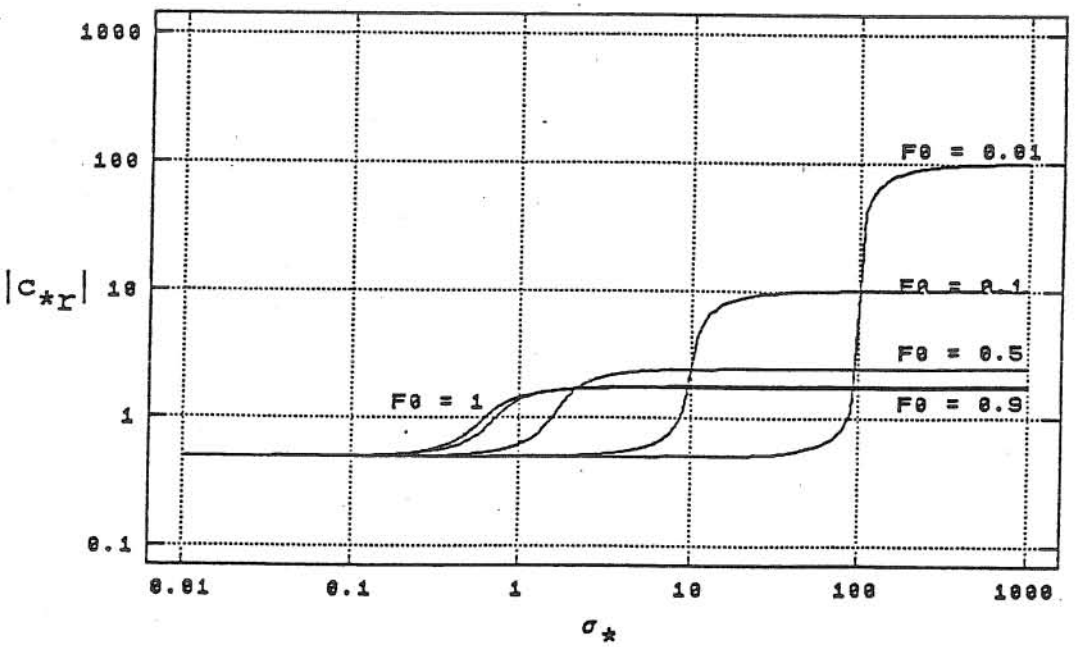

(c) $\beta = 2$, $k = k' = 1$

Fig. 8.1 (continued)

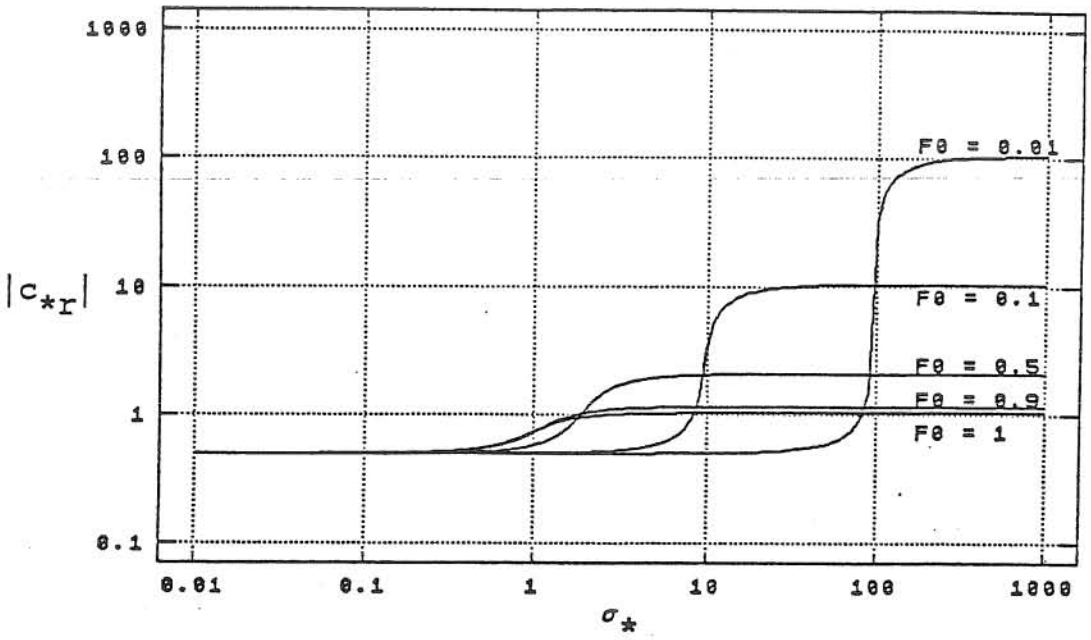

(d) $\beta = 1$, $k = 1.05$, $k' = 1$

Fig. 8.1 (continued)

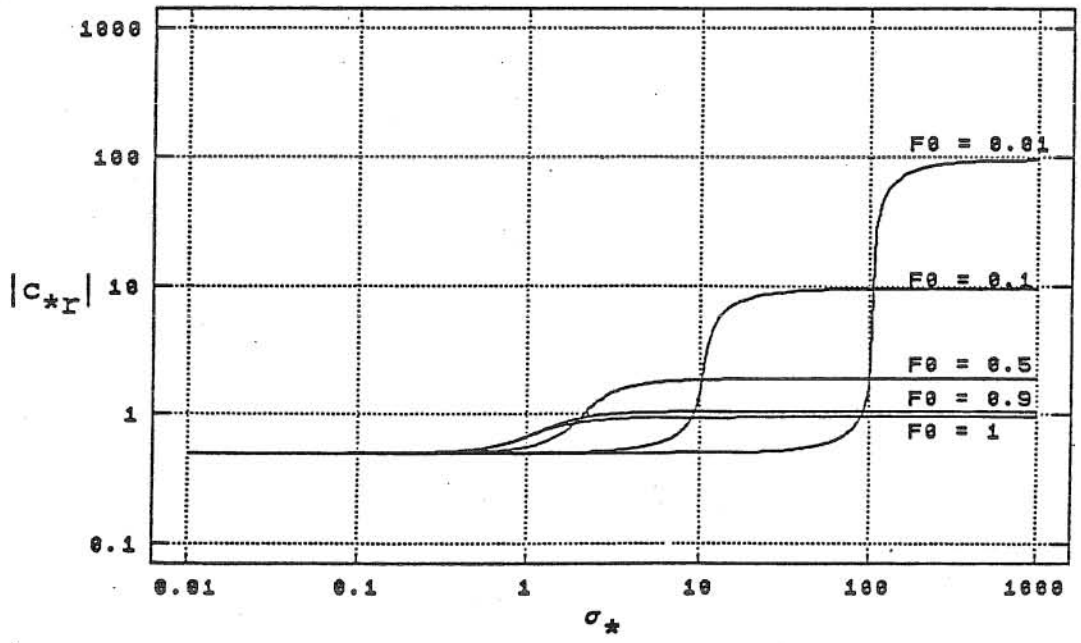

(e) $\beta = 1$, $k = 0.95$, $k' = 1$

Fig. 8.1 (continued)

Table 8.2 Dimensionless Relative Celerity, c_{*r}, for Various Dimensionless Wave Number, σ_*, and Froude Number, F_0

(a) $\beta = 1$, $k = k' = 1$

Dimensionless wave number	Froude number = 1	0.9	0.5	0.1	0.01
	Dimensionless relative celerity				
0.1	0.5019	0.5016	0.5006	0.5000	0.5000
0.2	0.5076	0.5065	0.5024	0.5001	0.5000
0.3	0.5173	0.5150	0.5054	0.5002	0.5000
0.4	0.5314	0.5272	0.5096	0.5004	0.5000
0.5	0.5503	0.5436	0.5153	0.5006	0.5000
0.6	0.5741	0.5648	0.5224	0.5009	0.5000
0.7	0.6028	0.5911	0.5312	0.5012	0.5000
0.8	0.6357	0.6228	0.5418	0.5016	0.5000
0.9	0.6712	0.6594	0.5545	0.5020	0.5000
1	0.7071	0.6995	0.5697	0.5025	0.5000
2	0.9087	0.9764	1.0000	0.5103	0.5001
3	0.9587	1.0505	1.5514	0.5241	0.5002
4	0.9767	1.0770	1.7553	0.5454	0.5004
5	0.9850	1.0892	1.8458	0.5770	0.5006
6	0.9896	1.0959	1.8938	0.6243	0.5009
7	0.9924	1.0999	1.9224	0.6985	0.5012
8	0.9941	1.1026	1.9408	0.8283	0.5016
9	0.9954	1.1044	1.9533	1.1177	0.5020
10	0.9963	1.1056	1.9622	2.2361	0.5025
11	0.9969	1.1066	1.9688	4.2981	0.5031
12	0.9974	1.1073	1.9738	5.5780	0.5036
13	0.9978	1.1079	1.9777	6.4178	0.5043
14	0.9981	1.1083	1.9808	7.0170	0.5050
15	0.9983	1.1087	1.9833	7.4669	0.5057
16	0.9985	1.1090	1.9853	7.8165	0.5065
17	0.9987	1.1092	1.9870	8.0951	0.5074
18	0.9988	1.1094	1.9884	8.3215	0.5083
19	0.9990	1.1096	1.9896	8.5085	0.5093
20	0.9991	1.1097	1.9906	8.6651	0.5103
22	0.9992	1.1100	1.9922	8.9109	0.5126
24	0.9993	1.1102	1.9935	9.0935	0.5151
26	0.9994	1.1103	1.9944	9.2331	0.5178
28	0.9995	1.1104	1.9952	9.3425	0.5208
30	0.9996	1.1105	1.9958	9.4297	0.5241
110	1.0000	1.1111	1.9997	9.9587	41.6741
210	1.0000	1.1111	1.9999	9.9887	87.9346
310	1.0000	1.1111	2.0000	9.9948	94.6544
410	1.0000	1.1111	2.0000	9.9970	96.9801
510	1.0000	1.1111	2.0000	9.9981	98.0589
610	1.0000	1.1111	2.0000	9.9987	98.6472
710	1.0000	1.1111	2.0000	9.9990	99.0032
810	1.0000	1.1111	2.0000	9.9992	99.2350
910	1.0000	1.1111	2.0000	9.9994	99.3944

Table 8.2 (continued)

(b) $\beta = 1.33$, $k = k' = 1$

Dimensionless wave number	Froude number = 1	0.9	0.5	0.1	0.01
	Dimensionless relative celerity				
0.1	0.1712	0.1709	0.1702	0.1700	0.1700
0.2	0.1750	0.1738	0.1709	0.1700	0.1700
0.3	0.1819	0.1789	0.1721	0.1701	0.1700
0.4	0.1930	0.1868	0.1739	0.1701	0.1700
0.5	0.2106	0.1987	0.1762	0.1702	0.1700
0.6	0.2398	0.2166	0.1791	0.1703	0.1700
0.7	0.2929	0.2450	0.1828	0.1704	0.1700
0.8	0.3994	0.2943	0.1873	0.1705	0.1700
0.9	0.5630	0.3889	0.1928	0.1707	0.1700
1	0.7050	0.5454	0.1996	0.1709	0.1700
2	1.0931	1.1406	0.7900	0.1735	0.1700
3	1.1533	1.2277	1.6372	0.1782	0.1701
4	1.1738	1.2570	1.8567	0.1856	0.1701
5	1.1831	1.2703	1.9503	0.1964	0.1702
6	1.1881	1.2775	1.9994	0.2127	0.1703
7	1.1912	1.2818	2.0285	0.2385	0.1704
8	1.1931	1.2846	2.0471	0.2842	0.1705
9	1.1945	1.2865	2.0598	0.3924	0.1707
10	1.1955	1.2878	2.0688	1.3905	0.1709
11	1.1962	1.2888	2.0755	4.2341	0.1710
12	1.1967	1.2896	2.0805	5.5731	0.1712
13	1.1971	1.2902	2.0844	6.4272	0.1715
14	1.1975	1.2907	2.0875	7.0319	0.1717
15	1.1977	1.2911	2.0900	7.4845	0.1719
16	1.1979	1.2914	2.0921	7.8355	0.1722
17	1.1981	1.2916	2.0938	8.1149	0.1725
18	1.1983	1.2918	2.0952	8.3419	0.1728
19	1.1984	1.2920	2.0964	8.5293	0.1732
20	1.1985	1.2922	2.0974	8.6861	0.1735
22	1.1987	1.2924	2.0991	8.9323	0.1743
24	1.1988	1.2926	2.1003	9.1150	0.1751
26	1.1989	1.2928	2.1013	9.2548	0.1761
28	1.1990	1.2929	2.1021	9.3642	0.1771
30	1.1991	1.2930	2.1027	9.4515	0.1782
110	1:1995	1.2936	2.1066	9.9806	41.6667
210	1.1995	1.2936	2.1068	10.0106	87.9368
310	1.1995	1.2936	2.1068	10.0167	94.6565
410	1.1995	1.2936	2.1068	10.0190	96.9822
510	1.1995	1.2936	2.1069	10.0200	98.0611
610	1.1995	1.2936	2.1069	10.0206	98.6494
710	1.1995	1.2936	2.1069	10.0209	99.0054
810	1.1995	1.2936	2.1069	10.0212	99.2372
910	1.1995	1.2936	2.1069	10.0213	99.3966

Table 8.2 (continued)

(c) $\beta = 2$, $k = k' = 1$

Dimensionless wave number	Froude number = 1	0.9	0.5	0.1	0.01
	Dimensionless relative celerity				
0.1	0.5070	0.5050	0.5009	0.5000	0.5000
0.2	0.5296	0.5207	0.5036	0.5001	0.5000
0.3	0.5737	0.5499	0.5083	0.5002	0.5000
0.4	0.6520	0.5985	0.5150	0.5004	0.5000
0.5	0.7862	0.6775	0.5240	0.5006	0.5000
0.6	0.9756	0.8026	0.5356	0.5009	0.5000
0.7	1.1576	0.9726	0.5503	0.5013	0.5000
0.8	1.2928	1.1438	0.5687	0.5016	0.5000
0.9	1.3877	1.2805	0.5917	0.5021	0.5000
1	1.4553	1.3820	0.6206	0.5026	0.5000
2	1.6651	1.6990	1.5538	0.5105	0.5001
3	1.7025	1.7547	2.0797	0.5246	0.5002
4	1.7155	1.7739	2.2471	0.5464	0.5004
5	1.7214	1.7828	2.3216	0.5790	0.5006
6	1.7247	1.7876	2.3612	0.6278	0.5009
7	1.7266	1.7905	2.3849	0.7052	0.5012
8	1.7279	1.7924	2.4002	0.8431	0.5016
9	1.7288	1.7937	2.4106	1.1632	0.5020
10	1.7294	1.7946	2.4180	2.4696	0.5025
11	1.7299	1.7953	2.4235	4.5133	0.5031
12	1.7302	1.7958	2.4277	5.7516	0.5036
13	1.7305	1.7962	2.4309	6.5705	0.5043
14	1.7307	1.7965	2.4335	7.1574	0.5050
15	1.7309	1.7968	2.4355	7.5992	0.5057
16	1.7310	1.7970	2.4372	7.9431	0.5065
17	1.7311	1.7971	2.4386	8.2174	0.5074
18	1.7312	1.7973	2.4398	8.4406	0.5083
19	1.7313	1.7974	2.4408	8.6251	0.5093
20	1.7314	1.7975	2.4417	8.7796	0.5103
22	1.7315	1.7977	2.4430	9.0223	0.5126
24	1.7316	1.7978	2.4441	9.2027	0.5151
26	1.7317	1.7979	2.4449	9.3407	0.5178
28	1.7317	1.7980	2.4455	9.4488	0.5208
30	1.7318	1.7981	2.4460	9.5352	0.5241
110	1.7320	1.7985	2.4492	10.0586	41.6980
210	1.7320	1.7985	2.4494	10.0883	87.9460
310	1.7320	1.7985	2.4495	10.0944	94.6649
410	1.7320	1.7985	2.4495	10.0966	96.9904
510	1.7320	1.7985	2.4495	10.0976	98.0691
610	1.7321	1.7985	2.4495	10.0982	98.6573
710	1.7321	1.7985	2.4495	10.0985	99.0133
810	1.7321	1.7985	2.4495	10.0988	99.2451
910	1.7321	1.7985	2.4495	10.0989	99.4045

Table 8.2 (continued)

(d) $\beta = 1$, $k = 1.05$, $k' = 1$

Dimensionless wave number	Froude number = 1	0.9	0.5	0.1	0.01
	Dimensionless relative celerity				
0.1	0.5021	0.5018	0.5006	0.5000	0.5000
0.2	0.5086	0.5074	0.5026	0.5001	0.5000
0.3	0.5198	0.5169	0.5059	0.5002	0.5000
0.4	0.5361	0.5309	0.5107	0.5004	0.5000
0.5	0.5580	0.5499	0.5170	0.5007	0.5000
0.6	0.5861	0.5746	0.5250	0.5010	0.5000
0.7	0.6204	0.6057	0.5348	0.5013	0.5000
0.8	0.6597	0.6435	0.5469	0.5018	0.5000
0.9	0.7017	0.6873	0.5614	0.5022	0.5000
1	0.7433	0.7347	0.5789	0.5028	0.5000
2	0.9582	1.0326	1.1044	0.5113	0.5001
3	1.0081	1.1060	1.6679	0.5267	0.5002
4	1.0258	1.1320	1.8633	0.5507	0.5004
5	1.0341	1.1440	1.9499	0.5869	0.5007
6	1.0386	1.1505	1.9959	0.6426	0.5010
7	1.0413	1.1544	2.0232	0.7343	0.5014
8	1.0431	1.1570	2.0408	0.9109	0.5018
9	1.0443	1.1588	2.0528	1.4132	0.5022
10	1.0451	1.1600	2.0614	3.4743	0.5028
11	1.0458	1.1609	2.0677	5.3001	0.5034
12	1.0463	1.1616	2.0725	6.4015	0.5040
13	1.0466	1.1622	2.0763	7.1497	0.5047
14	1.0469	1.1626	2.0792	7.6938	0.5055
15	1.0472	1.1630	2.0816	8.1071	0.5063
16	1.0474	1.1633	2.0835	8.4306	0.5072
17	1.0475	1.1635	2.0851	8.6898	0.5081
18	1.0477	1.1637	2.0865	8.9013	0.5092
19	1.0478	1.1639	2.0876	9.0765	0.5102
20	1.0479	1.1640	2.0886	9.2235	0.5114
22	1.0480	1.1642	2.0902	9.4550	0.5139
24	1.0482	1.1644	2.0914	9.6273	0.5166
26	1.0483	1.1646	2.0923	9.7594	0.5197
28	1.0483	1.1647	2.0930	9.8629	0.5231
30	1.0484	1.1648	2.0936	9.9457	0.5268
110	1.0488	1.1653	2.0973	10.4487	52.3096
210	1.0488	1.1653	2.0975	10.4773	93.4478
310	1.0488	1.1653	2.0976	10.4831	99.7970
410	1.0488	1.1653	2.0976	10.4853	102.0055
510	1.0488	1.1653	2.0976	10.4863	103.0318
610	1.0488	1.1653	2.0976	10.4868	103.5918
710	1.0488	1.1653	2.0976	10.4871	103.9309
810	1.0488	1.1653	2.0976	10.4874	104.1518
910	1.0488	1.1653	2.0976	10.4875	104.3036

Table 8.2 (continued)

(e) $\beta = 1$, $k = 0.95$, $k' = 1$

Dimensionless wave number	Froude number = 1	0.9	0.5	0.1	0.01
	Dimensionless relative celerity				
0.1	0.5016	0.5014	0.5005	0.5000	0.5000
0.2	0.5066	0.5057	0.5021	0.5001	0.5000
0.3	0.5149	0.5130	0.5048	0.5002	0.5000
0.4	0.5269	0.5235	0.5086	0.5004	0.5000
0.5	0.5428	0.5376	0.5136	0.5006	0.5000
0.6	0.5626	0.5554	0.5199	0.5008	0.5000
0.7	0.5862	0.5774	0.5276	0.5011	0.5000
0.8	0.6133	0.6035	0.5368	0.5014	0.5000
0.9	0.6426	0.6336	0.5479	0.5018	0.5000
1	0.6727	0.6666	0.5609	0.5023	0.5000
2	0.8573	0.9182	0.9054	0.5092	0.5001
3	0.9070	0.9923	1.4283	0.5215	0.5002
4	0.9251	1.0192	1.6410	0.5403	0.5004
5	0.9335	1.0317	1.7358	0.5677	0.5006
6	0.9381	1.0386	1.7862	0.6075	0.5008
7	0.9409	1.0427	1.8161	0.6674	0.5011
8	0.9427	1.0453	1.8354	0.7645	0.5014
9	0.9440	1.0472	1.8485	0.9478	0.5018
10	0.9449	1.0485	1.8578	1.4391	0.5023
11	0.9455	1.0495	1.8647	3.0862	0.5027
12	0.9460	1.0502	1.8700	4.6226	0.5033
13	0.9464	1.0508	1.8741	5.5947	0.5038
14	0.9467	1.0512	1.8773	6.2693	0.5045
15	0.9470	1.0516	1.8799	6.7674	0.5051
16	0.9472	1.0519	1.8820	7.1504	0.5059
17	0.9474	1.0522	1.8838	7.4534	0.5066
18	0.9475	1.0524	1.8852	7.6984	0.5075
19	0.9476	1.0525	1.8865	7.9000	0.5083
20	0.9477	1.0527	1.8875	8.0682	0.5093
22	0.9479	1.0529	1.8892	8.3315	0.5113
24	0.9480	1.0531	1.8905	8.5263	0.5135
26	0.9481	1.0533	1.8916	8.6750	0.5159
28	0.9482	1.0534	1.8924	8.7913	0.5186
30	0.9483	1.0535	1.8930	8.8839	0.5216
110	0.9487	1.0540	1.8970	9.4433	27.1723
210	0.9487	1.0541	1.8973	9.4749	82.0519
310	0.9487	1.0541	1.8973	9.4814	89.2157
410	0.9487	1.0541	1.8973	9.4837	91.6795
510	0.9487	1.0541	1.8974	9.4848	92.8200
610	0.9487	1.0541	1.8974	9.4854	93.4412
710	0.9487	1.0541	1.8974	9.4858	93.8170
810	0.9487	1.0541	1.8974	9.4860	94.0616
910	0.9487	1.0541	1.8974	9.4862	94.2297

Table 8.2 (continued)

(f) $\beta = 1$, $k = 1$, $k' = 1.05$

Dimensionless wave number	Froude number = 1	0.9	0.5	0.1	0.01
	Dimensionless relative celerity				
0.1	0.5018	0.5015	0.5006	0.5000	0.5000
0.2	0.5071	0.5061	0.5022	0.5001	0.5000
0.3	0.5161	0.5140	0.5051	0.5002	0.5000
0.4	0.5292	0.5253	0.5091	0.5004	0.5000
0.5	0.5465	0.5406	0.5144	0.5006	0.5000
0.6	0.5682	0.5600	0.5211	0.5009	0.5000
0.7	0.5944	0.5841	0.5293	0.5012	0.5000
0.8	0.6243	0.6130	0.5393	0.5015	0.5000
0.9	0.6567	0.6462	0.5511	0.5019	0.5000
1	0.6897	0.6827	0.5652	0.5024	0.5000
2	0.8832	0.9476	0.9513	0.5098	0.5001
3	0.9332	1.0218	1.4907	0.5228	0.5002
4	0.9512	1.0484	1.6990	0.5428	0.5004
5	0.9596	1.0609	1.7916	0.5723	0.5006
6	0.9642	1.0676	1.8407	0.6158	0.5009
7	0.9670	1.0717	1.8700	0.6825	0.5012
8	0.9688	1.0743	1.8888	0.7945	0.5015
9	0.9700	1.0761	1.9016	1.0228	0.5019
10	0.9709	1.0774	1.9107	1.7579	0.5024
11	0.9716	1.0784	1.9175	3.7212	0.5029
12	0.9721	1.0791	1.9226	5.1203	0.5035
13	0.9724	1.0797	1.9266	6.0197	0.5041
14	0.9728	1.0802	1.9297	6.6534	0.5047
15	0.9730	1.0805	1.9323	7.1256	0.5054
16	0.9732	1.0808	1.9343	7.4908	0.5062
17	0.9734	1.0811	1.9361	7.7808	0.5070
18	0.9735	1.0813	1.9375	8.0160	0.5079
19	0.9736	1.0814	1.9387	8.2099	0.5088
20	0.9737	1.0816	1.9398	8.3719	0.5098
22	0.9739	1.0818	1.9414	8.6260	0.5119
24	0.9740	1.0820	1.9427	8.8145	0.5143
26	0.9741	1.0822	1.9437	8.9584	0.5169
28	0.9742	1.0823	1.9445	9.0710	0.5197
30	0.9743	1.0824	1.9451	9.1609	0.5229
110	0.9746	1.0829	1.9490	9.7044	35.1740
210	0.9747	1.0830	1.9493	9.7352	85.0441
310	0.9747	1.0830	1.9493	9.7415	91.9753
410	0.9747	1.0830	1.9493	9.7438	94.3670
510	0.9747	1.0830	1.9493	9.7448	95.4754
610	0.9747	1.0830	1.9493	9.7454	96.0795
710	0.9747	1.0830	1.9494	9.7458	96.4450
810	0.9747	1.0830	1.9494	9.7460	96.6829
910	0.9747	1.0830	1.9494	9.7462	96.8465

Table 8.2 (continued)

(g) $\beta = 1$, $k = 1$, $k' = 0.95$

Dimensionless wave number	Froude number = 1	0.9	0.5	0.1	0.01
	Dimensionless relative celerity				
0.1	0.5020	0.5017	0.5006	0.5000	0.5000
0.2	0.5081	0.5070	0.5025	0.5001	0.5000
0.3	0.5186	0.5159	0.5056	0.5002	0.5000
0.4	0.5337	0.5290	0.5102	0.5004	0.5000
0.5	0.5541	0.5467	0.5161	0.5007	0.5000
0.6	0.5800	0.5696	0.5237	0.5009	0.5000
0.7	0.6114	0.5983	0.5330	0.5013	0.5000
0.8	0.6475	0.6330	0.5443	0.5017	0.5000
0.9	0.6862	0.6731	0.5579	0.5021	0.5000
1	0.7250	0.7168	0.5743	0.5026	0.5000
2	0.9336	1.0048	1.0512	0.5108	0.5001
3	0.9837	1.0786	1.6105	0.5254	0.5002
4	1.0015	1.1048	1.8101	0.5480	0.5004
5	1.0099	1.1169	1.8985	0.5819	0.5007
6	1.0144	1.1235	1.9455	0.6332	0.5009
7	1.0171	1.1275	1.9734	0.7157	0.5013
8	1.0189	1.1301	1.9914	0.8667	0.5017
9	1.0201	1.1319	2.0037	1.2423	0.5021
10	1.0210	1.1331	2.0124	2.8443	0.5026
11	1.0216	1.1341	2.0189	4.8212	0.5032
12	1.0221	1.1348	2.0238	6.0031	0.5038
13	1.0225	1.1354	2.0276	6.7933	0.5045
14	1.0228	1.1358	2.0306	7.3631	0.5052
15	1.0230	1.1361	2.0330	7.7935	0.5060
16	1.0232	1.1364	2.0350	8.1293	0.5069
17	1.0234	1.1367	2.0367	8.3977	0.5078
18	1.0235	1.1369	2.0380	8.6162	0.5087
19	1.0237	1.1371	2.0392	8.7971	0.5098
20	1.0238	1.1372	2.0402	8.9486	0.5108
22	1.0239	1.1374	2.0418	9.1869	0.5132
24	1.0240	1.1376	2.0430	9.3642	0.5158
26	1.0241	1.1378	2.0440	9.4999	0.5187
28	1.0242	1.1379	2.0447	9.6062	0.5219
30	1.0243	1.1379	2.0453	9.6912	0.5254
110	1.0247	1.1385	2.0491	10.2066	47.2912
210	1.0247	1.1385	2.0493	10.2359	90.7331
310	1.0247	1.1385	2.0494	10.2419	97.2597
410	1.0247	1.1385	2.0494	10.2441	99.5245
510	1.0247	1.1385	2.0494	10.2451	100.5761
610	1.0247	1.1385	2.0494	10.2456	101.1497
710	1.0247	1.1385	2.0494	10.2460	101.4970
810	1.0247	1.1385	2.0494	10.2462	101.7231
910	1.0247	1.1385	2.0494	10.2464	101.8786

Table 8.3 Rate of Change of Relative Difference of c_{*r} with respect to ß, k and k' for Various Wave Number, σ_*, and Froude Number, F_0

(a) ß = 1.33, k = k' = 1 vs. ß = 1, k = k' = 1 (ß varies 33%)

Dimensionless wave number	Froude number = 1	0.9	0.5	0.1	0.01
	Rate of change of relative difference of dimensionless relative celerity with respect to ß in %				
0.1	-199.65	-199.77	-199.98	-200.00	-200.00
0.2	-198.56	-199.06	-199.91	-200.00	-200.00
0.3	-196.49	-197.76	-199.80	-200.00	-200.00
0.4	-192.97	-195.64	-199.64	-200.00	-200.00
0.5	-187.03	-192.27	-199.42	-200.00	-200.00
0.6	-176.46	-186.80	-199.13	-200.00	-200.00
0.7	-155.81	-177.42	-198.75	-200.00	-200.00
0.8	-112.65	-159.84	-198.27	-200.00	-200.00
0.9	-48.87	-124.29	-197.65	-200.00	-200.00
1	-0.90	-66.76	-196.84	-200.00	-200.00
2	61.51	50.93	-63.63	-199.99	-200.00
3	61.52	51.12	16.75	-199.97	-200.00
4	61.15	50.65	17.50	-199.93	-200.00
5	60.93	50.36	17.16	-199.87	-200.00
6	60.80	50.19	16.90	-199.77	-200.00
7	60.71	50.09	16.72	-199.57	-200.00
8	60.66	50.02	16.60	-199.04	-200.00
9	60.62	49.97	16.52	-196.64	-200.00
10	60.59	49.93	16.46	-114.59	-200.00
11	60.57	49.91	16.41	-4.51	-200.00
12	60.55	49.89	16.38	-0.27	-200.00
13	60.54	49.87	16.35	0.45	-200.00
14	60.53	49.86	16.33	0.64	-200.00
15	60.52	49.85	16.31	0.71	-200.00
16	60.52	49.84	16.30	0.74	-200.00
17	60.51	49.83	16.29	0.74	-200.00
18	60.51	49.83	16.28	0.74	-200.00
19	60.50	49.82	16.27	0.74	-200.00
20	60.50	49.82	16.26	0.74	-200.00
22	60.49	49.81	16.25	0.73	-200.00
24	60.49	49.80	16.24	0.72	-200.00
26	60.49	49.80	16.23	0.71	-200.00
28	60.48	49.80	16.23	0.70	-200.00
30	60.48	49.79	16.22	0.70	-200.00
110	60.47	49.78	16.19	0.67	-0.05
210	60.47	49.78	16.19	0.67	0.01
310	60.47	49.78	16.19	0.66	0.01
410	60.47	49.78	16.19	0.66	0.01
510	60.47	49.78	16.19	0.66	0.01
610	60.47	49.78	16.19	0.66	0.01
710	60.47	49.78	16.19	0.66	0.01
810	60.47	49.78	16.19	0.66	0.01
910	60.47	49.78	16.19	0.66	0.01

Table 8.3 (continued)

(b) $\beta = 2$, $k = k' = 1$ vs. $\beta = 1$, $k = k' = 1$
(β varies 100%)

Dimensionless wave number	Froude number = 1	0.9	0.5	0.1	0.01
	Rate of change of relative difference of dimensionless relative celerity with respect to β in %				
0.1	1.02	0.67	0.06	0.00	0.00
0.2	4.34	2.79	0.25	0.00	0.00
0.3	10.89	6.78	0.58	0.00	0.00
0.4	22.69	13.52	1.05	0.00	0.00
0.5	42.87	24.62	1.69	0.00	0.00
0.6	69.95	42.10	2.53	0.00	0.00
0.7	92.04	64.54	3.61	0.00	0.00
0.8	103.36	83.64	4.97	0.01	0.00
0.9	106.75	94.20	6.71	0.01	0.00
1	105.82	97.58	8.94	0.01	0.00
2	83.24	74.00	55.38	0.04	0.00
3	77.58	67.03	34.05	0.10	0.00
4	75.64	64.72	28.02	0.19	0.00
5	74.76	63.67	25.78	0.33	0.00
6	74.28	63.11	24.68	0.56	0.00
7	73.99	62.78	24.06	0.97	0.00
8	73.81	62.56	23.67	1.78	0.00
9	73.68	62.42	23.41	4.07	0.00
10	73.59	62.31	23.23	10.44	0.00
11	73.52	62.23	23.09	5.01	0.00
12	73.47	62.17	22.99	3.11	0.00
13	73.43	62.13	22.91	2.38	0.00
14	73.40	62.09	22.85	2.00	0.00
15	73.38	62.06	22.80	1.77	0.00
16	73.36	62.04	22.76	1.62	0.00
17	73.34	62.02	22.73	1.51	0.00
18	73.32	62.00	22.70	1.43	0.00
19	73.31	61.99	22.68	1.37	0.00
20	73.30	61.98	22.66	1.32	0.00
22	73.28	61.96	22.63	1.25	0.00
24	73.27	61.94	22.60	1.20	0.00
26	73.26	61.93	22.58	1.17	0.00
28	73.25	61.92	22.57	1.14	0.00
30	73.25	61.91	22.56	1.12	0.00
110	73.21	61.87	22.48	1.00	0.06
210	73.21	61.87	22.48	1.00	0.01
310	73.21	61.86	22.48	1.00	0.01
410	73.21	61.86	22.47	1.00	0.01
510	73.21	61.86	22.47	1.00	0.01
610	73.21	61.86	22.47	1.00	0.01
710	73.21	61.86	22.47	1.00	0.01
810	73.21	61.86	22.47	1.00	0.01
910	73.21	61.86	22.47	1.00	0.01

Table 8.3 (continued)

(c) $\beta = 1$, $k = 1.05$, $k' = 1$ vs. $\beta = 1$, $k = k' = 1$ (k varies 5%)

Dimensionless wave number	Froude number = 1	0.9	0.5	0.1	0.01
	Rate of change of relative difference of dimensionless relative celerity with respect to k in %				
0.1	1.01	0.81	0.25	0.01	0.00
0.2	4.09	3.31	1.01	0.04	0.00
0.3	9.46	7.65	2.30	0.09	0.00
0.4	17.41	14.10	4.16	0.16	0.00
0.5	28.26	23.00	6.64	0.25	0.00
0.6	42.09	34.72	9.83	0.36	0.00
0.7	58.35	49.40	13.83	0.49	0.00
0.8	75.40	66.52	18.79	0.64	0.01
0.9	90.76	84.50	24.88	0.82	0.01
1	102.37	100.76	32.37	1.01	0.01
2	108.92	115.08	208.89	4.18	0.04
3	103.01	105.68	150.21	9.96	0.09
4	100.69	102.16	123.07	19.30	0.16
5	99.60	100.52	112.79	34.11	0.25
6	99.00	99.63	107.76	58.46	0.36
7	98.63	99.10	104.91	102.52	0.49
8	98.39	98.75	103.12	199.41	0.64
9	98.23	98.51	101.92	528.78	0.82
10	98.12	98.34	101.08	1107.55	1.01
11	98.03	98.22	100.46	466.24	1.23
12	97.96	98.12	100.00	295.29	1.46
13	97.91	98.05	99.64	228.09	1.72
14	97.87	97.99	99.36	192.90	2.00
15	97.84	97.94	99.13	171.46	2.31
16	97.81	97.90	98.95	157.13	2.63
17	97.79	97.87	98.79	146.94	2.98
18	97.77	97.84	98.66	139.35	3.36
19	97.76	97.82	98.56	133.51	3.76
20	97.74	97.80	98.46	128.90	4.18
22	97.72	97.77	98.32	122.12	5.11
24	97.70	97.74	98.20	117.42	6.14
26	97.69	97.72	98.12	114.00	7.29
28	97.68	97.71	98.05	111.43	8.56
30	97.67	97.70	97.99	109.43	9.96
110	97.62	97.62	97.65	98.41	510.41
210	97.62	97.62	97.63	97.83	125.39
310	97.62	97.62	97.62	97.72	108.66
410	97.62	97.62	97.62	97.67	103.64
510	97.62	97.62	97.62	97.65	101.43
610	97.62	97.62	97.62	97.64	100.25
710	97.62	97.62	97.62	97.64	99.55
810	97.62	97.62	97.62	97.63	99.09
910	97.62	97.62	97.62	97.63	98.78

Table 8.3 (continued)

(d) $\beta = 1$, $k = 0.95$, $k' = 1$ vs. $\beta = 1$, $k = k' = 1$ (k varies 5%)

Dimensionless wave number	Froude number = 1	0.9	0.5	0.1	0.01
	Rate of change of relative difference of dimensionless relative celerity with respect to k in %				
0.1	-1.00	-0.81	-0.25	-0.01	0.00
0.2	-4.07	-3.29	-1.01	-0.04	0.00
0.3	-9.33	-7.56	-2.29	-0.09	-0.00
0.4	-16.99	-13.82	-4.13	-0.16	-0.00
0.5	-27.23	-22.29	-6.58	-0.25	-0.00
0.6	-40.02	-33.20	-9.69	-0.36	-0.00
0.7	-54.87	-46.57	-13.55	-0.49	-0.00
0.8	-70.56	-62.00	-18.28	-0.64	-0.01
0.9	-85.29	-78.37	-24.01	-0.82	-0.01
1	-97.38	-93.88	-30.92	-1.01	-0.01
2	-112.99	-119.33	-189.14	-4.15	-0.04
3	-107.85	-110.74	-158.69	-9.81	-0.09
4	-105.66	-107.26	-130.27	-18.76	-0.16
5	-104.59	-105.60	-119.15	-32.45	-0.25
6	-104.00	-104.70	-113.69	-53.76	-0.36
7	-103.64	-104.15	-110.57	-88.92	-0.49
8	-103.41	-103.80	-108.63	-154.03	-0.64
9	-103.24	-103.55	-107.32	-303.96	-0.82
10	-103.13	-103.38	-106.40	-712.81	-1.01
11	-103.04	-103.25	-105.73	-563.93	-1.22
12	-102.98	-103.15	-105.23	-342.56	-1.46
13	-102.93	-103.07	-104.84	-256.48	-1.72
14	-102.89	-103.01	-104.53	-213.12	-2.00
15	-102.85	-102.96	-104.28	-187.36	-2.30
16	-102.83	-102.92	-104.08	-170.42	-2.62
17	-102.81	-102.89	-103.91	-158.52	-2.97
18	-102.79	-102.86	-103.77	-149.75	-3.34
19	-102.77	-102.84	-103.66	-143.03	-3.73
20	-102.76	-102.82	-103.56	-137.76	-4.15
22	-102.74	-102.79	-103.39	-130.05	-5.07
24	-102.72	-102.76	-103.27	-124.73	-6.08
26	-102.71	-102.74	-103.18	-120.89	-7.21
28	-102.70	-102.73	-103.10	-118.00	-8.45
30	-102.69	-102.72	-103.04	-115.77	-9.82
110	-102.64	-102.64	-102.66	-103.51	-695.96
210	-102.63	-102.64	-102.64	-102.87	-133.80
310	-102.63	-102.63	-102.64	-102.74	-114.91
410	-102.63	-102.63	-102.64	-102.70	-109.31
510	-102.63	-102.63	-102.63	-102.67	-106.85
610	-102.63	-102.63	-102.63	-102.66	-105.55
710	-102.63	-102.63	-102.63	-102.65	-104.77
810	-102.63	-102.63	-102.63	-102.65	-104.27
910	-102.63	-102.63	-102.63	-102.65	-103.92

Table 8.3 (continued)

(e) $\beta = 1$, $k = 1$, $k' = 1.05$ vs. $\beta = 1$, $k = k' = 1$ (k' varies 5%)

Dimensionless wave number	Froude number = 1	0.9	0.5	0.1	0.01
	Rate of change of relative difference of dimensionless relative celerity with respect to k' in %				
0.1	-0.50	-0.41	-0.13	-0.01	0.00
0.2	-2.04	-1.65	-0.50	-0.02	0.00
0.3	-4.68	-3.79	-1.15	-0.05	-0.00
0.4	-8.55	-6.94	-2.07	-0.08	-0.00
0.5	-13.74	-11.23	-3.30	-0.13	-0.00
0.6	-20.26	-16.78	-4.86	-0.18	-0.00
0.7	-27.86	-23.63	-6.81	-0.25	-0.00
0.8	-35.87	-31.55	-9.20	-0.32	-0.00
0.9	-43.34	-39.94	-12.11	-0.41	-0.00
1	-49.36	-47.81	-15.63	-0.50	-0.01
2	-55.98	-59.13	-97.38	-2.08	-0.02
3	-53.29	-54.70	-78.25	-4.92	-0.05
4	-52.17	-52.95	-64.17	-9.45	-0.08
5	-51.63	-52.12	-58.72	-16.43	-0.13
6	-51.33	-51.67	-56.04	-27.43	-0.18
7	-51.15	-51.40	-54.52	-45.97	-0.25
8	-51.03	-51.22	-53.57	-81.58	-0.32
9	-50.95	-51.10	-52.93	-169.80	-0.41
10	-50.89	-51.01	-52.48	-427.70	-0.50
11	-50.85	-50.95	-52.16	-268.44	-0.61
12	-50.81	-50.90	-51.91	-164.08	-0.73
13	-50.79	-50.86	-51.72	-124.05	-0.86
14	-50.77	-50.83	-51.57	-103.64	-1.00
15	-50.75	-50.81	-51.45	-91.42	-1.15
16	-50.74	-50.79	-51.35	-83.34	-1.31
17	-50.73	-50.77	-51.27	-77.64	-1.49
18	-50.72	-50.76	-51.20	-73.43	-1.67
19	-50.71	-50.74	-51.14	-70.20	-1.87
20	-50.70	-50.73	-51.09	-67.66	-2.08
22	-50.69	-50.72	-51.01	-63.94	-2.54
24	-50.68	-50.71	-50.95	-61.37	-3.05
26	-50.68	-50.70	-50.91	-59.50	-3.62
28	-50.67	-50.69	-50.87	-58.10	-4.24
30	-50.67	-50.68	-50.84	-57.02	-4.93
110	-50.64	-50.64	-50.66	-51.07	-311.95
210	-50.64	-50.64	-50.65	-50.76	-65.74
310	-50.64	-50.64	-50.64	-50.69	-56.61
410	-50.64	-50.64	-50.64	-50.67	-53.89
510	-50.64	-50.64	-50.64	-50.66	-52.69
610	-50.64	-50.64	-50.64	-50.65	-52.06
710	-50.64	-50.64	-50.64	-50.65	-51.68
810	-50.64	-50.64	-50.64	-50.65	-51.44
910	-50.64	-50.64	-50.64	-50.65	-51.27

Table 8.3 (continued)

(f) $\beta = 1$, $k = 1$, $k' = 0.95$ vs. $\beta = 1$, $k = k' = 1$ (k' varies 5%)

Dimensionless wave number	Froude number = 1	0.9	0.5	0.1	0.01
	Rate of change of relative difference of dimensionless relative celerity with respect to k' in %				
0.1	0.50	0.41	0.13	0.01	0.00
0.2	2.04	1.65	0.50	0.02	0.00
0.3	4.71	3.81	1.15	0.05	0.00
0.4	8.65	7.01	2.08	0.08	0.00
0.5	14.00	11.41	3.31	0.13	0.00
0.6	20.78	17.16	4.90	0.18	0.00
0.7	28.73	24.33	6.88	0.25	0.00
0.8	37.09	32.68	9.33	0.32	0.00
0.9	44.71	41.47	12.33	0.41	0.00
1	50.61	49.54	15.99	0.51	0.01
2	54.96	58.07	102.37	2.09	0.02
3	52.07	53.44	76.12	4.96	0.05
4	50.93	51.67	62.37	9.58	0.08
5	50.38	50.85	57.13	16.84	0.13
6	50.08	50.40	54.57	28.60	0.18
7	49.90	50.13	53.11	49.35	0.25
8	49.78	49.96	52.20	92.75	0.32
9	49.70	49.84	51.59	222.88	0.41
10	49.64	49.75	51.16	544.04	0.51
11	49.60	49.69	50.84	243.42	0.61
12	49.56	49.64	50.61	152.44	0.73
13	49.54	49.61	50.42	117.03	0.86
14	49.52	49.58	50.28	98.63	1.00
15	49.50	49.55	50.16	87.47	1.15
16	49.49	49.53	50.07	80.04	1.31
17	49.48	49.52	49.99	74.76	1.49
18	49.47	49.50	49.92	70.84	1.68
19	49.46	49.49	49.87	67.83	1.88
20	49.45	49.48	49.82	65.45	2.09
22	49.44	49.47	49.75	61.96	2.55
24	49.43	49.45	49.69	59.54	3.06
26	49.43	49.44	49.64	57.79	3.63
28	49.42	49.44	49.61	56.47	4.27
30	49.42	49.43	49.58	55.44	4.96
110	49.39	49.39	49.40	49.79	269.58
210	49.39	49.39	49.39	49.50	63.65
310	49.39	49.39	49.39	49.44	55.05
410	49.39	49.39	49.39	49.42	52.47
510	49.39	49.39	49.39	49.41	51.34
610	49.39	49.39	49.39	49.40	50.74
710	49.39	49.39	49.39	49.40	50.38
810	49.39	49.39	49.39	49.40	50.15
910	49.39	49.39	49.39	49.40	49.99

First, by comparing Fig. 8.1 (a) with Figs. 8.1 (b) and (c) or Table 8.2 (a) with Tables 8.2 (b) and (c), and referring to Tables 8.3 (a) and (b), the following conclusions on the effect of ß are observed:

(a) For various F_0 (in reality, it is an initial Froude number) considered, the dimensionless relative celerity increases very slowly with the dimensionless wave number in the range of low wave number, then it rises sharply from a small magnitude to a large one, and finally, it asymptotically reaches a constant value in the range of high wave number. In general, the smaller the Froude number, the later the time of sharp rise, and the larger the rise. If the dimensionless wave number corresponding to the sharp rise point is designated as a dimensionless rise wave number, it is approximately equal to the inverse of the Froude number. For example, if F_0 = 1, 0.5, 0.1 and 0.01, the rise wave number is approximately equal to 1, 2, 10 and 100, respectively. The variation of ß does not affect the regularity of variation of the relative celerity with the wave number, and it changes only the magnitude of the relative celerity. Obviously, based on the rise wave numbers, the effect of ß on the relative celerity can be divided into two regions: (i) One is after the rise wave numbers, in which the values of the relative celerity for cases of ß = 1.33 and 2 are greater than those of ß = 1, i.e., the relative celerity increases with increasing the value of ß. (ii) The other is before the rise wave numbers where values of the relative celerity for the case of ß = 2 are slightly greater than those of ß = 1, but for the case of ß = 1.33 the situation is opposite and the change seems to

be large, namely, as ß = 1, the relative celerity is almost equal to 0.5 for various wave numbers less than the rise wave numbers, but, as ß = 1.33, the magnitude of the relative celerity reduces to 0.17. These indicate that the effect of ß is wave-number dependent.

(b) The effect of ß on the relative celerity is also related to the Froude number. With increasing Froude number, the effect of ß becomes significant. For example, in Table 8.3 (b) with increasing ß from 1 to 2, for F_0 = 0.1, the rate of change of the relative difference of the relative celerity with respect to ß is only 1% for high wave numbers, while it reaches 73% for F_0 = 1.

(c) For the situation of large Froude number and low wave number, the impact of ß on the relative celerity is very significant. This partially explains why the impact of ß on the numerical solutions obtained in this study appears to be unimportant. The numerical testing has been focused on subcritical flow condition with F_0 less than 0.5, and the inflow considered is not a very slow-rising flood wave, and hence, the wave number is not low. Therefore, the impact of ß on the solutions of the equations seems small.

Secondly, by comparing Fig. 8.1 (a) with Figs. 8.1 (d) and (e), and Table 8.2 (a) with Tables 8.2 (d) and (e), and referring to Tables 8.3 (c) and (d), the following observations on the effect of k can be made:

(a) Similar to ß, the variation of k does not affect the pattern of variation of the relative celerity with the wave number, and it changes only the magnitude of the relative celerity. For

example, for k = 1.05, the values of the relative celerity for various Froude numbers and wave numbers are greater than those of k = 1 (designate this as amplification), and for k = 0.95, the values of the relative celerity become less than those of k = 1 (designate this as attenuation).

(b) By comparing Table 8.3 (c) with Table 8.3 (d), it is obvious that the attenuation of the relative celerity for the case of k < 1 is stronger than the amplification for the case of k > 1. This agrees with the result presented in Chapter 5 that the solution differences between the exact momentum and continuity equations and the Saint-Venant equations for k = 0.95 are greater than those for k = 1.05.

(c) The impact of k is also related to the dimensionless wave number. There are two ranges based on the rise wave number: (i) For wave numbers greater than the rise wave number, the impact of k is large. (ii) For wave numbers less than the rise wave number, the impact of k is small. For example, in Table 8.3 (c) with increasing k from 1 to 1.05, when F_0 = 0.5, for wave numbers greater than 2, the rate of change of the relative difference of the relative celerity with respect to k is approximately 100%; whereas for wave numbers less than 2, the rate becomes much smaller. This means that the impact of k on the solutions of the equations is important for high wave numbers.

(d) In the range of the wave number greater than the rise wave number, the impact of k seems to be unrelated to Froude number, because all the rates of change of the relative difference of the relative celerity with respect to k are approximately 100% for

various F_0 considered (see Tables 8.3 (c) and (d)). However, in the range of the wave number less than the rise wave number, the impact of k is related to Froude number.

(e) If Tables 8.2 (d) and (e) are compared with Tables 8.2 (b) and (c), and Tables 8.3 (c) and (d) with Tables 8.3 (a) and (b), it is obvious that the impact of k on the relative celerity is greater than that of ß, especially, for the situation of small Froude number and high wave number. This indicates that k is more important than ß. This conclusion is also in agreement with that presented in Chapter 5.

Third, by comparing Tables 8.2 (f) and (g) with Tables 8.2 (d) and (e), and Tables 8.3 (e) and (f) with Tables 8.3 (c) and (d), the effect of k' on the relative celerity is similar to that of k, but there are two differences:

(a) The change of the magnitude of the relative celerity due to the variation of k' is opposite to that of k, i.e., when k' increases from 1 to 1.05, the relative celerity decreases (attenuation), and when k' decreases from 1 to 0.95, the relative celerity increases (amplification).

(b) By inspecting Tables 8.3 (c), (d), (e) and (f), it is obvious that the effect of k' on the relative celerity is approximately half of that of k. This is also in agreement with the conclusion presented in Chapter 5.

8.2. Evaluation of Contributions of Terms by Using Price's Method

As described in section 3.3, Price (1985) introduced two parameters, $\varepsilon = \bar{h}/\overline{xS_0}$ and $\varsigma = \bar{Q}^2/(g\bar{A}^2\bar{h})$ where the 'bar' denotes the

scale of the variable, and rewrote the complete dynamic wave equation as

$$\frac{\varepsilon\varsigma}{A''}\left[\frac{\partial Q''}{\partial t''}+\frac{\partial}{\partial x''}\left(\frac{Q''^2}{A''}\right)\right]+\varepsilon\frac{\partial h''}{\partial x''}-S''_0+S''_f=0 \qquad (8.38)$$

in which the 'double prime' denotes the dimensionless form of the variable. For example, $Q''=Q/\bar{Q}$, $A''=A/\bar{A}$, $h''=h/\bar{h}$, $S''_0=S_0/\bar{S}_0$, $S''_f=S_f/\bar{S}_0$, $x''=x/\bar{x}$ and $t''=t/\bar{t}$.

By using Price's method, the exact momentum equation without considering the internal stresses term and two rates of spatial change of ß and k can be rewritten as follows

$$\frac{\varepsilon\varsigma}{A''}\left[\frac{\partial Q''}{\partial t''}+\beta\frac{\partial}{\partial x''}\left(\frac{Q''^2}{A''}\right)\right]+k\varepsilon\frac{\partial h''}{\partial x''}-(k-k')\varepsilon\frac{h''}{A''}\frac{\partial A''}{\partial x''}-S''_0+S''_f=0 \qquad (8.39)$$

in which, in addition to ß, k and k', all the quantities are the same as those in Eq. (8.38).

From Eq. (8.39), two points can be observed. One is that if the values of ß, k and k' are equal to unity, Eq. (8.39) becomes Eq. (8.38). The other point is that on the basis of the magnitudes of the two parameters, ε and ς, the relative contribution of each of the terms in Eq. (8.39) can be estimated. For example, if the value of ε is close to zero, the contributions of the local and convective acceleration terms, and the pressure term in Eq. (8.39) are insignificant, thus, they can be neglected and Eq. (8.39) becomes a kinematic wave approximation. If only the value of ς is very small, the contributions of the two acceleration terms can be ignored, thus Eq. (8.39) is simplified to a noninertia model.

Therefore, based on the magnitudes of two parameters, the results obtained in Chapter 6 can be evaluated. Four typical combinations of the coefficients ($\beta = 1$, $k = k' = 1$; $\beta = 1$, $k = 0.95$, $k' = 1$; $\beta = 1$, $k = 1.05$, $k' = 1$; and $\beta = 2$, $k = 0.95$, $k' = 1$) for the assigned conditions of rectangular channels with channel slope, $S_0 = 0.00019$, without or with downstream backwater effect are used as examples. The magnitudes of the two parameters ε and ς obtained at the cross-sectional position, $x/L = 25/27$, near downstream boundary for various cases investigated are displayed in Table 8.4.

Table 8.4 Magnitudes of Parameters, ε and ς, for Evaluating Contributions of Terms

		No backwater effect	$\partial h/\partial x > 0$ cases			$\partial h/\partial x < 0$ cases
			hd/h0=1.44	1.80	2.53	0.70
ß=1						
k'=1	ε	0.0049	0.0656	0.1024	0.2006	0.0157
k=1	ς	0.1531	0.0629	0.0322	0.0117	0.5046
ß=1						
k'=1	ε	0.0049	0.0655	0.1019	0.1980	0.0157
k=0.95	ς	0.1531	0.0629	0.0323	0.0118	0.5045
ß=1						
k'=1	ε	0.0049	0.0657	0.1029	0.2055	0.0157
k=1.05	ς	0.1531	0.0630	0.0322	0.0117	0.5046
ß=2						
k'=1	ε	0.0049	0.0654	0.1017	0.1976	0.0157
k=0.95	ς	0.1531	0.0629	0.0322	0.0118	0.5046

From Table 8.4, three observations can be obtained. First, when there is no backwater effect, the magnitude of ε is close to zero for various situations considered. This means that the

pressure term and the two acceleration terms are insignificant, and the kinematic wave is a proper approximation for the exact momentum equation. Second, when the flow profiles are the convectively decelerating type where $\partial h/\partial x > 0$, the magnitude of ε increases with increasing the downstream-boundary water depth and gradually develops to approach unity, but the magnitude of ς decreases with increasing downstream water depth and gradually becomes much less than unity. This means that the pressure term becomes important and the two inertial terms (local and convective accelerations) can be neglected, especially when the downstream water depth is large, i.e., the subcritical flow condition is subject to greater convective deceleration. Therefore, the noninertia model is a proper approximation. Third, for the convectively accelerating profiles, namely, the convectively accelerating subcritical flow, the magnitude of ς is greater than that of ε, but, the order of magnitude of ε is the same as that of product of ε and ς. This means that the contribution of the convective acceleration increases, and it is necessary to regard both the pressure term and the convective acceleration term. Thus, the quasi-steady dynamic wave model may be suitable. Therefore, Table 8.4 indicates that the results using the two parameters as a criterion to evaluate the contributions of the terms in the exact momentum equation are in agreement with those obtained in Chapter 6. In addition, it is obvious that the variations of the coefficients, ß and k, do not influence the pair of parameters because the magnitude of either ε or ς is basically the same for various combinations of the coefficients tested.

9. CRITERIA FOR SELECTION OF EQUATIONS AND APPROXIMATE MODELS

9.1. Criteria for Selection of Equations

The selection of equations means what kind of equations, i.e., the exact momentum and continuity equations or the Saint-Venant equations, will be used to solve a flood routing problem. The Saint-Venant equations are a special case of the exact momentum and continuity equations, i.e., the latter with $\beta = 1$, $k = k' = 1$ and without the internal stresses term and two rates of spatial change of β and k. Based on the difference between the solutions of the two formulations, criteria can be set up on the situations that the Saint-Venant equations can be a good approximation of the exact momentum and continuity equations.

As discussed in previous chapters, the maximum absolute and relative solution differences between the two sets of equations mainly depend on: (a) the values of the coefficients, β, k and k'; (b) the channel slope, S_0; (c) the flow Froude number; (c) the downstream boundary condition; and (d) the solution variables, h and V or Q.

From Chapter 7, in general, if the solution variable is Q, the difference in discharge between the solutions of the exact momentum and continuity equations and the Saint-Venant equations is insignificant, therefore, the Saint-Venant equations can be selected as a satisfactory approximation. However, from Chapter 5, the maximum solution differences in flow velocity V and flow depth h between the two sets of equations are significant for some situations, and the solution difference in the velocity are larger

than that in the flow depth. Thus, it is necessary to make different selection criteria for the flow velocity and flow depth.

In addition, because the maximum solution difference is closely related to the channel slope and downstream boundary condition, how to set up a good indicator to describe the two factors is an important problem. Different downstream boundary conditions, i.e., with or without backwater effect, can be identified by using the longitudinal gradient of the water depth, $\partial h/\partial x$. Hence, $\partial h/\partial x$ to the channel slope, S_0, ratio is a good and meaningful indicator to effectively link the two factors (the channel slope and downstream boundary condition). The different values of the ratio, $(\partial h/\partial x)/S_0$, for various downstream boundary conditions are shown in Fig. 9.1. For example, for uniform flow with no downstream backwater effect, $(\partial h/\partial x)/S_0 = 0$; for the downstream boundary condition with convectively decelerating type water surface profiles where $\partial h/\partial x > 0$, $(\partial h/\partial x)/S_0 > 0$, in which S_0 is defined as $-dZ/dx$ and Z is water surface elevation relative to a fixed datum; for the downstream boundary condition with convectively accelerating type profiles where $\partial h/\partial x < 0$, $(\partial h/\partial x)/S_0 < 0$. It is obvious that the stronger the convectively decelerating or accelerating subcritical flow, the larger the ratio, $(\partial h/\partial x)/S_0$, in the absolute value. The ratio, $(\partial h/\partial x)/S_0$, is a function of time and location for an unsteady flow. For simplicity and convenience, for the channel studied, the time-average difference of the water depth in the last 4-mile long reach (from x/L = 25/27 to 1) divided by the channel slope is taken approximately as the ratio of the longitudinal gradient of the water depth to the

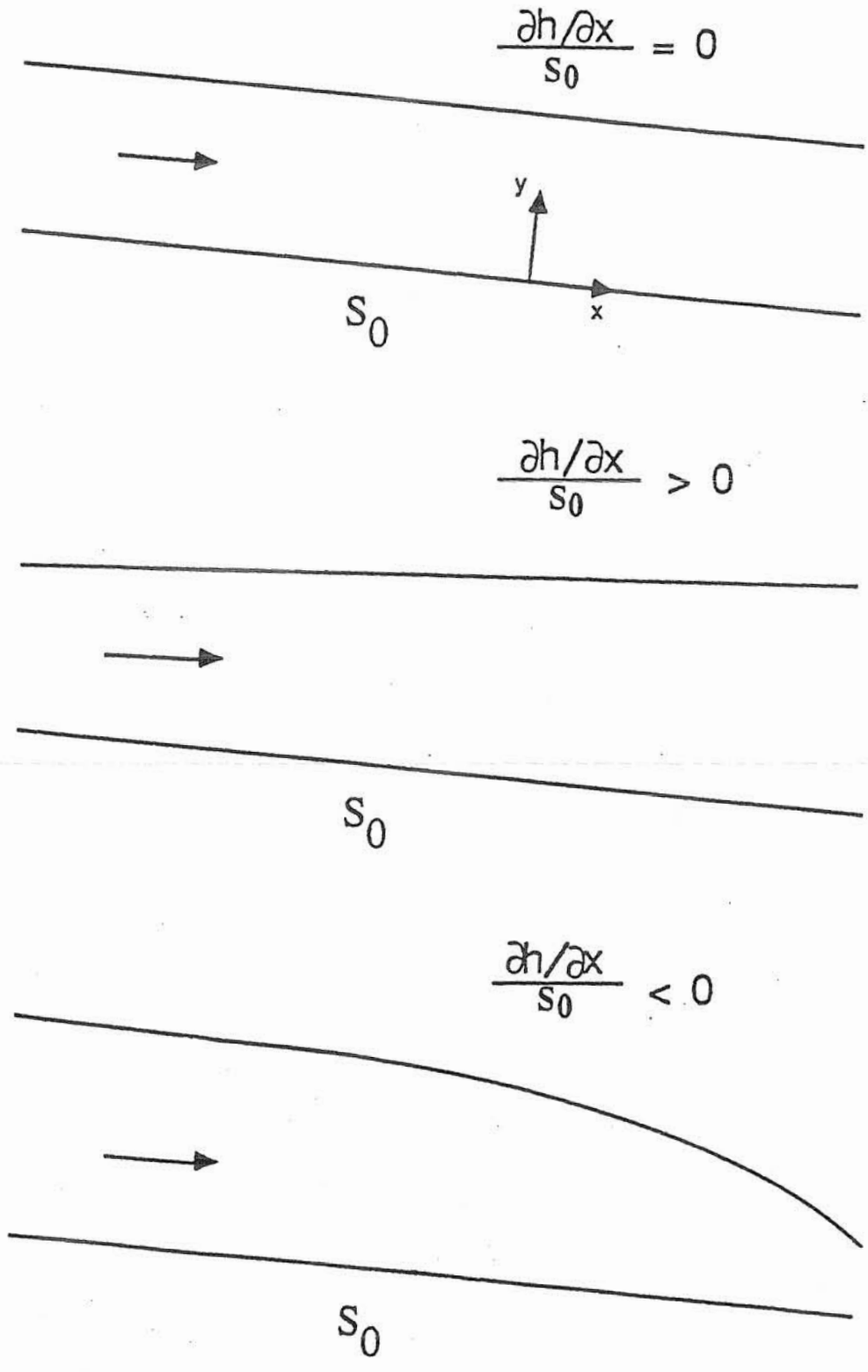

Fig. 9.1 Values of $(\partial h/\partial x)/S_0$ for Various Downstream Boundary Conditions

channel slope.

As to the flow Froude number, the initial steady-uniform-flow Froude number, $F_0 = V_0/(gh_0)^{1/2}$, is taken as an indicator to reflect the solution difference between the exact momentum and continuity equations and the Saint-Venant equations. Based on the results obtained from this study, if the initial steady-uniform-flow Froude number is small (e.g., less than 0.2), the difference between the solutions of the two sets of equations is large, otherwise, the difference is insignificant.

Furthermore, the selection of equations also depends on the required accuracy. If the required accuracy is not high, such as greater than 10% maximum relative solution difference, the Saint-Venant equations can replace the exact momentum and continuity equations for most flow and boundary conditions, but if the accuracy is limited to 5% maximum relative solution difference, for some flow and boundary conditions, such as channels with very curved bed, small slope and large downstream-backwater effect, only the exact momentum and continuity equations can provide reliable solutions.

Based on the results obtained in Chapter 5, if the 5% maximum relative solution difference is chosen as a required accuracy, it can be estimated that $|\partial h/\partial x|/S_0 = 0.25$ and 0.35 are two demarcation points for the flow velocity and flow depth, respectively. This means that, if the value of $|\partial h/\partial x|/S_0$ is less than 0.25 (or 0.35) and the solution variable is velocity (or flow depth), the Saint-Venant equations are a satisfactory approximation of the exact momentum and continuity equations, otherwise, selecting the

exact momentum equation is necessary. The two demarcation values of $(\partial h/\partial x)/S_0$ may be useful in flood routing. For unsteady flow, the value of $(\partial h/\partial x)/S_0$ can be continuously monitored. When the monitored value of $|\partial h/\partial x|/S_0$ is less than the demarcation value, the Saint-Venant equations can be used as a model to simulate flood routing; but when the monitored value of $|\partial h/\partial x|/S_0$ becomes greater than the demarcation value, the exact momentum equation should be used.

To sum up, the criteria for the selection of equations (simply designated as CSE) can be expressed as such a function

$$CSE = f(\beta, k, k', F_0, (\partial h/\partial x)/S_0, \text{ required accuracy})$$

and they are shown in Tables 9.1 (a) and (b) based on assuming 5% maximum relative solution difference as a error limit for the flow velocity and flow depth, respectively.

Table 9.1 Criteria for Selection of Equations

(a) Solution Variable, V

Values of ß and k	$F_0 < 0.2$		$0.2 < F_0 < 1$	
	$\lvert\partial h/\partial x\rvert/S_0$			
	< 0.25	> 0.25	< 0.25	> 0.25
	Recommended equations			
ß from 1 to 2				
0.98 < k < 1.02	Saint-Venant equations	Saint-Venant equations	Saint-Venant equations	Saint-Venant equations
k < 0.98 k > 1.02	Saint-Venant equations	Exact momentum and continuity equations	Saint-Venant equations	Saint-Venant equations

(b) Solution Variable, h

Values of ß and k	$F_0 < 0.2$		$0.2 < F_0 < 1$	
	$\lvert\partial h/\partial x\rvert/S_0$			
	< 0.35	> 0.35	< 0.35	> 0.35
	Recommended equations			
ß from 1 to 2				
0.97 < k < 1.03	Saint-Venant equations	Saint-Venant equations	Saint-Venant equations	Saint-Venant equations
k < 0.97 k > 1.03	Saint-Venant equations	Exact momentum and continuity equations	Saint-Venant equations	Saint-Venant equations

9.2. Criteria for Selection of Approximate Models

The selection of approximate models is definitely related to the relative contribution of each of the terms, i.e., the local acceleration, convective acceleration, pressure, friction slope and channel slope. From Chapter 6, the contributions of the terms mainly depend on the channel slope, S_0, the flow Froude number, and the downstream boundary condition. The downstream boundary condition has the most significant influence to the contributions of the terms. When no backwater effect exists and the Froude number is small, the friction slope and channel slope are the most important, and the other terms can be ignored. When there is a downstream backwater effect, i.e., the flow condition is dominated by the convectively decelerating or accelerating subcritical flow, the pressure term becomes very significant. For the convectively accelerating type profiles, the importance of the convective acceleration term increases.

In order to clearly set up criteria for the selection of various approximate models, Equation (8.40), which is as follows,

$$\frac{\varepsilon\varsigma}{A''}\left[\frac{\partial Q''}{\partial t''} + \beta\frac{\partial}{\partial x''}\left(\frac{Q''^2}{A''}\right)\right] + k\varepsilon\frac{\partial h''}{\partial x''} - (k-k')\varepsilon\frac{h''}{A''}\frac{\partial A''}{\partial x''} - S''_0 + S''_f = 0$$

is discussed again. In this equation, ς is equal to the square of the Froude number and ε is equal to $(\bar{h}/\bar{x})/S_0$. If $\varepsilon = (\bar{h}/\bar{x})/S_0$ is replaced by the ratio, $(\partial h/\partial x)/S_0$, on the basis of magnitudes of Froude number and $(\partial h/\partial x)/S_0$, the exact momentum equation can be transferred into various approximations. For example, if $(\partial h/\partial x)/S_0 = 0$, this equation is the kinematic wave approximation;

if $(\partial h/\partial x)/S_0 \approx 0$, but the flow Froude number is large, only the pressure term can be neglected, thus this equation becomes an approximation without the pressure term; if $|\partial h/\partial x|/S_0$ is large, i.e., the more convectively decelerating or accelerating subcritical flow condition, but the Froude number is small, this equation becomes the noninertia model. These analyses can be summarized in Table 9.2 to demonstrate the criteria for the selection of various approximate models.

Table 9.2 Criteria for Selection of Approximate Models

$(\partial h/\partial x)/S_0$ / F_0	<<0	0	>>0
Small	Noninertia	Kinematic wave	Noninertia
Large	Complete dynamic wave	Nonpressure	Complete dynamic wave

Finally, according to the above discussions, one example reflecting the boundaries between either different equations (the exact momentum and continuity equations and the Saint-Venant equations) and various approximate models can be roughly expressed in Fig. 9.2. Figure 9.2 is given only as an example. In order to obtain the actual regions for the equations and approximate models, further investigation is required.

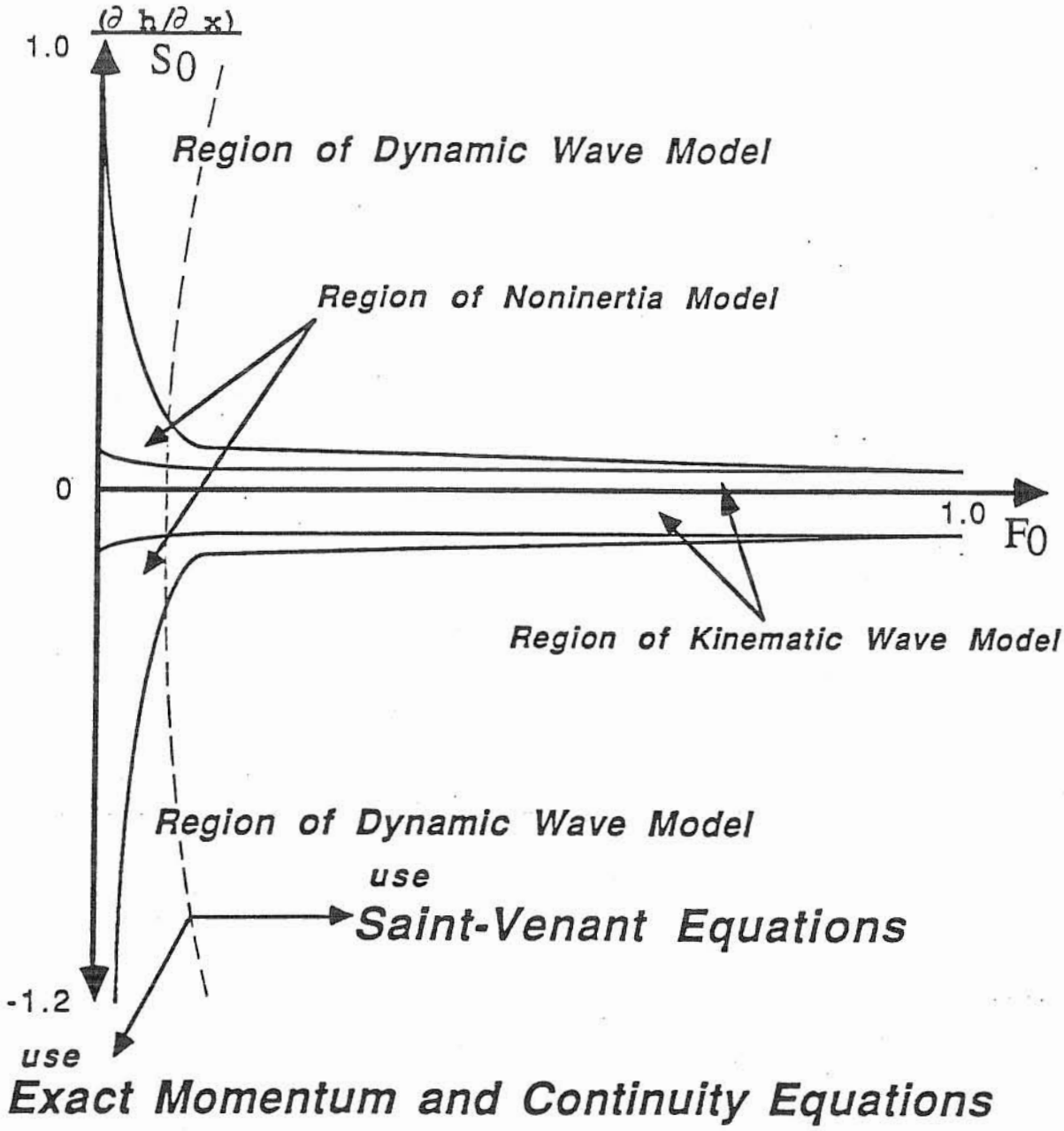

Fig. 9.2 Schematic of Applicable Regions for Different Equations & Approximate Models

10. CONCLUSIONS AND RECOMMENDATIONS

A systematic and comprehensive investigation of the sensitivity of the coefficients and terms in the exact momentum equation for unsteady subcritical flow in prismatic channels with fixed boundary has been conducted in this study. By analyzing the numerical results, the importance of the momentum flux correction coefficient (ß) and pressure correction coefficients (k and k'), and the relative contributions of the terms (local acceleration, convective acceleration, pressure, friction slope, channel slope, internal stresses) to the exact momentum equation for different cross-sectional shapes, channel slopes and downstream boundary conditions are summarized as follows

(a) On the basis of the results obtained from this study, among the coefficients, ß, k and k', the impact of k on the solutions of the equations is the largest, especially when the channel slope is small and the downstream backwater effect is significant (i.e., the longitudinal gradient of the water depth, $\partial h/\partial x$, differs significantly from the channel slope, S_0). However, usually the value of k is close to unity in most practical situations where the pressure distribution is nearly hydrostatic, unless the flow condition is significant convective acceleration, such as spillways and channels with sharply curved beds. In such special cases, the pressure distribution is very nonhydrostatic so that the value of k departs from unity.

(b) The impact of k' on the solutions of the equations is roughly equal to half of that of k.

(c) The impact of ß on the solutions of the equations is relatively small as compared to that of k. However, the combined impact of ß and k may become significant. If the flow velocity and pressure distributions of a real flow are extremely nonuniform and nonhydrostatic, the assumption of ß and k equal to unity will lead to a significant error.

(d) The impacts of these coefficients (ß, k and k') on the solutions of the equations are closely related to the Froude number, channel slope and downstream boundary condition. If the Froude number is small and the longitudinal gradient of the water depth, $\partial h/\partial x$, differs considerably from the channel slope (often associated with a significant downstream-boundary backwater effect where the convective deceleration or acceleration of the flow is strong), the difference between the solutions of the exact momentum and continuity equations and the Saint-Venant equations where $ß = k = k' = 1$ is significant.

(e) The effects of the coefficients (ß, k and k') on the solution of the flow velocity are greater than that on either the flow depth or discharge. This implies that flow velocity is more sensitive to the variations of the coefficients than the flow depth and discharge. Therefore, if the velocity is the required solution variable, the selection of the equations (the exact momentum and continuity equations or the Saint-Venant equations) must be done carefully.

(f) For channels with small slope and without backwater effect, the friction slope and channel slope are the most important among the terms in the momentum equation, and the two inertia terms

and the pressure term can be neglected. However, if there is a backwater effect, the relative importance of these terms is different. For convectively decelerating subcritical flow where $(\partial h/\partial x)/S_0 > 0$, the pressure term becomes very significant and its contribution becomes equal to or greater than that of either the friction slope or the channel slope. For convectively accelerating subcritical flow where $(\partial h/\partial x)/S_0 < 0$, the pressure term is also important. The increase of contribution of the pressure term implies the advantage of using the noninertia model when there exists a downstream backwater effect.

(g) When the water surface profile is of the convectively accelerating type, the contribution of the convective acceleration term increases relatively as compared to that for convectively decelerating water surface profiles.

(h) Generally speaking, the internal stress term is not significant, and can be ignored, provided there is no abrupt change in cross section along the channel.

(i) Similar to the internal stress term, the rates of spatial change of β and k can be disregarded in most situations. However, for some special cases, such as an abrupt change of channel cross section or bed profile, the changes of the velocity and pressure distributions along flow direction are large. Hence, the two rates are important to consider.

(j) From the above observations, it is clear that when the pressure distribution is nearly hydrostatic, i.e., gradually varied flow, the exact momentum equation can be approximated by the

complete dynamic wave equation. Otherwise, it is necessary to use the more complicated exact momentum equation.

(k) The noninertia model can serve as a good approximation of the exact momentum and continuity equations in most cases since the two acceleration terms are relatively small. The kinematic wave approximation can be used only when there is no downstream backwater effect.

(l) The key parameters for the selection of approximate models of the exact momentum and continuity equations are the Froude number and $(\partial h/\partial x)/S_0$. Alternatively, the relative celerity and logarithmic decrement of the shallow water wave can also be used (Table 8.1).

(m) The solution difference of the flow depths between the V-h form and Q-h form of the exact momentum and continuity equations is mostly insignificant. This means that either form of the equations can be selected for solving flow depth. However, the Q-h form is slightly preferred to the V-h form, because flow velocity is more sensitive to the variations of the coefficients (ß, k and k') than the flow depth or discharge.

(n) For a prismatic channel, the cross-sectional shape does not significantly affect the relative importance of the coefficients (ß, k and k') and the relative contributions of the terms in the exact momentum equation.

According to the analyses and results of this study, the following subjects are recommended for further investigation:

(a) First is to investigate the impacts of the coefficients and contributions of the terms for nonprismatic channels.

(b) Second is to study the impacts of the coefficients and contributions of the terms for different upstream inflows, and other types of the downstream boundary conditions.

(c) Third, because in reality it is impossible to change the value of only one coefficient while keeping other coefficients unchanged, further investigation of the relationships among the coefficients is necessary.

(d) Finally, it is important to collect data from laboratory experiments and perhaps also from the field for comparison and verification of the numerical results obtained from this study.

REFERENCES

Abbott, M. B., 1979. Computational Hydraulics: Elements of the Theory of Free Surface Flows. Pitman, Marshfield, Mass.

Akan, A. O., and Yen, B. C., 1977. A Nonlinear Diffusion-Wave Model for Unsteady Open-Channel Flow. Proceedings of 17th IAHP Congress, Germany, Vol. 2, pp. 181-190.

Akan, A. O., and Yen, B. C., 1981. Diffusion-Wave Flood Routing in Channel Networks. Journal of the Hydraulics Division, ASCE, Vol. 107, No. HY6, pp. 719-732, June.

Amein, M., 1966. Streamflow Routing on Computer by Characteristics. Water Resources Research, Vol. 2, No. 1, pp. 123-130.

Amein, M., 1968. An Implicit Method for Numerical Flood Routing. Water Resources Research, Vol. 4, No. 4, pp. 719-726, August.

Amein, M., and Chu, H. L., 1975. Implicit Numerical Modeling of Unsteady Flows. Journal of the Hydraulic Division, ASCE, Vol. 101, No. HY6, pp. 717-731, June.

Amein, M., and Fang, C. S., 1970. Implicit Flood Routing in Natural Channels. Journal of the Hydraulics Division, ASCE, Vol. 96, No. HY12, pp. 2481-2500, December.

Ball, J. E., 1988. Modelling of Unsteady Flows in Urban Drainage Works Including Some Effects on Manholes. Ph. D. Thesis Presented to the University of Newcastle, Austraria.

Baltzer, R. A., and Lai, C., 1968. Computer Simulation of Unsteady Flows in Waterways. Journal of the Hydraulics Division, ASCE, Vol. 94, No. HY4, pp. 1083-1117, July.

Chang, F. F. M., and Richards, D. L., 1971. Deposition of Sediment in Transient Flow. Journal of the Hydraulics Division, ASCE, Vol. 97, No. HY6, pp. 837-849, June.

Chaudhry, Y. M., and Contractor, D. N., 1973. Application of the Implicit Method to Surges in Open Channels. Water Resources Research, Vol. 9, No. 6, pp. 1605-1612, December.

Chow, V. T., 1959. Open-Channel Hydraulics. Mcgraw-Hill Book Co., Inc., New York.

Chen, C. L., and Chow, V. T., 1971. Formulation of Mathematical Watershed-Flow Model. Journal of the Engineering Mechanics Division, ASCE, Vol. 97, No. EM3, pp. 809-828, June.

Courant, R., and Friedricks, W. R., 1948. Supersonic Flow and Shock Waves. Interscience Press, New York, N. Y.

Cunge, J. A., Holly, F. M. and Verwey, A., 1981. Practical Aspects of Computational River Hydraulics. Pitman, Marshfield, Mass.

Fletcher, A. G., and Hamilton, W. S., 1967. Flood Routing in An Irregular Channel. Journal of the Engineering Mechanic Division, ASCE, Vol. 93, No. EM3, pp. 45-62, June.

Fread, D. L., 1971. discussion of Implicit Flood Routing in Natural Channels by Michad Amein and Ching S. Fang, Journal of the Hydraulics Division, ASCE, Vol. 97, No. HY7, pp. 1156-1159, July.

Fread, D. L., 1973. Technique for Implicit Dynamic Routing in Rivers with Tributaries. Water Resources Research, Vol. 9, No. 4, pp. 918-926, August.

Fread, D. L., 1979. Applicability Criteria for Kinematic and Diffusion Routing Models. Report, No. 1.

Goldberg, D. E., and Wyile, E. B., 1983. Characteristics Method Using Time-line Interpolations. Journal of Hydraulics Division, ASCE, Vol. 109, No. 5, pp. 670-683.

Harder, J. A., and Armacost, L. V., 1966. Wave Propagation in Rivers. Hydraulic Engineering Laboratory Report No. 1, Ser. 8, University of California, Berkeley, June.

Harley, B. M., 1967. Linear Routing in Uniform Open Channels. M. Eng. Sc. Thesis, National University of Ireland.

Hartree, D. R., 1952. Some Practical Methods of Using Characteristics in the Calculation of Nonsteady Compressible Flows. Los Alamos Sci. Lab. [Report] LA-HU-1.

Hayami, S., 1951. On the Propagation of Flood Waves. Bull. 1, Disaster Prevention Res. Inst., Kyoto Univ., Kyoto, Japan.

Henderson, F. M., 1966. Open Channel Flow. The Macmillan Publishing Co., Inc., New York.

Isaacson, E., Stoker, J. J., and Troesch, B. A., 1956. Numerical Solution of Flood Prediction and River Regulation Problems. Report No. IMM-205 and IMM-235, Institute of Math. and Mech., New York Univ., N.Y.

Iwasaki, T., 1967. Flood Forecasting in the River Kitakami. Proceedings, International Hydrology Symposium, Fort Collins, Colorado, September 6-8, Vol. 1, pp. 103-112.

Joliffe, I. B., 1984. Computation of Dynamic Waves in Channel Networks. Journal of Hydraulic Engineering, ASCE, Vol. 110, No. 10, pp. 1358-1370, October.

Jolly, J. P., and Yevjevich, V., 1974. Simulation Accuracies of Gradually Varied Flow. Journal of Hydraulic Engineering, ASCE, Vol. 100, No. 7, pp. 1011-1030, July.

Katopodes, N. D., 1982. On Zero-inertia and Kinematic Waves. Journal of Hydraulics Division, ASCE, Vol. 108, No. HY11, pp. 1380-1387.

Keefer, T. N., 1974. Desktop Computer Flow Routing. Journal of the Hydraulics Division, ASCE, Vol. 100, No. HY7, pp. 1047-1058, July.

Keulegan, G. H., 1938. Laws of Turbulent Flow in Open Channel. Journal of Research, U.S. National Bureau of Standards, Vol. 21, Research Paper 1151, pp. 707-741, December.

Keulegan, G. H., and Patterson, G. W., 1943. Effect of Turbulence and Channel Slope on Translation Waves. Journal of Research,U.S. National Bureau of Standards, Vol. 30, Research Paper 1544, pp. 461-512, June.

Kolupaila, S., 1956. Methods of Determination of the Kinetic Energy Factor. The Port Engineer, Calcutta, India, Vol. 5, No. 1, pp. 12-18, January.

Lai, C., 1965a. Flow of Homogeneous Density in Tidal Reaches, Solution by the Method of Characteristics. Open-file Report 65-93, U.S. Geological Survey, Denver, Colo.

Lai, C., 1986. Numerical Modeling of Unsteady Open Channel Flow. Advances in Hydroscience, B. C. Yen, ed., Vol. 14, Academic Press, Orlando, Fla., pp. 161-333.

Lai, C., 1988. Comprehensive Method of Characteristics Models for Flow Simulation. Journal of Hydraulic Engineering, ASCE, Vol. 114, No. 9, pp. 1074-1097, September.

Liggett, J. A., and Woolhiser, D. A., 1967. The Use of the Shallow Water Equations in Runoff Computation. Proceedings, Third Annual American Water Resources Conference, San Francisco, California, pp. 117-126.

Liggett, J. A., and Woolhiser, D. A., 1967. Difference Solutions of the Shallow-Water Equations. Journal of the Engineering Mechanics Division, ASCE, Vol. 93, No. EM2, pp. 39-71, April.

Liggett, J. A., 1975. Basic Equation of Unsteady Flow. Unsteady Flow in Open Channels, K. Mahmood and V. Yevjevich, eds. Water Resources Publications, Fort Collins, Colo., Vol. 1, pp. 29-62.

Liggett, J. A., and Cunge, J. A., 1975. Numerical Methods of Solution of the Unsteady Flow Equations. Unsteady Flow in Open Channels, K. Mahmood and V. Yevjevich, eds. Water Resources Publications, Fort Collins, Colo., Vol. 1.

Lighthill, M. J., and Whitham, G. B., 1955. On kinematic Waves: I Flood Movement in Long Rivers. Proceeding, Royal Society of London, Series A, Vol. 229, May.

Lin, P. N., 1952. Numerical Analysis of Continuous Unsteady Flow in Open Channels. Transactions, American Geophysical Union, Vol. 33, No. 2, pp. 227-234, April.

Lister, M., 1960. The Numerical Solution of Hyperbolic Partial Differential Equations by the Method of Characteristics. in A. Ralston and H. S. Wilf, Mathematical Methods for Digital Computers, John Wiley and Sons, Inc., New York.

Mahmood, K. and Yevjevich, V., 1975. Unsteady Flow in Open Channels, Vols. I and II. Water Resources Publications, Littleton, Colo.

Martin, C. S. and Wiggert, D. C., 1975. Discussion of Simulation Accuracies of Gradualy Varied Flow. Journal of the Hydraulics Division, ASCE, Vol. 101, No. HY7, pp. 1021-1024.

Medowell, D. M., 1976. Modeling Methods for Unsteady Flows. Proc. Int. Symp. Unsteady Flow in Open Channels, Int. Assoc. Hydraul. Res., Newcastle-upon-Tyne, England, pp. B1-10.

Miller, W. A., and Cunge, J. A., 1975. Simplified Equation of Unsteady Flow. Unsteady Flow in Open Channels, K. Mahmood and V. Yevjevich, eds. Water Resources Publications, Fort Collins, Colo., Vol. 1, pp. 183-257.

Miller, W. A. and Yevjevich, V., 1975. Unsteady Flow in Open Channels, Vol. III. Water Resources Publications, Littleton, Colo.

Overton, D. E., 1972. Kinematic Flow on Long Impermeable Planes. Water Resources Bulletin, American Water Resources Association, Vol. 8, No. 6, pp. 1198-1204, December.

Ponce, V. M., and Simons, D. B., 1977. Shallow Wave Propagation in Open Channel Flow. Journal of the Hydraulics Division, ASCE, Vol. 103, No. HY12, pp. 1461-1476, December.

Ponce, V. M., Li, R. M., and Simons, D. B., 1978. Applicability of Kinematic and Diffusion Models. Journal of the Hydraulics Division, ASCE, Vol. 104, No. HY3, pp. 353-360, March.

Ponce, V. M., and Simons, D. B., 1978. Convergence of Four-Point Implicit Water Wave Models. Journal of the Hydraulics Division, ASCE, Vol. 104, No. HY7, pp. 947-958, July.

Ponce, V. M., 1989. Stream Channel Routing. Engineering Hydrology Principles and Practices, Ponce, V. M. ed. Prentice Hall Inc., New Jersey, pp. 270-305.

Ponce, V. M., 1990. Generalized Diffusion Wave Equation with Inertial Effects. Water Resources Research, Vol. 26, No. 5, pp. 1099-1101, May.

Price, R. K., 1974. Comparison of Four Numerical Methods for Flood Routing. Journal of the Hydraulics Division, ASCE, Vol. 100, No. HY7, pp. 879-899, July.

Price, R. K., 1985. Flood Routing. Developments in Hydraulic Engineering - 3, P. Novak, ed. Elsevier Applied Science Publishers, London and New York, pp. 129-173.

Quinn, F. H., and Wylie, E. B., 1972. Transient Analysis of the Detroit River by the Implicit Method. Water Resources Research, Vol. 8, No. 6, pp. 1461-1469, December.

Ragan, R. M., 1965. Synthesis of Hydrographs and Water Surface Profiles for Unsteady Open Channel Flow with Lateral Inflows. Ph.D. Dissertation, Cornell University Water Resources Center, Ithaca, New Youk, February.

Richtmyer, R. D., 1957. Difference Methods for Initial-value Problems, Interscience, N.Y.

Rouse, H., 1965. Critical Analysis of Open-channel Resistance. Journal of the Hydraulics Division, ASCE, Vol. 91, No. HY4, PP. 1-25, July.

Schmitz, G., and Edenhofer, J., 1980. Considering a New Way to Solve Saint-Venant Equations. Proc. Int. Conf. on Water Resour. Dev. Int. Assoc. Hydraul. Res. Asian and Pacific Reg. Div., Taipei, Taiwan, Vol. 2, pp. 821-832.

Schmitz, G., and Edenhofer, J., 1983. Flood Routing in the Danube River by the New Implicit Method of Characteristics (IMOC) Proc. Int. Conf. on Appl. Math. Modelling Mitteilungen des Inst. fur Meereskunde der 3rd Univ. Hanburg, West Germany.

Sevuk, A. S., 1973. Unsteady Flow in Sewer Networks. Ph. D. Thesis presented to the University of Illinois at Urbana-Champaign, Illinois.

Sevuk, A. S., and Yen, B. C., 1973. A Comparative Study on Flood Routing Computation. Proceeding, International Symposium on River Mechanics, Vol. 3, pp. 275-290, Bangkok, Thailand, January.

Sevuk, A. S., and Yen, B. C., 1973. Comparison of Four Approaches in Routing Flood Wave through Junction. Proceeding of the 15-th Congress, International Association for Hydraulic Research, Vol. 5, pp. 169-172, September.

Sivaloganathan, K., 1978. Flood Routing by Characteristic Methods. Journal of the Hydraulics Division, ASCE, Vol. 104, No. HY7, pp. 1075-1091, July.

Sridharan, K., and Kumar, M., 1981. Parametric Study of Flood Wave Propagation. Journal of the Hydraulics Division, ASCE, Vol. 107, No. HY9, pp. 1061-1076, September.

Stoker, J. J., 1953. Numerical Solution of Flood Prediction and River Regulation Problems-Report I-Derivation of Basic Theory and Formulation of Numerical Methods of Attack. Report No. IMM-200, Institute of Math. Sciences, New York Univ. N.Y.

Strelkoff, T., 1969. One-Dimensional Equations of Open-Channel Flow. Journal of the Hydraulics Division, ASCE, Vol. 95, No. HY3, pp. 861-876, May.

Strelkoff, T., 1970. Numerical Solution of Saint-Venant equations. Journal of the Hydraulics Division, ASCE, Vol. 96, No. HY1, pp. 223-253, January.

Tingsanchali, T., and Manandhar, S. K., 1985. Analytical Diffusion Model for Flood Routing. Journal of Hydraulic Engineering, ASCE, Vol. 111, No. 3, pp. 435-454, March.

Wang, S. H., and Yen, B. C., 1987. A Study on the Linearized Non-Inertia Analytical Solution for Unsteady Open Channel Flow. Taiwan Water Conservancy Quarterly, Vol. 35, No. 1.

Weinmann, P. E., and Laurenson, E. M., 1979. Approximate Flood Routing Methods: A Review. Journal of the Hydraulics Division, ASCE, Vol. 105, No. HY12, pp. 1521-1536, December.

Woolhiser, D. A., and Liggett, J. A., 1967. Unsteady, One-dimensional Flow over a Plane - the Rising Hydrograph. Water Resources Research, Vol. 3, No. 3, pp. 753-771, 3rd Quarter.

Wormleaton, P. R., and Karmegam, M., 1984. Parameter Optimization in Flood Routing. Journal of Hydraulic Engineering, ASCE, Vol. 110, No. 12, pp. 1799-1814, December.

Wylie, E. B., 1970. Unsteady Free-Surface Flow Computions. Journal of the Hydraulics Division, ASCE, Vol. 96, No. HY11, pp. 2241-2251, November.

Wylie, E. B., 1980. Inaccuracies in the Characteristics Method. Proc. Ann. Hydraul. Spec. Conf., ASCE, 28th, Chicago, Illinois, pp. 165-176.

Yen, B. C., 1971. Spatially Varied Open-Channel Flow Equations. Research Report No. 51. Water Resour. Cent., Univ. of Illinois at Urbana-Champaign, Illinois.

Yen, B. C., 1973. Open-Channel Flow Equations Revisited. Journal of the Engineering Mechanics Division, ASCE, Vol. 99, No. EM5, pp. 979-1009, October.

Yen, B. C., 1975. Open Channel Roughness: A Review of Manning's Roughness Factor. Sonderforschungsbereich 80 Rept. No. SFB80/T/57. Univ. of Karlsruhe, Karlsruhe, Federal Republic of Germany.

Yen, B. C., 1979. Unsteady Flow Mathematical Modeling Techniques. In: H. W. Shen (Editor), Modeling of River. Wiley-Interscience, New York, N. Y., pp. 13.1-13.33.

Yen, B. C., 1986. Hydraulics of Sewers. Advances in Hydroscience, Vol. 14, B. C. Yen, ed. Academic Press, Orlando, Fla., pp. 1-122.

Yen, B. C. and Sevuk, A. S., 1975. Discussion of Simulation Accuracies of Gradually Varied Flow. Journal of the Hydraulics Division, ASCE, Vol. 101, No. HY6, PP. 786-787, June.

Yen, B. C., and Wenzel, H. G., 1970. Dynamic Equation for Steady Spatially Varied Flow. Journal of the Hydraulics Division, ASCE, Vol. 96, No. HY3, pp. 801-814, March.

Yen, B. C., Wenzel, H. G., and Yoon, Y. N., 1972. Resistance Coefficients for Steady Spatially Varied Flow. Journal of the Hydraulics Division, ASCE, Vol. 98, No. HY8, pp. 1395-1409, August.

Yevjevich, V., and Barnes, A. H., 1970. Flood Routing through Storm Drains. Final Report, Colorado State Univercity, Fort Collins, Colorado.

Yu, Y. S., and McNown, J. S., 1964. Runoff from Impervious Surfaces. Journal of Hydraulic Research, Vol. 2, No. 1, pp. 3-24.